Titre: Title:	Conditional simulation of IRF-k in the petroleum industry and the expert system perspective
Auteur: Author:	Roussos Dimitrakopoulos
Date:	1989
Type:	Mémoire ou thèse / Dissertation or Thesis
Référence: Citation:	Dimitrakopoulos, R. (1989). Conditional simulation of IRF-k in the petroleum industry and the expert system perspective [Thèse de doctorat, Polytechnique Montréal]. PolyPublie. https://publications.polymtl.ca/57959/

UNIVERSITÉ DE MONTRÉAL

CONDITIONAL SIMULATION OF IRF-k IN THE PETROLEUM INDUSTRY AND THE EXPERT SYSTEM PERSPECTIVE

par

Roussos DIMITRAKOPOULOS

DÉPARTEMENT DE GÉNIE MINÉRAL

ÉCOLE POLYTECHNIQUE

THÈSE PRÉSENTÉE EN VUE DE L'OBTENTION
DU GRADE DE PHILOSOPHIAE DOCTOR (Ph.D.)
(GÉNIE MINÉRAL et GÉNIE CIVIL)

Juin 1989

ISBN 0-315-52684-X

UNIVERSITÉ DE MONTRÉAL

ÉCOLE POLYTECHNIQUE

Cette thèse intitulée:

CONDITIONAL SIMULATION OF IRF-k IN THE PETROLEUM INDUSTRY AND THE EXPERT SYSTEM PERSPECTIVE

présentée par: Roussos Dimitrakopoulos

en vue de l'obtention du grade de: Ph.D.

a été dûment acceptée par le jury d'examen constitué de:

M. Guy Perrault, Ph.D., président

M. Michel Soulié, D.Sc.A., directeur de thèse

M. Alexandre Desbarats, Ph.D.

M. Pierre Montes, Ph.D.

SOMMAIRE

La chute spectaculaire des prix du pétrole enregistrée ces dernières années et la baisse graduelle des perspectives d'exploration, orientent l'industrie du pétrole vers l'exploration de gisements connus. Par ailleurs, le relèvement de la productivité exige de mieux comprendre et d'utiliser correctement les caractéristiques naturelles d'un gisement, en procédant à sa caractérisation avancée. La caractérisation avancée d'un gisement comporte deux aspects interconnectés: 1) l'aspect géologique-qualitatif qui permet d'appréhender le gisement comme un phénomène naturel, 2) l'aspect quantitatif-numérique, qui permet la représentation numérique "équivalente" sous forme d'un maillage servant aux études de simulation de l'écoulement du gisement.

D'importants progrès ont été réalisés dans l'amélioration de l'aspect qualitatif de la caractérisation des gisements. Par contre l'aspect numérique reste peu développé. En outre, les progrès réalisés dans d'autres secteurs se rapportant à la simulation des gisements, telle que les formulations complexes de transport des fluides, les méthodes numériques approfondies, les super-ordinateurs, etc. ont fait ressortir davantage le besoin d'améliorer la fiabilité, la certitude et le niveau de précision de la caractérisation quantitative-numérique des gisements. Afin d'améliorer la description numérique des gisements, la présente étude propose des méthodes géostatistiques avancées, dans le cadre de la théorie des fonctions aléatoires intrinsèques d'ordre k

(FAI-k). Les techniques géostatistiques ont des propriétés qui revêtent un intérêt particulier pour la caractérisation des gisements. En effet, 1) elles permettent de quantifier les propriétés inhérentes aux gisements géologiques comme la zonation, la continuité, la dérive et les anisotropies; 2) elles fournissent directement depuis l'échelle de la carotte et des données d'enregistrement jusqu'à l'échelle du modèle de bloc de gisement, des estimations non biaisées sur les propriétés des roches qui serviront de données géologiques pour les études de simulation de l'écoulement du gisement; 3) elles produisent des représentations simulées de variables pertinentes reproduisant les variations **in-situ** des propriétés des roches qui serviront à vérifier la sensibilité des résultats de la simulation de l'écoulement aux données géologiques.

Dans ce travail, nous avons donné une grande importance à l'élaboration et à la présentation point par point d'une technique complète pour la simulation conditionnelle de la FAI-k. Cette dernière est une méthode stochastique qui génère la réalisation de phénomènes non-stationnaires (comme les propriétés des roches des gisements de pétrole dans bien des cas), reproduisant ainsi la covariance généralisée, et les valeurs des données disponibles aux endroits d'échantillonnage. La technique envisagée nécessite les étapes suivantes: 1) simulation en direct des méthodes de Wiener-Levy et leur intégration; 2) l'utilisation de la méthode des bandes de retour pour générer des réalisations en R^n; 3) conditionnement par rapport aux données

disponibles; et 4) vérification de la covariance généralisée reproduite à l'aide de variogrammes généralisés.

L'estimation du tenseur effectif de perméabilité est un problème bien connu de la caractérisation des gisements. On a tenté à plusieurs reprises de le régler, mais aucune solution générale définitive n'a jamais été proposée. Nous proposons ici une nouvelle approche dans un cadre stochastique en deux étapes. La première étape de ce processus porte sur la simulation conditionnelle des perméabilités scalaires dans un maillage à haute densité, représentant le gisement d'hydrocarbures à l'échelle macroscopique. La réalisation de simulations conditionnelles des perméabilités par point reproduit l'histogramme et le variogramme (ou la covariance) des données disponibles ainsi que les mesures prises aux lieux d'échantillonnge. L'étape suivante porte sur la reconstruction simultanée des composantes du tenseur effectif des perméabilités à l'échelle mégascopique, représentant le modèle de gisement utilisé dans les simulations d'écoulement. Dans cette dernière étape, les résultats publiés tirés de la solution des équations d'écoulement en ce qui concerne les milieux poreux statistiquement anisotropes au moyen de la théorie du continum stochastique, sont généralisés pour des blocs finis et utilisés en même temps que les caractéristiques statistiques des perméabilités par point obtenus par simulation conditionnelle.

Les techniques dont il est question aux paragraphes précédents ont servi à caractériser numériquement le gisement de Crystal Viking

dans le centre-sud de l'Alberta. Plus précisément, à l'aide de la description géologique qualitative détaillée du gisement, on a d'abord évalué les limites des unités géologiquement homogènes de ce gisement avant d'en simuler deux réalisations conditionnelles. À l'intérieur de ces limites, les propriétés des roches du gisement (porosité, perméabilité, saturation en huile résiduelle et saturation en eau) sont évaluées et simulées conditionnellement à l'aide des structures de corrélation de chaque variable par unité géologique du gisement. C'est ainsi que le gisement de Crystal Viking est entièrement caractérisé. Les modèles numériques obtenus serviront aux simulations d'écoulement dans d'autres études.

Bien que les techniques géostatistiques présentent d'importants avantages, elles sont difficiles sur le plan théorique et opérationel. Par ailleurs, l'industrie du pétrole ne dispose pas toujours du savoir-faire nécessaire. On propose donc une approche pour le transfert des connaissances impliquées. Cette approche revêt la forme d'une nouvelle théorie appelée "la théorie de la géostatistique artificiellement intelligente". Cette théorie est basée sur le point de vue que le géostatisticien est un processeur de symboles représentant tous les aspects des connaissances dans le domaine. La théorie proposée a des avantages opérationnels indéniables; un système informatique peut lui être intégré pour reproduire les activités du géostatisticien. D'après la théorie proposée, on présente un petit système appelé BOU-1. Ce système calcule des variogrammes expérimentaux et malgré sa simplicité, on constate

qu'il est compatible avec un géostatisticien. En outre, le BOU-1 possède toutes les propriétés que commande la théorie proposée; c'est en effet à tous égards un processeur de symboles représentant les connaissances géostatistiques. La théorie proposée et les expériences qui s'y rattachent suggèrent que l'édification d'un système expert autorisant la caractérisation géostatistique des gisements est une entreprise parfaitement réalisable.

ABSTRACT

The drastic fall of oil prices during the last years, together with the gradual reduction of exploration prospects, has imposed a strategic shift of the Petroleum Industry towards the enhanced exploitation of known reservoirs. Enhanced productivity, however, requires a better understanding and the proper utilization of the natural characteristics of a reservoir, i.e. advanced reservoir characterization. Reservoir characterization incorporates two sequentially interrelated aspects: (i) the geological-qualitative, providing the understanding of a petroleum reservoir as a natural phenomenon; and (ii) the quantitative-numerical, providing the "equivalent" numerical representation of the reservoir in the form of a grid to be used in reservoir flow simulation studies.

Significant advances have been made to date in improving the qualitative aspect of reservoir characterization; however, the same is not true for the numerical aspect. In addition, advances in other areas related to reservoir simulation, such as sophisticated fluid transport formulations, elaborate numerical methods, super-computers, etc. have further emphasized the need to improve-upgrade reliability, certainty, and level of detail in quantitative-numerical reservoir characterization. To contribute in upgrading numerical reservoir description, this study presents and develops elaborated geostatistical methods within the framework of the theory of Intrinsic Random Functions

of order k (IRF-k). Geostatistical techniques have properties of particular interest and importance to reservoir characterization. They (i) quantify inherent geological reservoir properties such as zonation, continuity, trends and anisotropies; (ii) provide, directly from the scale of core and log data to the scale of the reservoir block model, unbiased estimates of reservoir-rock properties to be used as geological input to reservoir flow simulation studies; and (iii) generate conditionally simulated representations of pertinent variables reproducing the **in-situ** variation of rock properties to be used to check the sensitivity of flow simulation results to geological input.

Particular emphasis is given to the development and presentation of a comprehensive step-by-step technique for the conditional simulation of IRF-k. The latter is a stochastic method that generates realizations of non-stationary phenomena (such as rock properties of petroleum reservoirs, in many cases), reproducing their generalized covariance and honoring the available data at sampled locations. The technique proposed requires the following steps: (i) on line simulation of Wiener-Levy processes and of their integrations; (ii) use of the turning bands method to generate realizations in R^n; (iii) conditioning to the available data; and (iv) verification of the reproduced generalized covariance using generalized variograms.

The estimation of the effective permeability tensor is a well known problem in reservoir characterization. Several attempts have been

made to tackle the problem; however, none introduced a general definitive solution. A new approach is proposed here, within a stochsatic framework and in the form of a two step process. The first step of this process includes the conditional simulation of scalar point permeabilities on a dense grid representing the hydrocarbon reservoir at the macroscopic scale. Conditionally simulated realizations of point permeability at the latter scale reproduce the histogram and variogram function of the available data as well as measurements at sampled locations. The next step includes the simultaneous reconstruction of the components of the effective permeability tensor at the megascopic scale, representing the reservoir block model as used in flow simulations. In the latter step, published results derived from the solution of flow equations for statistically anisotropic porous media using the stochastic continuum theory are generalized for finite blocks and utilized together with statistical characteristics of the conditionally simulated point permeabilities.

The techniques discussed in the previous paragraphs are used to numerically characterize the Crystal Viking field in south-central Alberta. More specifically, using the detailed geological-qualitative description of the field, the boundaries of the geologically homogeneous zones of the Crystal reservoir are first estimated and then two realizations are conditionally simulated. Within the boundaries of the units, the reservoir rock properties: porosity, permeability, residual oil saturation and water saturation, are estimated and conditionally

simulated using the correlation structures of each variable per geological unit of the reservoir. Thus, the Crystal Viking reservoir is completely characterized. The numerical models produced will be used as input to flow simulations in future studies.

Although geostatistical techniques have significant advantages, they are theoretically and operationally difficult. Furthermore, the required know-how is not yet widely available in the Petroleum Industry. A perspective is therefore suggested for the transfer of the knowledge involved, and is in the form of a new theory termed "theory of Artificially Intelligent Geostatistics". The theory is based on the view that the Geostatistician is a processor of symbols representing all aspects of this knowledge in the domain. The proposed theory has significant operational advantages; that is, a computer system can be built to reproduce the activities of a Geostatistician. Based on the proposed theory, a small system named BOU-1 is presented. The system undertakes the task of calculating experimental variograms and, although simple, it is shown to be compatible with a geostatistician. In addition, BOU-1 has all properties that the proposed theory called for; it is in all its basic aspects a processor of symbols representing geostatistical knowledge. The proposed theory and relevant experimentation suggest that future building of an Expert System for geostatistical reservoir characterization is indeed a feasible perspective.

ACKNOWLEDGEMENTS

I would like to thank all those who directly and indirectly helped me to carry out this study. In particular, I am grateful to Michel David for his guidance, encouragment and unconditional support in every aspect of my presence at Ecole Polytechnique. He has been the fundamental force behind both my scientific pursues and the accomplishment of this thesis. I am most thankful to Michel Soulié, who undertook my supervision during the last year of my studies, and provided me with advise, constructive discussions and financial support. Acknowledgments are also in order to Wayne Griffin, who although did not contribute directly to this study, tought me in the past basic geostatistics and, most importantly, how to work.

I am also thankful to the Institute of Sedimentary and Petroleum Geology, Calgary, and the Department of Suplies and Services for financing the major part of this study though the Unsolicited Proposals Program (DSS contract 01SG.23294-6-0842). More specifically, I would like to thank Dr. R. Macqueen, who as the scientific authority on the above contract, has been most helpful, and Dr. A. Foscolos who suggested and encouraged the work on the Crystal Viking field. Many thanks are also in order to Westcoast Petroleum, and particulary John Clark for providing data from Crystal, cooperation, advice and encouragment, as well as to G. Reinson for his help with log correlations. Additional financial support was provided by Ecole Polytechnique in the form of

research expences. For this I am thankful to R. Lévesque and the Dept. de Génie minéral. I would also like to thank Graduate Studies and particulary Dr. Tanguay for removing differencial fees, a financial burden for foreign students.

I wish to also thank A. Desbarats for his most constructive comments and help, particularly on the problem of permeability estimation, G. Christakos for his critical comments on conditional simulations of IRF-k, and P. Montes for his detailed review of this thesis. I am al so thankful to A. De Iure for editorial assistance, and D. Marcotte for his help in the Laboratoire de Géostatistique.

Many thanks are in order to Centre Dévelopment et Technologie of Ecole Polytechnique and particularly to Carol Guérin for efficiently administrating the DSS contract related to any studies as well as taking care of most of the production of this manuscript. Thanks are also in order to Danielle Therrien and Hélène Lalumière for the final preparation of this thesis; the secretaries of Génie minéral and particularly to Lucie Corbeil, have been most helpfull during my presence at Polytechnique.

Finally, I wish to thank my parents for their encouragment in my endeavors and pursues, and my friends Desolina, Vaso, Aphrodite, Prokopis, Dimitri and Alan who made life easier during the times of distress and anxiety.

TABLE OF CONTENTS

TABLE OF CONTENTS (Cont'd)

TABLE OF CONTENTS (Cont'd)

TABLE OF CONTENTS (Cont'd)

TABLE OF CONTENTS (Cont'd)

LIST OF FIGURES

LIST OF FIGURES (cont'd)

LIST OF FIGURES (cont'd)

LIST OF FIGURES (cont'd)

LIST OF FIGURES (cont'd)

LIST OF FIGURES (cont'd)

LIST OF FIGURES (cont'd)

LIST OF FIGURES (cont'd)

LIST OF FIGURES (cont'd)

LIST OF FIGURES (cont'd)

LIST OF FIGURES (cont'd)

LIST OF FIGURES (cont'd)

LIST OF FIGURES (cont'd)

LIST OF FIGURES (cont'd)

LIST OF TABLES

1. GENERAL INTRODUCTION

The continuous stochastic process approach to the estimation and/or simulation of space dependant data in Geosciences, termed Geostatistics, was introduced long time ago (Matheron, 1965), and today has developed into a collection of techniques used worldwide by the Mining Industry. In the Petroleum Industry, however, Geostatistics has, to date, found very limited use. This must be attributed to the fact that little has been done in adapting and developing the techniques to the peculiarities of oil exploration and development, and that geostatistical theory is still considered as mathematically obscure and operationally difficult.

During the last years, due to both economic hardship as well as a reduction of the possible new large oilfield discoveries, the Petroleum Industry has been directed towards a more efficient exploitation of known reservoirs using enhanced recovery techniques. Enhanced productivity, however, requires a better understanding and description of the natural characteristics of reservoirs, upon which better recovery processes can be designed, tested and implemented. The forecasting of the behavior of reservoirs under given recovery techniques is performed through reservoir flow simulation studies. The numerical description of the reservoir in a form of a grid (matrix of numbers) constitutes a

large part of the input to the flow simulator. The reliability and accuracy of the numerical description of the reservoir are crucial to the results of the simulation and depend upon the methodology as well as techniques used for the inference of the numerical models or reservoir properties.

It is the aim of this study to present the generalized theory of linear geostatistics termed "intrinsic random functions of order-k" or IRF-k (Matheron, 1973; Chiles, 1977) for reservoir characterization, develop a comprehensive step by step technique for the conditional simulation of IRF-k in three-dimensions, and furthermore, develop the methodology required in modeling characteristics of petroleum reservoirs as well as to suggest how the properties of these models should be used.

The IRF-k theory represents the generalized linear geostatistical theory as it relaxes the major assumption commonly made about the phenomenon to be modelled, namely stationarity. In simple terms, stationarity implies that first and second order moments are invariant under translation in space. This, however, is not necessarily true, particularily in the presence of distinct trends (drifts), as is very common is sedimentary deposits (Rendu and David, 1977) such as oil deposits (Delfiner **et al.**, 1983). It is easy to show that stationarity depends on the scale of examination of a phenomenon. In addition the stationary case is a simple derivation of the IRF-k theory.

Historically, the first attempt to remove the stationarity assumption is found in "Universal Kriging" (Matheron, 1969). Universal Kriging requires the splitting of a phenomenon into a stationary random component and a drift of a polynomial form. This dichotomic approach, however, creates a "vicious circle" (Chauvet and Galli, 1982), as it requires one to estimate one unknown component from another.

Geostatistics provides two different techniques and consequently models, namely, unbiased minimum estimation variance (estimated mean or kriged) and conditionally simulated model. The latter is a combination of kriged values and simulated correlated variates. Conditionally simulated models faithfully mimic the spatial variability of the phenomenon under study and can be used as possible representations of the real fluctuation of the phenomenon, thus providing planners and operators with "what if" tools. Conditional simulation of IRF-k is seen as the most generalized form of linear geostatistics and, in this sense, it is used in the title of this study.

The key to the application of geostatistics for modelling characteristics of oil deposits is the sequence of methodological steps to be followed, so that transformation of geological realities into mathematical abstraction is possible. It has been shown (Dimitrakopoulos, 1985) that such a transformation is valid only if an oil deposit is divided into different geologically homogeneous domains and each domain is treated separately. Geologically, homogeneous domains are

represented by the different sedimentary facies and depositional environments of the deposit. However, one should keep in mind that such a methodological approach introduces to the final numerical model the subjectivity of a geological interpretation.

IRF-k represents a generalized mathematical theory. However, it should be clear from previous statements that the knowledge of the theory itself is not a sufficient condition for an operator to carry out a successful application. In addition to the theoretical background, methodological and empirical knowledge are needed.

The geostatistical knowledge and expertise required for applications are not generally available in the Petroleum Industry. A perspective for the transfer of geostatistical knowledge is therefore seen as part of the aim of this study. Expert systems, i.e. computer programs with knowledge in a given domain, are suggested as the perspective for the required knowledge transfer. A geostatistical theory upon which such systems may be built has been developed and termed "theory of artificially intelligent geostatistics". Accordingly, the geostatistician is seen as a processor of geostatistical symbols representing his knowledge in the domain. The theory introduces developments in the field of artifical intelligence to the geostatistical world. The major dynamic consequence of such an introduction is that geostatistical procedures can be advanced to the extent that a system can be designed and implemented to carry out complete geostatistical studies using a

very simple input. Then, the operator of such a system will not be required to have any particular knowledge of geostatistical theory or experience in the domain. Another important characteristic of such a system is that it will be able to reason about its decisions and actions during the operation.

1.1 Previous Work

Applications of the IRF-k theory in the Petroleum Industry are limited and mostly related to IRF-0 (stationary phenomena). In the relevant literature, one may distinguish studies related to (i) oil exploration and (ii) oil reservoir characterization, evaluation, and development.

Haas and Jousselin (1975) as well as Hass and Viallix (1976) use data from geophysical surveys such as arrival time and seismic velocity to map geological horizons and estimate boundaries of oil impregnated layers. Seismic data are also used by Olea and Davis (1977) to map geological formations in the Magellan Basin, South America. Maps are produced using universal kriging and maps of "residuals" are used to detect locations of possible hydrocarbon accumulations. David **et al.** (1986) use the IRF-k theory and seismic information to map a part of the continental slope off the east coast of the U.S. They also extensively discuss manipulation of large data sets in the form of seismic lines. Dowd (1984) constructs geological models of a major oil

bearing formation of a large area in the North Sea from well data by conditionally co-simulating two variables. These variables are the total thickness of the formation and the ratio of the thickness of each of the four units of the formation to the total thickness. Different co-realizations can then be used to interpret the possible geological features of the area.

Specialized geostatistical techniques (Chiles, 1976) have also been used. The first, termed "external drift", combines the use of "accurate" data from wells with "inaccurate" data from seismic surveys. The second integrates well measurements of elevations with dip information, for example, from dipmeter logs. Some examples of both techniques applied in the mapping of geological horizons are given by Delfiner **et al.** (1983).

More recent geostatistical theoretical developments include techniques which allow mapping of surfaces from seismic data in the presence of faults (Marechal, 1984) and techniques allowing the use of data in the form of inequality constraints. The latter techniques has been developed either as a combination of kriging and quadratic minimization (Dubrule and Kostov, 1986), or in terms of a Bayesian-type formalism termed "soft kriging" (Kostov and Journel, 1985). Bayesian kriging has also been used to estimate surfaces using data from both seismic surveys and exploratory wells (Omre, **et al.**, 1988). Factorial kriging (Galli **et al.**, 1984), a combination of spectral methods with

kriging, has also been used in detecting geochemical anomalies, which may suggest the existence of oil accumulations (Galli, 1985; personal communication).

With the exception of factorial kriging, the specialized geostatistical techniques described in the previous paragraph can, in addition to their use in oil exploration, find very significant applications in oil-reservoir characterization. This becomes apparent considering the lack of large number of wells in most oil deposits and the "fuzzy" nature of certain phenomena such as the oil-water contact (Kostov and Dubrule, 1986), etc.

Haas and Mollier (1974) as well as Haas and Jousselin (1975) present case studies where reservoir parameters such as porosity and reservoir boundaries are kriged and then a volumetric calculation of the oil in place is derived. Delfiner and Chiles (1977) use conditional simulation of IRF-1 to provide different realizations of the top of a dome shaped reservoir. These models are then used to derive a probabilistic estimate of hydrocarbons in place. The use of geostatistical techniques to derive reserve estimates of hydrocarbon accumulations is discussed and compared to traditional methods by Jones (1984).

Delfiner **et al.** (1983) provide some examples of two-dimensional mapping of reservoir characteristics such as depth to the top of the reservoir, thickness, porosity and water saturation. Helwick and

Luster (1984) construct two-dimensional co-realizations of porosity and permeability to derive permeability estimates which are then used for fluid-flow simulation. Simulated fields representing sand-shale sequences with given variograms are used by Desbarats (1987a, b) as the basis for numerical estimation of effective (block) permeability. Deutsch (1986) uses a technique termed "power averaging", based on Desbarats work and an empirical formulae for two component materials suggested by Korvin (1982).

Geostatistical techniques have also been used in non-conventional oil deposits. Dimitrakopoulos (1985) estimates and conditionally simulates the oil content and boundaries of oil saturated geologically homogeneous zones in the Athabasca tar sands, Alberta. Dowd and Royle (1977) as well as Zwicky (1977) present variograms of percent weight oil from the same deposit. Examples of mapping the oil content of oil shales using IRF-k is given by Davis and David (1978).

1.2 Philosophy and Objectives of this Study

The title of a dissertation is descriptive of its content. It may, in addition, be indicative of an underlying philosophy as is the present case. Developments in science and engineering are viewed as being invoked by reality, interact with it and should produce useable results which can further interact with the real world. The Petroleum Industry represents such a real world, where needs are recognized and

and research is directed to satisfy them. The major recognition here is the need for better numerical reservoir characterization. With the gradual shifting of the Industry towards more efficient exploitation of existing reservoirs, it has been widely recognized (Lake and Carroll, 1986) that quantitative description of reservoir-rock variables must be improved to provide more accurate and reliable numerical equivalents of reservoirs.

Stochastic methods in the form of geostatistics are chosen for numerical-quantitative reservoir characterization. This choice is not accidental; rather it relates to the understanding of hydrocarbon reservoirs as natural geological phenomena. The formation of an oil deposit is a combination of independant physical processes in time and space. These processes include burial of organic rich sediments, maturation of organic matter, migration, entrapment and accumulation of migrating hydrocarbons and, in some cases, post-entrapment alterations. As an end result of these processes, it should be apparent that an oil deposit is not a random phenomenon. The configuration and the distribution and fluctuation in space of the characteristics of a hydrocarbon accumulation depend upon the trapping situation and the properties and spatial distribution of the rock bodies which host the hydrocarbons. The properties of the reservoir rock are themselves a result of their depositional setting, post-depositional diagenetic alterations and structural deformation. As a result, the characteristics of a reservoir and their spatial distribution and variability are not random, certainly

not on a macro-scale. To recognize oil reservoirs as a non random natural phenomenon entails to the search for methods and techniques which can indeed quantify inherent geological reservoir properties such as zonation, continuity, trends and anisotropies. This is precisely what geostatistical methods uniquely provide.

It was stated earlier, that the present study also aims to provide a perspective for geostatistical knowledge and expertise transfer to the Petroleum Industry. This is a further recognition of reality. To recall a philosophical term used by the fathers of artificial intelligence, we live and function in a certain "Zeitgeist", that is the milieu of our times with its technological trends and advances. Both the availability of technology and need for knowledge transfer are real and this should be recognized particularly in applied sciences. Consequently, to case efforts after the identification of a problem, and the development of proper methodology and solutions, would be incomplete without considering who, how, when and what the end users need. It would, furthermore, be incompatible with the claim that realities should be or are recognized.

The specific objectives of this study are as follows:

i) The examination of the nature of reservoir-rock variables such as porosity, permeability, water and residual oil saturations, the

review of the basic aspects of the IRF-k theory and the outline of the advantages of the theory with respect to reservoir characterization.

ii) The development of a comprehensive step by step technique for the conditional simulation of IRF-k including the non-conditional simulation.

iii) The development of a simple, workable approximation for the reconstruction of the effective block permeability tensor. This is meant to be examined within the limits of this study and in the sense of improving current Industry practices.

iv) The complete and detailed numerical-quantitative characterization of all pertinent variables of the Crystal Viking reservoir in south-central Alberta.

v) The provision of an expert system perspective for the transfer of geostatistical knowledge and expertise to the Petroleum Industry by developping a theory upon which the perspective can be materialized in the future.

Each of the above objectives is tackled and developed separately in the following chapters.

2. GEOSTATISTICAL MODELING OF RESERVOIR-ROCK PROPERTIES

2.1 Introduction

The actual performance of a reservoir during production is predicted from reservoir simulation studies. A controlling factor in the quality of predictions is the numerical description of reservoir-rock properties such as porosity, permeability and fluid saturations (Coats, 1982; Aziz and Settari, 1979; Haldorsen; 1983). Furthermore, while the sophistication of fluid transport formulations, numerical methods and numerical models continues to increase, quantitative geological modelling remains significantly less advanced. As a result, prediction problems arise from unreliable reservoir description (Haldorsen, 1986). For these reasons, it has already been suggested (Haldorsen, 1986, 1983) that more emphasis be given to increasing the sophistication and reliability of quantitative reservoir characterization.

During the last few years, attempts at reservoir description (Lake and Carroll, 1986) have had two major aspects. The first is qualitative-geological and the second quantitative-numerical. Although attention was given and progress has been made in the former (Krause **et al.**, 1987; Reinson **et al.**, 1988), there is much room for

improvement in the latter, so that qualitative information provided by the first aspect can be translated into a usable reservoir model.

The present study is a natural step in the continuing effort to improve geological reservoir description. It attempts to provide basic elements of a generalized stochastic framework (Gel'fand and Vilenkin, 1964; Matheron, 1973) which will allow an effective transformation of geological descriptions to computer processable numerical equivalents. The reasons that stochastic models, as opposed to deterministic, are chosen are due to: (i) Geological variables exhibit a locally random behavior (Fig. 2.1), but on average there is a structural aspect in spatial variability (correlation structure) which is expressed with the similarity of neighboring values (Fig. 2.2). The stochastic approach (ii) enables the estimation of large volumes from core samples using best (optimal) estimators; (iii) provides a measurement of uncertainty in the above estimation; and (iv) allows the generation (simulation) of fields of values which 'look like' reality in terms of their variation pattern. The stochastic framework in modelling geological variables was originally introduced in the mining industry (Matheron, 1965; David, 1977; Journel and Huijbregts, 1978) and found extensive use in ground water hydrology (Delhomne, 1979; Neuman, 1982). In reservoir engineering, few authors have attempted to use stochastic methods for parameter estimation (Hewett, 1986; Da Costa e Silva, 1985) or simulation (Dimitrakopoulos, 1985; Desbarats, 1987, 1987b, 1988) using restricting (stationary) assumptions.

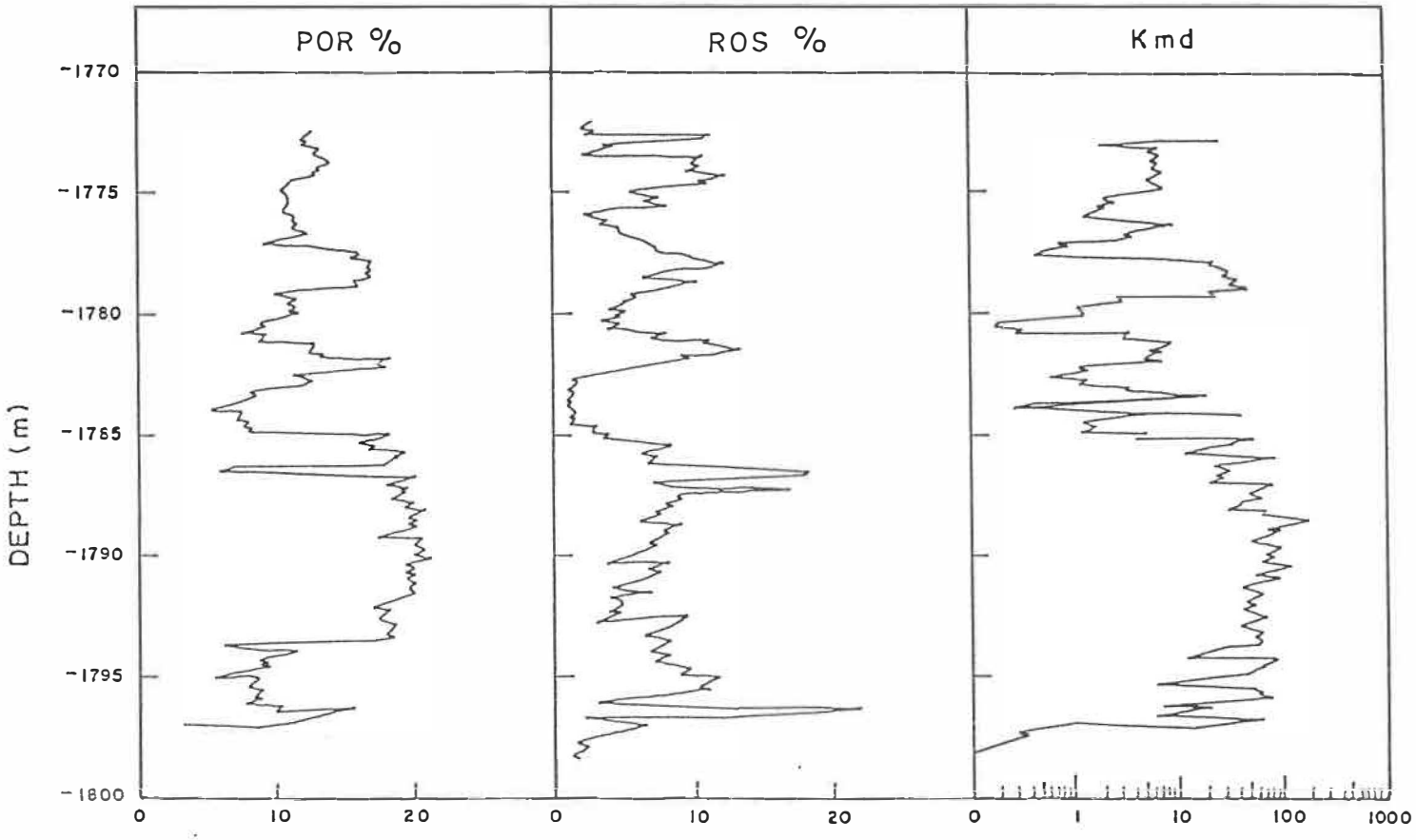

FIGURE 2.1: Profiles of porosity (POR), residual oil saturation (ROS) and permeability showing random components of spatial variation.

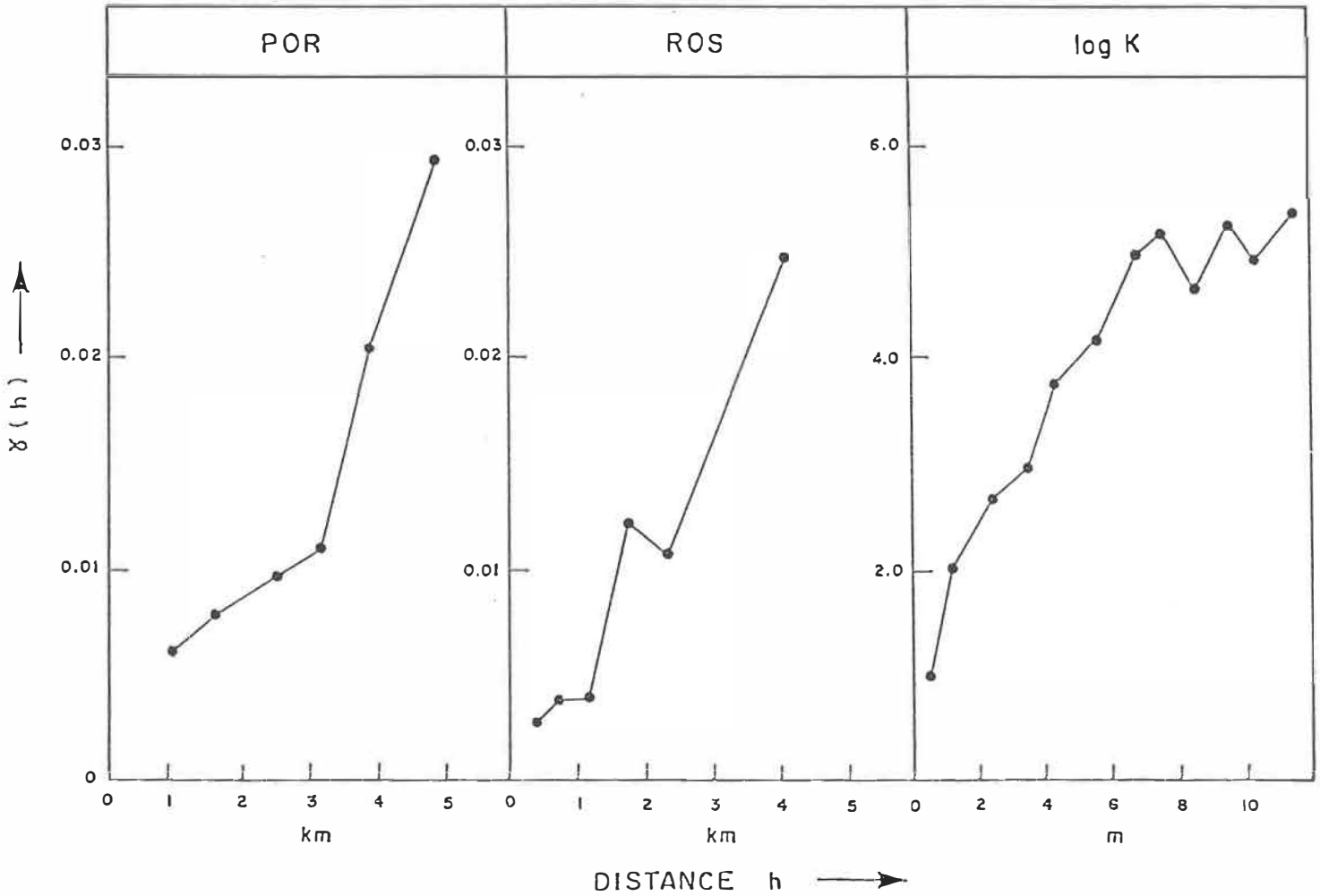

FIGURE 2.2: Experimental variograms of porosity (POR), residual oil saturation (ROS) and permeability (k) showing the correlation structures of the respective variables.

2.2 Stochastic Conception of Porous Media and the Problem of Changing Scales

The consideration of fluid flow through a porous medium introduces the concept of continuum, which implies a statistical averaging of properties over the volume of the medium within which the flow occurs. In addition, it implies that flow appears within volumes larger than a representative elementary volume (Bear, 1968), i.e. at least larger than a single pore and in fact larger than a sufficient number of pores to permit statistical averaging of properties (Fig. 2.3). Note that different views on this formulation have also been expressed (Baveye and Sposito, 1984).

The dependance of the flow equation formulation on statistical averaging over some volume introduces the known problem of scale (Bear, 1968; Bear and Braester, 1972). Two conceptual scales associated with porous media will be considered here. Following previously established terminology (Pickens **et al.**, 1977; Haldorsen, 1983), we will consider the macroscopic scale which represents a volume v of about a core plug, and the megascopic representing volume V of the size of grid blocks used in flow simulation studies.

Probabilistic definition of porous media at different scales, was long introduced (Prager, 1961; Matheron 1967; Deffeyes **et al.**, 1985) and follows the idea of a porous medium as an aggregation of

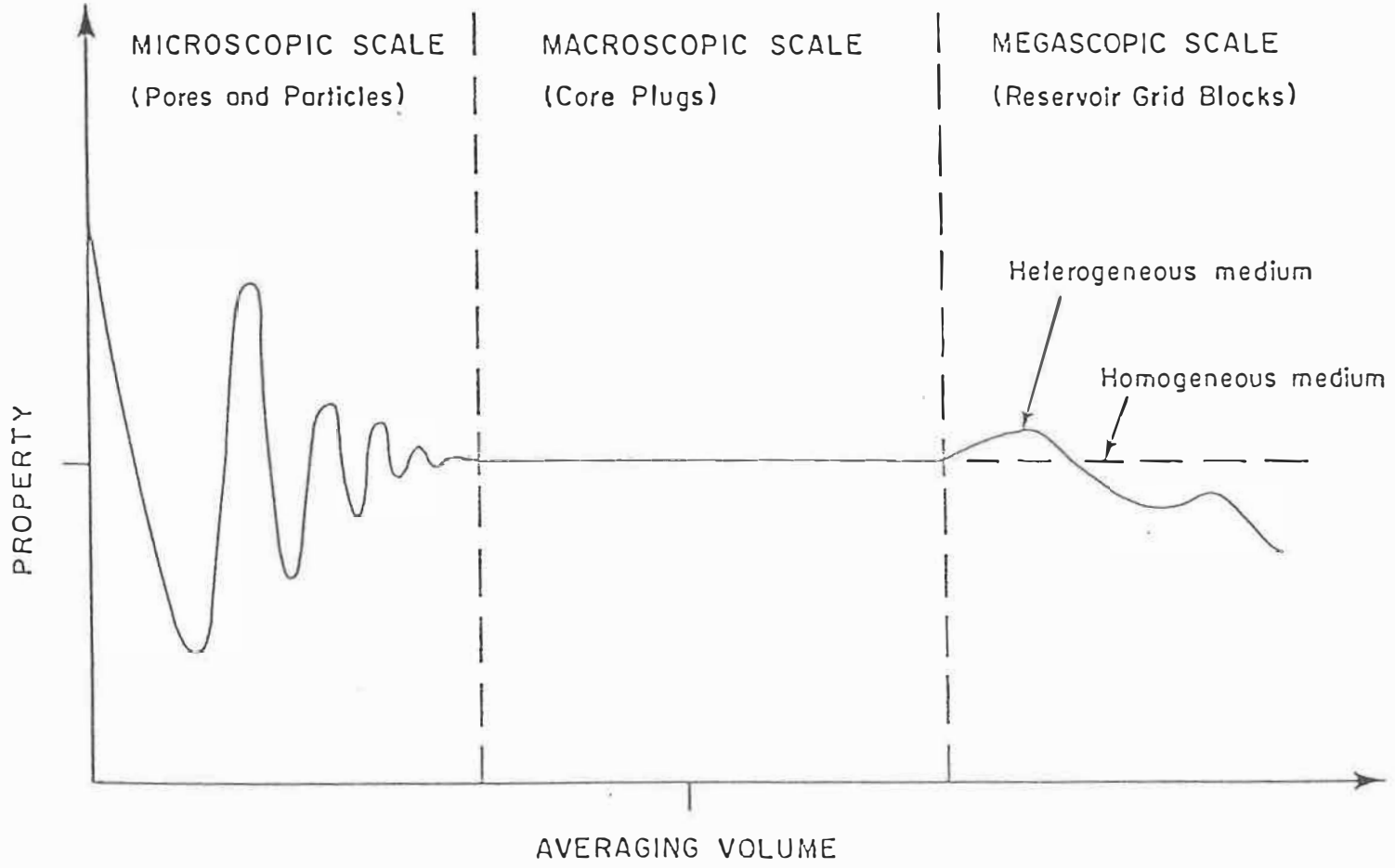

FIGURE 2.3: Property of a porous medium plotted as function of the averaging volume. (Modified after Pickens et al., 1977)

particles and void spaces more or less frequently distributed over the whole. Accordingly, on the microscopic scale we may consider a random function I(x) such that

$$I(x) = \begin{cases} 1 & \forall\ x \in A \\ 0 & \forall\ x\ A \end{cases}$$

where A is a set of space occupied by particles (grains) and $x \in R^3$.

The probability of point x hitting a grain when put randomly in domain $\underline{v}$ of volume v of a porous medium is

$$p_v = \int_{\underline{v}} I(x) \frac{dx}{v}$$

The pore space fraction of volume $\underline{v}$, or porosity, may be defined as $q_v = 1 - E[p_v]$ where E denotes mathematical expectation. Similarly any property Z_v may be defined at the present scale.

On the macroscopic scale, it is reasonable to assume that properties are more or less homogeneous and isotropic. This, however, is not always valid on the megascopic scale (Fig. 2.3). In the latter case and in terms of random functions, a parameter Z_V of a porous medium may be

$$Z_V = \frac{1}{V} \int_V Z(x)\, dx \qquad (2.1)$$

where Z(x) is a point random function representing the macroscopic scale. Note that a volume v on the latter scale is effectively a point compared to the megascopic volume V. In practice, a limited number of measurements of Z(x) at a discrete set of points within domain V are available. Then, the estimation of Z_V may be formulated as a linear weighted average of available values at x_a, a = 1,...,N such that

$$Z_V^* = \sum_{a=1}^{N} \lambda^a Z(x_a)$$

In the following sections, a stochastic methodology on how Z_V can be estimated from available data as well as how different realizations of Z_V can be numerically simulated is presented. Note that Equation (2.1) is not valid for permeability, which is separately discussed in Chapter 4.

2.3 Formulation of Geostatistical Estimation Theory

The generalized theory of the stochastic mathematical formalism for the estimation of characteristics of reservoir-rock properties has been termed the "theory of intrinsic random functions of order k" (or IRF-k) and developed by Matheron (Matheron, 1971, 1973). It represents a particular case of generalized stochastic processes with stationary increments of order k as defined by Gel'fand and Vilenkin (Gel'fand and

Vilenkin, 1964), in combination with Wiener's optimal estimators (Wiener, 1949).

2.3.1 Generalized increments of order k

Let $Z(x)$ be a function in R^n and consider the linear combination $Z(\lambda_m)$ such that

$$Z(\lambda_m) = \sum_{a=1}^{N} \lambda^a Z(x_a) \qquad (2.2)$$

where λ^a are weights and $Z(x_a)$ values of $Z(x)$ at point x_a.

$Z(\lambda_m)$ is by definition a generalized increment of order k (GI-k) if and only if the weights λ^a and points x_a have the property

$$\sum_{a=1}^{N} \lambda^a f^l(x_a) = 0, \quad l = 1,\ldots,(n+k)!/n!k! \qquad (2.3)$$

where $f^l(x)$ are monomials of degree k of the coordinates x, N the number of sample points, and n the dimensions in space. If $Z(x)$ has a polynomial component (trend), it will not contribute to the increment and thus the $k^{th}+1$ order increment $Z(\lambda_m)$ filters out polynomials of degree k.

As an example, it follows from Equation (2.3) that in order for $Z(\lambda m)$ to be a GI-k with k = 0,1,2 in R^3 of $Z(x)$, the weights λ^a must be as follows

for k = 0: $\sum_{a=1}^{N} \lambda^a = 0$

k = 1: $\sum_{a=1}^{N} \lambda^a = 0, \quad \sum_{a=1}^{N} \lambda^a x_a = 0, \quad \sum_{a=1}^{N} \lambda^a y_a = 0, \quad \sum_{a=1}^{N} \lambda^a z_a = 0$

k = 2: $\sum_{a=1}^{N} \lambda^a = 0, \quad \sum_{a=1}^{N} \lambda^a x_a = 0, \quad \sum_{a=1}^{N} \lambda^a y_a = 0, \quad \sum_{a=1}^{N} \lambda^a z_a = 0,$

$$\sum_{a=1}^{N} \lambda^a x_a y_a = 0, \quad \sum_{a=1}^{N} \lambda^a x_a z_a = 0, \quad \sum_{a=1}^{N} \lambda^a y_a z_a = 0,$$

$$\sum_{a=1}^{N} \lambda^a x_a^2 = 0, \quad \sum_{a=1}^{N} \lambda^a y_a^2 = 0, \quad \sum_{a=1}^{N} \lambda^a z_a^2 = 0.$$

2.3.2 Intrinsic random functions of order k

An intrinsic random function of order k (IRF-k) is a random function whose k^{th}-increments are weakly stationary. More specifically, if Z(x) is an IRF-k in R^n, the GI-k $Z(\lambda_m)$ such that

$$Z(\lambda m) = \sum_{a=1}^{N} \lambda^a Z(x_a + x) \qquad (2.4)$$

has a mean and variance independant of x.

It has been shown (Matheron, 1973) that if we replace Z(x) with any combinations {Y(x) + m(x)} where Y(x) is a random function such as

$$E[Y(x)] = 0$$

and m(x) a random function such that

$$E[Z(x)] = m(x) = \sum_{l=1}^{(n+k)!/n!k!_l} A_l f^l(x) \qquad (2.5)$$

where A_l are random coefficients and f^l known functions, the GI-k $Z(\lambda_m)$ remains the same. Then an IRF-k can be seen as an equivalent to a class of functions with random polynomial components up to order k.

It follows from above that the first order moment of an IRF-k is

$$E[Z(\lambda_m)] = 0 \qquad (2.6)$$

and the second order moment is

$$Var[Z(\lambda_m)] = E[Z(\lambda_m)]^2 = \sum_{a=1}^{N} \sum_{b=1}^{N} \lambda^a \lambda^b K(x_a - x_b) \qquad (2.7)$$

where K(h) is a covariance function representing a class of equivalent functions termed generalized covariance (GC). A GC is a characteristic function for a class of random functions and it is defined up to an even polynomial of degree ≤ 2k. It is the covariance of an IRF-k.

The models of GC-k used in practice and the associated monomials in R^3 of the GI-k of Equation (2.3) are as follows

for k = 0 (stationary case)

$$K(h) = c\delta + a_o |h|$$

and

$$f^l(x) = \{1\}$$

for k = 1 (linear drift)

$$K(h) = c\delta + a_o|h| + a_1|h|^3$$

and

$$f^l(x) = \{1,x,y,z\}$$

for k = 2 (quadratic drift)

$$K(h) = c\delta - a_o |h| + a_1 |h|^3 - a_2 |h|^5$$

and

$$f^l(x) = \{1,x,y,z,xz,yz,xy,x^2,y^2,z^2\}$$

c is a positive constant and δ a Dirac δ-function. $c\delta$ represents possible random variation and is termed nugget effect. Coefficients of the above GC's satisfy the constraints

$$a_0, a_2 \geq 0 \text{ and } a_1 \geq -2 \sqrt{\frac{5}{3}\frac{n+3}{n+1}} a_0 a_2 \text{ in } R^n.$$

The inference of a GC-k in terms of the order k and the coefficients a_k, may be formulated as a minimization problem (Davis and David, 1978), least-square regression (Delfiner, 1975), quadratic, maximum likelihood or minimum norm estimation (Kitanidis, 1983).

2.3.3 Estimation using the IRF-k model

Let $z(x_a)$ with a = 1,...,N be a set of values from one realization of an IRF-k Z(x) at x_a in R^n. The average value of $z_V(x_o)$ over

domain V centered at point x_o of the same realization is estimated by a linear weighted average of the available values as

$$z_V^*(x_o) = \sum_{a=1}^{N} \lambda^a z(x_a)$$

or in terms of IRF-k

$$Z_V^*(x_o) = \sum_{a=1}^{N} \lambda^a Z(x_a)$$

For the estimator $Z_V^*(x_o)$ to be unbiased, the following condition must be satisfied

$$E[Z_V^*(x_o) - Z_V(x_o)] = 0$$

which requires

$$\sum_{a=1}^{N} \lambda^a f_v^l(x_a) = f_V^l(x_o) \qquad (2.8)$$

For the estimator $Z_V^*(x_o)$ to be best, the estimation variance σ^2_{IRF} must be minimal under the constraints imposed by Equation (2.8). Then, it is

$$\sigma^2_{IRF} = \text{Var}\,[Z^*_V(x_o) - Z_V(x_o)]$$

$$= \sum_{a=1}^{N}\sum_{b=1}^{N} \lambda^a\lambda^b K(v_a,v_b) - 2\sum_{a=1}^{N}\lambda^a K(v_a,V) + K(V,V)$$

Using the standard Lagrangian technique under the constraints in Equation (2.8) σ^2_{IRF} is minimized if we consider

$$\phi = \sigma^2_{IRF} - 2\sum_{l=1}^{(n+k)!/n!k!}\mu_l\left(\sum_{a=1}^{N}\lambda^a f^l_v(x_a) - f^l_V(x_o)\right)$$

$$\partial\phi/\partial\lambda^a = 0, \quad \forall \quad a = 1,\ldots, \quad N$$

and

$$\partial\phi/\partial\mu_l = 0, \quad \forall \quad l = 1,\ldots, \quad (n+k)!/n!$$

we conclude

$$\sum_{b=1}^{N}\lambda^b K(v_a,v_b) - \sum_{l=1}^{(n+k)!/!k!}\mu_l f^l_{x_a} = K(v_a,V)$$

$$\sum_{a=1}^{N}\lambda^a f^l_v(x_a) = f^l_v(x_o) \qquad (2.9)$$

where μ_l are Lagrange multipliers, and $K(v_a,V)$ and $K(v_a,v_b)$ the average

GC value between volumes v_a, v_b and V.

From equations (2.9), it can be shown, that the estimation variance σ^2_{IRF} is

$$\sigma^2_{IRF} = K(V,V) + \sum_{l=1}^{(n+k)!/n!k!} \mu_l f^l_v(x_o) - \sum_{a=1}^{N} \lambda^a K(v_a,V) \qquad (2.10)$$

Equations (2.9) represent the system of equations in estimating with the IRF-k model. It is clear that system (2.9) allows the calculation of the weights λ^a so that the estimator $Z^*_V(x_o)$ is unbiased and optimal in the least-square sence. The only requirement for the calculation of $\{\lambda^a, a=1,\ldots,N\}$ is the knowledge of the GC K(h), and the order of the polynomial drift.

2.3.4 The common case of IRF-0

When the order of an IRF is 0, the mean m(x) given in Equation (2.5) becomes a constant

$$E[Z(x)] = m(x) = A^1 f^1(x) = m$$

and Equations (2.9) and (2.10) reduce and may be rewritten respectively as

$$\sum_{b=1}^{N} \lambda^b \gamma(v_a,v_b) + \mu_o = \gamma(v_a,V)$$

$$\sum_{a=1}^{N} \lambda^a = 1 \qquad (2.11)$$

and

$$\sigma^2_{IRF} = \sum_{a=1}^{N} \lambda^a \gamma(v_a,V) + \mu_o - \gamma(v,v) \qquad (2.12)$$

where γ represents the average variogram value among volumes v_a,v_b and V. The variogram function related to the GC when k = 0 by the relation $\gamma(h) = K(0)-K(h)$ is defined as

$$\gamma(h) = \tfrac{1}{2} \text{ var } [Z(x)-Z(x+h)]$$

$$= \frac{1}{2V} \int_{\underline{V}} [Z(x) - Z(x+h)]^2 dx \qquad (2.13)$$

where V is the domain over which variable Z(x) is defined, and h is the distance between two points.

The variogram is a very common tool in stochastic estimation, and unlike ordinary covariances it is always defined. It is estimated from a set of data by

$$\gamma^*(h) = \frac{1}{2N} \sum_{i=1}^{N} [Z(x_i) - Z(x_i+h)]^2 \qquad (2.14)$$

A limited number of functions are admissible variograms (Matheron, 1971; Christakos, 1984) with the most common being the spherical

$$\gamma(h) = C\,[1.5(h/R) - 0.5\,(h/R)^3] \text{ when } h \leq R$$

$$= C \qquad \text{when } h > R \qquad (2.15)$$

where h is distance, R is the range or correlation scale, and C is the sill (Figures 2.4 and 2.5).

2.4 Conditional Simulation Using Generalized Covariances

The stochastic model considers a characteristic of an oil deposit as a realization of a random function, which can be estimated as described in the previous paragraphs. However the estimation, although unbiased and optimal, is a smoothing operation. It is possible to generate different realizations, i.e. numerical models mimicking the spatial variation of the real deposit as well as reproducing the data and their statistical properties.

Conditional simulation of an IRF-k Z(x) in R^3 is the technique which, given realizations (data) of Z(x) at points $\{x_a, a=1,...,N\}$ and the corresponding GC, allows the construction of different realizations of Z(x) with the following two properties: (i) Reproduce the given realizations at $\{x_a, a=1,...,N\}$; (ii) Reproduce the GC of Z(x).

Consider an IRF-k S(x) with the same GC as Z(x). We can write

$$S(x) = S^*(x) + [S(x) - S^*(x)]$$

The conditional simulation of Z(x) $\{x_a, a=1,...,N\}$ and GC K(h) is then defined as

$$Z_{cs}(x) = Z^*(x) + [S(x) - S^*(x)] \qquad (2.16)$$

$Z_{cs}(x)$ will reproduce the data x_a since $Z^*(x_a) = Z(x_a)$ and $S(x_a) = S^*(x_a)$, because kriging estimators are exact interpolators (Matheron, 1971).

Taking the k^{th} increment of $Z_{cs}(x)$ at any point x_b we have

$$\sum_{b=1}^{N} \lambda^b Z_{cs}(x_b) = \sum_{b=1}^{N} \lambda^b Z^*(x_b) + \sum_{b=1}^{N} \lambda^b \, (S(x_b) - S^*(x_b))$$

then it is

$$\text{Var}\left[\sum_{b=1}^{N}\lambda^{b}Z_{cs}(x_b)\right]=\text{Var}\left[\sum_{b=1}^{N}\lambda^{b}Z^{*}(x_b)\right]+\text{Var}\left[\sum_{b=1}^{N}\lambda^{b}(S(x_b)-S^{*}(x_b))\right]$$

which leads to (Delfiner, 1975).

$$\text{Var}\left[\sum_{b=1}^{N}\lambda^{b}\,Z_{cs}(x_b)\right]=\text{Var}\left[\sum_{b=1}^{N}\lambda^{b}\,Z(x_b)\right] \qquad (2.17)$$

The above shows that indeed the $Z_{cs}(x)$ has the same GC as the original $Z(x)$.

In order to produce $Z_{cs}(x)$, realizations of an IRF-k $S(x)$ must be available, as required by Equation (2.16). These realizations are generated in a two step process detailed in Chapter 3. Briefly, the two steps required are (i) the simulation of Wiener-Levy processes on lines, and (ii) the addition of the contribution from each line in two or three dimensional space using the turning bands method (Matheron, 1973).

2.5 Conditional Simulation Using Variograms

Conditional simulation using variograms is extensively discussed elsewere (Journel, 1984). A short outline is given have.

The conditional simulation of $Z(x)$ $\{x_a, a=1,...,N\}$ with $\gamma(h)$ is defined as

$$Z_{cs}(x) = Z^*(x) + [Z_s(x) - Z_s^*(x)] \qquad (2.18)$$

The defined random function $Z_{cs}(x)$ has the following properties: (i) reproduces the variogram mean and variance of $Z(x)$, and (ii) reproduces the available data.

For the conditional simulation $Z_{cs}(x)$ in Equation (2.18) a realization of $Z(x)$ such as $Z_s(x)$ is required. The latter realization is generated by (i) simulating random numbers on lines, (ii) imposing appropriate moving averages, and (iii) using the turning bands method to construct two or three dimensional simulations with a given variogram.

In practice, conditional simulation with a GC or a variogram requires the following steps:

1) simulation of a regular grid of values with the same GC or variogram of the data,
2) estimation of the grid points using the original data,
3) estimation of the grid points using the simulated values at the sample points and the CG or variogram of the data,
4) summation on each grid point of the corresponding values from steps (1) and (2) and subtraction of the value from step (3).

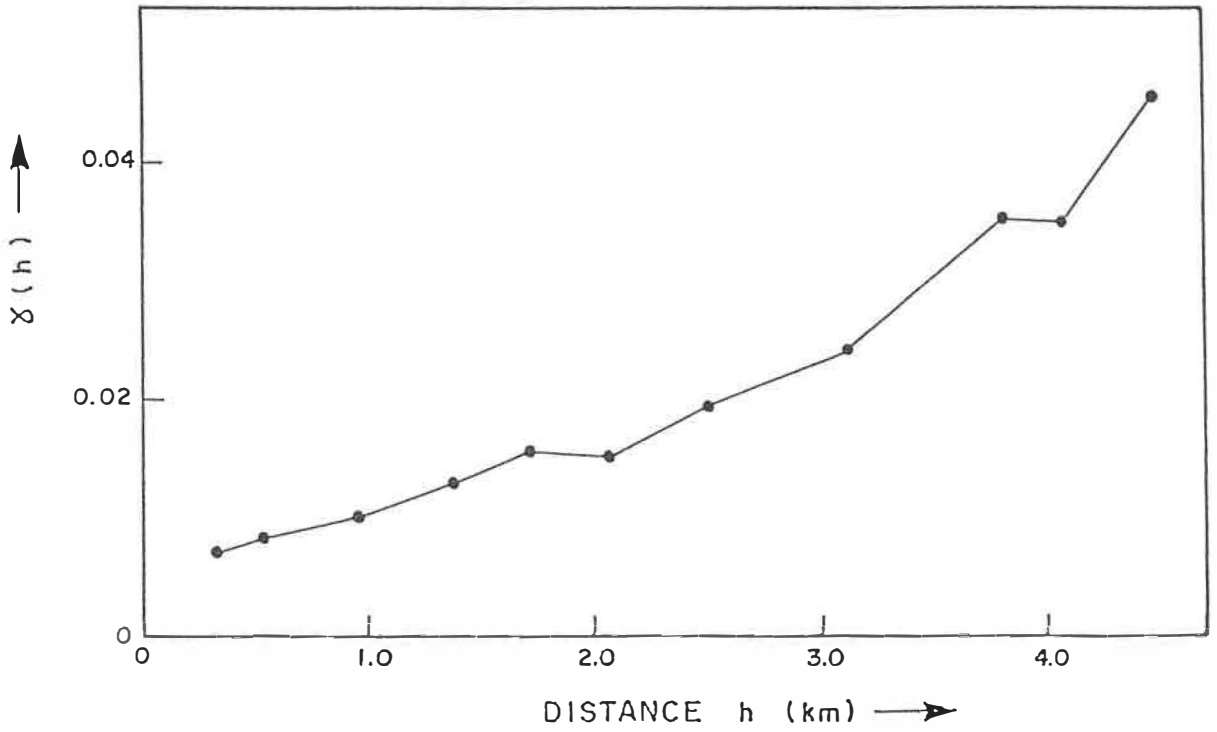

FIGURE 2.4: Experimental variogram of water saturation

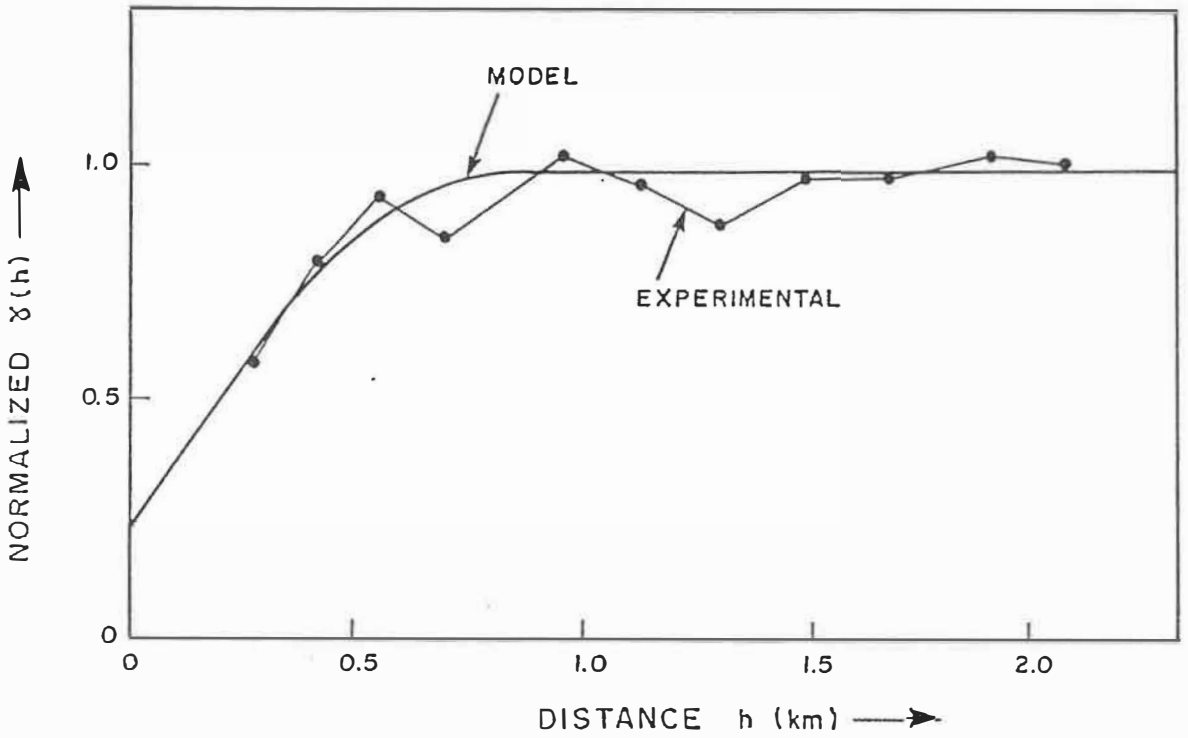

FIGURE 2.5: Experimental variogram of weight percent oil and fitted spherical variogram model.

2.6 Applicational Aspects and Examples

The first step in any application of stochastic models is the evaluation of the correlation structure of the variable under study. Accordingly, the experimental variogram, as defined in Equation (2.14), is calculated and subsequently modeled. An experimental variogram may exhibit two possible general patterns. In the first, the values of the experimental variogram steadily increase with distance as is the case of the variograms of porosity and residual oil saturation in Figure 2.2, and water saturation in Figure 2.4. In the second, the experimental variogram increases first but after some distance, called correlation scale or range or zone of influence, more or less stabilizes about a value, called sill, as in the case of permeability in Figure 2.2 and weight percent oil content in Figure 2.5.

A steadily increasing experimental variogram indicates the existence of trends in the variable under study. This is relatively common in reservoir-rock variables and represents a quantification of geological trends within a reservoir. Mathematically and in terms of random functions, the existence of trends is expressed by Equation (2.5). The IRF-k theory is specifically designed to handle the existence of trends. More precisely, by considering generalized increments of order k, the existing trends are filtered out as expressed by Equation (2.6). The most important intricacy in the presence of trends is the inference of

the generalized covariance. The experimental variograms, are useful in demonstrating the existence of trends.

The inference of the generalized covariance of a set of data is automated, based on several techniques mentioned earlier. The application of one of these techniques provides the admissible generalized covariances for k = 0,1,2, which are the common cases. In addition, statistics which evaluate each model are provided from a standard procedure, which is the re- estimation of known data from surrounding values and the evaluation of estimation errors. For example, given a set of 144 data points which represent depths from the mean sea level to the top of the Crystal Viking reservoir in south-central Alberta, the possible generalized covariance models were found to be $K(h) = 27.41$, $K(h) = -0.026633|h|$, and $K(h) = -0.020327|h| + 0.000867|h|^3$ with k = 1. Of these, the third one was selected as it gave the smallest average error. The inferred generalized covariance was subsequently used for the estimation of the regional top of Crystal reservoir depicted in Figure 2.6. The estimation applied has also produced the associated estimation errors mapped in Figure 2.7. Note that, as is logical, the estimation error increases around the margins of the area where the well control is poor.

An additional example is given in Figure 2.8, a cross-section taken from a three-dimensional estimated model of residual oil saturation (ROS) of the Crystal reservoir. Data from core analyses were used

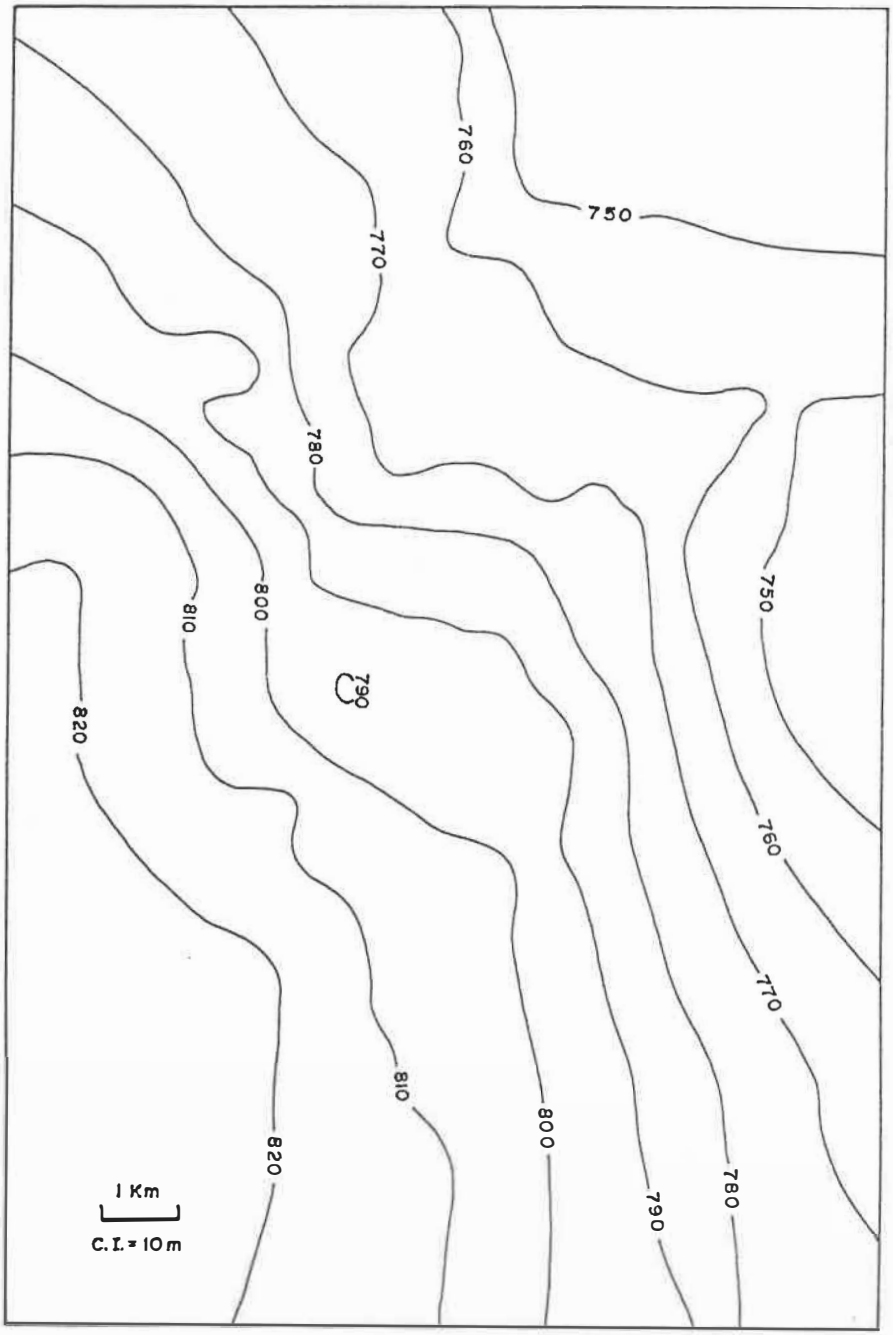

FIGURE 2.6: Estimated structure of the regional top of the Crystal Viking reservoir, Alberta.

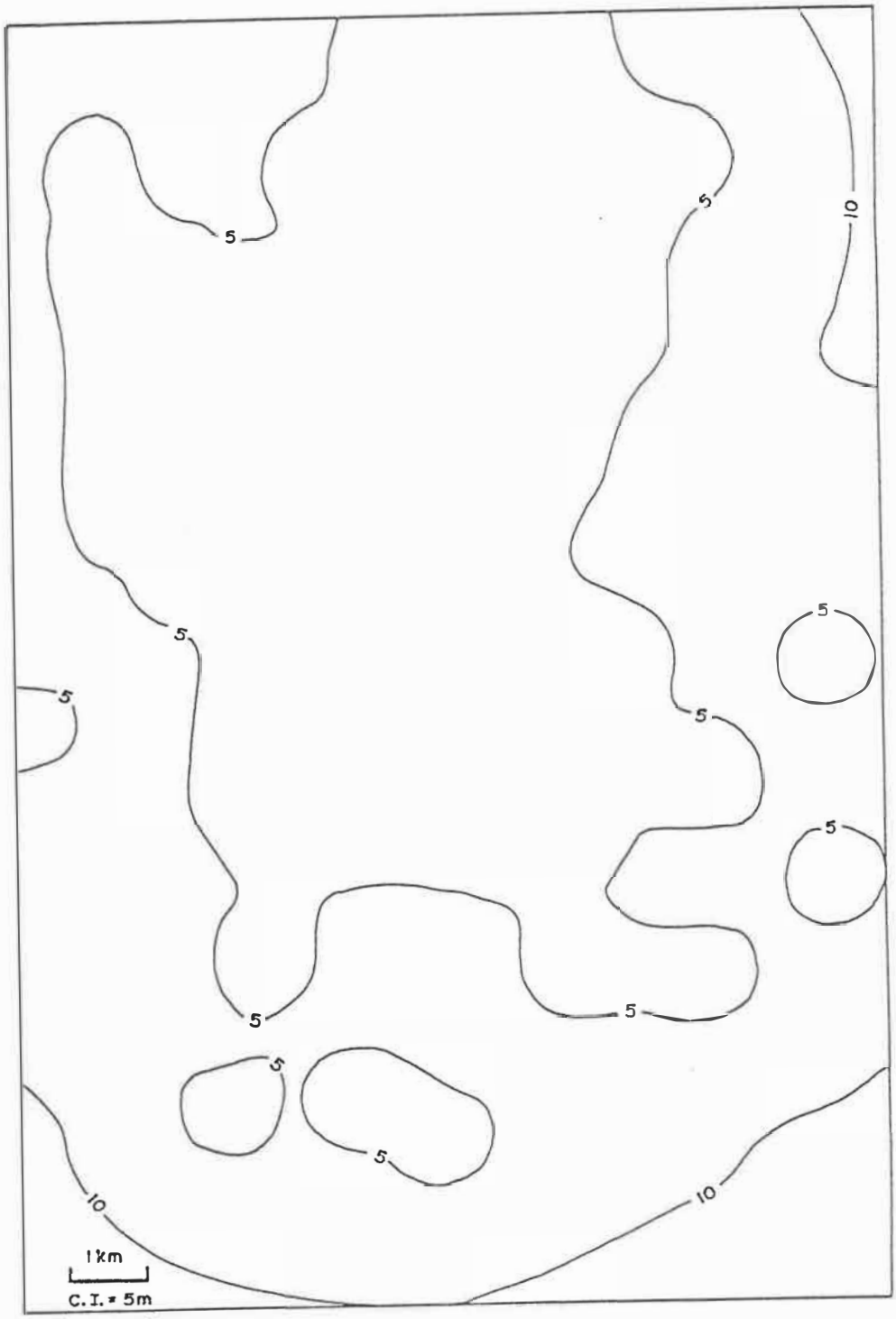

FIGURE 2.7: Map of the estimation error associated with the structure of the top of the Crystal Viking reservoir in Figure 2.6 .

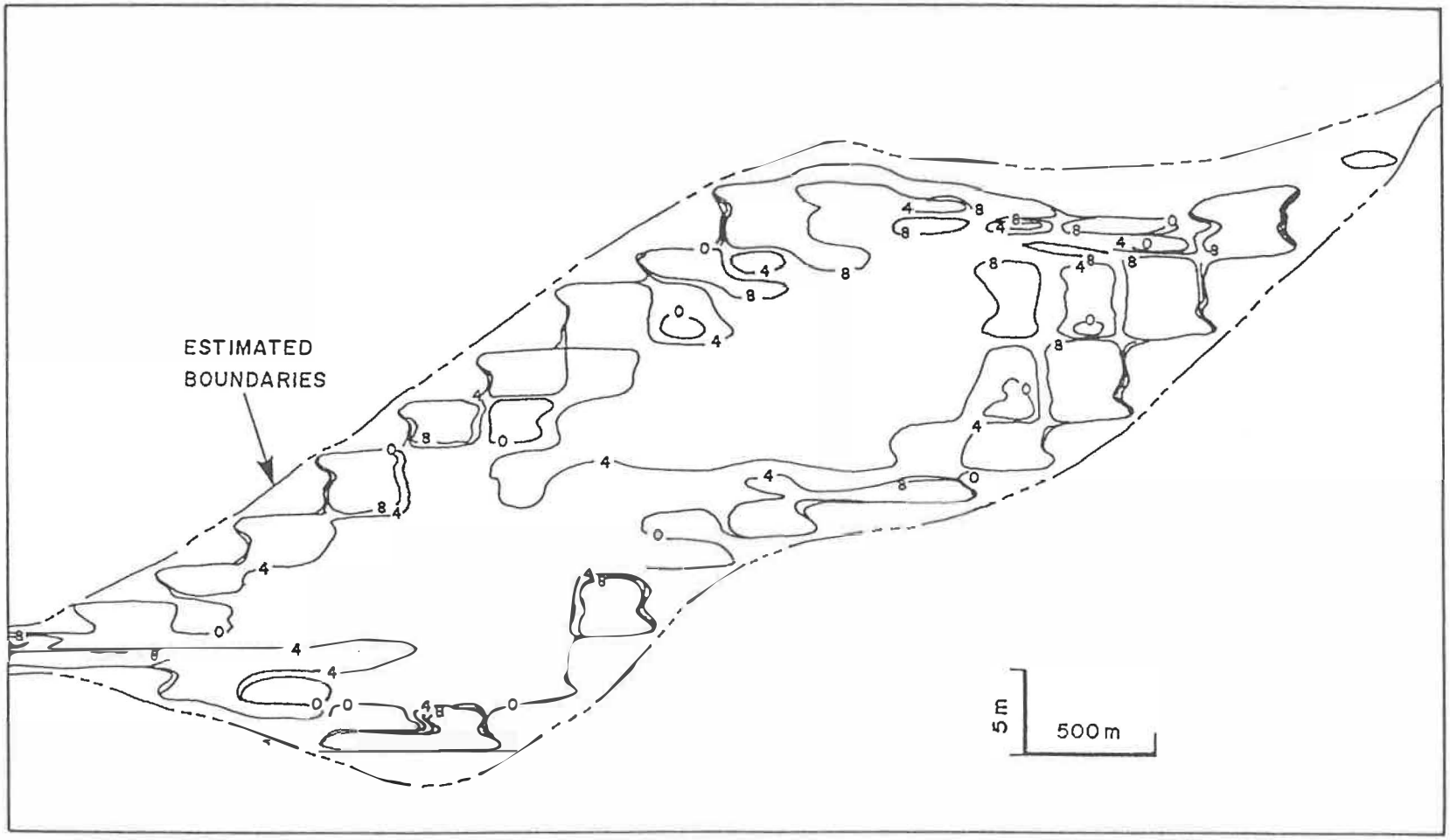

FIGURE 2.8: Cross-section of percent residual oil saturation taken from an estimated 3-D model of the Crystal Viking reservoir, Alberta.

to directly estimate the average value of ROS over grid blocks with a resolution of 300 x 300 x 1 metres.

In the case that the experimental variogram of a data set reaches a sill, then an admissible variogram model is fitted. This is demonstrated in Figure 2.5 where the spherical variogram model below

$$\gamma(h) = 0.25 + 0.75\ [1.5(h/900) - 0.5(h/900)^3] \qquad \forall\ h \leq 900\ m$$

$$\gamma(h) = 1.0 \qquad \forall\ h > 900\ m$$

is fitted to the experimental points. The fitted model may then be used for estimation and error assessment using Equations (2.11) and (2.12). An example is given in Figure 2.9, a cross-section taken from a three-dimensional model of estimated weight percent oil saturation in part of the Athabasca oil sands deposit, Alberta. The depicted model was constructed using different variogram models and data for each of the different horizontal geological zones present. In this way, qualitative characteristics of every zone are incorporated into the model. The associated estimation error is given in Figure 2.10.

The simplified estimation Equations (2.11) and (2.12) are easier to apply than the respective generalized Equations (2.9) and (2.10). This is why they are most commonly used in the Mining Industry. Trends are not uncommon in mineral deposits. In practice, however, estimation

of a grid point or volume proceeds using a restricted number of surrounding data from relatively small distances. Then, it might be possible to ignore the presence of trends and use a variogram model which only fits the first few experimental variogram values, ignoring the restof the actual correlation structure of the phenomenon under study. The use of the generalized or the simplified equations is related to the objectives of modelling. Unlike the mining industry, the Petroleum Industry is more interested in conditionally simulated models than smooth estimated ones. It is important to check the sensitivity of flow simulations to possible realistic variations of the reservoir-rock describing input. This can only be done objectively using conditionally simulated models of the variables. If it is found that these models do not influence the flow simulation, then estimated models of the variable may be used as they represent the average of a very large number of conditionally simulated realizations.

In the practice of conditional simulation, the presence of trends cannot be ignored and bypassed. The only possibility is to use Equation (2.16) which defines the conditional simulation using generalized covariances. Equation (2.18) is only applicable in the case of variograms with a sill.

To demonstrate the differences between estimation and conditional simulation, Figures 2.11 and 2.12 present, somehow differently, the thickness of a pay zone from a part of the Athabasca deposit. In Figure

2.11, thickness is estimated and as such, it represents a smoothed reality. In Figure 2.12, thickness is conditionally simulated and evidently it is a "lookalike" of the real variation.

Examples of three-dimensional conditional simulations are presented in Figures 2.13 and 2.14. The former shows a cross-section of conditionally simulated boundaries and weight percent oil saturation from a pay zone of a part of the surface minable area of the Athabasca oil sands. In this case, Equation (2.18) was used. Figure 2.14 depicts a horizontal section from a three-dimensional conditionally simulated grid of porosity from a unit (H) within the Crystal reservoir. Equation (2.16) was used for the construction of this model. For the conditional simulations, the available data were mainly from core analysis. In addition, measurements from porosity logs were used in some wells with no core data. Although, porosity data from logs are not as accurate as core data, they are better than any estimate. However, it is important to specify that inference of a GC or a variogram should be done using only one source of data as mixing may produce erroneous results.

Finally, it should be stressed that in the application of stochastic models, attention should be paid to the geological characteristics and heterogeneities of the reservoir under study (Dimitrakopoulos, 1985), as geological controls critically influence the results of numerical characterization.

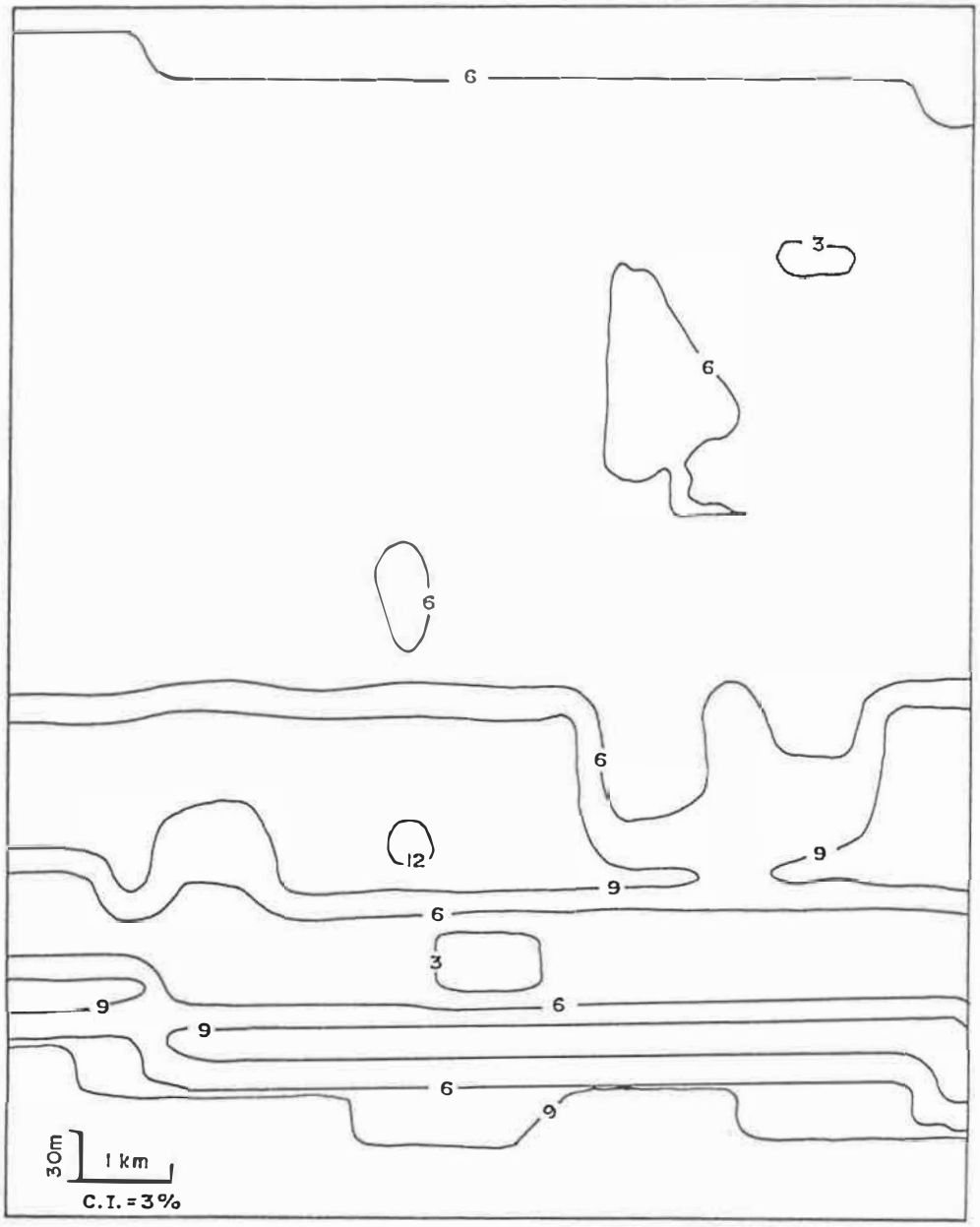

FIGURE 2.9: Cross-section of percent of weight oil from an estimated 3-D model of a part of the Athabasca oil sands deposit, Alberta.

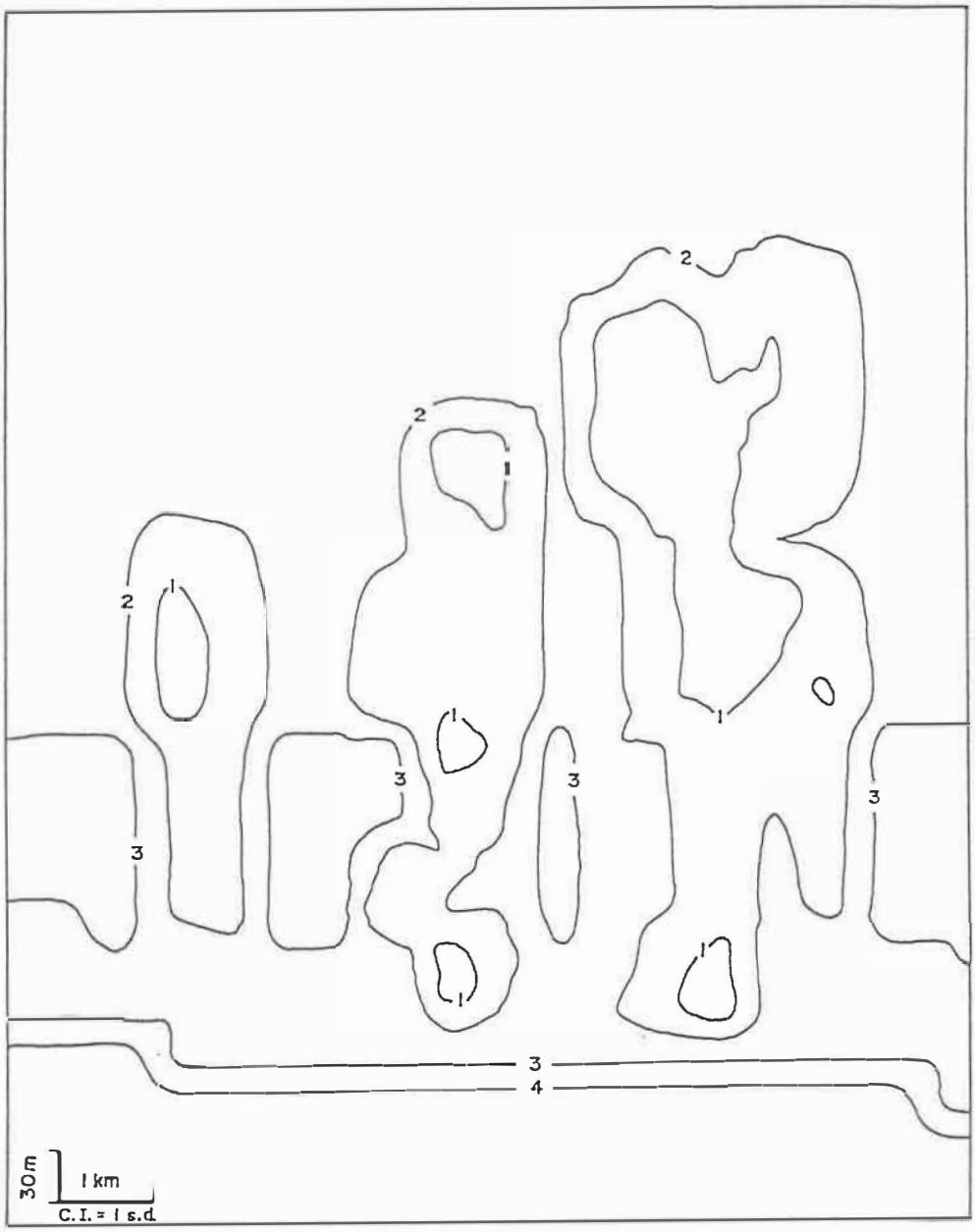

FIGURE 2.10: Map of estimation error associated with Figure 2.9.

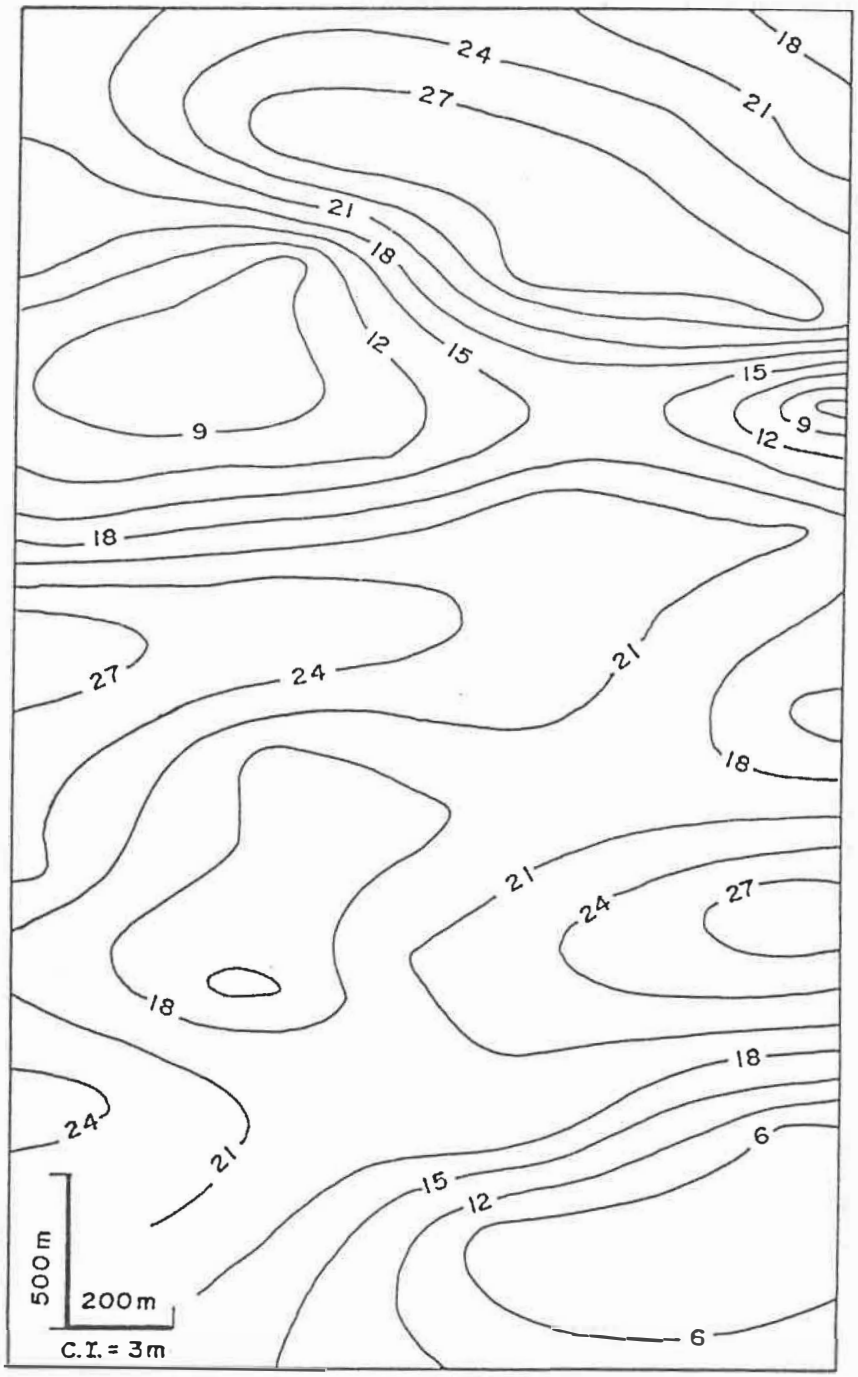

FIGURE 2.11: Estimated thickness of a pay zone in part of the Athabasca oil sands deposit, Alberta.

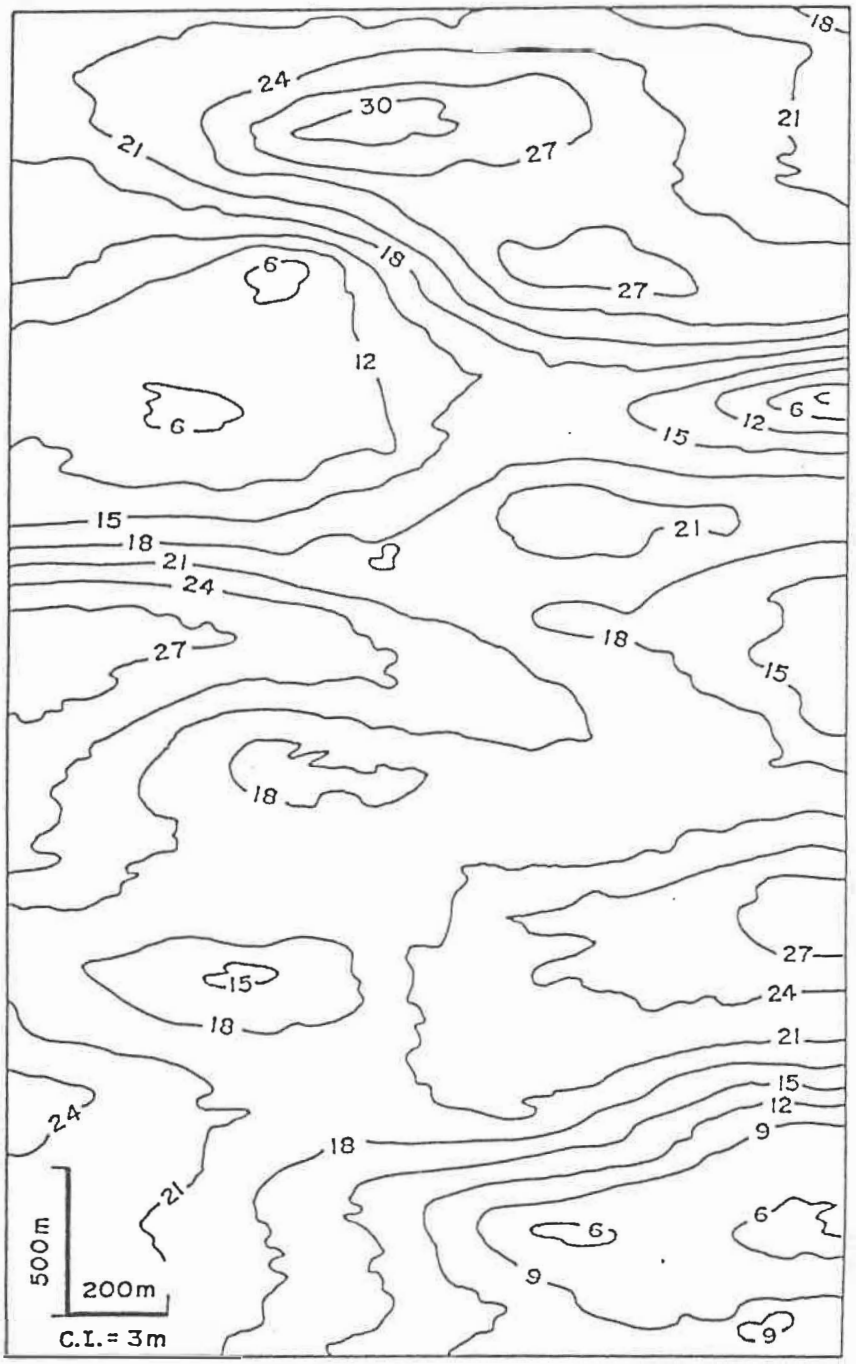

FIGURE 2.12: Conditionally simulated thickness of the same pay zone shown in Figure 2.11 .

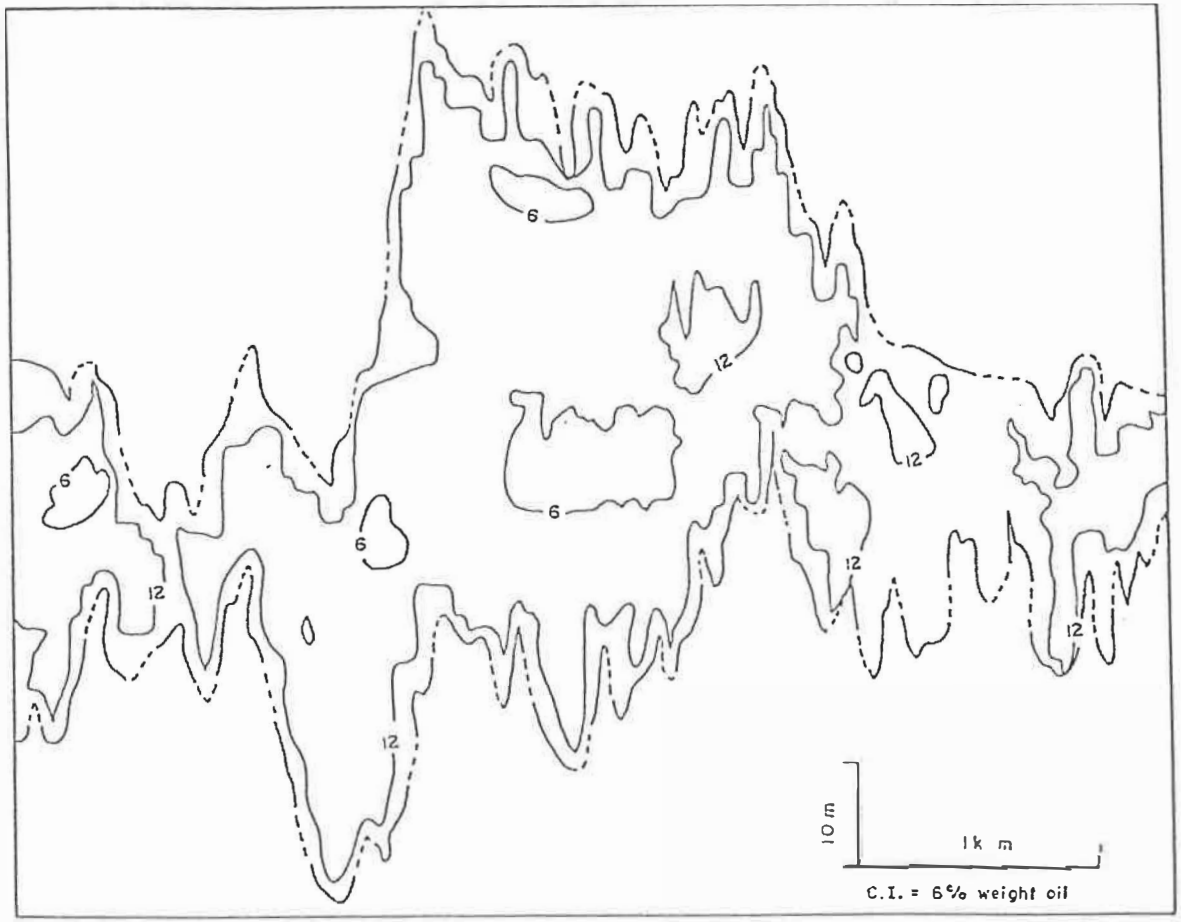

FIGURE 2.13: Cross-section of conditionally simulated boundaries and weight percent oil saturation from a pay zone from a part of the Athabasca oil sands.

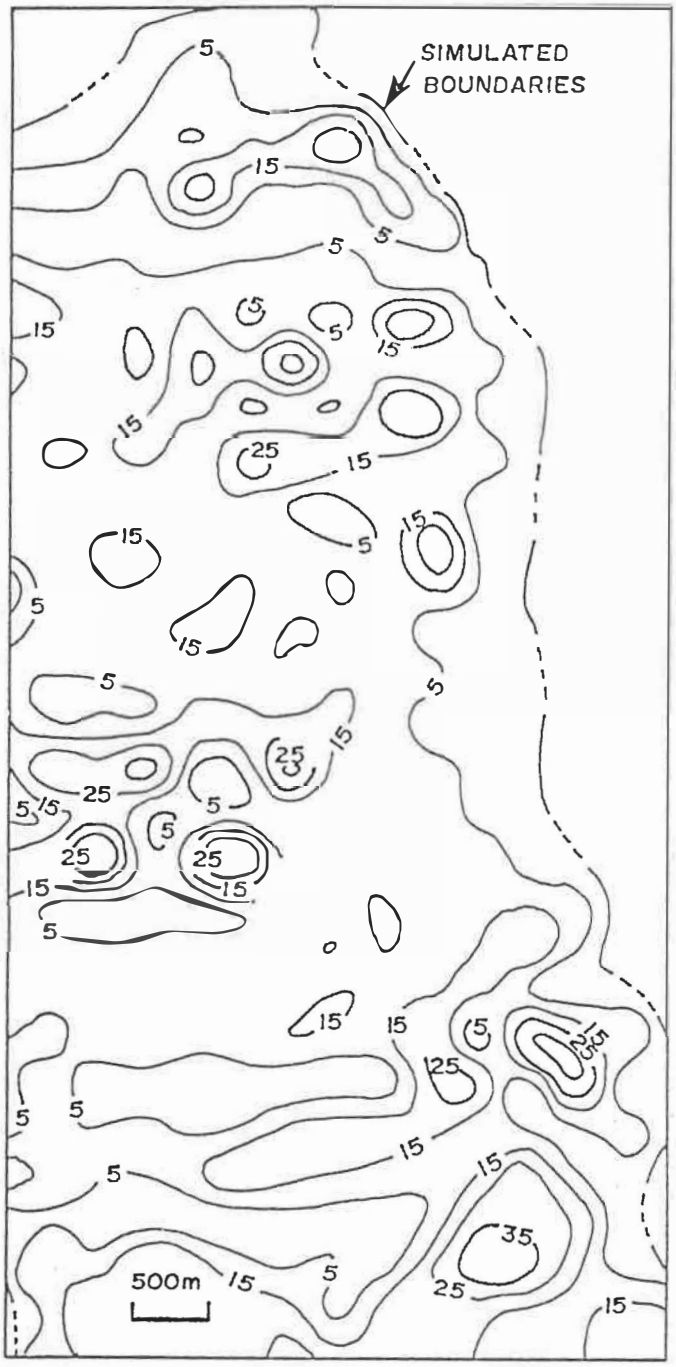

FIGURE 2.14: Horizontal section from a 3-D conditionally simulated grid of porosity from a unit within the Crystal Viking reservoir.

2.7. Summary

The need to provide reliable detailed numerical models describing the variability of geological reservoir-rock properties leads to the application of stochastic methodology.

The theory of intrinsic random functions of order k is a convenient mathematical formulation which leads to models which:

(i) account for the correlation structure of a variable which in turn 'passes' qualitative information to numerical models;

(ii) account for the naturally occurring trends within reservoirs;

(iii) provide best unbiased linear estimation;

(vi) are uniquely appropriate in performing direct estimations on the megascopic scale using data from the macroscopic one;

(v) provide assessment of the estimation in terms of an estimation error; and

(vi) can uniquely provide conditionally simulated realities of any pertinent variable, which may be used to check the sensitivity of flow simulations to reservoir describing input.

The above characteristics suggest that stochastic methodology, as outlined, is very promising in terms of advancing the sophistication of numerical reservoir characterization to the current levels of reservoir simulation.

In the following chapter the technique of conditional simulation of IRF-k, outlined in section 2.4, is developed in detail.

3. CONDITIONAL SIMULATION OF INTRINSIC RANDOM FUNCTIONS OF ORDER k

3.1 Introduction

Conditional simulation of stationary natural processes was introduced in Geostatistics by Journel (1974). Several aspects and developements on stationary simulations have recently been presented (Christakos, 1987; Davis, 1987; Mantoglou, 1987; Luster, 1985). However, conditional simulation of non-stationary stochastic fields has seldomly been addressed since the first use of the technique in two dimensions, (Chiles 1977) despite the fact that geological variables commonly exhibit distinct trends. Such variables are properties of petroleum reservoirs like porosity, fluid saturations, boundaries, etc. as shown in Chapter 2. As in the stationary case, conditional simulations of non-stationary fields which mimic the spatial variability of the actual phenomenon under study can be generated. The latter property is of particular interest in sensitivity studies. In the petroleum industry, for example, it is fundamental to assess the sensitivity of reservoir flow simulations to possible variations of the geological input. This can be done objectively by using realistic representations of the fluctuation of the pertinent variables as provided by conditional simulations.

In the present study, a comprehensive step-by-step procedure of conditional simulation of non-stationary physical processes is developed, within the framework of the theory of intrinsic random functions of order k and the turning bands method (Matheron, 1973). More specifically, the procedure includes the following steps. First, the Wiener-Levy process is used to simulate an IRF-k in R^1. Then, simulations in R^n are obtained by summing contributions from those in R^1. The conditioning process is described and the quality of the simulations is examined using experimentally calculated generalized variograms. In order to gain some insight into practical aspects of the proposed technique, examples in two and three dimensions are given.

3.2 Non Conditional Simulations

3.2.1 The Wiener-Levy process

A Wiener-Levy or Brownian motion process is a stochastic process $\{W(x), x \geq 0\}$ in R^1 with the following properties (Parzen, 1962; Antelman and Savage, 1965)

i) $\{W(x), x \geq 0\}$ has stationary independent increments

ii) for all $x > 0$: $W(x)$ is normally distributed

iii) for all $x > 0$: $E[W(x)] = 0$

iv) $W(0) = 0$.

As a consequence of (i) and (iv), to state the probability law of $W(x)$, it is sufficient to state the probability law of $[W(x + h) - W(x)]$ with $x + h > x$. Because of (ii), the increment $[W(x + h) - W(x)]$ is normal and its law is determined by its mean and variance. It is

$$E[W(x + h) - W(x)] = 0 \tag{3.1}$$

and

$$\mathrm{Var}[W(x + h) - W(x)] = \sigma^2 |h| \tag{3.2}$$

where σ^2 is an empirical characteristic of the process in hand.

In the discrete case, the Wiener-Levy process $W_o(x)$ is an IRF-0 with the following additional characteristics (Orfeuil, 1972)

v) for all $i \in [1,...,n]$: $W_o(x_i) = W_o(x_{i-1}) + R_i$

vi) for all $x \in [x_i, x_{i+1}[$: $W_o(x) = W_o(x_i)$

where $\{R_i, i = 1,...,N\}$ is a set of independent random variables with realizations of values +1 or -1 and probability of occurence 1/2. Note that relation (iii) is valid in the discrete case if R_i is gaussian.

In addition, one may consider the p^{th}, $p \neq 0$, integration $W_p(x)$ of a $W_o(x)$ process in R^1 such that

$$W_p(x) = \int_o^x \frac{(x-u)^{p-1}}{(p-1)!} W_o(u)\, du, \quad p = 1, \ldots, k \qquad (3.3)$$

The descrete integration of Wp(x) is defined as

vii) $W_p(0) = 0$ for all $p \geq 1$

viii) $W_p(x_i) = W_p(x_{i-1}) + eW_{p-1}(x_i)$, for all $p > 1$

where e is the norm of vector $\vec{e} = \overline{x_o x_1} = \overline{x_i x_{i+1}}$

ix) for all $x \in [x_i, x_{i+1}[: W_p(x) = W_p(x_i)$

For the discrete process $W_o(x)$, it is easy to show that equation (3.1) is valid, i.e.

$$E[W_o(x_i)] = E[W_o(x_{i-1}) + R_i]$$

$$= E[W_o(0) + \sum_{j=1}^{i} R_j]$$

Table 3.1: Representation of an IRF-k in terms of Wiener-Levy processes and corresponding GC in R^1 for order $k \leq 2$.

k	Y(x)	$K_1(h)$
0	$b_0 W_0(x)$	$-b_0^2 w\|h\|$
1	$b_0 W_0(x) + b_1 W_1(x)$	$-b_0^2 w\|h\| + b_1^2 \frac{w}{3!}\|h\|^3$
2	$b_0 W_0(x) + b_1 W_1(x) + b_2 W_2(x)$	$-b_0^2 w\|h\| + [b_1^2 - 2b_0 b_2]\frac{w}{3!}\|h\|^3 - b_2^2 \frac{w}{5!}\|h\|^5$

$$= \sum_{j=1}^{i} E[R_j]$$

$$= \sum_{j=1} E[\tfrac{1}{2}(1) + \tfrac{1}{2}(-1)] = 0 \text{ , for all } x$$

In addition, it is

$$\text{Var}[W_o(x + h) - W_o(x)] = E[(W_o(x + h) - W_o(x))^2]$$

$$= E[(\sum_{p=i+1}^{j} R_p)^2] = (j-i)\, E[R^2]$$

where $R = R_p$, for all p, and i and j are defined by

$$x \in [x_i, x_{i+1}[$$

$$x+h \in [x_j, x_{j+1}[$$

$$j > i.$$

Setting $(j-i)e = |h|$, one obtains

$$\text{Var}[W_o(x + h) - W_o(x)] = \frac{|h|}{e} E\,[R^2]$$

which becomes

$$\text{Var}\,[W_o(x + h) - W_o(x)] = \frac{1}{e}\,|h| \qquad (3.4)$$

Since

$$\text{Var}\,[W_o(x + h) - W_o(x)] = -2K_o(h)$$

Eq. (3.3) shows that the generalized covariance (GC) of $W_o(x)$ will be

$$K_o(h) = -\frac{1}{2e}\,|h| \qquad (3.5)$$

In conclusion, one can construct a realization of a Wiener-Levy process $W_o(x)$ in R^1 by simply generating random numbers of +1 or -1 drawn from a normal distribution with zero mean and variance of 1 and by applying properties (v) and (vi). The produced realization will have a GC $K(h) = -|h|$ (Fig. 3.1). From this, realizations of the p^{th} summation of $W_o(x)$ can be generated.

3.2.2 Simulation of IRF-k in R^1

It has been shown (Matheron, 1973) that an IRF-k in R^1 admits a polynomial generalized covariance (GC) if and only if it admits the representation

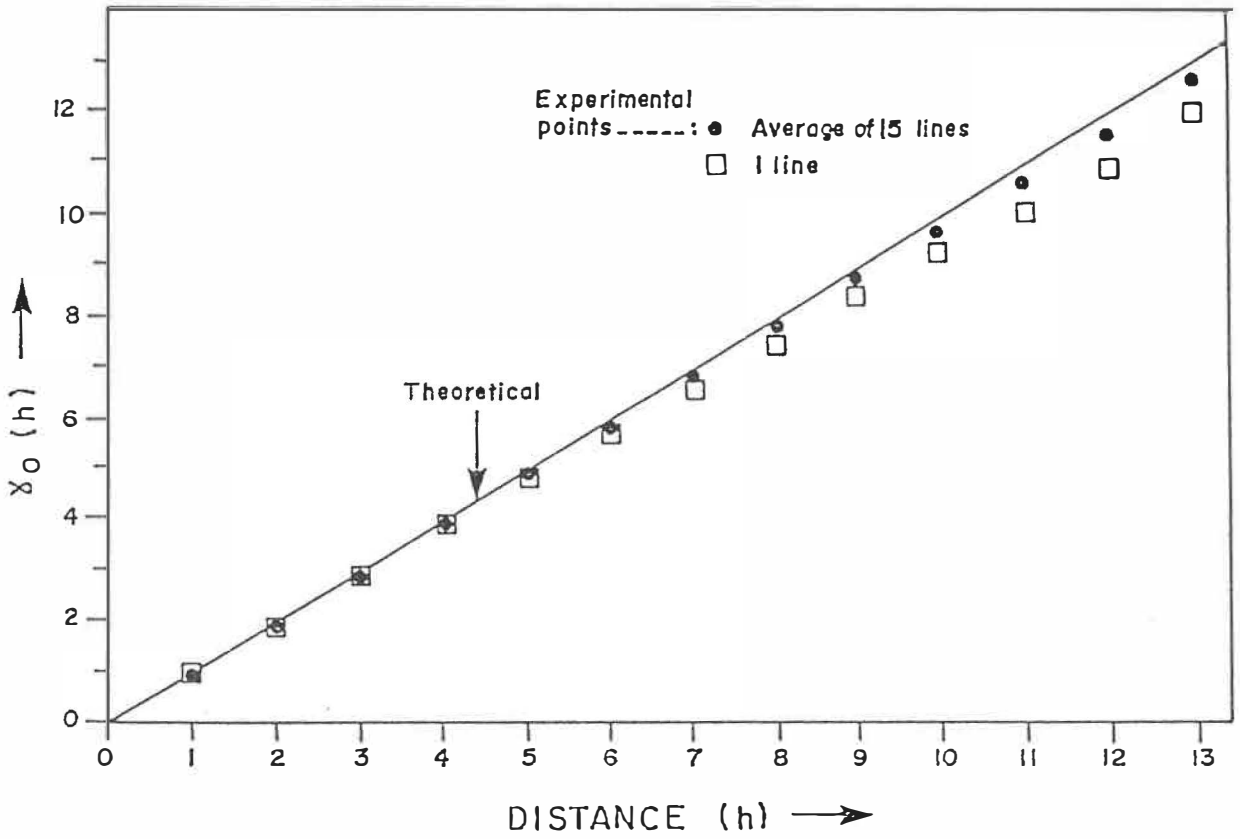

Figure 3.1: Experimental and theoretical variograms of realizations of Wiener-Levy processes on lines with $k(h) = -|h|$.

$$Y(x) = b_o W_o(x) + b_1 \int_o^x W_o(u)\, du + \ldots + b_k \int_o^x \frac{(x-u)^{k-1}}{(k-1)!} W_o(u)\, du \quad (3.6)$$

with b_p real coefficients, and $W_o(x)$ a representation of an IRF-0 with a GC such that $K(h) = - |h|$.

Equation (3.6) may be rewritten as

$$Y(x) = \sum_{p=0}^{k} b_p W_p(x) \quad (3.7)$$

where $W_p(x)$ is defined in (3.3).

$W_p(x)$ is an IRF-p with a GC-p

$$K_p(h) = \frac{(-1)^{p+1}}{(2p+1)!} |h|^{2p+1}, \; p = 0, \ldots, k \quad (3.8)$$

Note that since $W_p(x)$ is an IRF-p it is also an IRF-k for all $p \leq k$.

If $Y(x)$ is an IRF-k in R^1 which admits the representation (3.6) or its equivalent (3.7), and the linear combination

$\sum_{a=1}^{n} \lambda_a Y(x_a)$ is a GI-k, then

$$\text{Var}\left[\sum_{a=1}^{n}\lambda_a Y(x_a)\right] = \sum_{a=1}^{n}\sum_{b=1}^{n}\lambda_a\lambda_b K_1(x_a - x_b) \tag{3.9}$$

where $K_1(h)$, $h = x_a - x_b$, is the GC-k of $Y(x)$.

In addition, taking (3.7) into account one finds

$$\text{Var}\left[\sum_{a=1}^{n}\lambda_a Y(x_a)\right] = E\left[\left(\sum_{a=1}^{n}\lambda_a Y(x_a)\right)\left(\sum_{b=1}^{n}\lambda_b Y(x_b)\right)\right]$$

$$= E\left[\left(\sum_{a=1}^{n}\lambda_a\left(\sum_{p=0}^{k}b_p W_p(x_a)\right)\right)\left(\sum_{b=1}^{n}\lambda_b\left(\sum_{q=0}^{k}b_q W_q(x_b)\right)\right)\right]$$

$$= \sum_{a=1}^{n}\sum_{b=1}^{n}\lambda_a\lambda_b\left[\sum_{p=0}^{k}\sum_{q=0}^{k}b_p b_q E(W_p(x_a)W_q(x_b))\right]$$

$$= \sum_{a=1}^{n}\sum_{b=1}^{n}\lambda_a\lambda_b\left[\sum_{p=0}^{k}\sum_{q=0}^{k}b_p b_q\, K_{p,q}(x_a - x_b)\right] \tag{3.10}$$

where $K_{p,q}(h)$ is the cross GC of the IRF-k's $W_p(x)$ and $W_q(x)$.

It follows from (3.9) and (3.10) that the GC of $Y(x)$ is

$$K_1(h) = \sum_{p=0}^{k}\sum_{q=0}^{k}b_p b_q K_{p,q}(h)$$

$$= \sum_{p=0}^{k} b_p^2 K_{p,p}(h) + 2 \sum_{q=0}^{k-1} \sum_{p>q} b_q b_p K_{p,q}(h) \qquad (3.11)$$

where (see Appendix A)

$$K_{p,q}(h) = (-1)^{p+1} \frac{w}{(p+q+1)!} |h|^{p+q+1}, \quad p \geq q \qquad (3.12)$$

Equations (3.11) and (3.12) lead to

$$K_1(h) = \sum_{p=0}^{k} a'_p (-1)^{p+1} \frac{w}{(2p+1)!} |h|^{2p+1} \qquad (3.13)$$

with

$$a'_p = (-1)^{p+1} (b_p)^2 + \sum_{i=\max(0,2p-k)}^{p-1} (-1)^{i+1} 2 b_i b_{2p-i} \qquad (3.14)$$

From equations (3.13) and (3.14), Table 3.1 may be constructed showing the representation of an IRF-k in terms of Wiener-Levy processes and corresponding GC in R^1 for $k \leq 2$.

It follows from above that realizations of an IRF-k in R^1 with given polynomial GC with real coefficients can be generated from realisations of the processes $W_o(x)$ and $W_p(x)$, provided that the appropriate

coefficients are calculated. For example, if k=2 and the required GC in R^1 is

$$K_1(h) = -a_o|h| + \frac{a_1}{3!}|h|^3 - \frac{a_2}{5!}|h|^5$$

it is sufficient to simulate a realization of the IRF-2

$$Y(x) = b_o W_o(x) + b_1 W_1(x) + b_2 W_2(x)$$

where the coefficients are calculated by solving the system

$$b_o^2 = a_o$$

$$3\ (b_1^2 - 2b_o b_2) = a_1$$

$$5\ (b_2^2 = a_2)$$

What needs to be shown next is how from simulations of an IRF-k in R^1, realizations in R^n can be constructed and what the relations between the coefficients of the one-dimensional and n-dimensional GC's must be in order for the n-dimensional realization to have a specific GC.

3.2.3 The Turning Bands Method and Simulation of IRG-k in R^n

It has been shown (Matheron, 1973) that if Y(x) is an IRF-k in R^1 with GC $K_1(h)$ an IRF-k in R^n is defined such that:

$$Z_s(x) = Y(<x, s>) \tag{3.15}$$

where s is a unit vector chosen randomly from a unit sphere in R^n with probability distribution $\bar{w}_n$ concentrated in the sphere and invariant under translation. Then, $Z_s(x)$ has an isotropic GC such that

$$K_n(h) = \int K_1(<h, s>)\, \bar{w}_n\, ds \tag{3.16}$$

Equation (3.16) defines a one-to-one mapping of the GC-k in R^1 to an isotropic GC-k in R^n and it is called the turning bands operator (T_n).

For the operator T_n the equivalent GC's in R^1 and R^n are respectively the following

$$K_1(h) = \sum_{p=0}^{k} (-1)^{p+1} a_p \frac{|h|^{2p+1}}{(2p+1)!} \tag{3.17}$$

and

$$K_n(h) = \sum_{p=0}^{k} (-1)^{p+1} a_p B_{n,p} \frac{|h|^{2p+1}}{(2p+1)!} \qquad (3.18)$$

with

$$B_{n,p} = p!\ \Gamma\left(\frac{n}{2}\right) / \left[\pi^{1/2}\Gamma(p+(1/2)(1+n))\right]$$

It follows that if a random field having polynomial GC with coefficients, say C_p, is to be simulated in R^n, the coefficients a_p of the corresponding C_p in R^1 are

$$a_p = \frac{C_p}{B_{n,p}} \qquad (3.19)$$

From equation (3.19) it follows, for example, that in R^2 and for $k = 2$,

$$a_o = \frac{\pi}{2} C_o$$

$$a_1 = \frac{9\pi}{2} C_1$$

$$a_2 = \frac{(15)^2\pi}{2} C_2$$

Finally, if the appropriate random fields in R^1 can be simulated, then a n-dimensional field can be constructed by applying

$$Z_s(x) = \frac{1}{N^{1/2}} \sum_{i=1}^{N} Y_i (<x, s_i>) \qquad (3.20)$$

which is the discrete approximation of (3.15) with N being the number of independant one-dimensional random fields (Fig. 3.2).

3.3 Conditional Simulation of Random Fields with Generalized Covariances

Conditional simulation of an IRF-k Z(x) in R^n is a technique which, given values of Z(x) at particular points $\{x_a, a = 1,..., N\}$ and the corresponding GC, allows the construction of different realizations of Z(x) which have the following two properties

i) honor the given data available at $\{x_a, a = 1,...,N\}$;
ii) reproduce the GC of Z(x).

Consider an IRF-k S(x) with the same GC as Z(x) but not correlated to it. S(x) can be simulated as previously shown in section 2.4. One can write

$$S(x) = S^*(x) + [S(x) - S^*(x)]$$

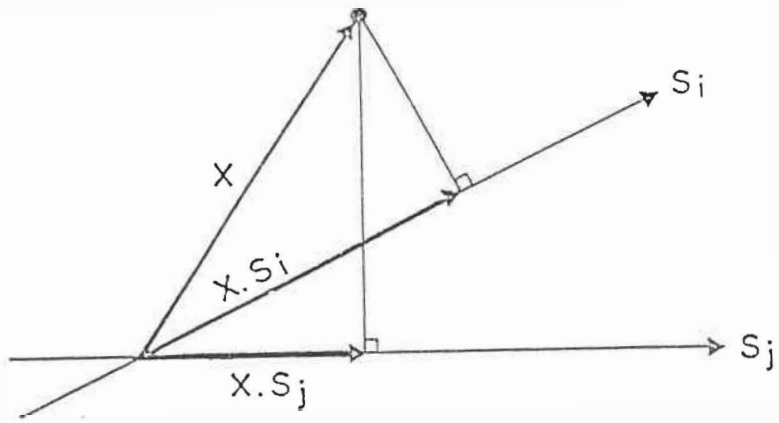

Figure 3.2: Schematic representation of the turning bands operator.

The conditional simulation of Z(x), {xa, a = 1,...,N} with GC K(h) is then defined as

$$Z_{cs}(x) = Z^{*}(x) + [S(x) - S^{*}(x)] \qquad (3.21)$$

Where $S^{*}(x)$ is an estimate of S(x), as if S(x) is only now in at {xa, a = 1,...,N}.

Apparently, $Z_{cs}(x)$ will reproduce the data $\{x_a\}$ because $Z^{*}(x_a) = Z(x_a)$ and $S(x_a) = S^{*}(x_a)$, which follows from the exactness of the kriging estimator.

Consider now the covariance between the kriging error and all increments of order k. It has been shown (Delfiner, 1976) that they are orthogonal to each other

$$\mathrm{Cov}[Z(x_o) - Z^{*}(x_o), \sum_{a=1}^{N} \lambda^{a} Z(x_a)] = 0$$

Taking the k^{th} increment of $Z_{cs}(x)$ at any point x_a one finds

$$\sum_{b=1}^{N} \lambda^{b} Z_{cs}(x_b) = \sum_{b=1}^{N} \lambda^{b} Z^{*}(x_b) + \sum_{b=1}^{N} \lambda^{b} (S(x_b) - S^{*}(x_b))$$

then it is

$$\mathrm{Var}[\sum_{b=1}^{N} \lambda^{b} Z_{cs}(x_b)] = \mathrm{Var}[\sum_{b=1}^{N} \lambda^{b} Z^{*}(x_b)] + \mathrm{Var}[\sum_{b=1}^{N} \lambda^{b} (S(x_b) - S^{*}(x_b))]$$

and as Z(x) and S(x) have the same GC

$$\mathrm{Var}\Big[\sum_{b=1}^{N}\lambda^{b}Z_{cs}(x_b)\Big] = \mathrm{Var}\Big[\sum_{b=1}^{N}\lambda^{b}Z(x_b)\Big]$$

The above shows that indeed $Z_{cs}(x)$ and $Z(x)$ have the same generalized covariance. Furthermore, one can show that the estimation variance of $Z_{cs}(x)$ is twice the estimation variance of $Z^{*}(x)$. Indeed

$$E[(Z(x_a) - Z_{cs}(x_a))^2] = E[(Z(x_a) - Z^{*}(x_a) - (S(x_a) - S^{*}(x_a)))^2]$$

$$= E[(Z(x_a)-Z^{*}(x_a))^2+(S(x_a)-S^{*}(x_a))^2-2(Z(x_a)-Z^{*}(x_a))(S(x_a)-S^{*}(x_a))]$$

$$= E[(Z(x_a) - Z^{*}(x_a))^2] + E[(S(x_a) - S^{*}(x_a))^2]$$

$$= 2\,E[(Z(x_a) - Z^{*}(x_a))^2] \qquad (3.22)$$

3.4 Verification of Simulations Using Generalized Variograms

The reproduction of a given generalized covariance of a conditionally or non-conditionally simulated realization of an IRF-k may be checked by comparing the experimental and theoretical generalized variograms (GV) in different directions. GV's are simpler to obtain but directly related to GC's. Aspects of the GV related to the present subject are presented next. Additional information may be found elsewere (Christakos, 1984; Chiles, 1979).

The generalized variogram of order k in R^1 is

$$\gamma_k(h) = \frac{1}{C_{2k+2}^{k+1}} \text{VAR}\,[\Delta_k\,(x,h)] \qquad (3.23)$$

where $\Delta_k\,(x,h)$ is a generalized increment of order k (GI-k) such that

$$\Delta_k(x,h) = \sum_{i=0}^{k+1} (-1)^i\, C_{k+1}^i\, Y(x+ih) \qquad (3.24)$$

where $C_{K+1}^i = \binom{k+1}{i}$

Note that, the GI-k in Eq. (3.24) is stationary if Y(x) is an IRF-k, and therefore $\gamma_k(h)$ in expression (3.23) is independent of x. In addition, considering relations shown in Appendix B, it is

$$\text{VAR}\,[\Delta_k(x,h)] = E[(\Delta_k(x,h))^2]$$

$$= \sum_{i=0}^{k+1} \sum_{j=0}^{k+1} (-1)^{i+j}\, C_{k+1}^i\, C_{k+1}^j\, K((i-j)h)$$

$$= \sum_{m=-k-1}^{k-1} (-1)^m\, C_{2(k+1)}^{m+k+1}\, K(mh)$$

and therefore

$$\gamma_k(h) = \frac{1}{C_{2k+2}^{k+1}} \sum_{m=-(k+1)}^{k+1} (-1)^m C_{2(k+1)}^{k+1+m} K(mh) \qquad (3.25)$$

From Eq. (3.25), the relations between generalized covariances and generalised variograms for k=0,1,2 in R^1 may be derived. More specifically, it is

$$\gamma_0(h) = K(0) - K(h)$$
$$\gamma_1(h) = K(0) - 4/3\ K(h) + 1/3\ K(2h)$$
$$\gamma_2(h) = K(0) - 3/2\ K(h) + 3/5\ K(2h) - 1/10\ K(3h) \qquad (3.26)$$

The experimental generalized variogram may be calculated from

$$\gamma_k^*(h) = \frac{1}{C_{2(k+1)}^{k+1} N_h} \sum_{i=1}^{N_h} [\Delta_K(x,h)]^2 \qquad (3.27)$$

where N_h is the number of finite differences $\Delta(x,h)$ available (eq. the number of pairs Y(x+h)-Y(x) if k=0). From Eqs. (3.27) and (3.24) it follows that for k = 0,1,2 it is

$$\gamma_0^* = \frac{1}{2N_h} \sum_{i=1}^{N_h} [Y(x) - Y(x+h)]^2$$

$$\gamma_1^* = \frac{1}{6N_h} \sum_{i=1}^{N_h} [Y(x) - 2Y(x+h) + Y(x+2h)]^2 \qquad (3.28)$$

$$\gamma_2^* = \frac{1}{20N_h} \sum_{i=1}^{N_h} [Y(x) - 3Y(x+h) + 3Y(x+2h) - Y(x+3h)]^2$$

Concluding, Eqs. (3.28) show how the experimental generalized variograms of a realization of an IRF-k can be calculated for the common cases of k=0,1,2 in one direction. Then they can be compared to the theoretical ones given by Eqs. (3.26) to verify the reproduction of the GV and therefore the GC.

3.5 Two- and Three-Dimensional Examples

Realizations of an IRF-2 with generalized covariance

$$K(h) = - |h| + 0.1 |h|^3 - 0.001 |h|^5$$

have been simulated in two and three dimensions. The two dimensional realization (Fig. 3.3) is on a 40 x 40 regular grid of 1600 points and has been constructed using 90 equally spaced one-dimensional simulations. The three-dimensional realization is on a 20 x 20 x 20 regular grid of 8000 points. It has been produced by summing 15 simulations on lines joining the mid-points of the opposite edges of a regular icosahedron, as is the standard practice (Journel, 1974). A horizontal section from the middle of the generated grid is presented in Figure 3.4.

The reproduction of the GC was tested by calculating directional experimental generalized variograms and comparing them to the theoretical one. In the two-dimensional example experimental GV's of order 2 were calculated along axes x, y and the two diagonals. The comparison to the theoretical one is shown in Figure 3.5. In the three-dimensional case experimental GV's of order 2 were calculated along the three orthogonal axes and compared to the theoretical one in Figure 3.6. Both comparisons suggest that the initial generalized covariance has been preserved reasonably well. The observed differences between simulated and theoretical values should be attributed to the discretezation involved in the one-dimensional simulations and the finite number of lines used.

The conditional simulation of IRF-k is next applied to 'real life' data from the Crystal Viking oil field, Alberta (Reinson, 1985). The first application involves elevations in meters below the mean sea level of the bottom of the Crystal Field using data from 144 wells. The GC inferred from the data set is of order 1 and has the form

$$K(h) = - 0.027691 \left|h\right| + 0.000344 \left|h\right|^3$$

A realization of the bottom of the Crystal Field (Fig. 3.7) was simulated on a grid of 38 x 50 points with a grid spacing of 300 metres The reproduction of the GC is verified using the four one-dimensional GV's shown in Figure 3.8. The second application includes the genera-

tion of a realization of percent porosity from a sedimentary unit within the Crystal reservoir. Available data include 186 regularized samples of 1 metre length representing porosity derived from core analyses. The GC inferred from the data is of order 0 and geometrically anisotropic in two dimensions with

$$K_{hor}(h) = 0.52 \times 10^{-3} - 0.666 \times 10^{-6} \left|h\right|$$

$$K_{vert}(h) = 0.52 \times 10^{-3} - 0.121 \times 10^{-3} \left|h\right|$$

A realization of porosity was conditionally simulated on a regular grid of 19 x 32 x 105 points with a resolution of 300 metres horizontally and 1 metre vertically. The geometric anisotropy was treated by properly scaling the grid. A horizontal section and a cross section from a generated realization of porosity are presented in Figures 3.9 and 3.10 respectively. The quality and reproduction of the GC is checked by computing experimental GV's of order zero on the horizontal and vertical planes. The results are plotted in Figures 3.11 and 3.12 respectively and show that preservation of the GC is excellent.

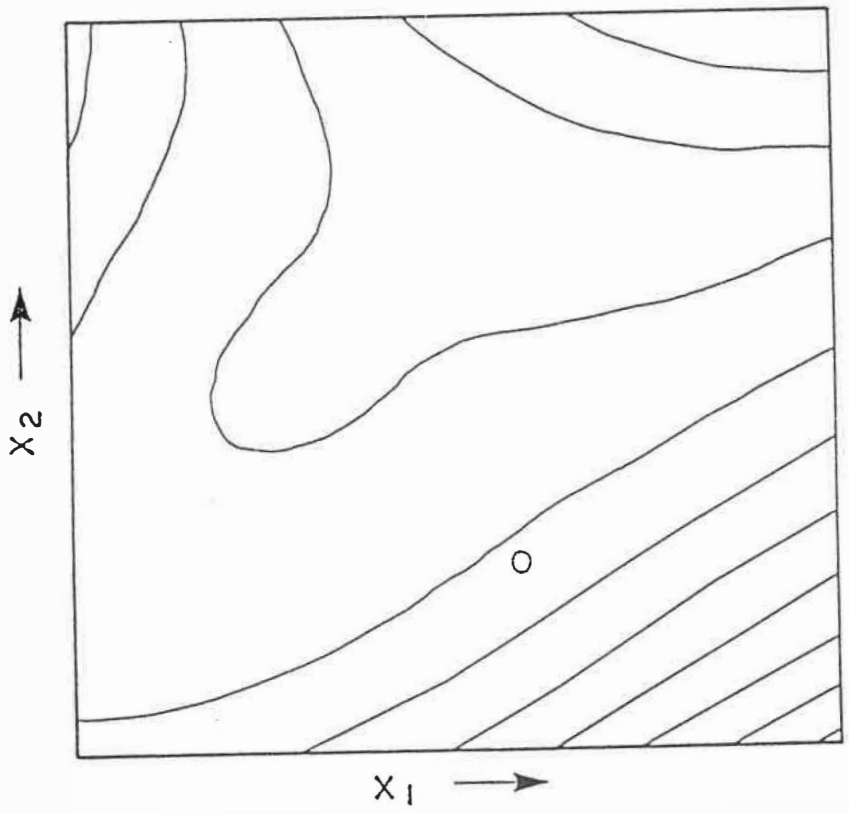

Figure 3.3: Contour map of a non conditional simulation of an IRF-2 in two dimensions.

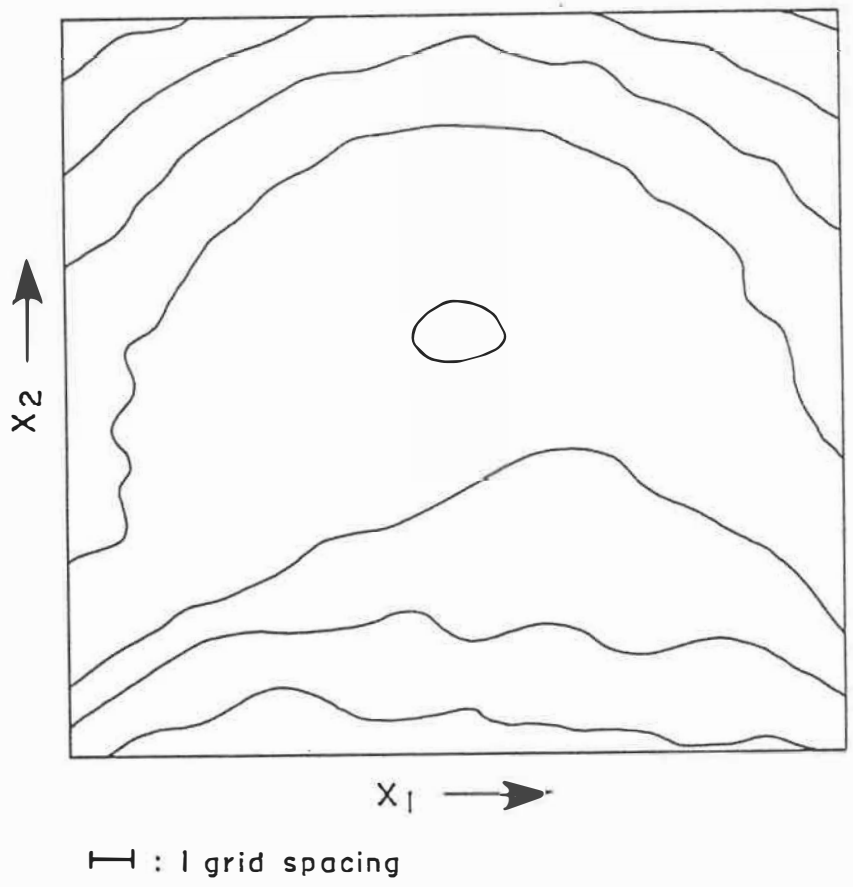

FIGURE 3.4: Cross-section from a non conditionally simulated realization of an IRF-2 in three dimensions.

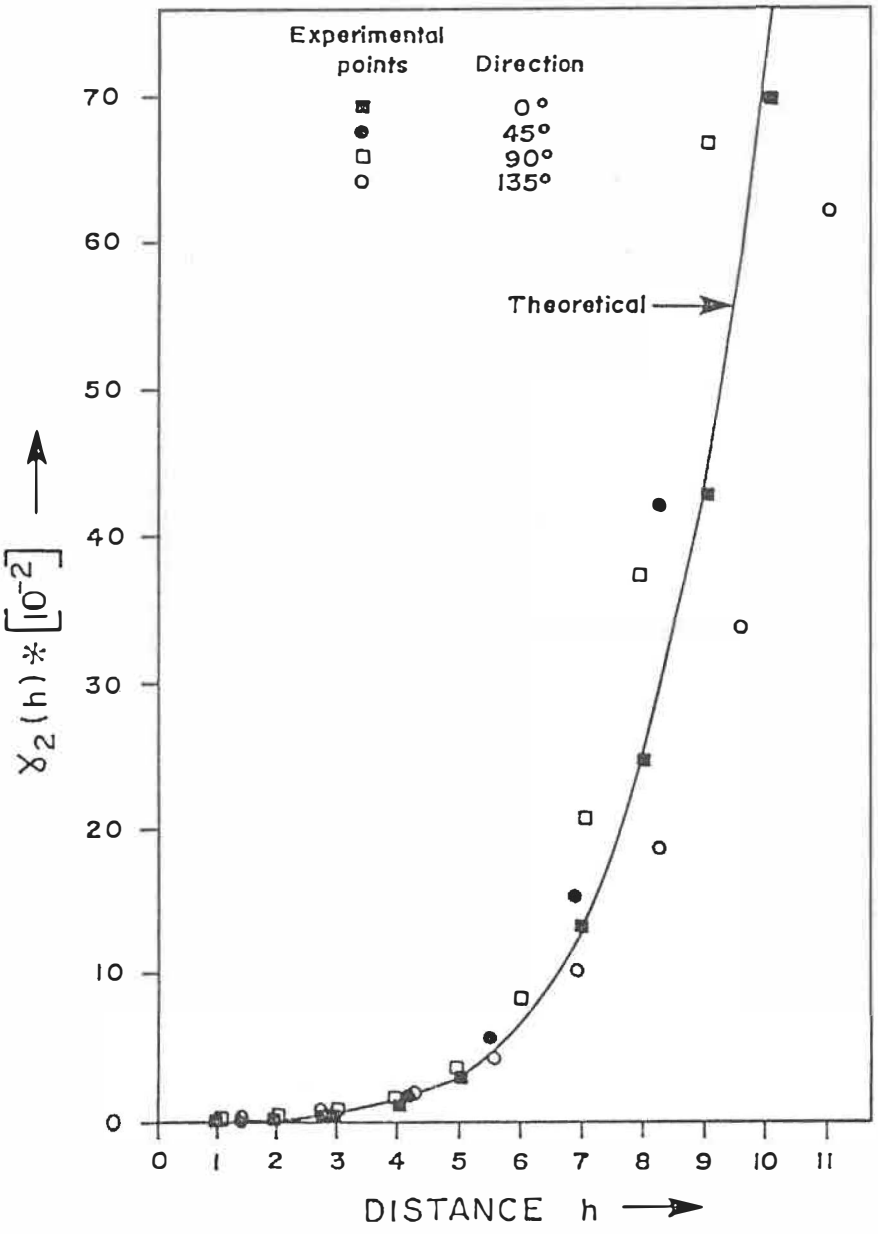

FIGURE 3.5: Experimental and theoretical generalized variograms of a simulated realization of an IRF-2 in two dimensions.

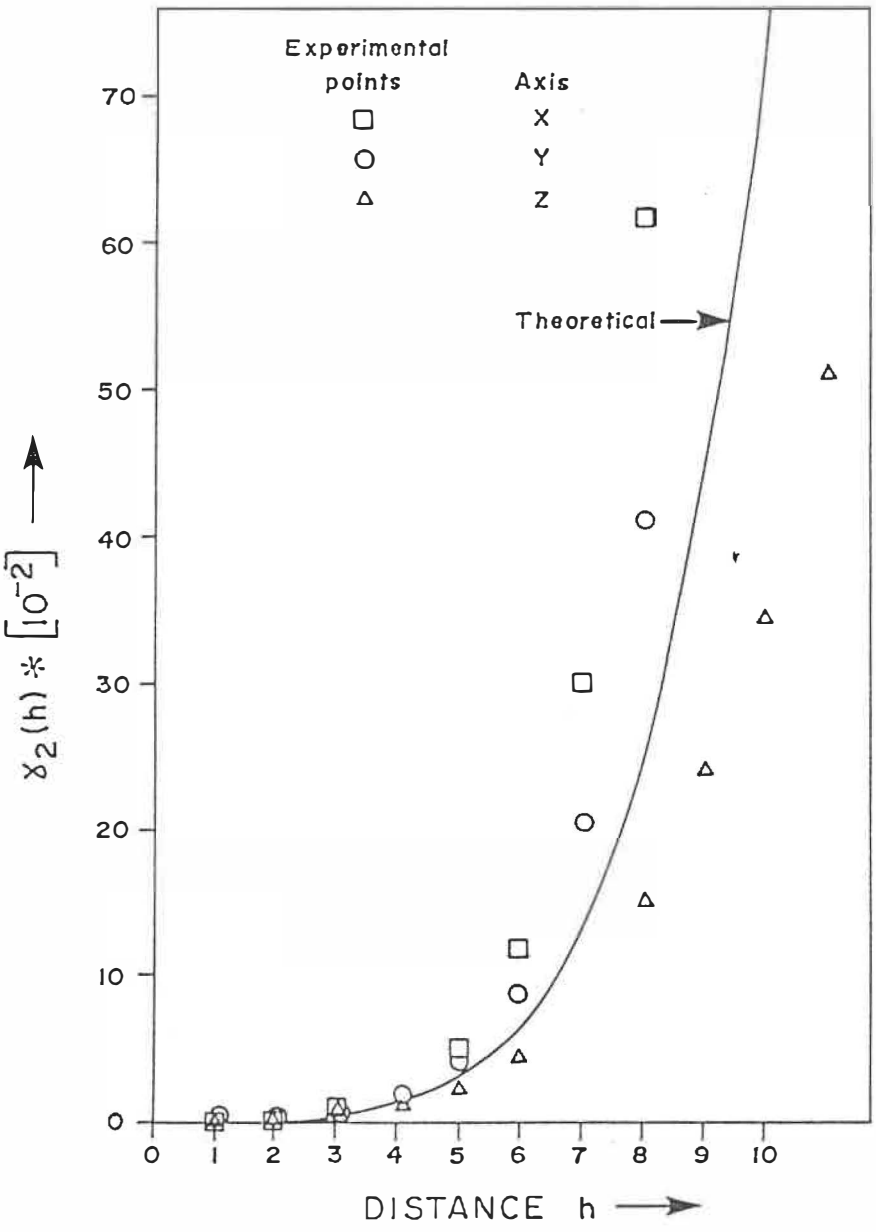

FIGURE 3.6: Experimental and theoretical generalized variograms of a simulated realization of an IRF-2 in three dimensions.

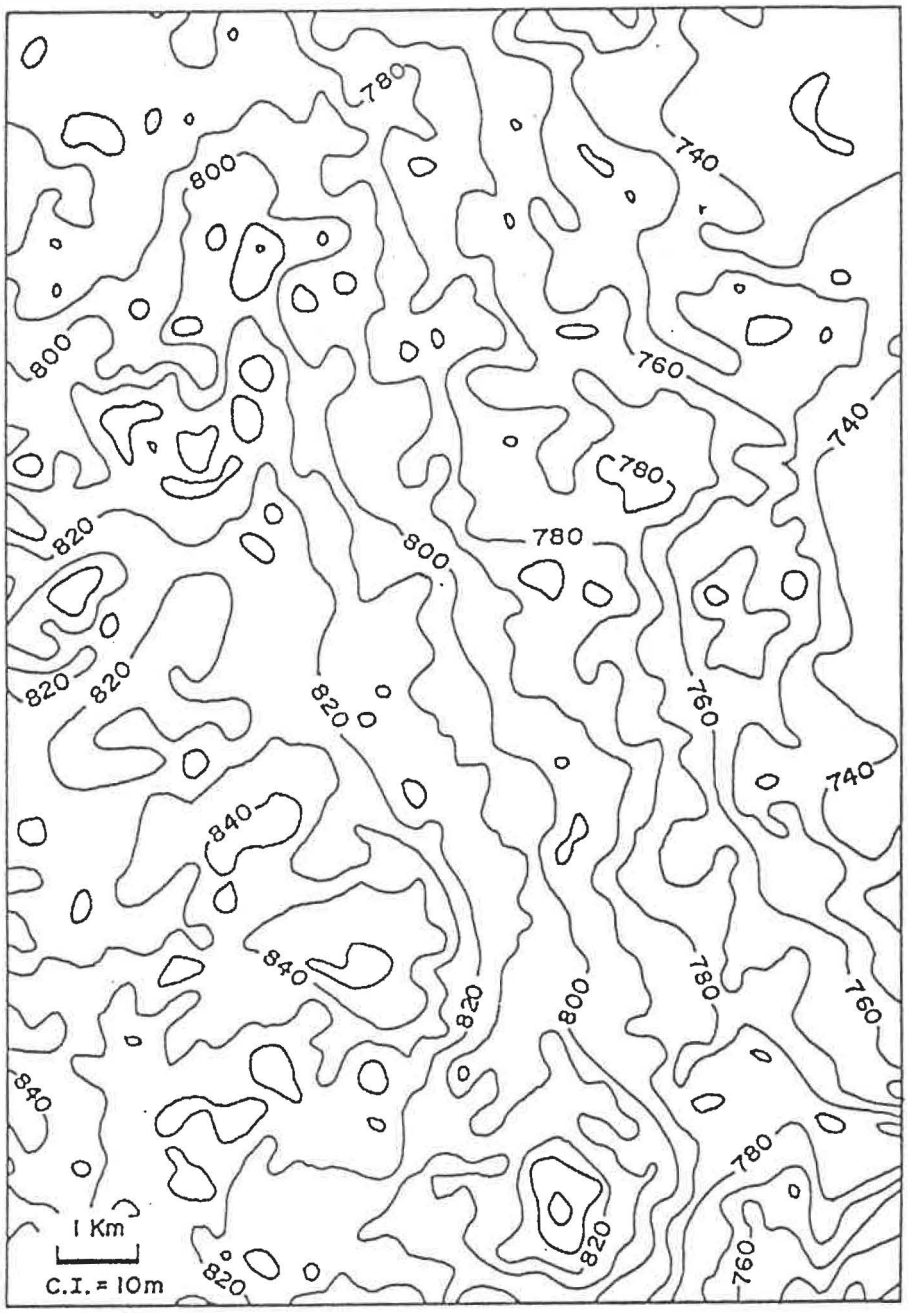

FIGURE 3.7: Contour map of conditionally simulated realization of the bottom of the Crystal Viking reservoir Alberta.

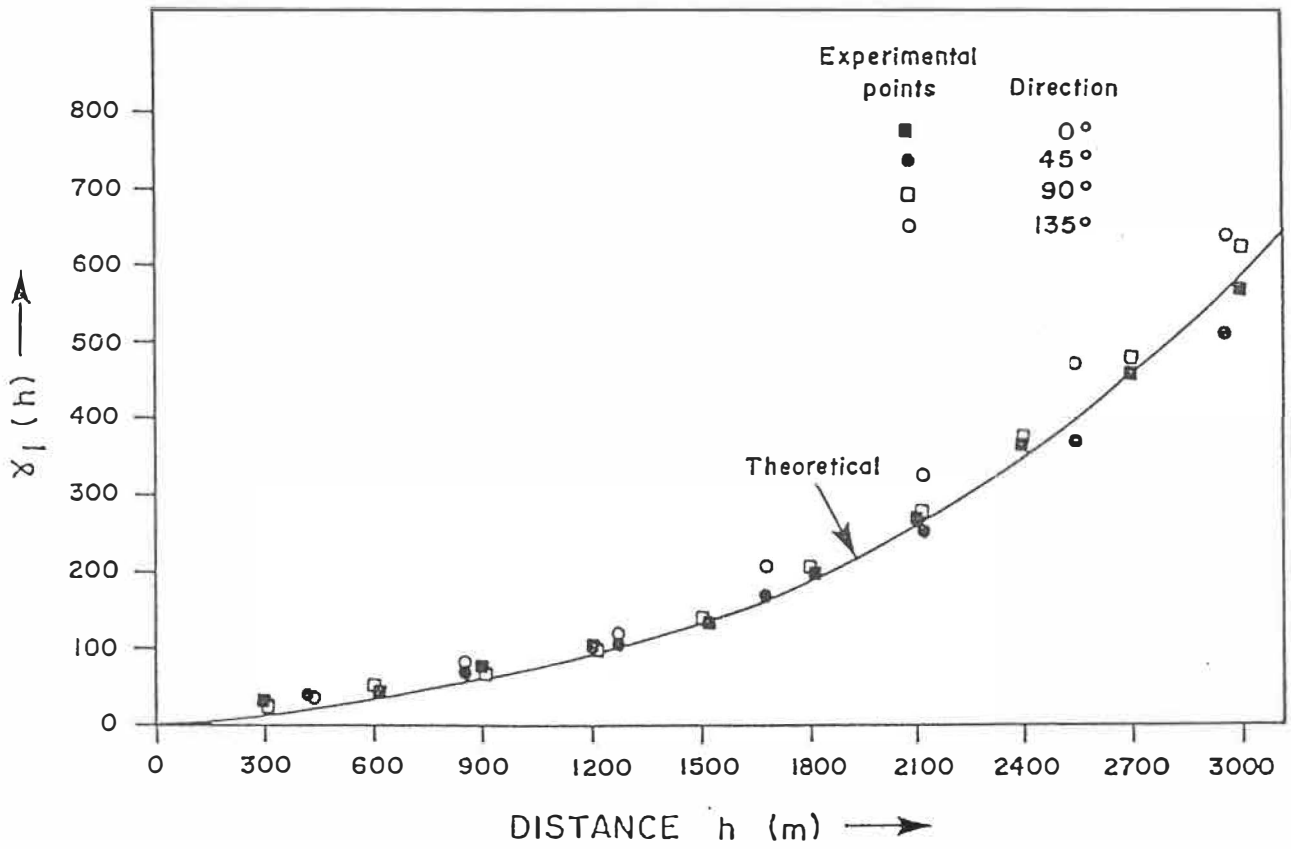

Figure 3.8: Experimental and theoretical generalized variograms of the realization of the bottom of the Crystal Viking reservoir, Alberta, in Figure 7.

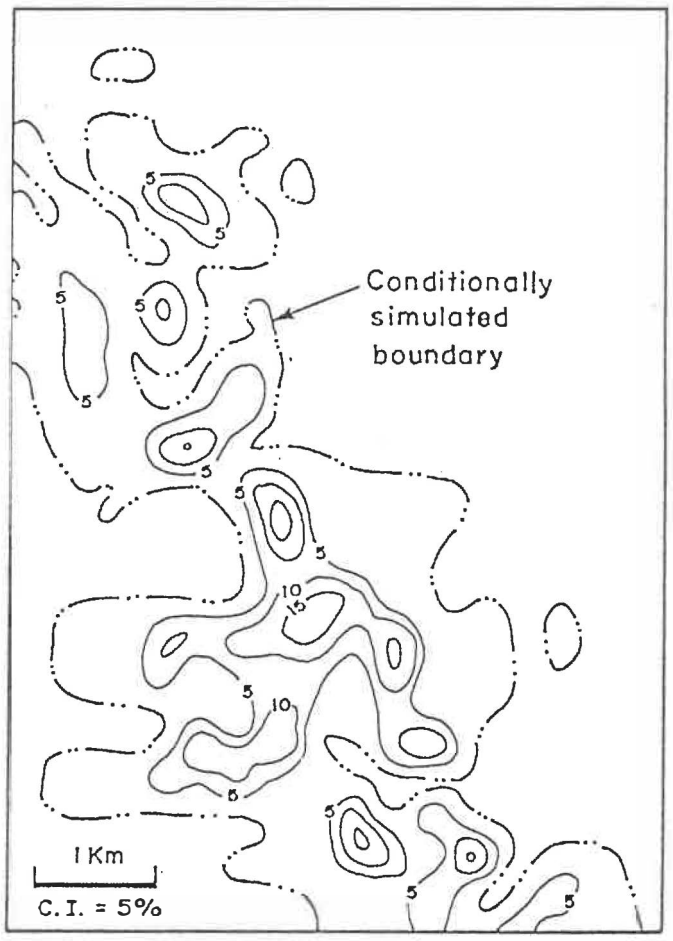

FIGURE 3.9: Horizontal section from a three dimensional conditionally simulated realization of porosity of a sedimentary unit within the Crystal Viking reservoir, Alberta .

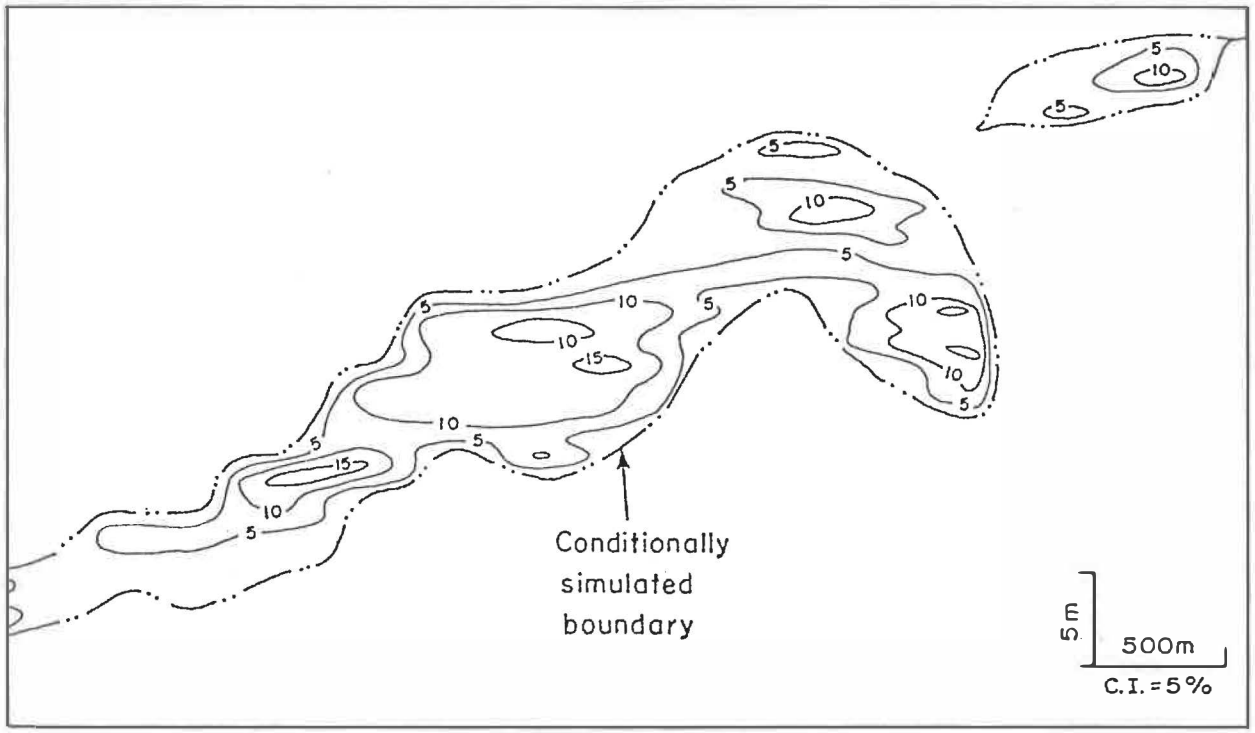

FIGURE 3.10: Cross-section from a three-dimensional conditionally simulated realization of porosity of a sedimentary unit within the Crystal Viking reservoir, Alberta.

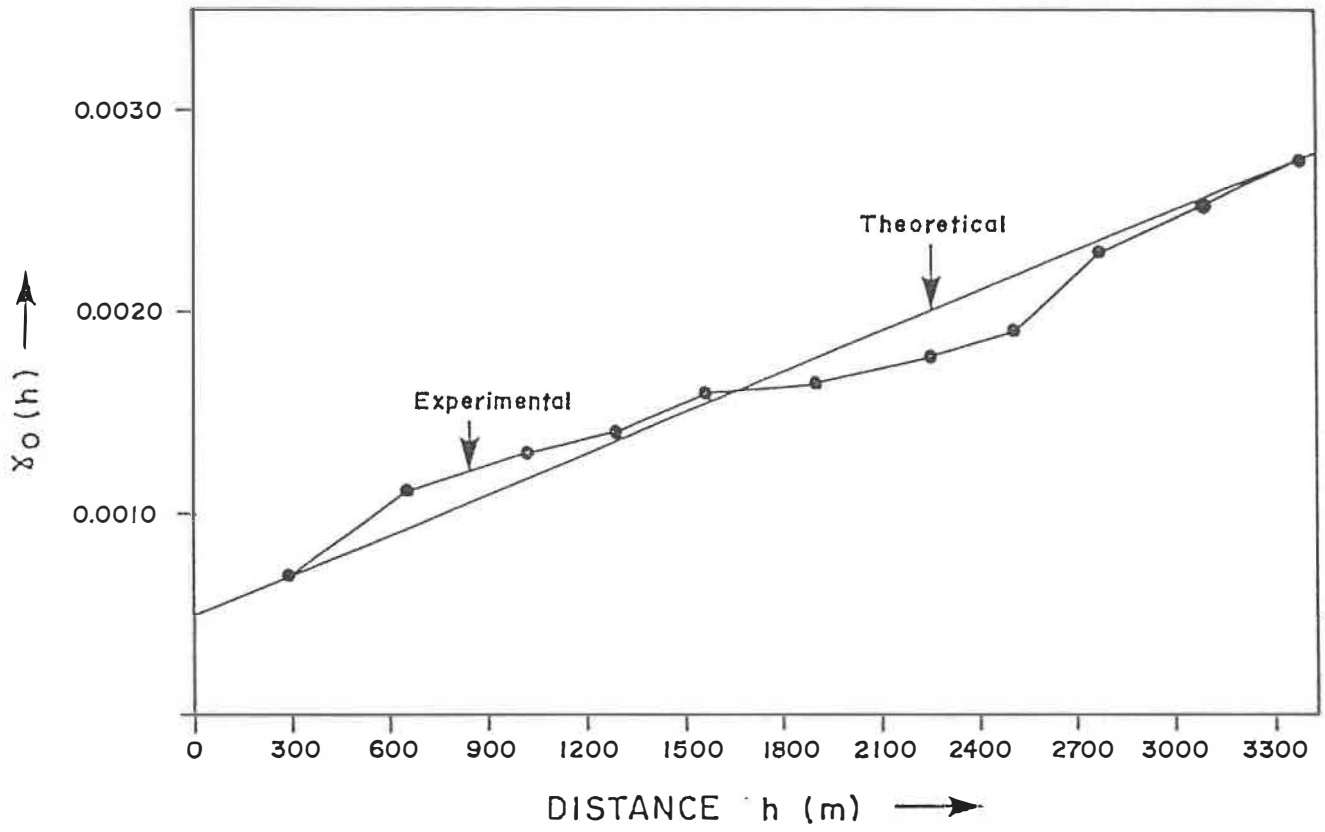

Figure 3.11: Horizontal experimental and theoretical generalized variograms of the conditionally simulated realization of porosity in Figures 9 and 10.

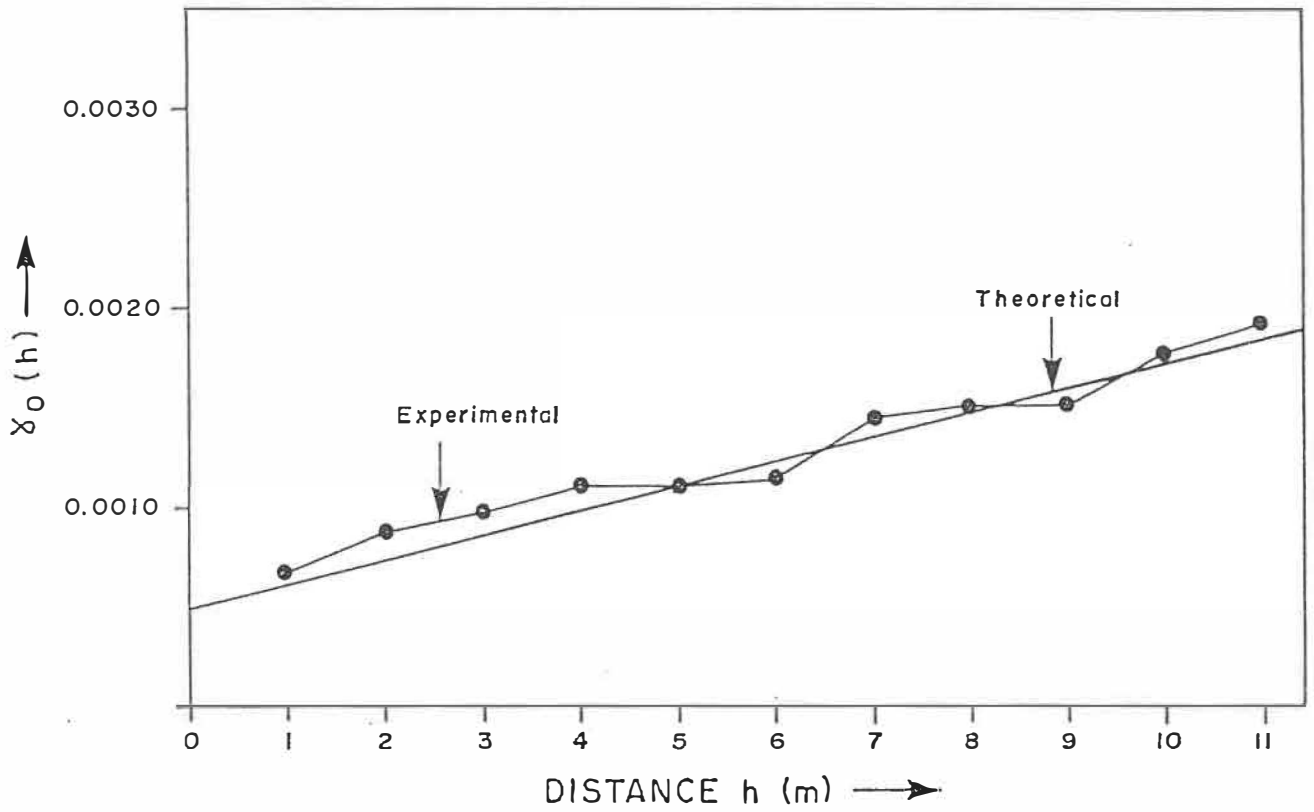

Figure 3.12: Vertical experimental and theoretical generalized variograms of the conditionally simulated realization of porosity in Figure 9 and 10.

3.6 Summary

A comprehensive step by step technique for the conditional simulation of IRF-k has been presented. The turning bands operator transforms the problem of simulating n-dimensional random fields into simulation in R^1. On line realizations of an IRF-k are generated using Wiener-Levy processes and their summations. The calculation of the appropriate coefficients for the processes on lines, so that they reproduce the GC of the IRF-k in R^1, is of main importance here. Next, by a folding back procedure realizations of IRF-k in R^n are constructed.

Given the non conditional simulations, conditional simulation of an IRF-k may be defined as the sum of an estimated random function using the IRF-k theory and a correla variate with the same GC as the process under study. Conditional simulations of random fields honor the data values available and reproduce the GC of the physical process. Verification of the latter is performed in this study by using generalized variograms.

The examples presented show that the conditional simulation of IRF-k is feasible and produces realistic results. Furthermore, it is particularly flexible and accounts for anisotropies in the simple case of linear GC's.

Conditional simulations of IRF-k can be used to model most of the reservoir-rock properties. However, the non additive permeability requires special treatment, and it is discressed separately in the following chapter.

4. GEOSTATISTICAL ESTIMATION OF THE EFFECTIVE PERMEABILITY TENSOR FOR THREE-DIMENSIONAL PETROLEUM RESERVOIR SIMULATORS

4.1 Introduction

The understanding, prediction and history maching of reservoir performance during production as well as the optimization of hydrocarbon recovery are based on reservoir flow simulation studies. In these studies, the reservoir is represented by a large grid of rectangular blocks. Effective reservoir-rock properties such as porosity, permeability, fluid saturations etc., are then assigned to each of these blocks. The assignment of a representative value for each of these variables to each grid block is of critical significance for the simulation results (Haldorsen, 1983; Coats, 1982; Aziz and Settari, 1979). It is a problem of interpolation and simultaneous change of scale, and it is based on measurements from a limited number of core samples, geophysical logs, and the geological characterization of the reservoir. The most challenging reservoir-rock property is permeability, whose non-additive character does not permit the direct estimation of

effective block equivalents from the available core measurements, thus requiring the development of specialized techniques.

Permeability refers to the ability of a porous medium to transmit fluids. It is the single most important geological property effecting subsurface flow, and reservoir simulation depends critically upon its accurate estimation. To date, considerable efforts have been made to tackle the calculation of permeability in heterogeneous geological formations. These efforts may be classified in three groups. The first includes numerical methods based on Monte Carlo simulations as introduced by Warren and Price (1961), improved to account for spatially correlated permeabilities (Smith and Freeze, 1979; Smith and Schwarts, 1981) and developed for sand-shale sequences by Desbarats (1987a, b, c). Combination of averaging formulae (Korvin, 1981) with simulations have also been attempted (Deutch, 1986). The next group includes streamline methods based on the geometry of discontinuous shales in sand-shale sequences, and on a stream tube concept (Haldorsen and Lake, 1982; Begg and King, 1985; Begg **et al.,** 1985). The third group includes analytical methods based either on a self-consistent approach (Dagan, 1979) or on perturbation methods for statistically isotropic (Matheron, 1967; Bark **et al.,** 1978; Gutjahr **et al.** 1978) and statistically anisotropic formations (Gelhar and Axness, 1983). To this last group, experimentation with the quantity of flow in order to derive upper and lower limits for effective block permeabilities (Le Loc'h, 1987) may be added.

The different approaches taken in the above studies have significantly contributedto the understanding of the factors controlling permeability. However, together with advantages, all these methods havetheir limitations. Numerical methods although more general are approxi- mate, tedious and their performance critically depends upon the relative lengths of the discretization grid and the correlation scale of permea- bility. Streamline methods are suitable for only a limited number of simple shale configurations and low shale fractions. Analytical methods may be restricted by assumptions of isotropy or by limits in the distribution and shape of the spatial correlation of permeability. Nervertheless, it is possible to expand the existing techniques and extent their applicability, thus providing significant improvements of the current practices.

In the present study, the estimation of effective permeability is examined within a geostatistical framework (David, 1977; Journel and Huijbregts, 1978), where permeability is considered as second-order stationary and ergodic random function, characterized by and predicted from a limited number of statistical moments. Accordingly, an **ad-hoc** generalization of the results of Gelhar and Axness (1983) to finite fields, such as flow simulator grid blocks, is developed in the following sections. The proposed methodology is illustrated in an example from the 'H' pool of the Crystal Viking field, south-central Alberta (Figure 4.1).

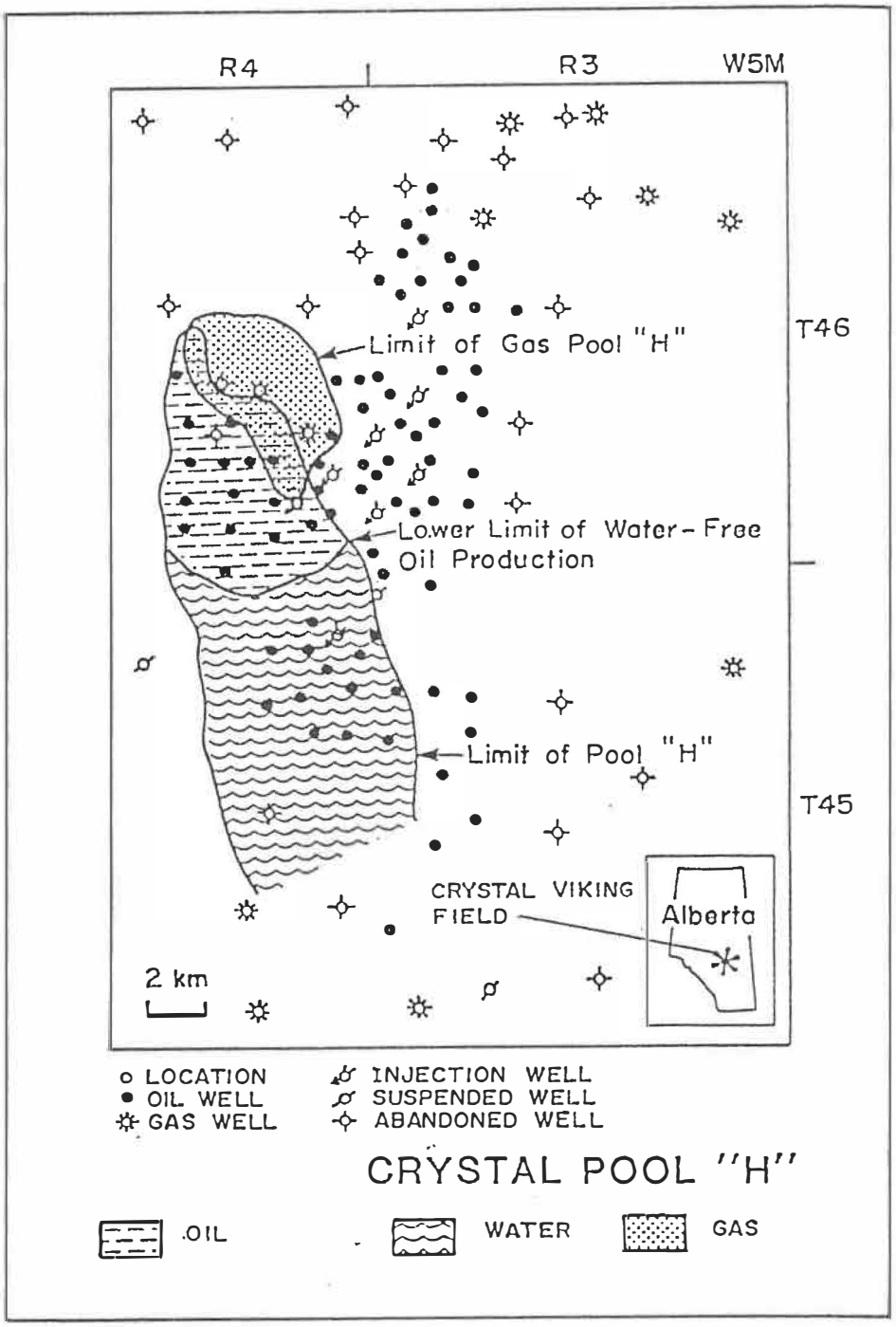

FIGURE 4.1: Limits and well control of the Crystal Viking pool 'H', Alberta (modified after Reinson et al., 1988).

4.2 Geostatistical Formulation

The basic concepts and definitions for the geostatistical estimation of the effective permeability for three-dimensional grid blocks, as required in petroleum reservoir simulation studies, are presented in this section.

Consider point permeability K(x) at point (x) in R^3 as a scalar, second order stationary and ergodic random function (RF). Then, the natural logarithm of K(x), Y(x) = ln K(x) is also a second order stationary RF with first and second order moments given by

$$E[Y(x)] = a \tag{4.1a}$$

$$Var[Y(x)] = \sigma(0) = \sigma^2 \tag{4.1b}$$

$$Cov[Y(x), Y(x+h)] = \sigma(h) \tag{4.1c}$$

$$\gamma(h) = \sigma^2 - \sigma(h) \tag{4.1d}$$

where a and σ^2 real constants, and $\sigma(h)$, $\gamma(h)$ the autocovariance and variogram functions respectivelly. The ensemble geometric mean of K(x) is defined by

$$K_G = e^{E[Y(x)]} = e^a \tag{4.2}$$

The arithmetic spatial average of Y(x) over volume v is defined by

$$Y_v = \frac{1}{v}\int_v Y(x)\,dx \qquad (4.3)$$

As a combination of the RF's Y(x) in volume v, Y_v is also a RF with

$$E[Y_v] = \frac{1}{v}\int_v E\,[Y(x)] = a \qquad (4.4a)$$

$$\mathrm{Var}[Y_v] = \frac{1}{v^2}\int_v\int_v \sigma(|r-s|)\,dr\,ds$$

$$= \bar{\sigma}(v,v) = \sigma^2 - \bar{\gamma}(v,v) \qquad (4.4b)$$

where $\bar{\sigma}(v,v)$ or $\bar{\gamma}(v,v)$ represent the average values of $\sigma(h)$ or $\gamma(h)$ when the extremities of vector h independatly describe volume v, and are calculated from charts (David, 1977).

Next, one may consider the spatial geometric average of K(x) over volume v defined by

$$K_v = \exp\left(\frac{1}{v}\int_v Y(x)\,dx\right) = e^{Y_v} \qquad (4.5)$$

If Y(x) is a multivariate normal random function, Y_v is also multivariate normal then, considering the properties of the log normal distribution (Aitchison and Brown, 1957), the mean and variance of K_v are given by

$$E[K_v] = E[e^{Y_v}] = K_G \left(e^{\frac{\bar{\sigma}(v,v)}{2}}\right) \tag{4.6a}$$

and

$$Var[K_v] = Var[e^{Y_v}] = E[K_v]^2 \left(e^{\bar{\sigma}(v,v)} - 1\right) \tag{4.6b}$$

Note that, if Y(x) is not assumed multivariate normal, then using a Taylor series expansion of e^{Y_v} and dropping the terms of third order of higher, the mean and variance of K_v are approximated by the above relations. In addition, the moments in equations (4.6) depend on the volume v through $\bar{\sigma}(v,v)$, and furthermore under ergodic assumptions, as the average volume becomes large, it is

$$\lim_{v \to \infty} E[K_v] = K_G \tag{4.7a}$$

and

$$\lim_{v \to \infty} Var[K_v] = 0 \tag{4.7b}$$

It is apparent that the ensemble geometric mean K_G defined by equation (4.2) and the spatial geometric average K_v defined in equation (4.5) are two distinct quantities, related by equation (4.7a).

4.3 Effective Permeability Estimation of Reservoir Blocks

Using the basic definitions previously described, an **ad-hoc** method for the effective permeability estimation of finite three dimensional anisotropic fields is developed in the present section, based on results by Gelhar and Axness (1983). The above authors derived, using a perturbation approach, an approximate analytical expression for the estimation of the effective permeability of infinite flow fields with anisotropic exponential spatial correlation. The latter may be expressed in the form of an exponential variogram

$$\gamma(h) = \sigma^2 \left(1-\exp\left(-\frac{h_i}{\lambda_i}\right)\right) \qquad (4.8)$$

where h_i denotes distance, λ_i the range of correlation with i=1,2,3. Accordingly, the effective permeability $K_{E_{ij}}$ is

$$K_{E_{ij}} = K_G \exp\left(\sigma^2(\tfrac{1}{2}-g_{ij})\right) \qquad (4.9)$$

where g_{ij} is a quantity depending on the anisotropy ratio and obtained by charts in Gelhar and Axness (1983). The results summarized above suggest that is infinite fields $K_{E_{ij}}$ is estimated by the combination K_G and a correction factor as shown in equation (4.9). A similar combination of K_V and a correction factor may be then used for finite fields, such as reservoir grid blocks. Considering the relation between K_V and K_G in (4.7a) the following approximation is suggested

$$K_{E_{ij}} = K_v \exp(\bar{\gamma}(v,v)\ (\tfrac{1}{2}-g_{ij})) \qquad (4.10)$$

Note that as volume $v \to \infty$ equation (4.10) becomes the same as equation (4.9). This may be considered as a justification for approximating K_E by equation (4.10). It remains that in practice K_v is not known for every grid block. It is, however, possible to provide estimates using the technique of conditional simulation, described in section 2.5.

For the conditional simulation, available point log-permeability measurements at data locations and their variograms are used to provide realistic representations of the actual point log-permeabilities Y(x) at every point in the reservoir. Then the conditionally simulated point log-permeabilities within every reservoir grid block can be used to provide estimates of K_v such that

$$K_v^* = \exp\left(\frac{1}{N} \sum_{i=1}^{N} Y_{cs}(x)\right) \qquad (4.11)$$

where $Y_{cs}(x)$ are the N conditionally simulated point log-permeabilities within volume v. Considering equation (4.11), equation (4.10) may be then approximated by

$$K_{E_{ij}} = K_v^* \exp(s^2(\tfrac{1}{2}-g_{ij})) \qquad (4.12)$$

where s^2 is an estimate of $\overline{\gamma}(v,v)$ calculated as the variance of the simulated points within the reservoir grid block. s^2 provides different estimates for $\overline{\gamma}(v,v)$ for every reservoir grid block and seems, at present, preferable to $\overline{\gamma}(v,v)$. The latter, is a single value for every reservoir block given a specific variogram $\gamma(h)$ of point log-permeabilities.

In the practice of reservoir simulation, it is required that the effective horizontal and vertical permeabilities are assigned to each of the reservoir grid blocks. This is obtained by considering the apropriate g_{ij}.

4.4 Applicational Aspects and Limitations of the Proposed Methodology

The methodology proposed for the determination of the effective permeability of reservoir grid blocks has limitations. These arise mainly from the formulation of equations (4.9) and (4.12).

It is assumed that the log-permeability Y(x) follows a gaussian law. However, it is common in practice that Y(x) has a bi- or multi-modal distribution. The multi-modality of the distribution of Y(x) and

in fact any other reservoir-rock property suggest that different geological units may be mixed. It is possible that given a detailed geological description of a reservoir in terms of sedimentary facies, diagenetic zones and structural deformations, different geologically homogeneous zones within the reservoir can be established so that each zone exhibits a uni-modal distribution. Therefore, if sufficient geological information is not available then the proposed method may not be suitable, depending on the shape of the distribution of Y(x).

The spatial variability of permeability represented by the variogram (4.1d) is strictly assumed to be exponential as in (4.8). Although the shape of the covariance does not represent a problem, the fact that the model can not account for a possible nugget effect, i.e. a percentage of random variation or variation due to measurement errors, could be a limitation. It should, however, be pointed out that the effect of neglecting a nugget effect, if present, is not clear. It seems, however, that the nugget effect, if present, acts as a filter on the influence of the largest (horizontal) correlation scale (Desbarats, 1988). The latter is indicated by two observations. First, it has been suggested from simulation experimentations (Warren and Price, 1961) that if no correlation structure is present (pure nugget effect), effective permeabilities tend towards the geometric mean of the permeability field. Second, it is apparent in equation (4.9), that as the horizontal range increases relative to the vertical one, the effective horizontal and vertical permeabilities tend towards the arithmetic and harmonic

means respectively and thus are moving away from the geometric mean. The above observations suggest that neglecting the nugget effect when present may have an apparent impact only in cases of a very large anisotropy ratio. In the latter case, results from equation (4.9) will tend to overestimate the horizontal and underestimate the vertical effective permeabilities.

Equation (4.9) provides exact results when the anisotropy ratio $\rho \to \infty$, i.e. in the ideal case of perfectly layered media. It concludes that the effective horizontal permeability is the arithmetic mean, and that the effective vertical permeability is the harmonic mean of the elementary permeabilities K(x). The validity of the above results are demonstrated in several studies (Gutjahr **et al.,** 1978; Dagan, 1979).

The two steps of the proposed methodology are developed within a geostatistical framework where ergodicity is an implicit assumption. In general, ergodicity requires the overall scale of the problem to be large compared to the correlation scale of the natural logarithm of point permeability. This may be verified when the variograms of Y(x) exhibit destinct sills indicating that the correlation scale is indeed small relative to the problem scale.

The application of the present method requires that every grid block in the reservoir is discretized in smaller sub-blocks on which

conditional simulation will be performed. Although discretization is standard practice in numerical applications, the optimal discretization lengths are not known. It is therefore suggested that discretization lengths are chosen as small as possible within the limitations of the available computer hardware.

The determination of the effective permeability tensor in the present study was investigated relative to the needs of reservoir flow simulation. The latter signifies that the important flow parameter is the average quantity of fluid which leaves the reservoir or is pumped into it. In such a case the stochastic flow solutions of Gelhar and Axness (1983) or the methodology developed here will provide, within the limitations already discussed, realistic results. It is important to note, however, that in other applications where the flow parameter of interest is the variability of the hydraulic head the approach may produce misleading results. This is due to the fact that the variation of the hydraulic head, unlike the quantity of flow, is substantially dependant on the geometry and orientation of possible localized impermeable barriers or high permeable pockets.

4.5 Field Application

In this section, the use of the proposed methodology is illustrated in an example from pool 'H' of the Crystal Viking oil field in south-central Alberta (Fig. 4.1). Pool 'H' of the Crystal field is a

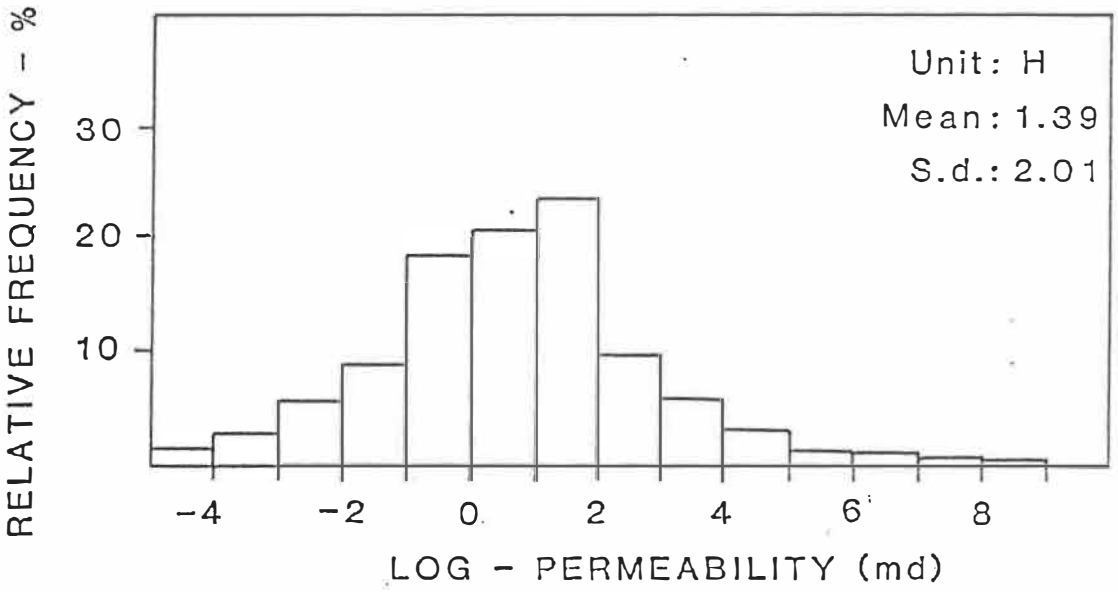

FIGURE 4.2: Histograms of the logarithmic transform of permeability core measurements from the Crystal Viking pool 'H'.

shallow channel-bar sandstone body representing the final episode of bay-fill facies deposition under transgressive conditions (Reinson **et al.**, 1988) and it can be considered, in terms of its sedimentary facies, as a geologically homogeneous unit with more or less horizontal stratification.

Data on permeability from core analyses are available from 28 wells within the limits of pool 'H'. The histogram of natural logarithm of the data is presented in Figure 4.2. The shape of the distribution in the last figure indicates that the distribution is uni-modal and thus the belief that pool 'H' represents a geologically homogeneous unit is statistically supported. Furthermore, the same figure suggests that one may safely consider that permeability in the pool under investigation follows a log-normal law. The experimental horizontal and vertical logarithmic variograms of the data are presented in Figs. 4.3 and 4.4 respectively. The apparent stability of both experimental variograms at larger distance suggests that the present problem is examined at a sufficiently large scale to ensure that ergodic assumptions are reasonably met. The fitted exponential models (Eq. (4.6)) are also presented on the same figures. Both variogram models tend towards a sill of 4.01 md^2, while correlation distances are 150 m and 4 m for the horizontal and vertical variograms respectively. The anisotropy ratio is 37.5 and the corresponding values for parameters g_{11} and g_{33} are 0.02 and 0.95 respectively.

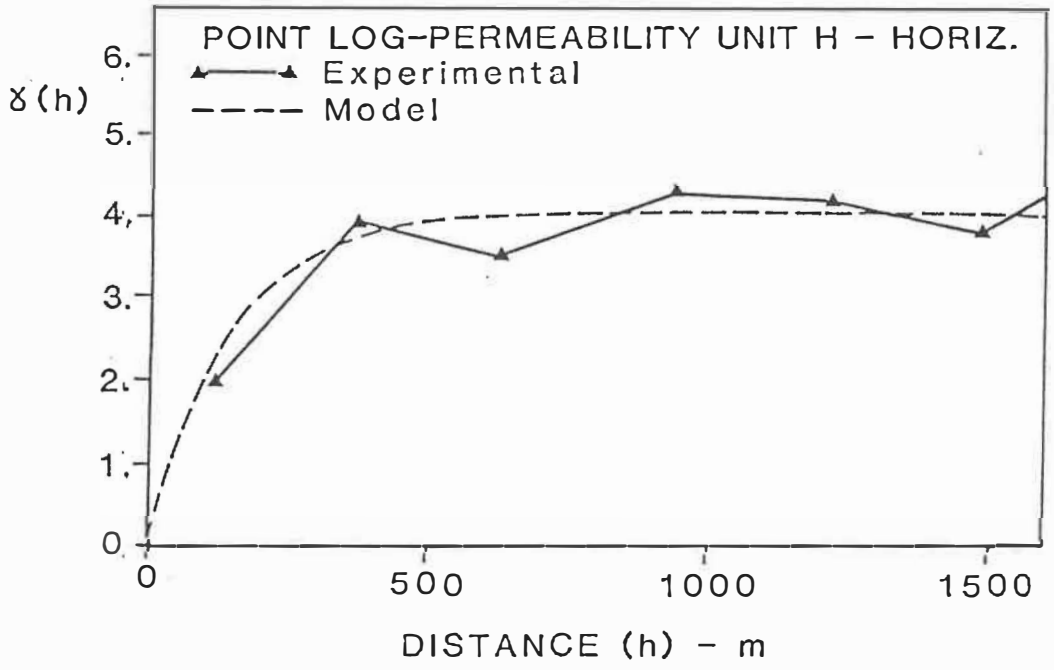

FIGURE 4.3: Horizontal experimental and fitted exponential model variograms of macroscopic log-permeability in pool 'H'.

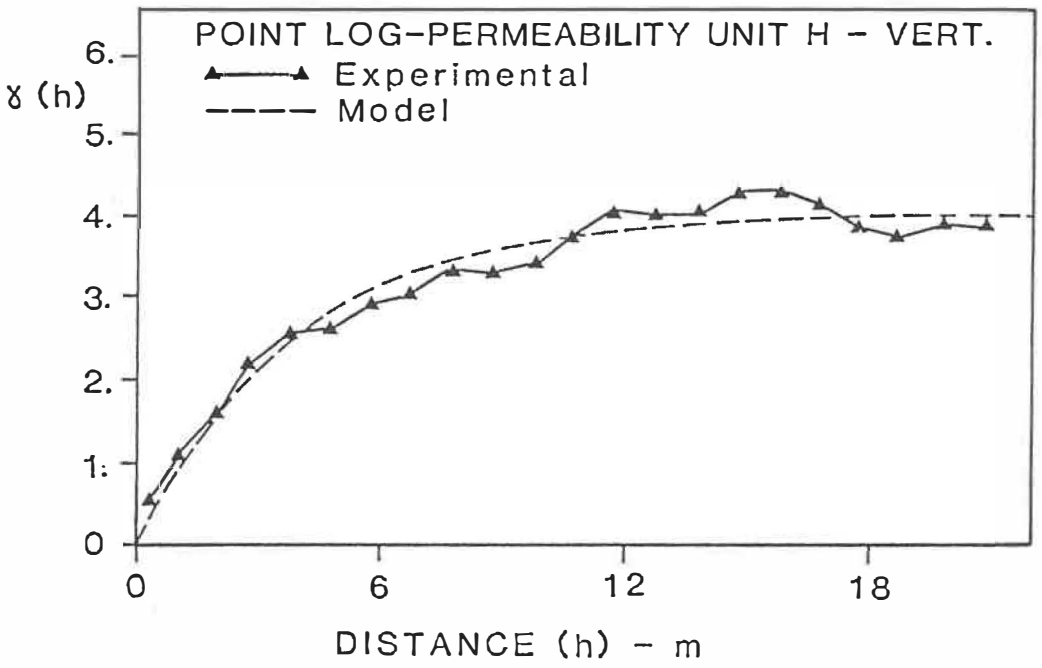

FIGURE 4.4: Vertical experimental and fitted exponential model variograms of macroscopic log-permeability in pool 'H'.

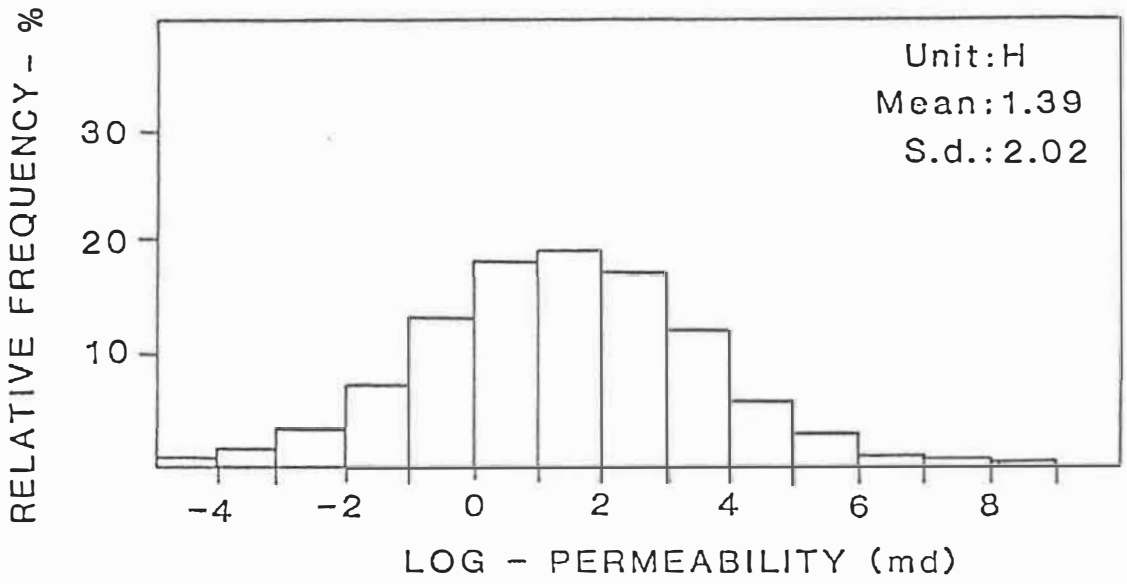

FIGURE 4.5: Histogram of the conditionally simulated macroscopic log-permeabilities.

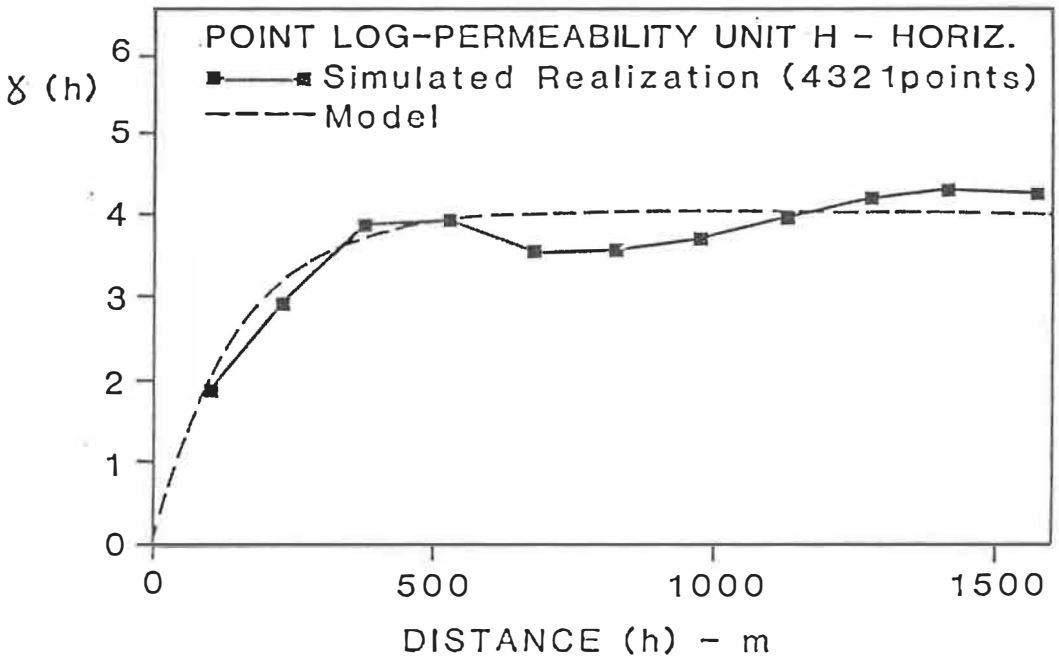

FIGURE 4.6: Horizontal variogram of conditionally simulated macroscopic log-permeabilities compared to the theoretical model.

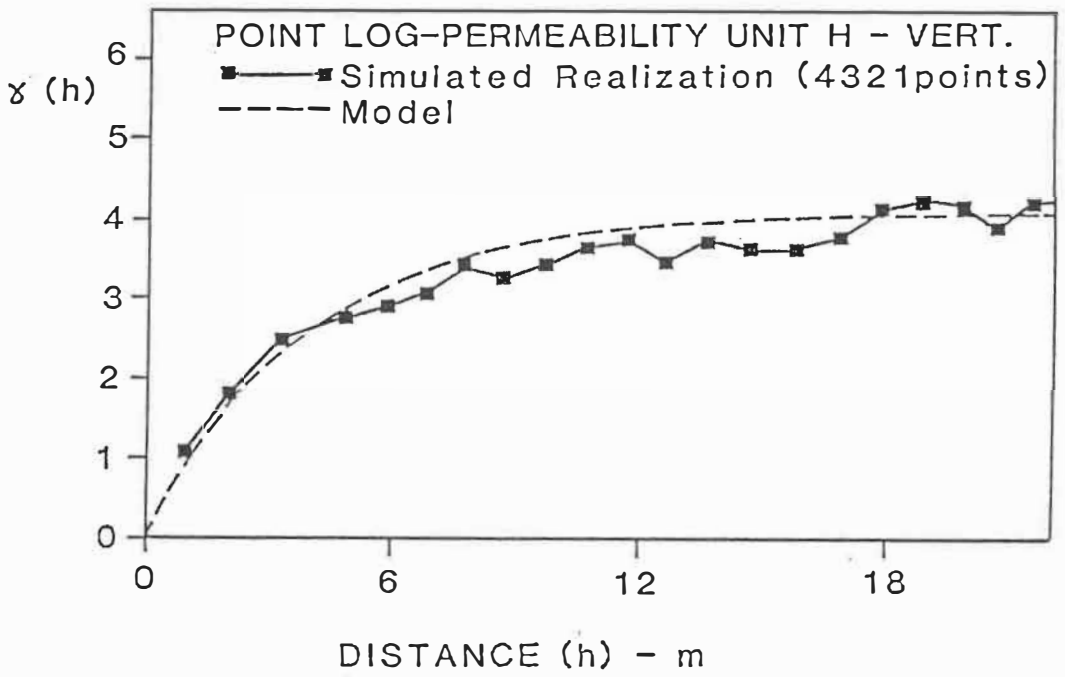

FIGURE 4.7: Vertical variogram of conditionally simulated macroscopic log-permeabilities compared to the theoretical model.

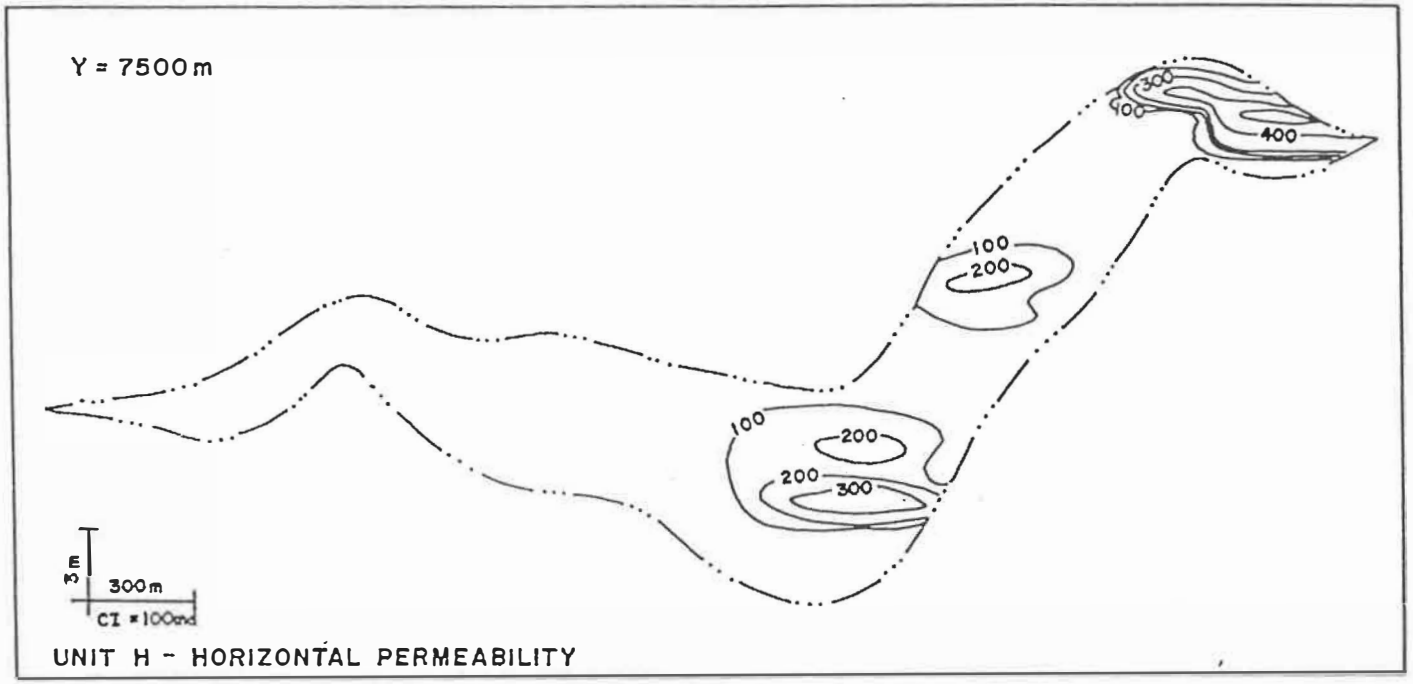

FIGURE 4.8: Cross-section from pool 'H' showing the variation of the reconstructed effective horizontal component of the permeability tensor.

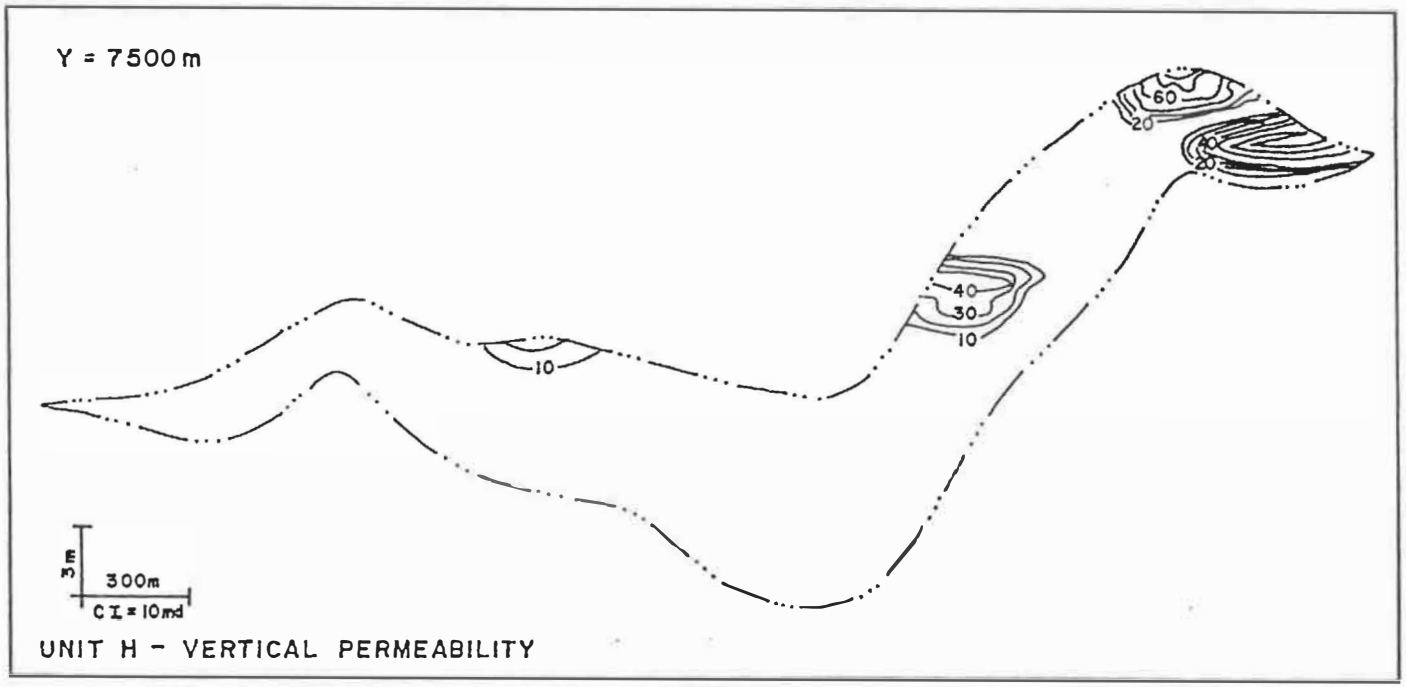

FIGURE 4.9: Cross-section from pool 'H' showing the variation of the reconstructed effective vertical component of the permeability tensor.

Following the approach presented in the previous paragraphs, the logarithmic transforms of macroscopic permeabilities are first conditionally simulated on a dense grid of resolution 30 x 30 m horizontally and 0.5 m vertically. Given that the grid chosen to represent the block model of the pool (megascopic scale) is of 300 x 300 m horizontal and 1 m vertical resolution, the grid for the conditional simulation used here seems sufficiently dense. Nevertheless, the criterion for the chosen grid density is, in this case, the limits of the available computer memory. The total number of conditionally simulated points within the boundaries of pool 'H' are 307000. The histogram of these points is presented in Figure 4.5. Representative horizontal and vertical variograms of the simulated point log-permeabilities are depicted in Figs. 4.6 and 4.7 respectively.

The horizontal and vertical components of the effective permeability tensor are estimated for every one of the 1535 blocks representing pool 'H' at the megascopic scale. The estimation of the components of the effective permeability is based on the geometric mean and variance of the 200 conditionally simulated macroscopic permeabilities in each block as well as the anisotropy ratio of the field. In Fig. 4.8 a cross-section showing the variation of the estimated horizontal permeabilities is presented. The corresponding vertical permeabilities are depicted in Fig. 4.9. The arithmetic, harmonic and geometric means of the same section are plotted in Figs. 4.10, 4.11 and 4.12 respectively. Comparison of the above figures shows, as expected, that the estimated

horizontal permeabilities are higher than the geometric mean while the vertical ones are lower. Furthermore, the horizontal and vertical permeabilities are bounded by the arithmetic and harmonic means respectively. The variation of the logarithmic variance of the section in the previous figures is presented in Fig. 4.13.

4.6 Conclusions

A new approximate approach is used to estimate the components of the effective permeability tensor at the scale of reservoir grid blocks as used in flow simulations, from the sample scale. The suggested methodology is a two step process which includes first the conditional simulation of scalar permeabilities on a high density grid of points representing the reservoir at a fine scale. The second step is the averaging of the simulated values within each grid block using an **ad-hoc** generalization of a Gelhar and Axness (1983) formulae, for the estimation of the effective permeability tensor.

The proposed approach attempts to provide a simple substitute to the direct estimation of effective properties of large reservoir volumes from core data, since direct estimation is not applicable in the case of permeability. Although it has limitations, like any other method proposed for the permeability problem, it provides the means for significantly improving the existing practices at least in the cases of reservoirs

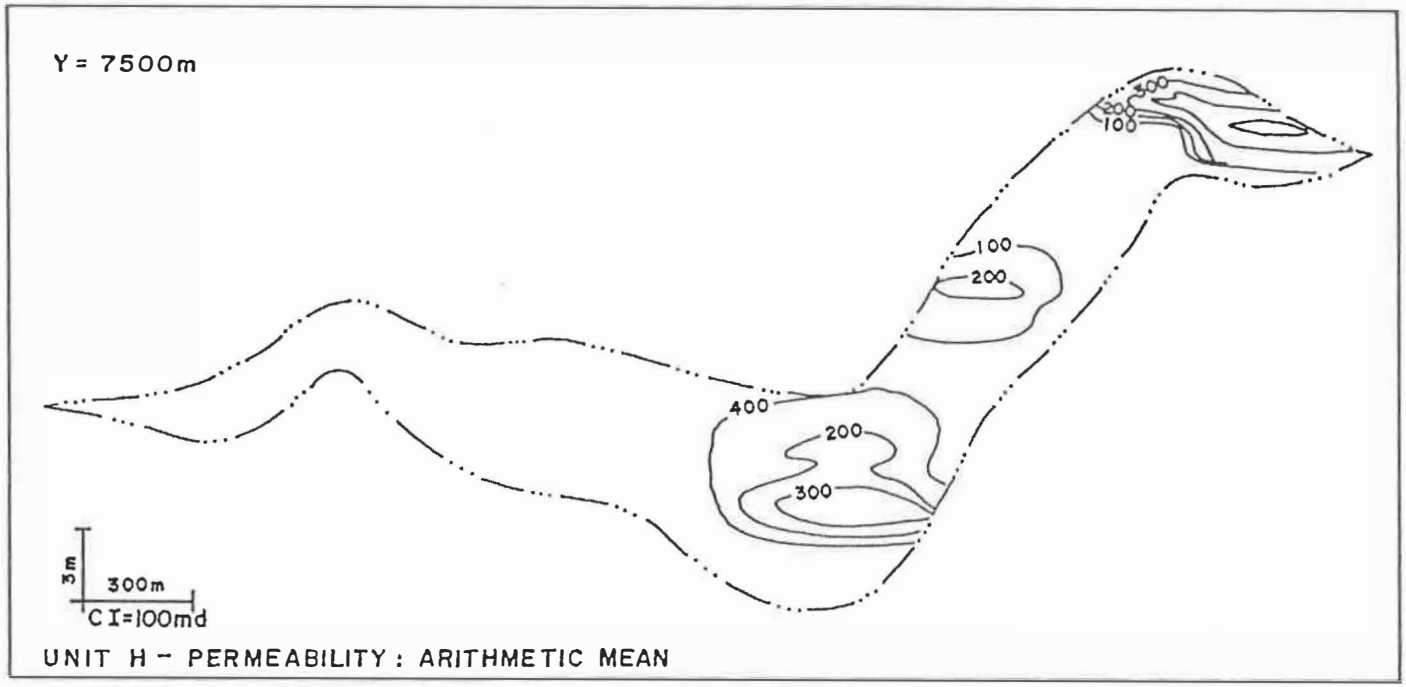

FIGURE 4.10: The same cross-section as in Figs. 4.8 and 4.9 showing the variation of the arithmetic mean of macroscopic permeabilities.

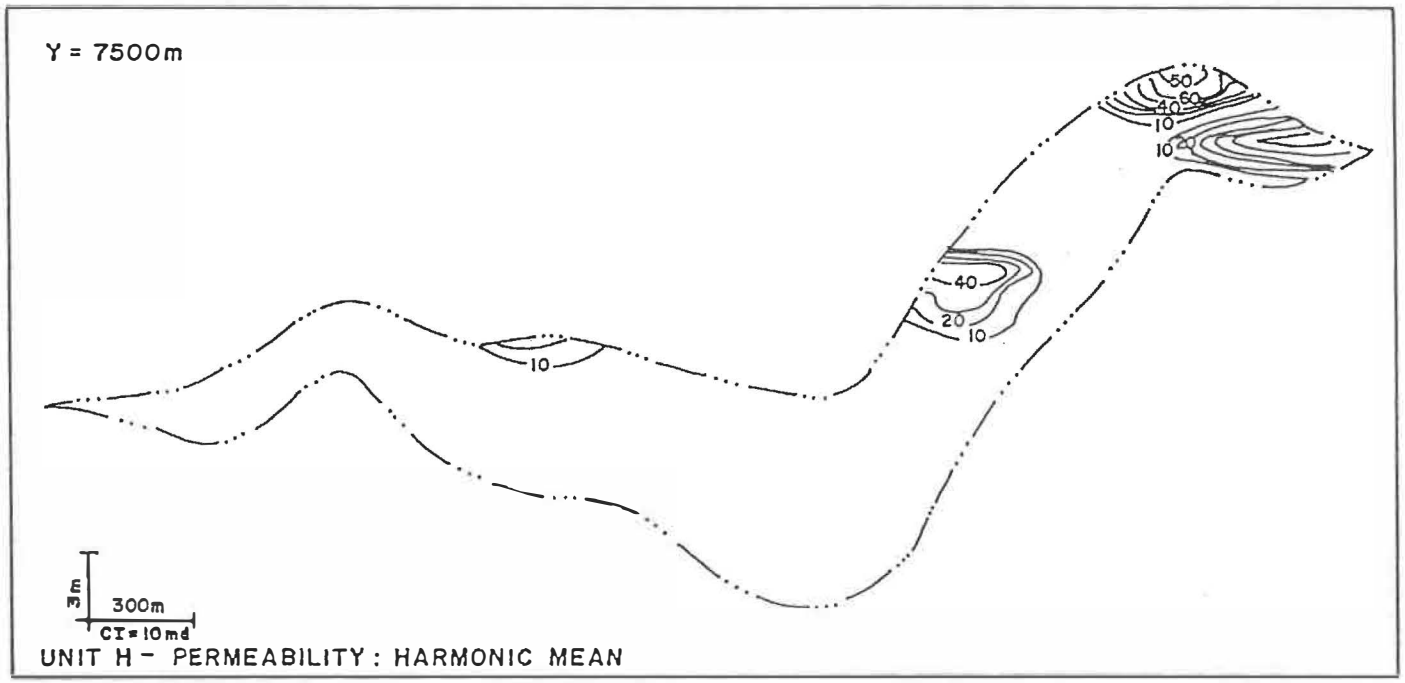

FIGURE 4.11: The same cross-section as in Figs. 4.8 and 4.9 showing the variation of the harmonic mean of macroscopic permeabilities.

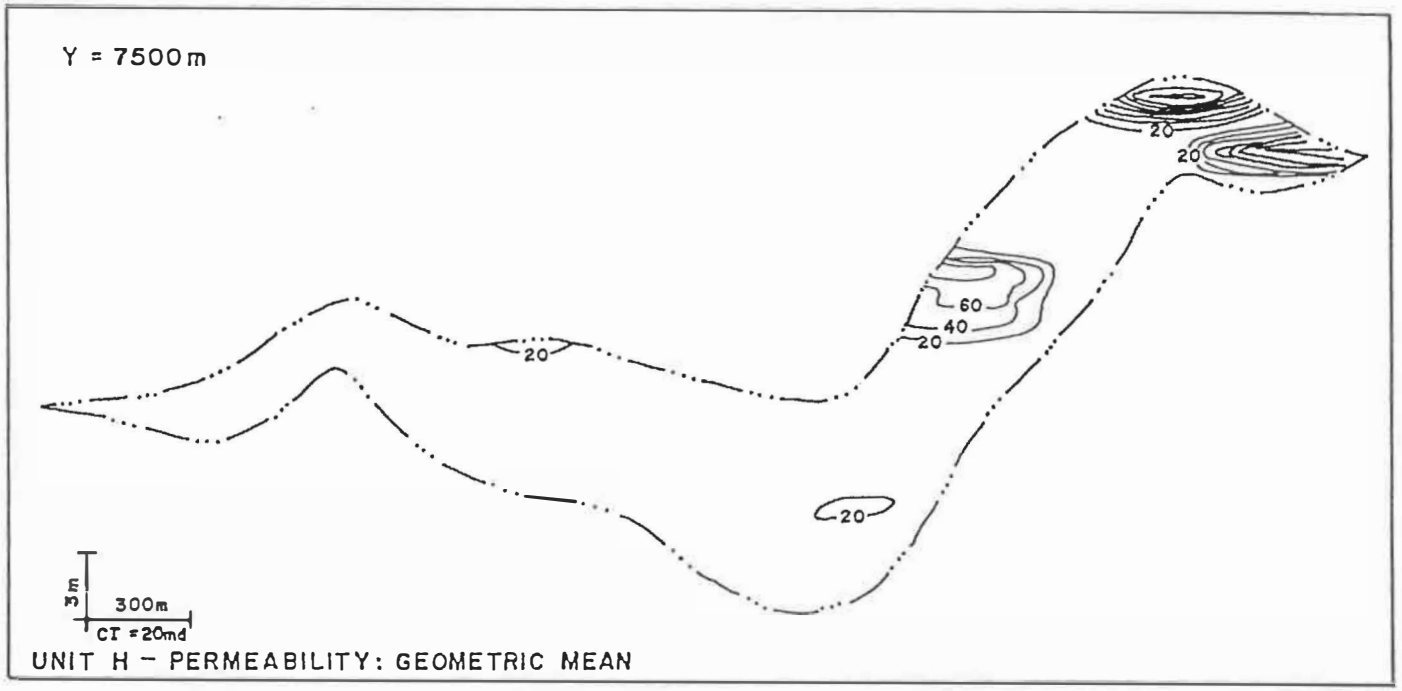

FIGURE 4.12: The same cross-section as in Figs. 4.8 and 4.9 showing the variation of the geometric mean of macroscopic permeabilities.

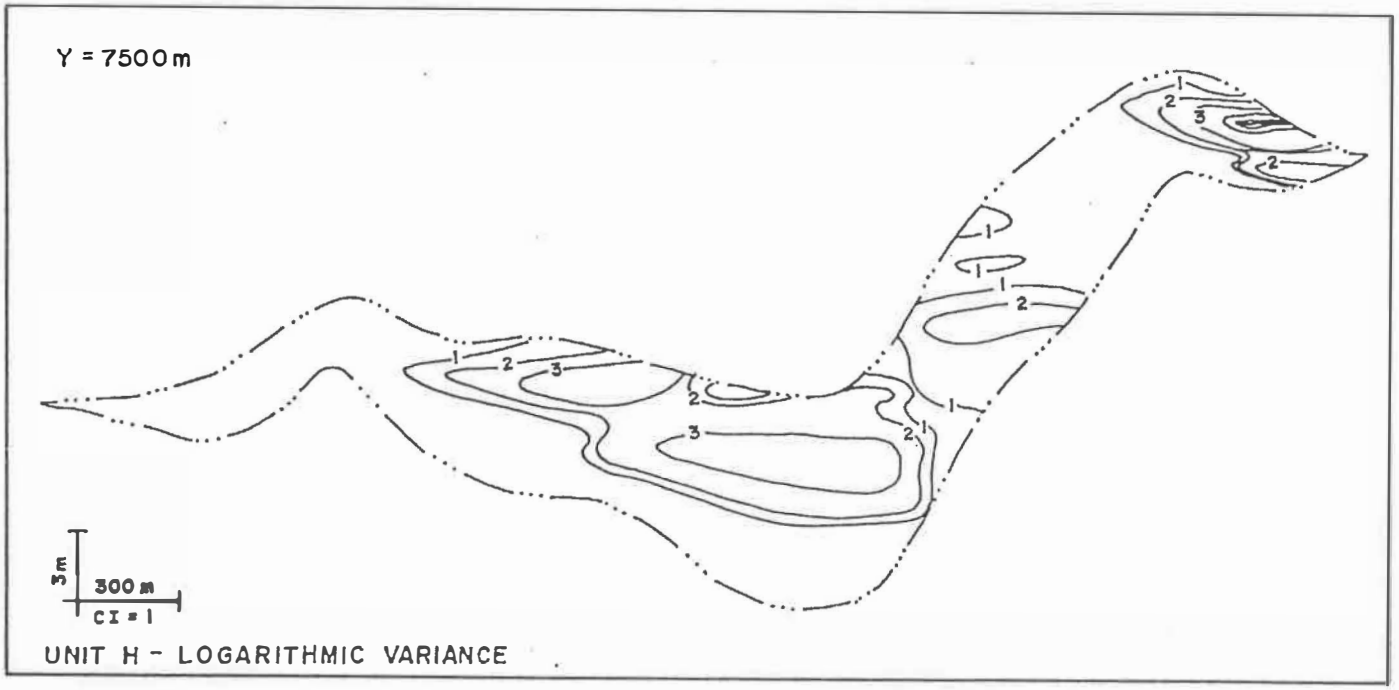

FIGURE 4.13: The same cross-section as in Figs. 4.8 and 4.9 showing the variation of the logarithmic variance of conditionally simulated points within reservoir grid block .

with sufficient geological control to distinguish geologically homogeneous units. The method is demonstrated with an application at the Crystal Viking pool 'H', representing a single sedimentary unit.

5. QUANTITATIVE-NUMERICAL CHARACTERIZATION OF THE CRYSTAL VIKING FIELD, SOUTH-CENTRAL ALBERTA: AN INTEGRATED APPROACH

5.1 Introduction

The Crystal Viking Field is located in south-central Alberta (Figure 4.1) and situated in a north-south orientation within the regional facies of the Lower Cretaceous Viking Formation (Beaumont, 1984; Reinson and Foscolos, 1986) of the western Canadian sedimentary basin. Crystal is a substantial oil field and it has been in production since the early eighties. In order to understand the complexities, assess the primary recovery trends, and predict the behavior of the reservoir particularly under secondary oil recovery schemes, detailed studies were undertaken (Reinson, 1985) to geologically describe and characterize the field. The natural step succeeding the qualitative-geological analysis of the Crystal reservoir is its quantitative-numerical characterization. This is approached with the view expressed in the last few years (Lake and Carroll, 1986) that more emphasis should be given to developing more elaborate and reliable reservoir models.

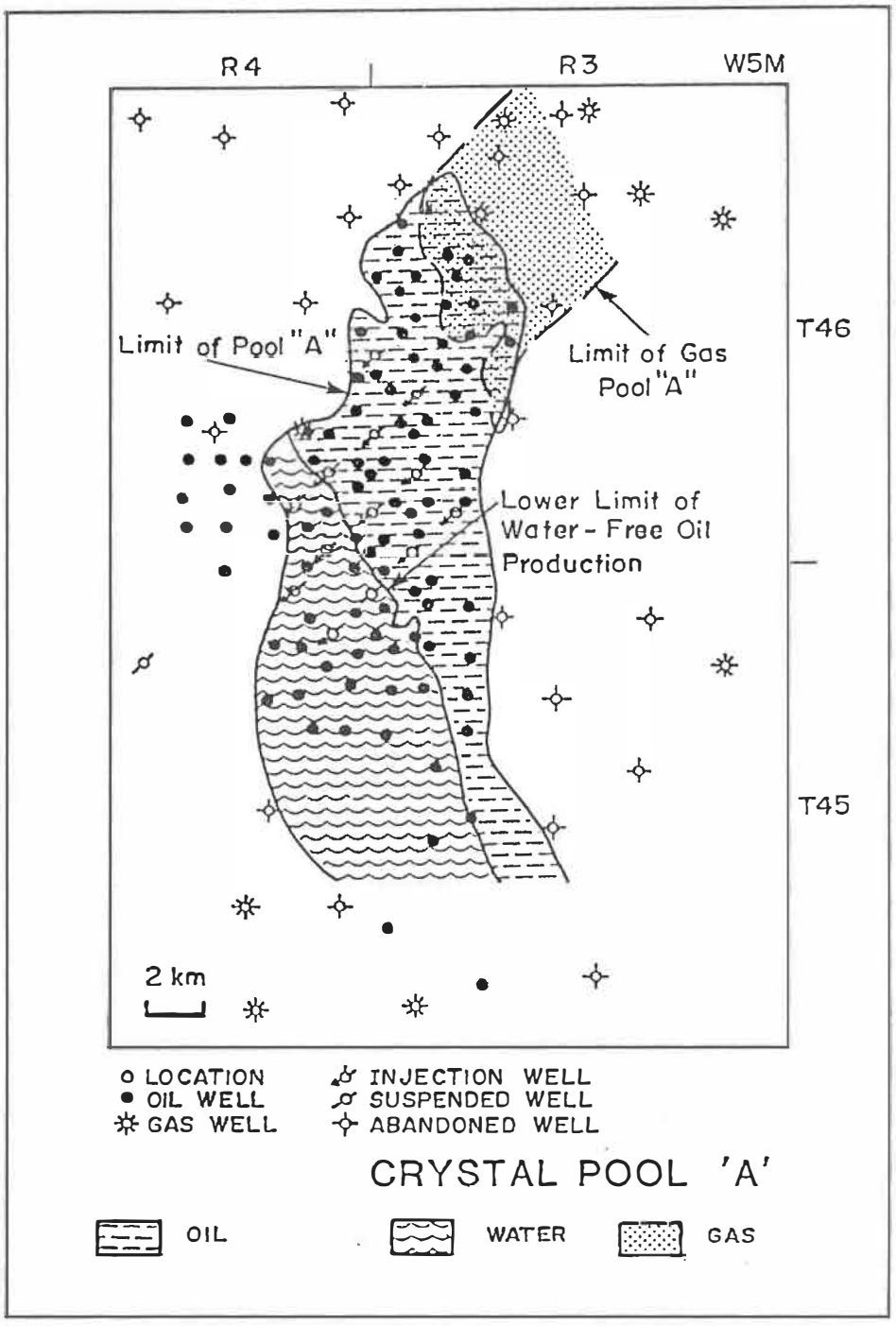

FIGURE 5.1: Pool 'A' of the Crystal Viking field south-central Alberta .

An integrated approach is followed in the quantitative description of the Crystal reservoir, and is based on two aspects: first, a detailed sedimentological model is available to serve as a basis, that is to define distinct, geologically homogeneous units (zones). Second, a geostatistical methodology is utilized. The latter is founded on the statistical analysis of patterns of variations (correlation structures) of available data sets within individual units of the reservoir, accomodating thus the transformation-integration of qualitative descriptions to quantitative models. The use of the geostatistical methods in terms of the theory of intrinsic random functions of order k (Matheron, 1973) has additional significant advantages for reservoir characterization. Geostatistical techniques lead to numerical models which (i) account for naturally occurring correlations, anisotropies and trends within reservoirs; (ii) provide a statistically best, linear, unbiased estimation and estimation variance; (iii) are uniquely appropriate for the direct estimation of effective properties of large volumes from core samples or log measurements; and (iv) can be used to generate simulated realities of any pertinent variable.

The present study was undertaken to complete the characterization of the Crystal Viking reservoir by providing quantification of zonation, continuity, trends, anisotropies and, most importantly, spatial variation of geological variables, upon which the evaluation and assessment of secondary or enchanced oil recovery techniques could be based. Specific objectives of the present study include (i) the complete

quantitative characterization of the Crystal Viking reservoir in terms of sedimentary unit boundaries, porosity, permeability, water saturation and residual oil saturation; and (ii) the demonstration of methodology, abilities and advantages of a synergetic application of geostatistical techniques to petroleum reservoirs.

5.2 Geology of the Crystal Viking Field

The geology of the Crystal Viking field is detailed in terms of sedimentary facies, depositional environments and stratigraphic relationships in Reinson et al. (1988). Accordingly, two major sedimentary facies are distinguished within the reservoir, which ranges up to 30 meters thick. These facies are estuary tidal-channel and estuary bay-fill facies deposited under transgressive conditions. The deposition of the tidal-channel facies is attributed to three successive and partially superimposed channel depositional events. These are referred to as stages A, B and C and correspond to the three distinct sandstone units which constitute the bulk of the reservoir, that is, the Crystal 'A' pool (Figure 5.1). In most of the field the three depositional stages are partially superimposed with downcutting and scouring relationships, while towards the north the three stages diverge. In the southernmost part of Crystal, channel stages appear to amalgamate into one sand body where the different stages bodies are not clearly distinguishable.

The estuary bay-fill facies are divided into subtidal estuarine muddy subfacies (EM) and shallow channel-bar sandstone subfacies (H). The muddy deposits separate the shallow channel-bar facies from the tidal-channel facies of the 'A' pool creating an impermeable barrier, attributing to the hydrodynamically separate 'H' pool (Figure 4.1) within the shallow channel-bar sands. These sands thin-out in the north, while in the south they merge with the tidal channel sands from which they cannot always be distinguished. Schematic cross-sections from north to south depicting the sand bodies A, B, C, H and the muddy deposits EM are presented in Figure 5.2.

The five distinct sedimentary units A, B, C, EM and H form the geological basis in the application of geostatistical techniques for the numerical characterization of the Crystal reservoir.

5.3 Geostatistical Methods

The geostatistical techniques used for the quantitative characterization of the Crystal Viking field are based on the "theory of intrinsic random functions of order k" or IRF-k (Matheron, 1973). A comprehensive presentation and discussion on advantages and applicability of the theory in reservoir characterization problems was detailed in Chapter 2.

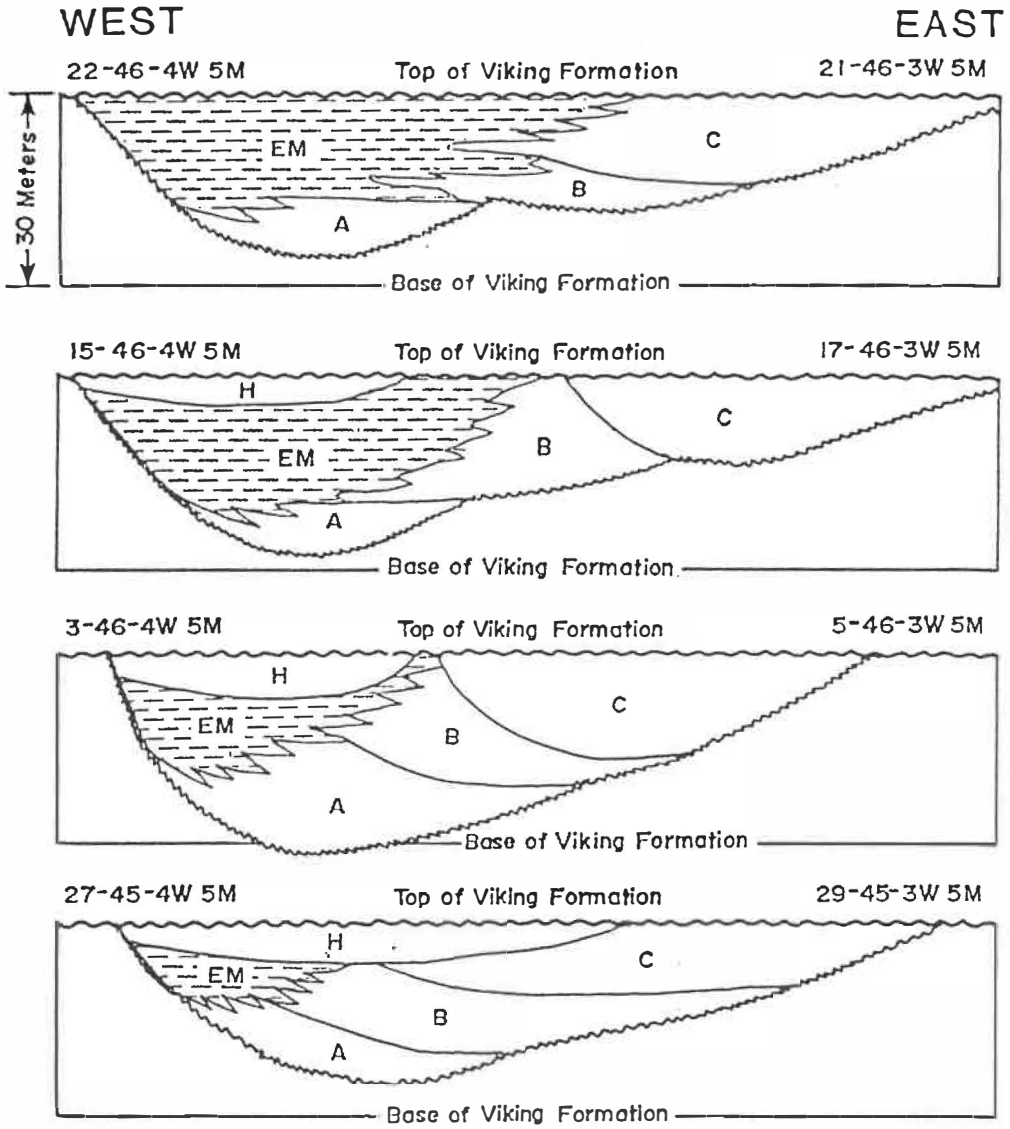

FIGURE 5.2: Schematic cross-sections representing the different depositional units of the Crystal Viking field from north to south (modified after Reinson **et al.**, 1988).

5.4 Data Base Construction

Extensive core data and high-quality geophysical logs are available for the Crystal Field, due both to its recent discovery and development, and to detailed facies analysis studies. Within the area of the field (Figures 4.1 and 5.1), there are 140 wells, of which 112 lie within the limits of 'A' and 'H' pools.

From the available data two major sets are constructed. The first includes the tops and bottoms of the five distinct units in every well in meters below the mean sea level. Tops and bottoms are picked from the available core descriptions for 74 wells while the rest are picked from well-logs. The locations of the wells are also recorded in meters east and north from the lower left corner of the study area.

The second data set includes data on porosity, permeability, residual oil saturation from 74 wells within the limits of the reservoir, derived from core analyses. In addition, the data set includes measurements of water saturation from resistivity logs from 92 wells. Water saturations are calculated from resistivity logs using Archie's equation for clean sands, and it is considered a good approximation, although it may slightly overestimate the actual water saturation when sandstones are not particularly clean. It should also be noted that porosity measurements from porosity logs are included in the data set when core measurements are not available. However, log derived

porosities were not used to provide any statistics on porosity. Finally, every measurement of the present data set is identified and coded with respect to the unit (H, EM, C, B and A) to which it belongs, using the first data set.

5.5 Data Statistics

Simple statistics in terms of histograms of the data sets are presented in this section per variable and unit. Note that unit EM representing shales is of no interest and therefore excluded.

In Figure 5.3 the relative frequency histograms of core sample porosity for units H, C, B and A are presented. They appear to follow a normal distribution as is usually the case with porosities, although units C, B and A exhibit slightly positive skewness. Average porosities range from 9 to 11% with standard deviations ranging from 3 to 4%.

Relative frequency histograms of the log derived water saturations are depicted in Figure 5.4. Apparently, water saturations in units C, A and B exhibit a slight negative skewness. The distribution in unit A with most of the samples over 50% reflects the fact that it is mostly below the oil-water contact as it is known from production data of pool 'A'. Average water saturations range from 58% to 70% with standard deviations from 10 to 18%. The high average water saturations per unit reflect the fact that the water-oil contact of the reservoir

particularily in the 'A' pool, is not a 'clear cut' but rather it is controlled by the sedimentary facies of the reservoir and is thus quite "dispersed" depending on continuity of the facies.

In Figure 5.5, the relative frequency distributions of core sample residual oil saturation are shown. Apparently, the distributions aremore "flat" and skewed than the ones of the previous variables. Furthermore, units H, B and A exhibit a clear bimodality with a large percentage of samples below 1%. The bimodal behavior of these histograms can be explained if one considers the fact that units H, B and A also exhibit high water saturations and the data contributing to bimodality most likely represent samples with very high water saturation and no hydrocarbons in place. Average residual oil saturations range from 3 to 8% with standard deviations from 3 to 5%.

Finally, the histograms of the logarithmic transform of core permeabilities are presented in Figure 5.6. Relative frequency histograms of log-permeability reasonably approximate normal distributions, suggesting that permeability, as is commonly the case, is lognormally distributed. Average permeabilities range from 10 to 26 md with standard deviations from 13 to 32 md. Statistics of permeability data per unit are summarized in Table 5.1.

The histograms of the pertinent variables present some average characteristics of the available data. The most important of these is

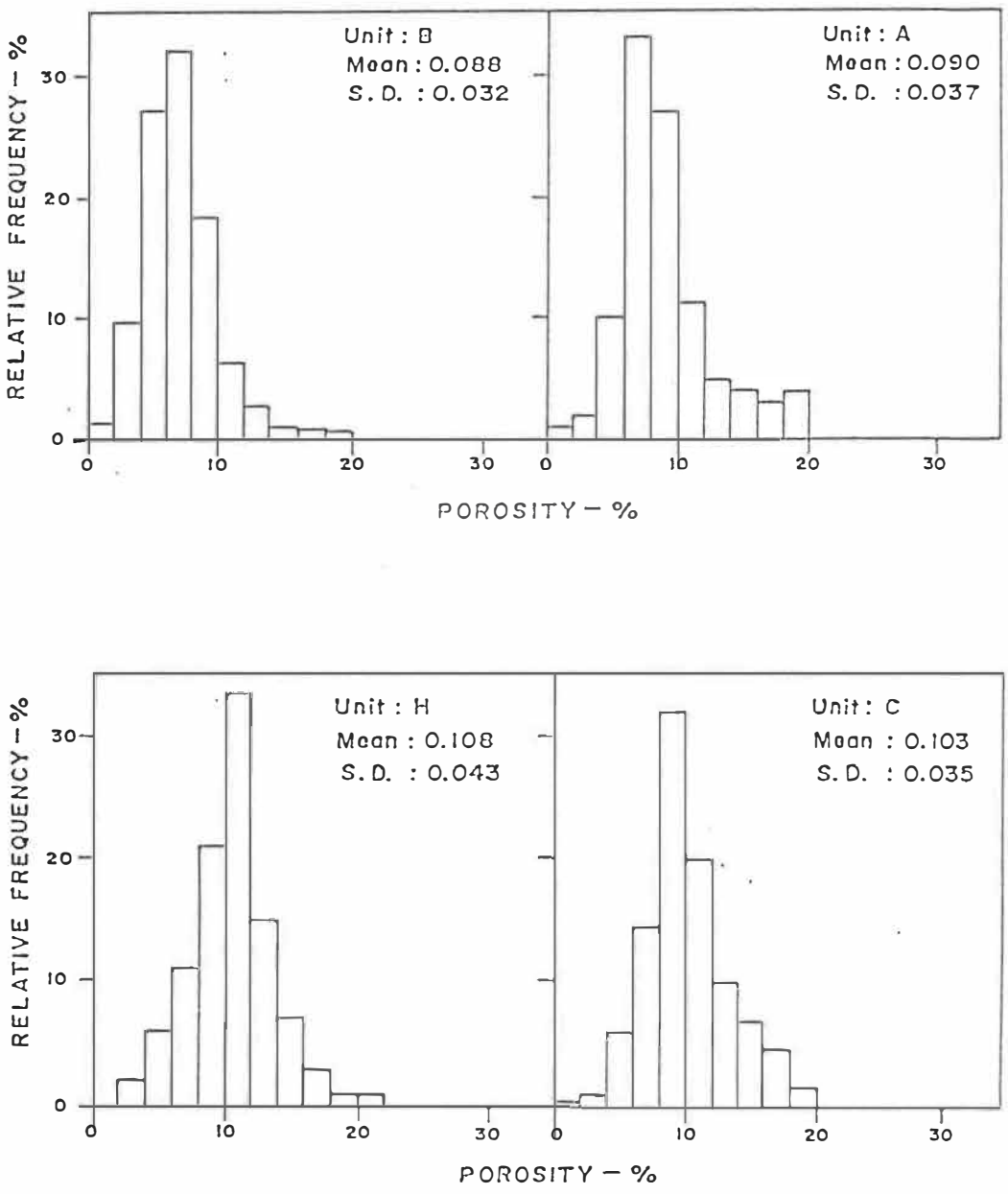

FIGURE 5.3: Relative frequency histograms of core sample porosity per unit of the Crystal field .

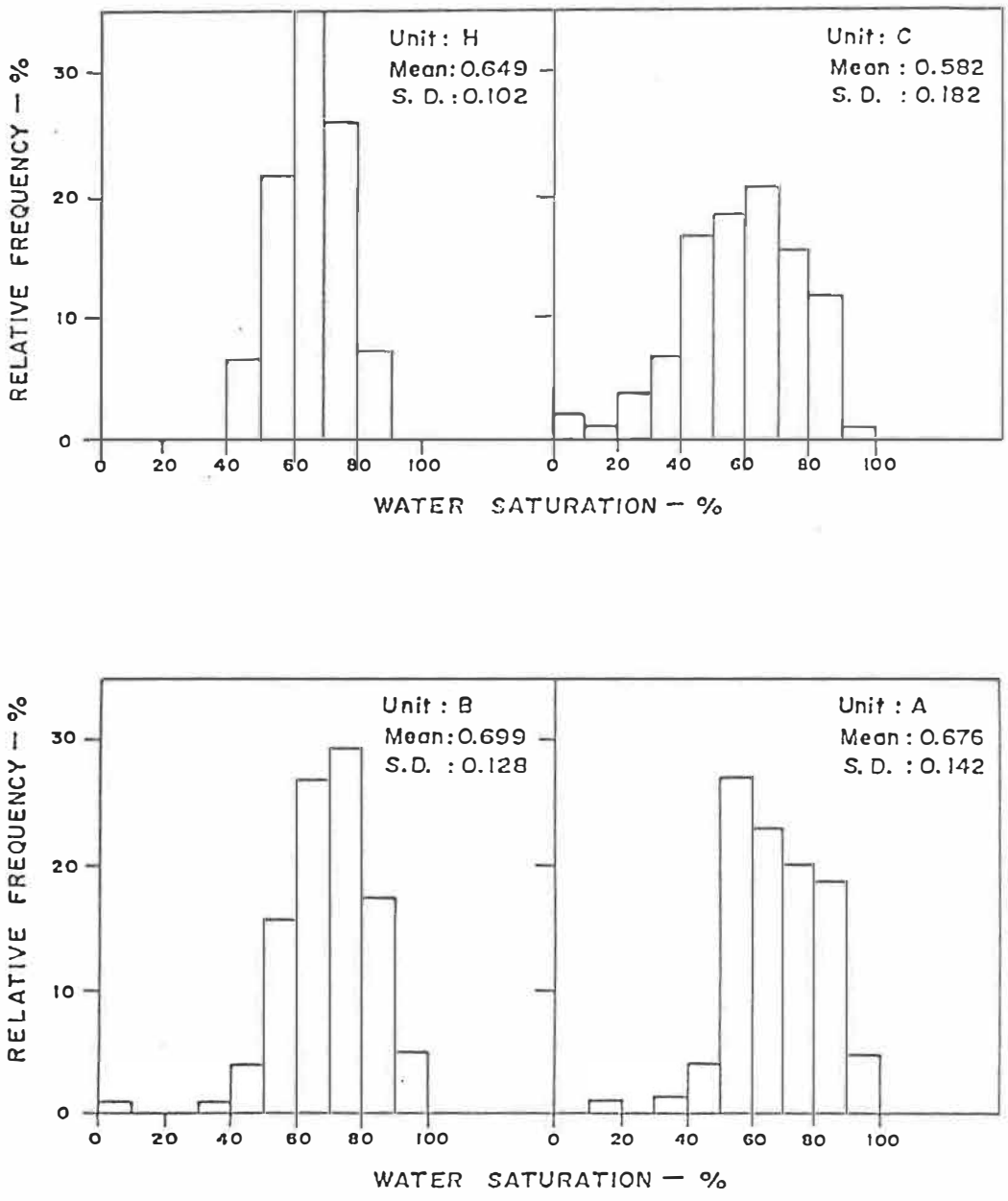

FIGURE 5.4: Relative frequency histograms of log derived water saturation per unit of the Crystal Viking field .

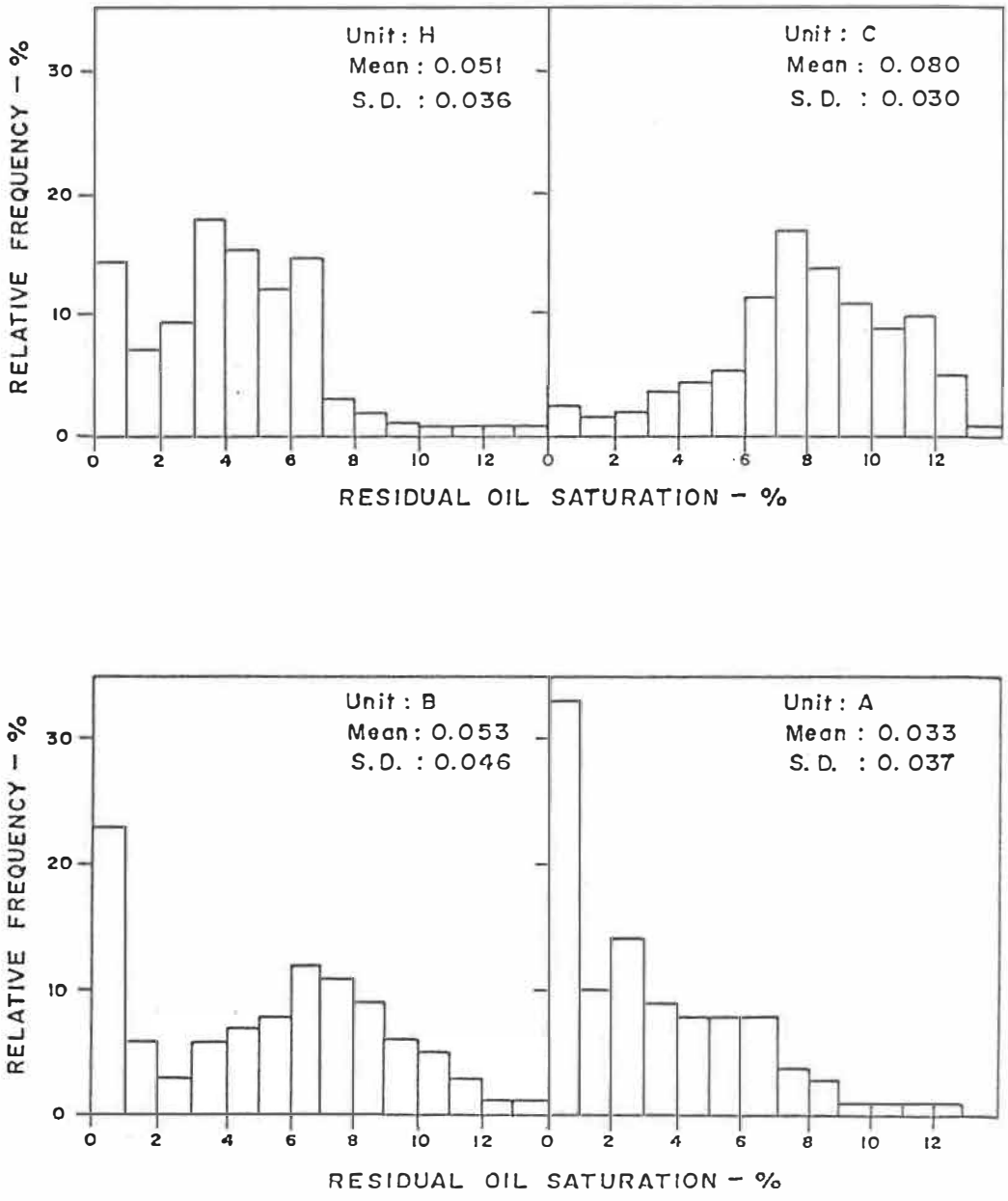

FIGURE 5.5: Relative frequency histograms of core sample residual oil saturation per unit of the Crystal field .

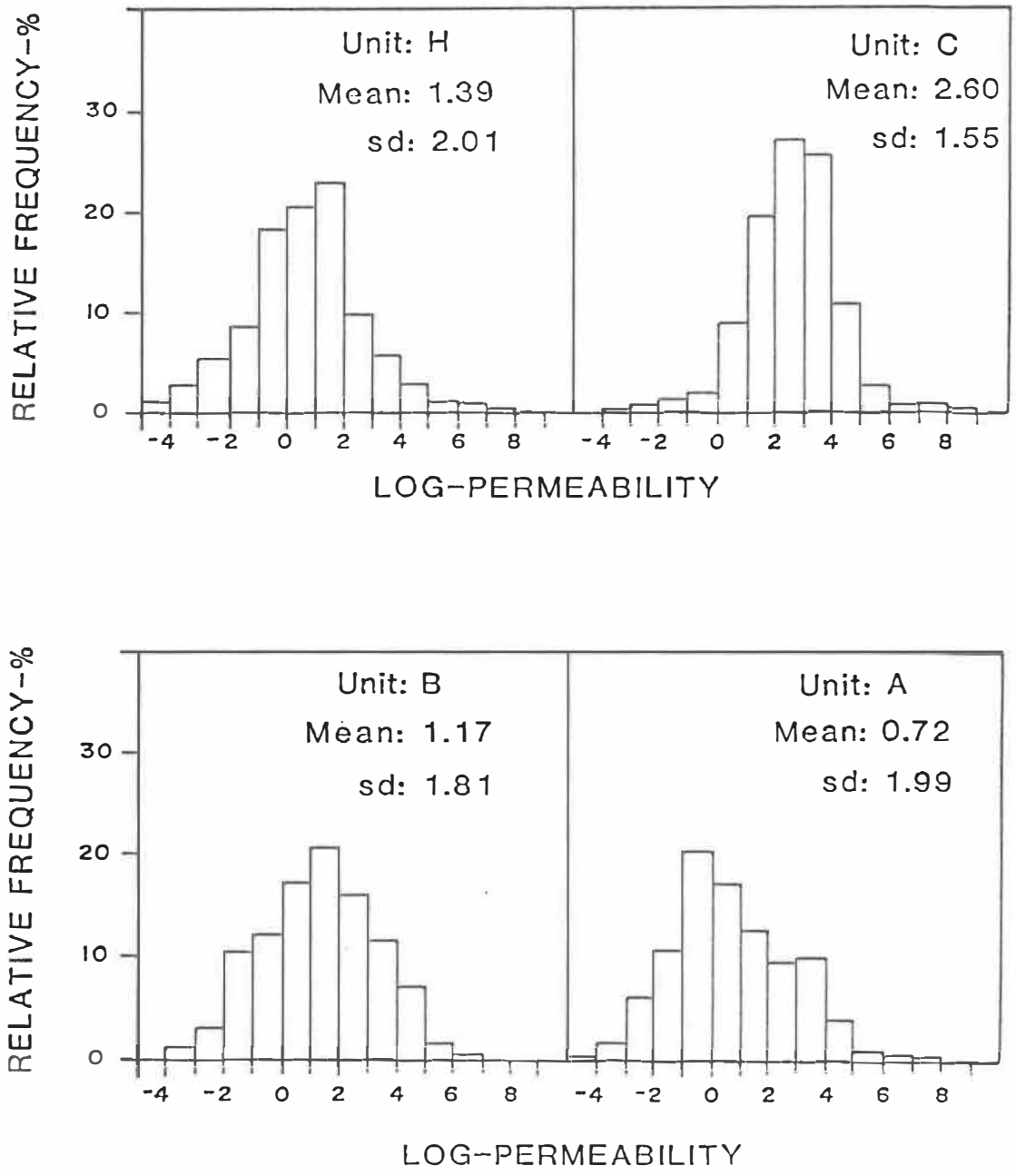

FIGURE 5.6: Relative frequency histograms of core sample log-permeability per unit of the Crystal field .

TABLE 5.1 - Summary statistics of core sample permeabilities and log-permeabilities per unit of the Crystal reservoir.

	Permeability (md)		Log-permeability	
Unit	Mean	Standard Deviation	Mean	Standard Deviation
H	19.11	32.13	1.39	2.02
C	26.42	29.87	2.60	1.56
B	10.91	16.91	1.17	1.81
A	10.58	13.71	0.72	1.99

that they exhibit unimodal distributions, with the exception of residual oil saturation in some of the units. The unimodality of the distributions may be seen as a statistical verification that indeed the sedimentary units H, C, B and A represent single populations as far as their properties are concerned. It could be suggested that, perhaps, additional units could be defined to accomodate the bimodality of residual oil saturation histograms in units H, B and A. This could be done if it was possible to clearly identify the oil-water contact. The latter, however, is not identifiable because water saturation is not controlled by gravity but rather by the sedimentary facies, their interrelations and continuity. In addition, further subdivision of the reservoir could create other implications such as insufficient data in the new units to perform statistical analysis. Finally, it should be noted that the IRF-k theory does not impose any restrictions on the data statistics. The only exception is permeability as it is later discussed.

5.6 Inherent Structural Characteristics of the Data

The average variation patterns (structures) of all pertinent variables for each sandstone unit in the Crystal field are quantified, in the present section, in the form of generalized covariances or variograms.

First, the order k and coefficients of the corresponding generalized covariances of the tops and bottoms of units H, EM, C, B and A

are inferred from the data using a minimization technique (Davis and David, 1978). The corresponding order and coefficients for all units are given in Table 5.2. The existing trend in all data sets is linear (k=1) most likely reflecting the general south-east dip of the reservoir in combination with its north-south channel-like shape.

The generalized covariances of core sample porosities are calculated for both the horizontal plane (well to well) and vertically (down-hole) for every unit. All generalized covariances are inferred from the corresponding experimental variograms presented for units H, C, B and A in Figures 5.7, 5.8, 5.9 and 5.10 respectively. The experimental variograms suggest, in all data sets and directions, the existance of a constant trend (k=0). The coefficients of the generalized covariances are calculated from the equivalent variograms fitted to the experimental variograms and are given in Table 5.3. The experimental variograms also indicate the existence of anisotropies expressed with the more rapid increase of the variogram values in the vertical variograms than in the horizontal ones. This suggests better continuity on the plane, which is expected considering the natural near-horizontal stratification of the reservoir. Furthermore, experimental variograms exhibit fluctuation around the fitted models. In general, such fluctuations reflect either simple sampling variations or structural aspects such as the clustering or alternation of low and high values. The fluctuation of the present experimental variograms should most likely be attributed to sampling variations, since persistant or distinct periodicity do not appear.

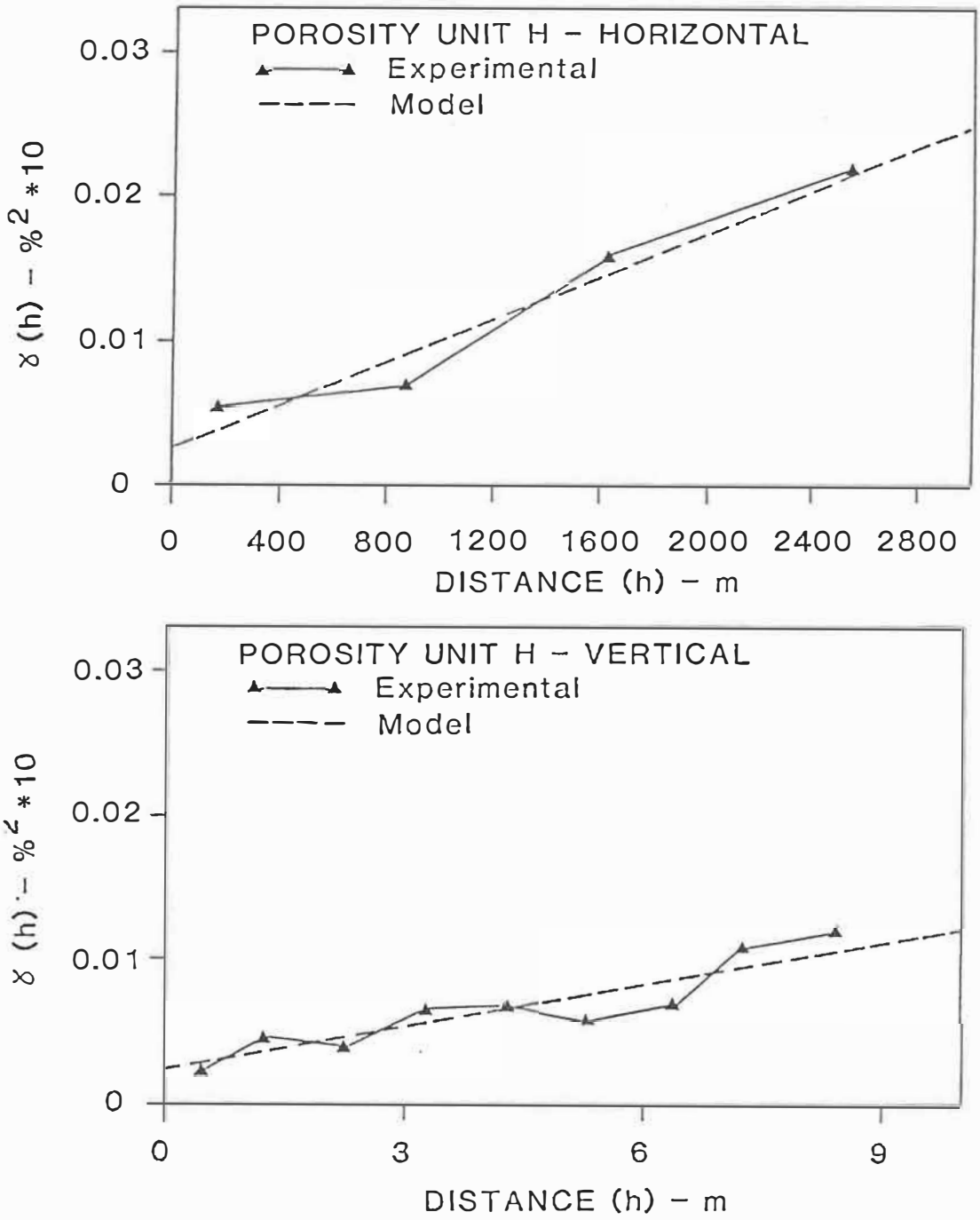

FIGURE 5.7: Experimental and model variograms of core sample porosity in unit H; average horizontal (top) and vertical (bottom).

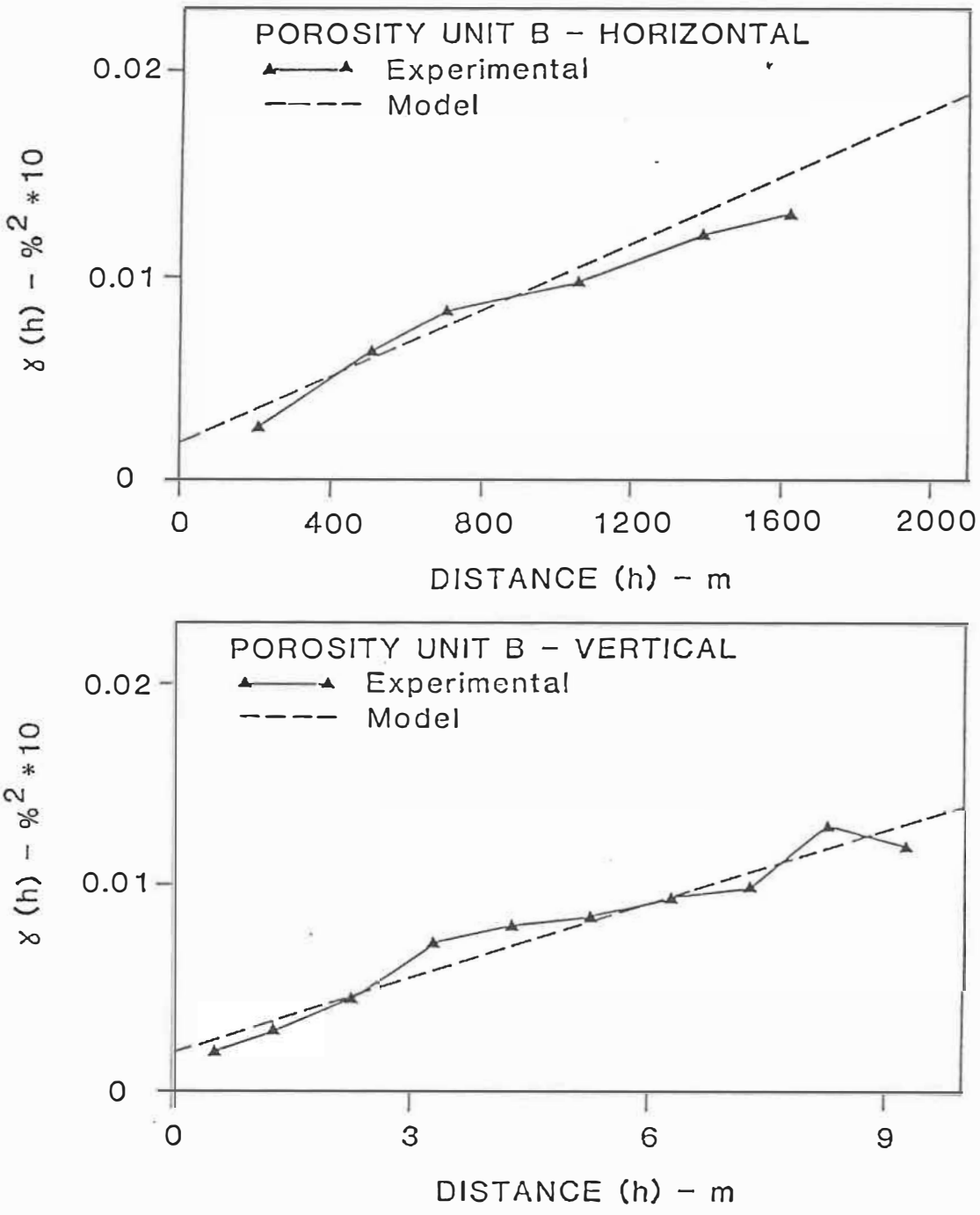

FIGURE 5.8: Experimental and model variograms of core sample porosity in unit C; average horizontal (top) and vertical (bottom) .

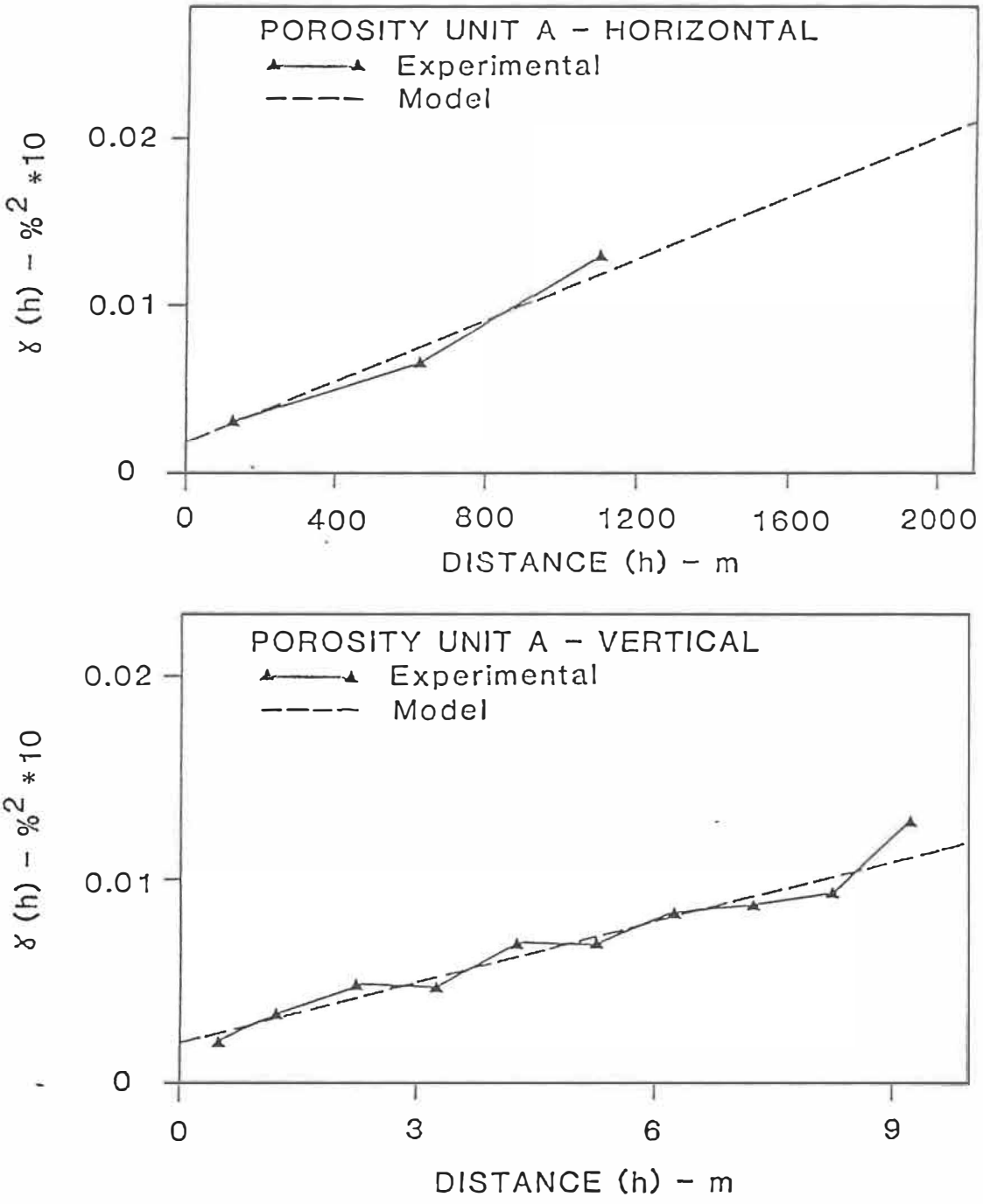

FIGURE 5.9: Experimental and model variograms of core sample porosity in unit B; average horizontal (top) and vertical (bottom).

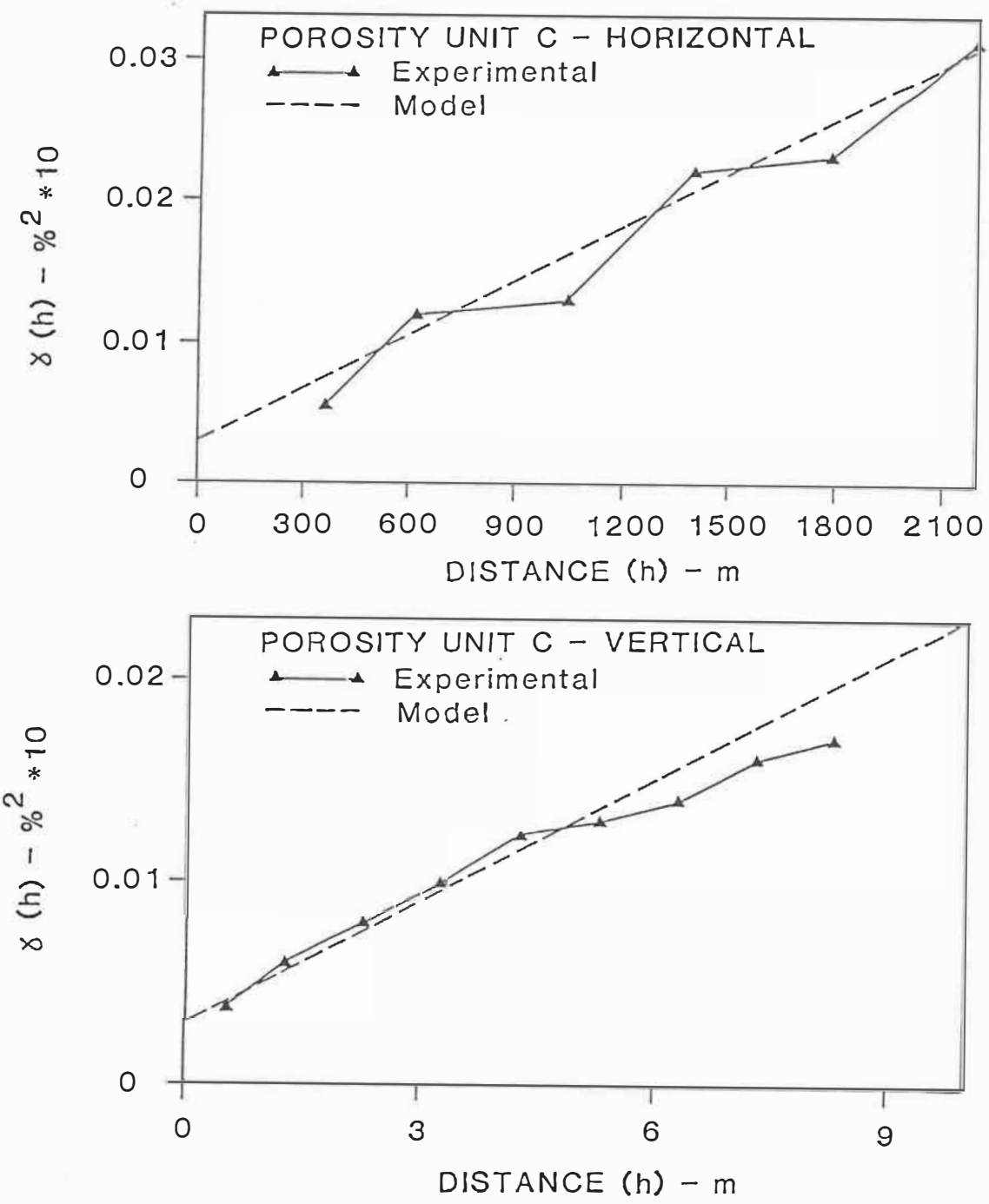

FIGURE 5.10: Experimental and model variograms of core sample porosity in unit A; average horizontal (top) and vertical (bottom) .

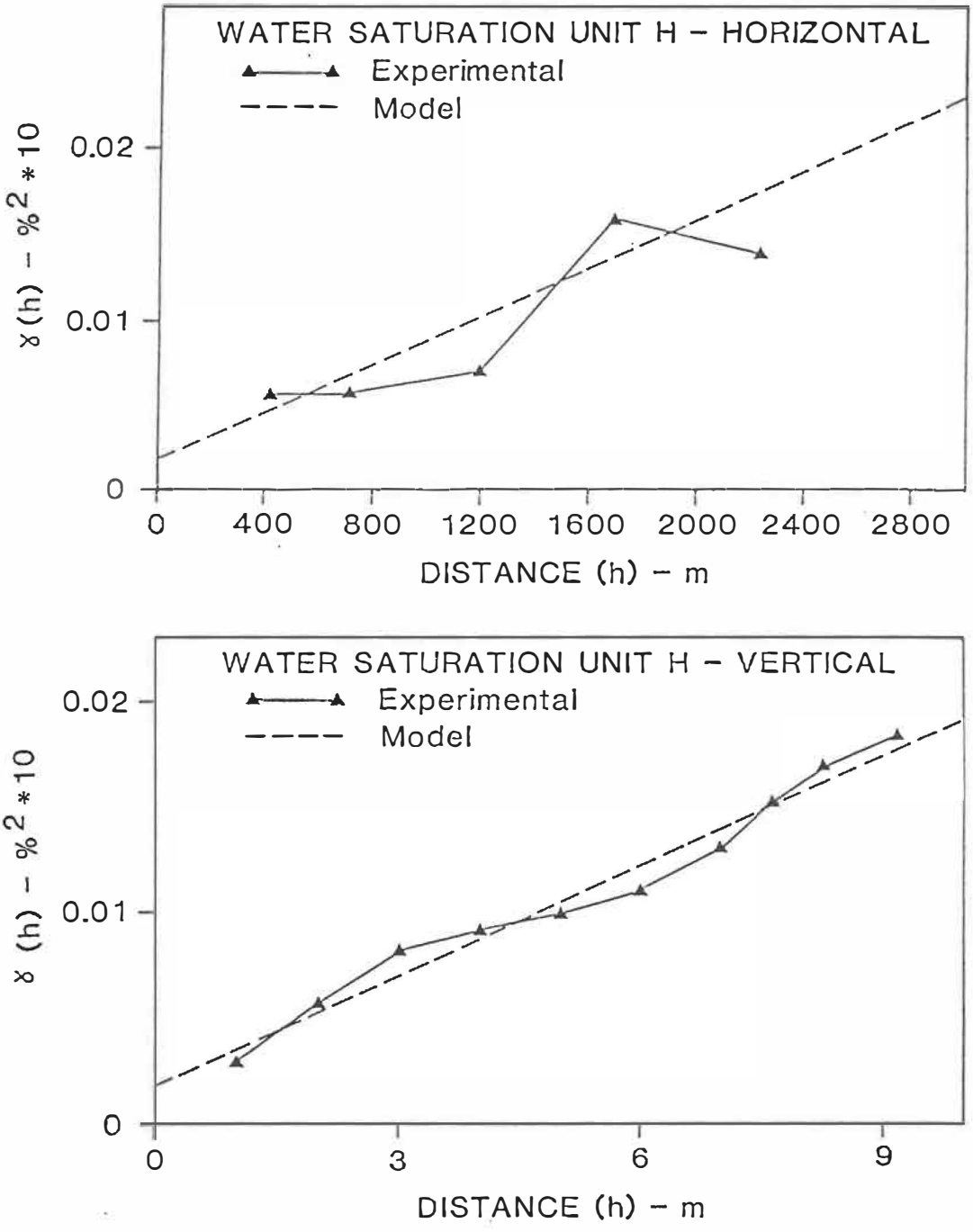

FIGURE 5.11: Experimental and model variograms of log derived water saturation in unit H; average horizontal (top) and vertical (bottom) .

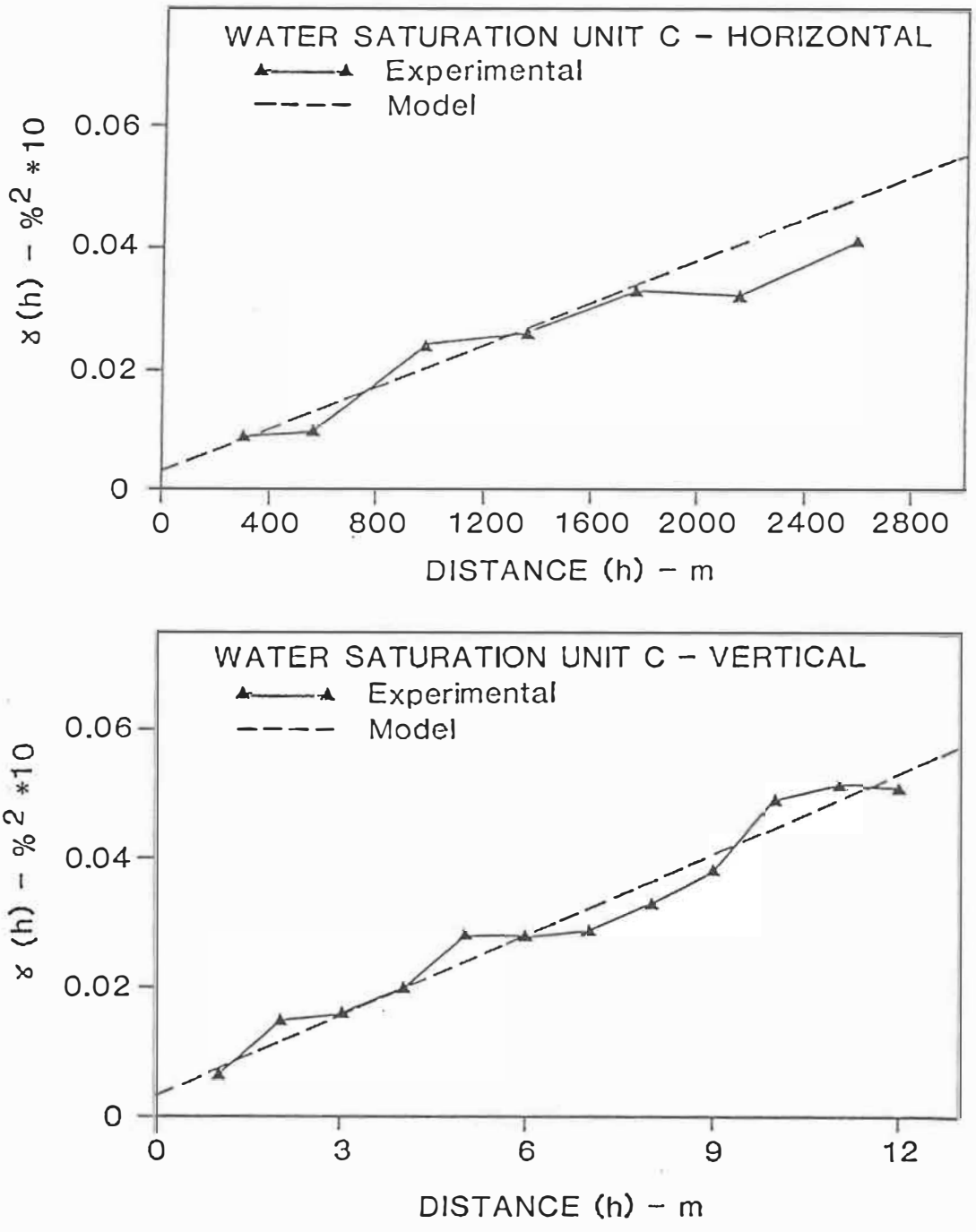

FIGURE 5.12: Experimental and model variograms of log derived water saturation in unit C; average horizontal (top) and vertical (bottom) .

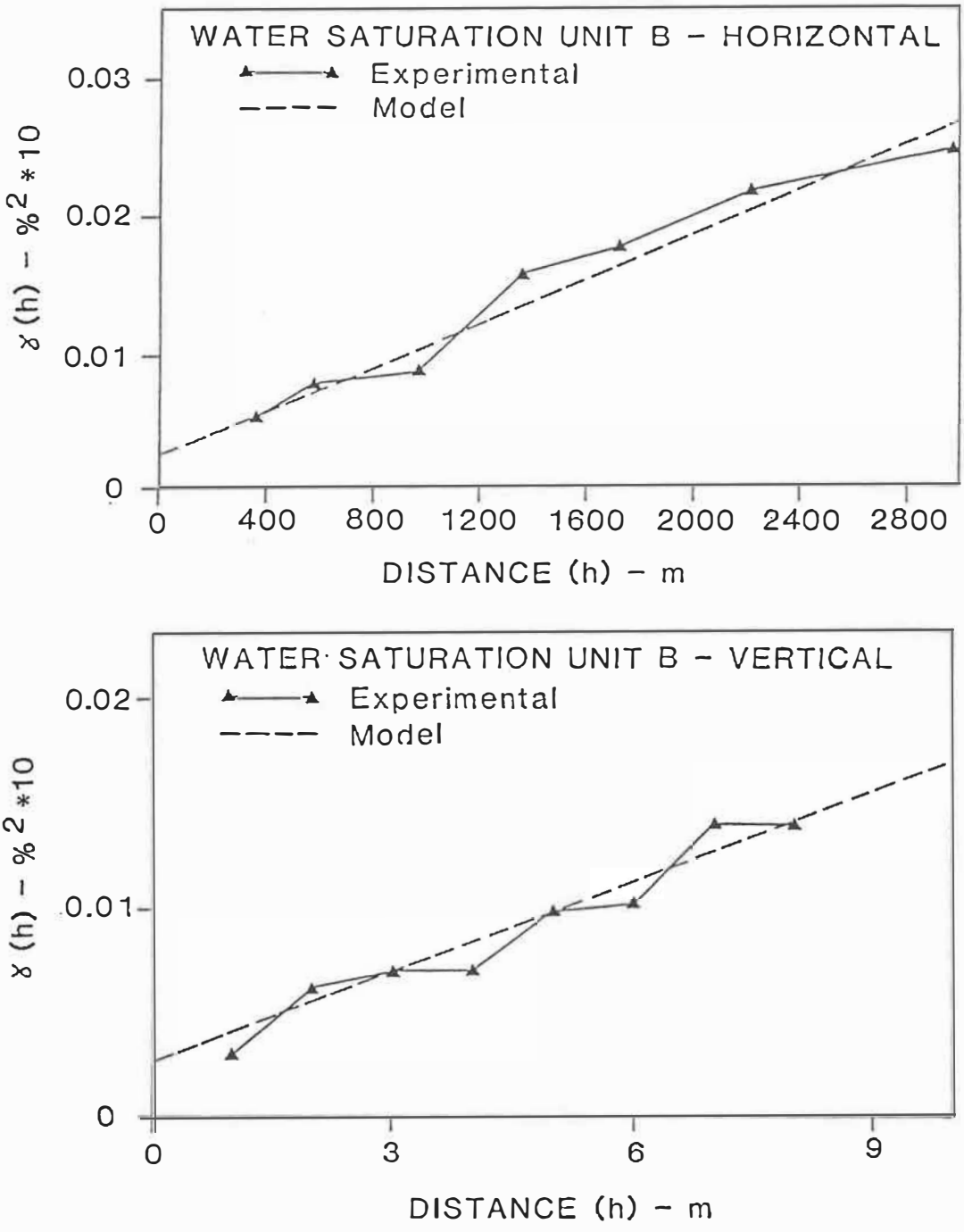

FIGURE 5.13: Experimental and model variograms of log derived water saturation in unit B; average horizontal (top) and vertical (bottom) .

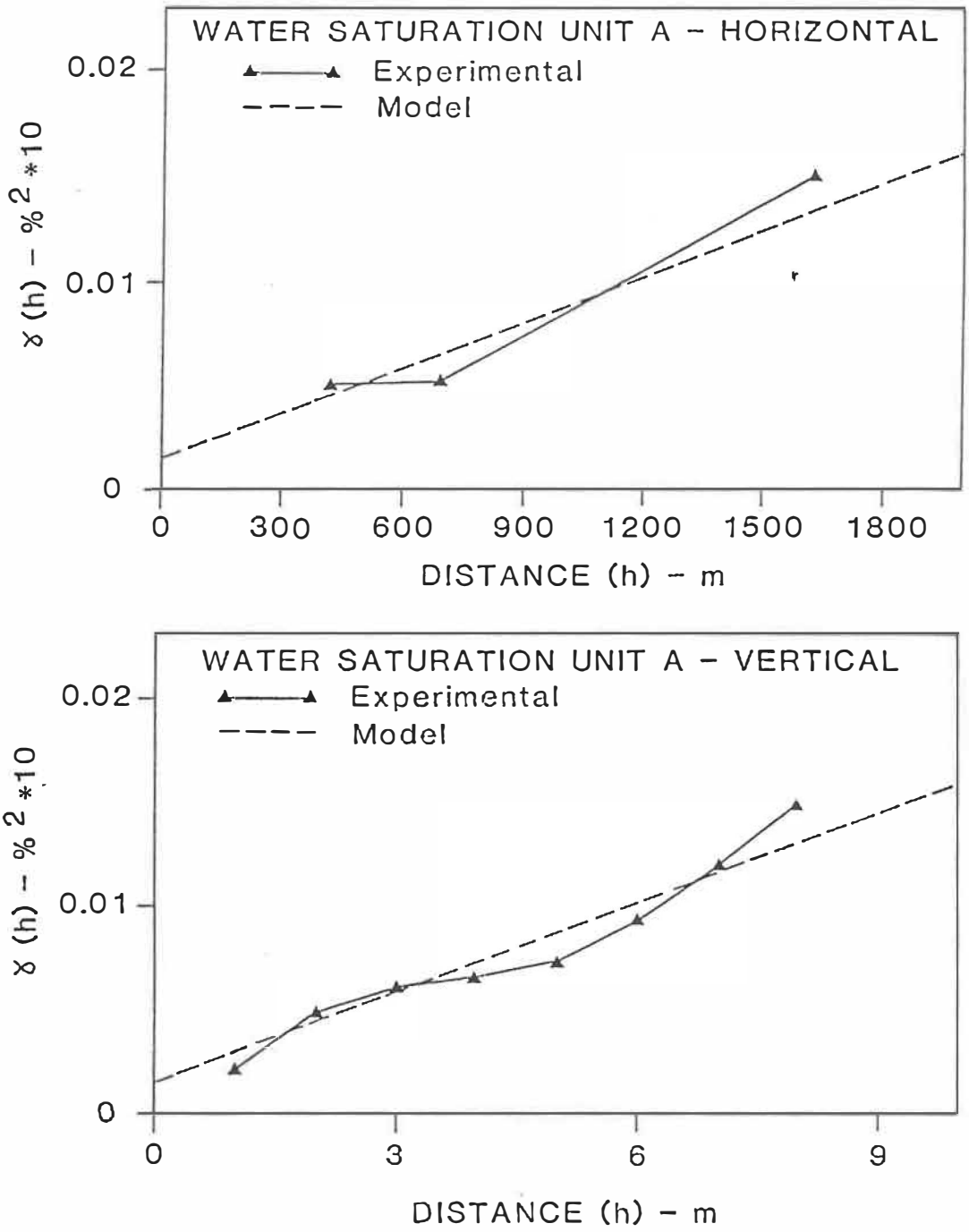

FIGURE 5.14: Experimental and model variograms of log derived water saturation in unit A; average horizontal (top) and vertical (bottom) .

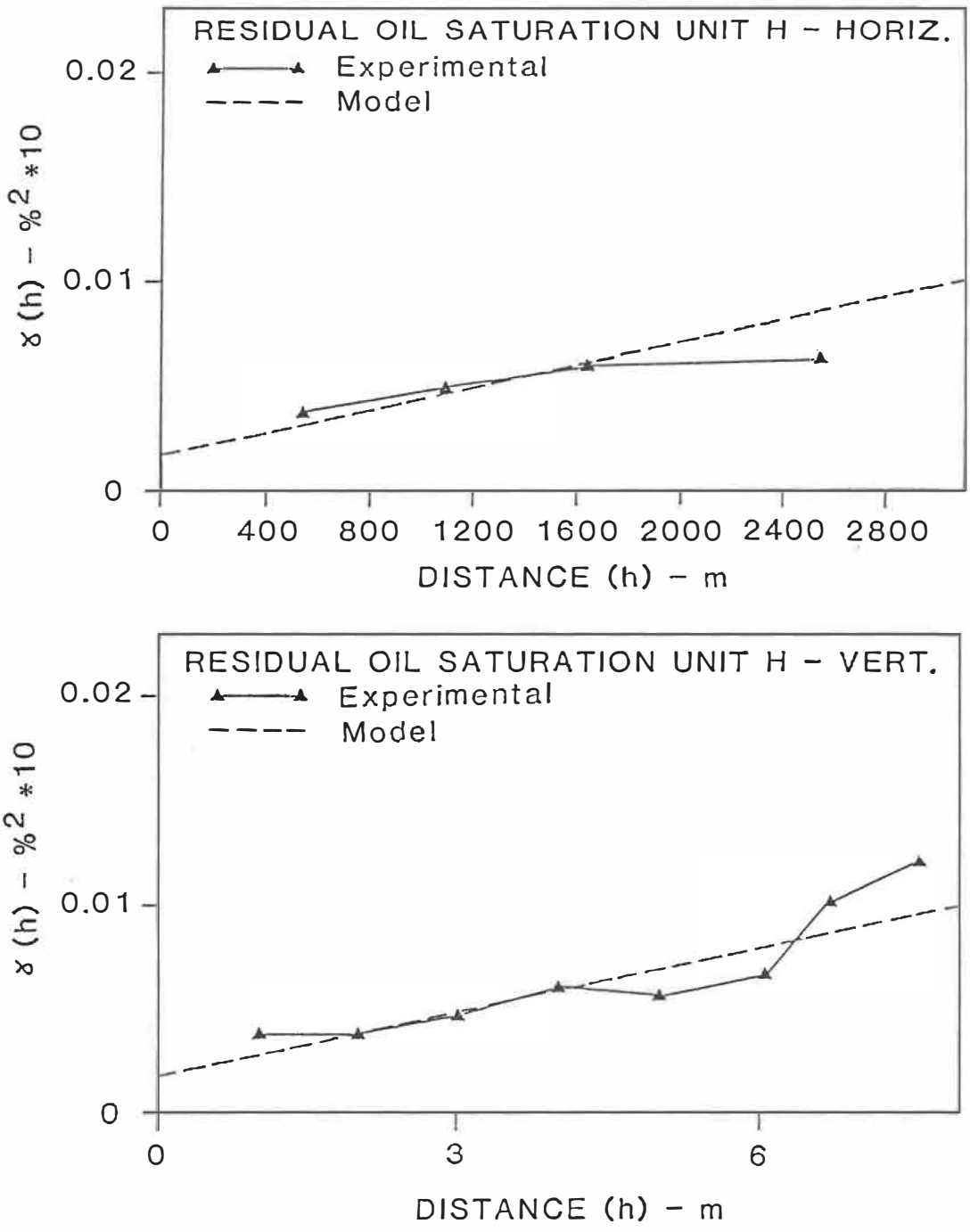

FIGURE 5.15: Experimental and model variograms of core sample residual oil saturation in unit H; average horizontal (top) and vertical (bottom) .

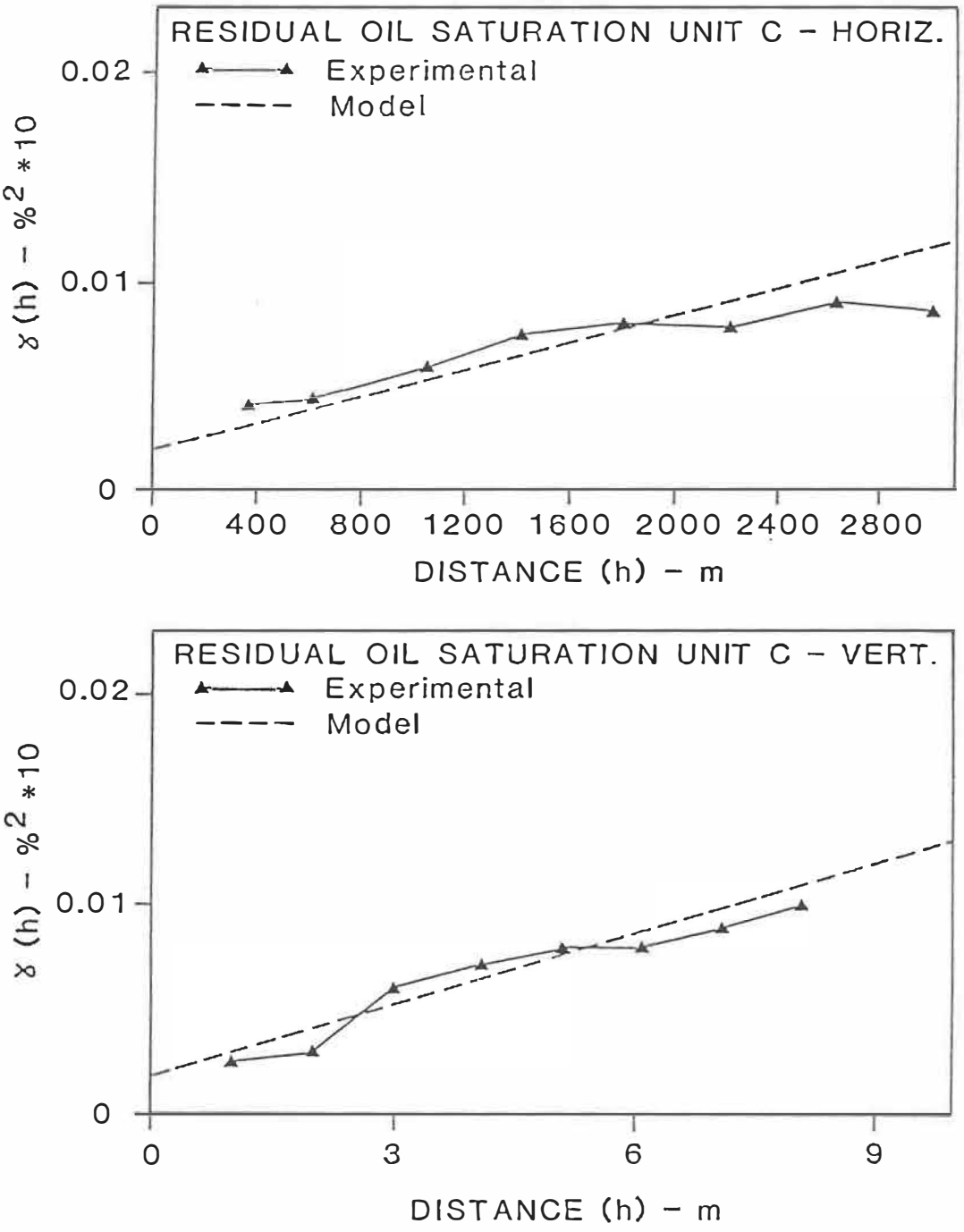

FIGURE 5.16: Experimental and model variograms of core sample residual oil saturation in unit C; average horizontal (top) and vertical (bottom) .

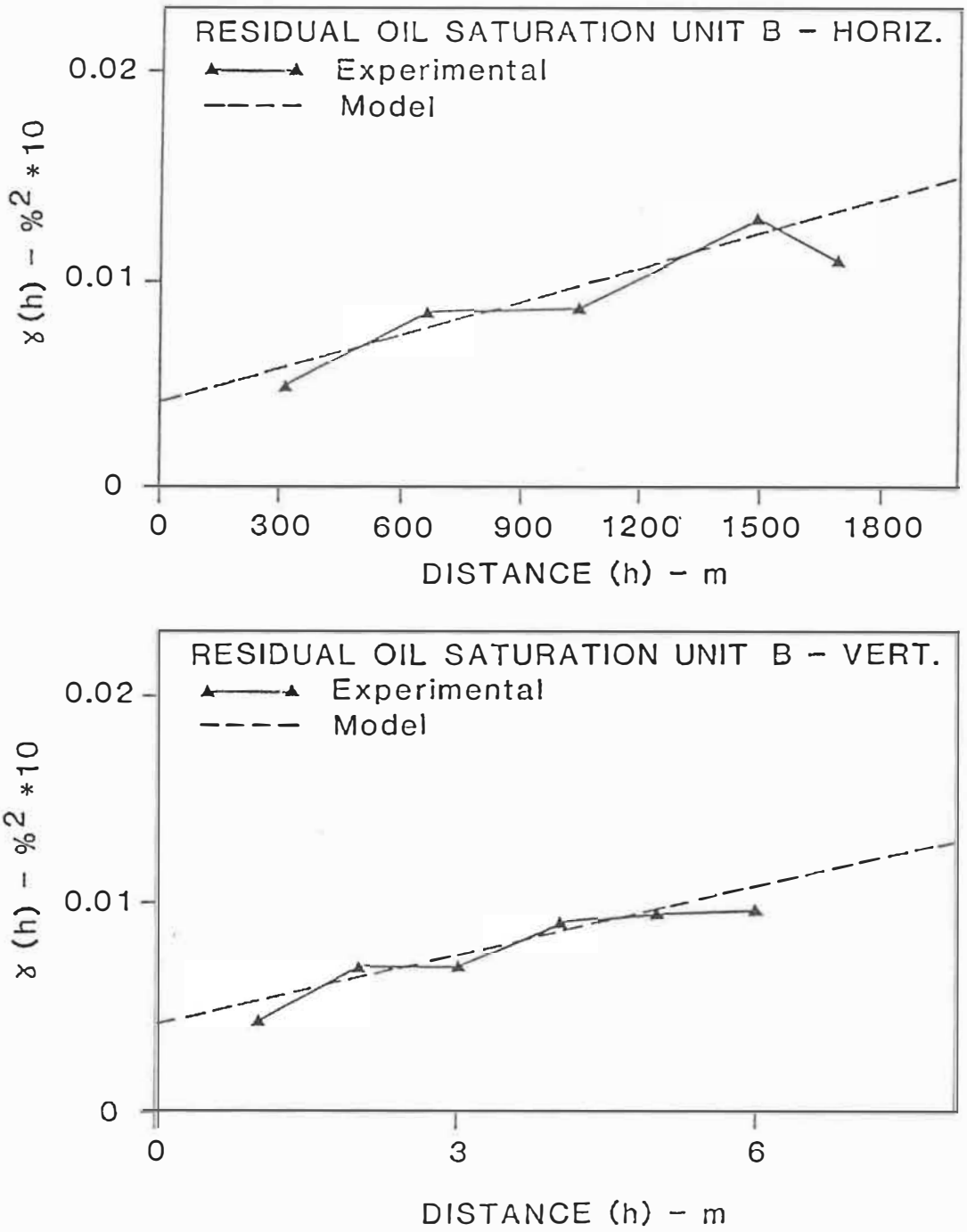

FIGURE 5.17: Experimental and model variograms of core sample residual oil saturation in unit B; average horizontal (top) and vertical (bottom) .

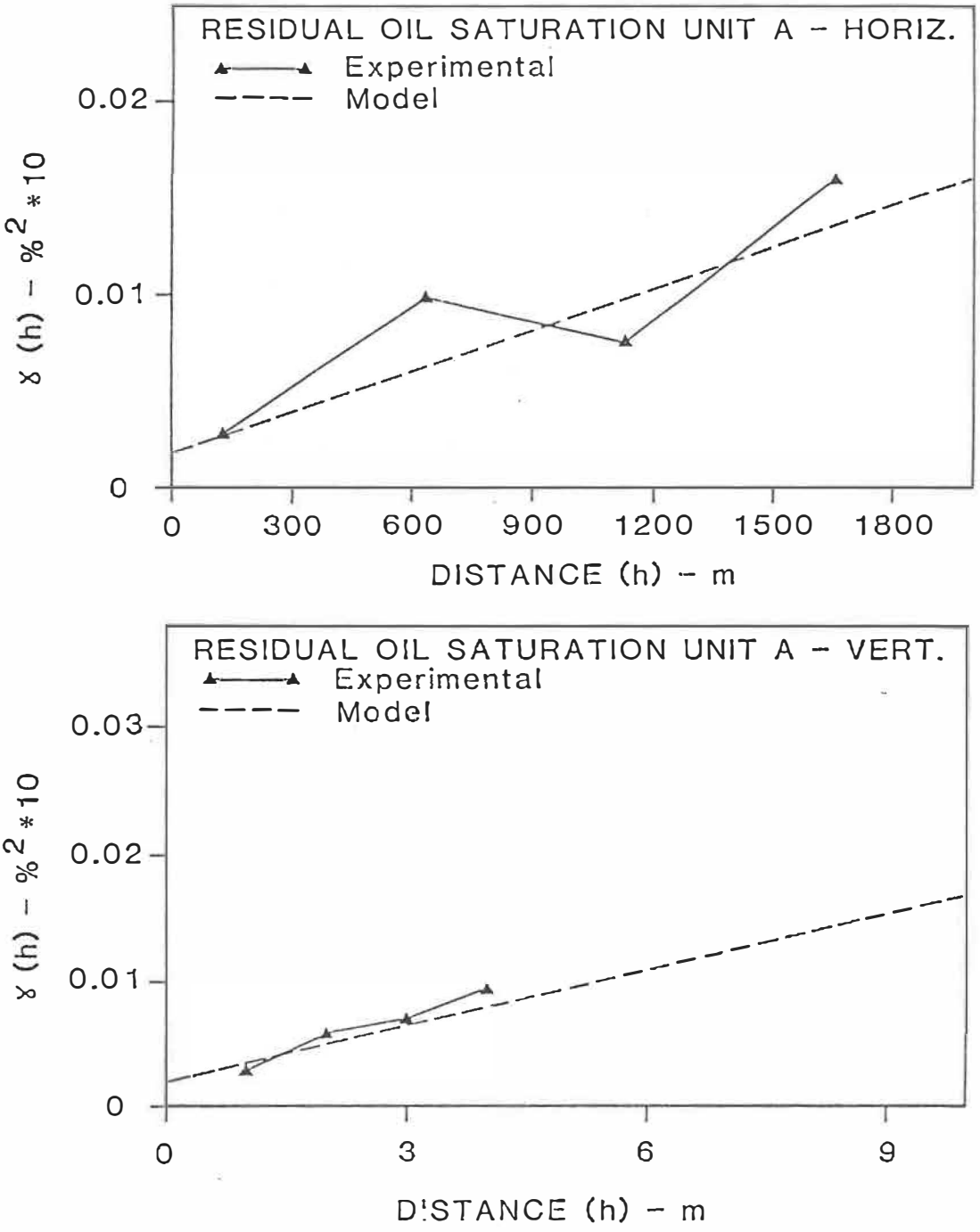

FIGURE 5.18: Experimental and model variograms of core sample residual oil saturation in unit A; average horizontal (top) and vertical (bottom) .

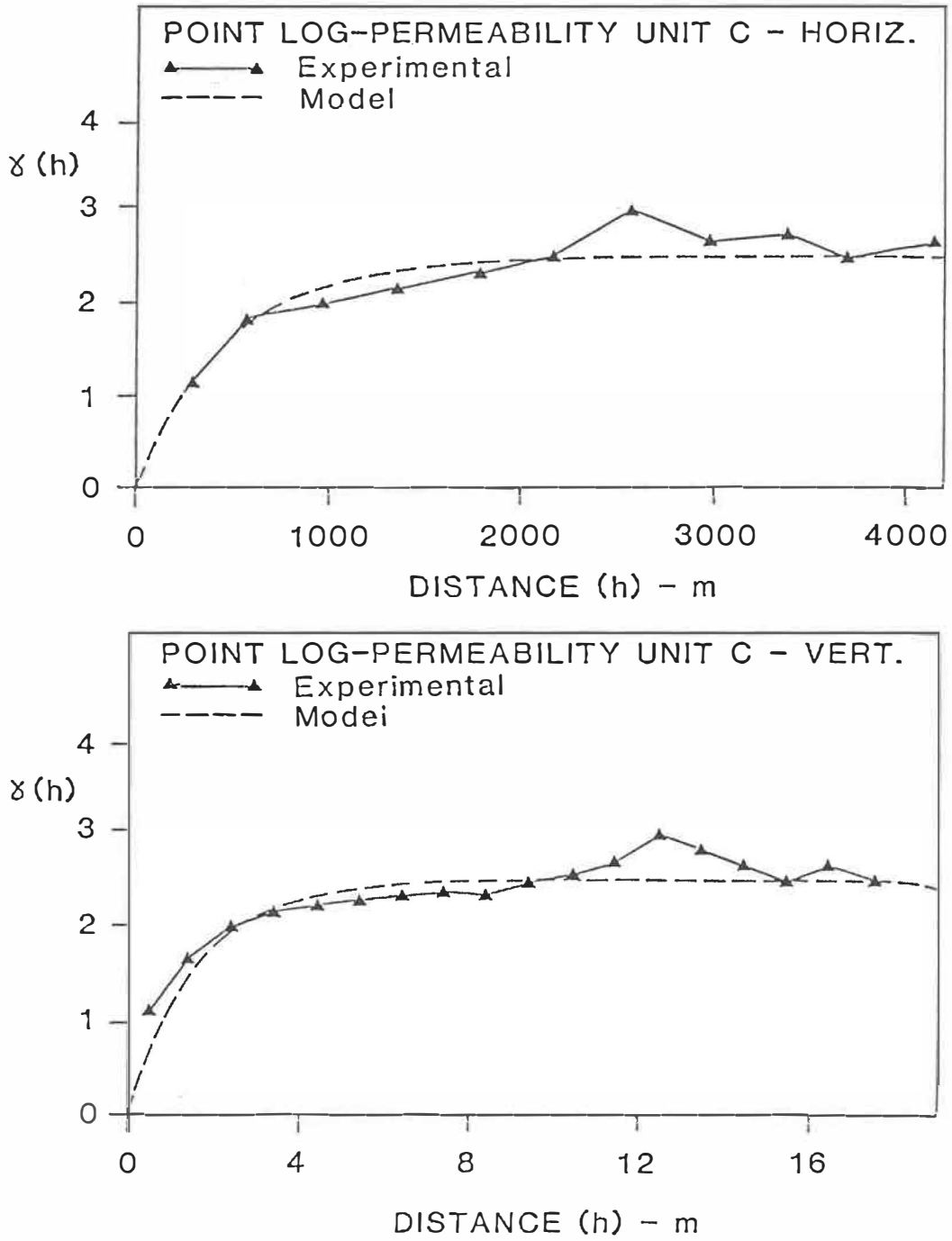

IGURE 5.19: Experimental and model variograms of core sample permeability in unit C; average horizontal (top) and vertical (bottom) .

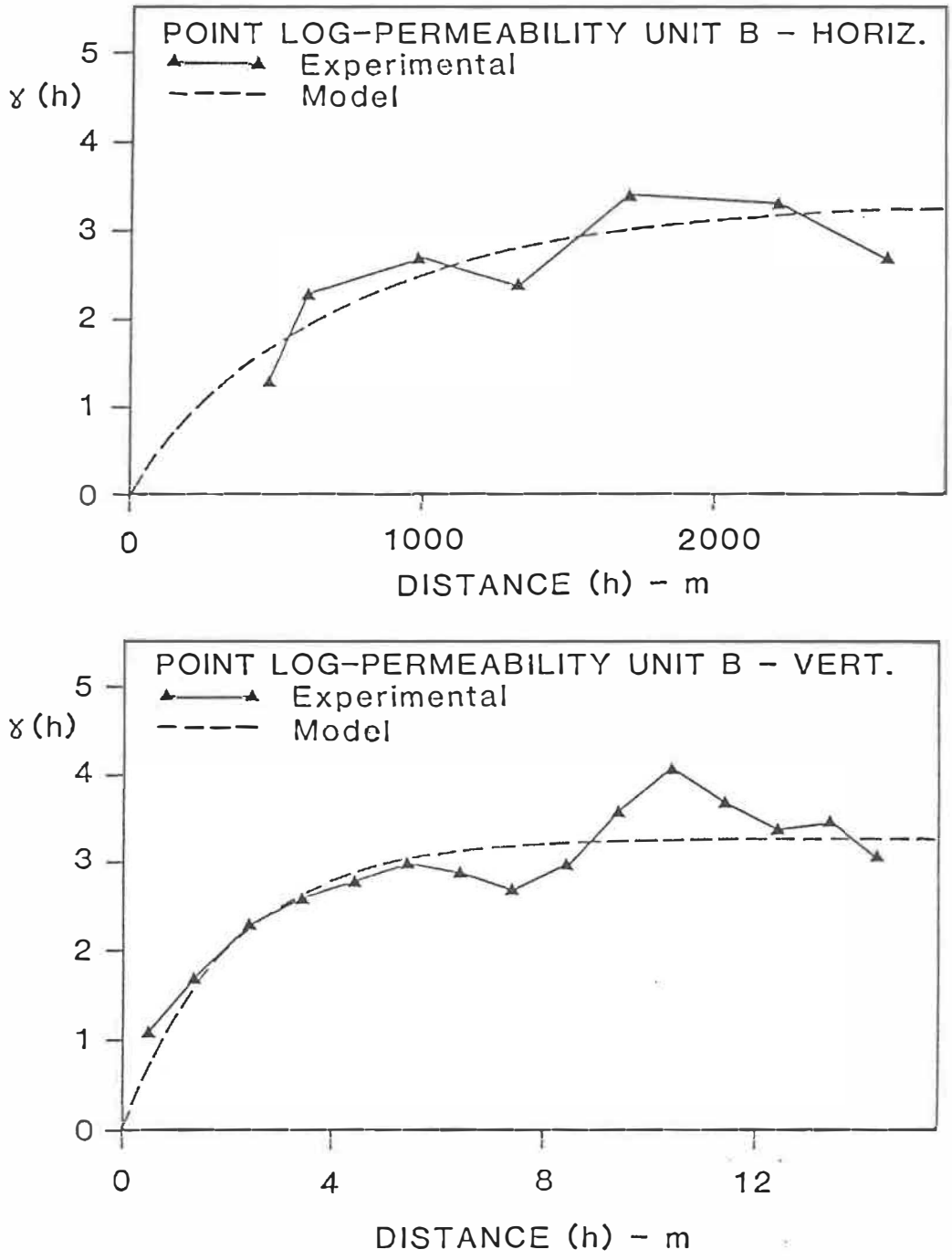

FIGURE 5.20: Experimental and model variograms of core sample permeability in unit B; average horizontal (top) and vertical (bottom) .

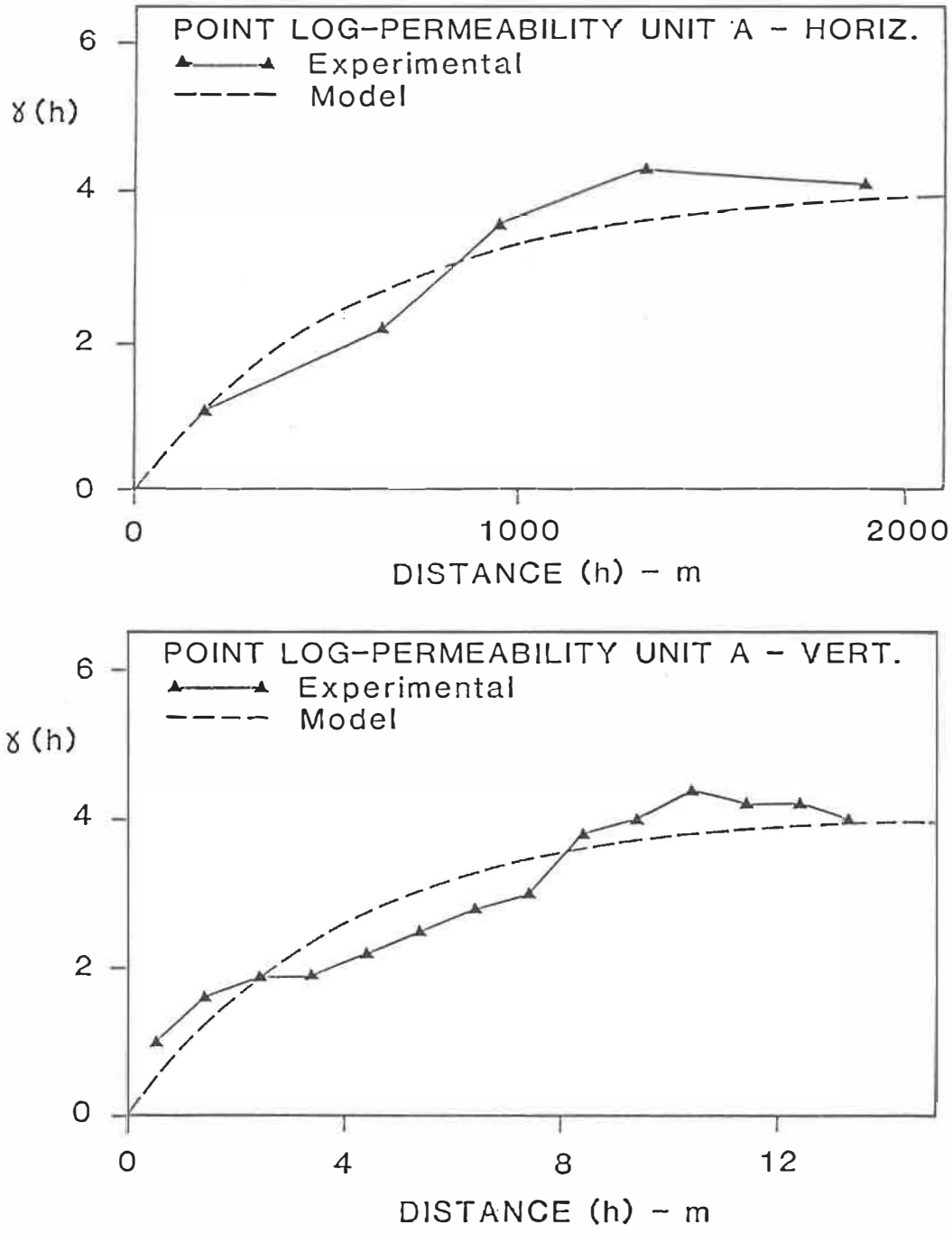

FIGURE 5.21: Experimental and model variograms of core sample permeability in unit A; average horizontal (top) and vertical (bottom) .

The generalized covariances of log derived water saturations are also calculated from experimental variograms depicted in Figures 5.11, 5.12, 5.13 and 5.14 for units H, C, B and A respectively. As in the case of porosities, experimental variograms indicate the existence of constant trends (k=0) in all units and directions. In addition, they indicate the presence of anisotropies with water saturations varying, on average, slower from well to well than down-hole. The coefficients of the generalized covariances for water saturations for every unit are derived from their equivalent variograms and are summarized in Table 5.4.

The experimental variograms of core sample residual oil saturation are presented in Figures 5.15, 5.16, 5.17 and 5.18 for units H, C, B, and A respectively. They also indicate the presence of both a constant trend (k=0) and anisotropies. Again, down-hole residual oil saturation variograms increase faster than well-to-well ones. The coefficients of the generalized covariances as derived from their equivalent variograms are given in Table 5.5.

Experimental horizontal and vertical variograms of the logarithmic transforms of core sample permeabilities are calculated for each of the units H, C, B and A and presented in Figures 4.6 and 4.7 and 5.19 to 5.21 respectively. The log-permeabilities are used because this is appropriate with lognormal variables (David, 1977), as well as due to restrictions imposed by the assumptions made in estimating effective

TABLE 5.2 - Generalized covariances of the tops and bottoms of the different units of the Crystal reservoir.

Unit	Order k	Nugget Effect $c\delta$	Coefficient a_0	Coefficient a_1
Top of H	1	0.0	0.020327	0.000867
Top of EM	1	0.0	0.031176	0.0
Top of C	1	0.0	0.048809	0.0
Top of B	1	0.0	0.052577	0.0
Top of A	1	0.0	0.032296	0.0
Bottom of A	1	0.0	0.027691	0.000344

TABLE 5.3 - Generalized covariances of core sample porosities per unit of the Crystal reservoir.

Unit	Order k	Nugget Effect $c\delta$ (*10^3)	Coefficient a_0		Coefficient a_1
			Horizontal (*10^6)	Vertical (*10^3)	
H	0	0.250	0.760	0.946	--
C	0	0.307	0.121	0.199	--
B	0	0.187	0.797	0.122	--
A	0	0.202	0.883	0.131	--

TABLE 5.4 - Generalized covariances of log derived water saturations per unit of the Crystal reservoir.

Unit	Order k	Nugget Effect $c\delta$(*10^3)	Coefficient a_0		Coefficient a_1
			Horizontal (*10^6)	Vertical (*10^3)	
H	0	1.701	6.872	1.512	--
C	0	1.652	8.571	2.002	--
B	0	2.529	0.786	1.449	--
A	0	1.481	7.602	1.453	--

TABLE 5.5 - Generalized covariances of core sample residual oil saturation per unit of the Crystal reservoir.

Unit	Order k	Nugget Effect $c\delta$ (*10^3)	Coefficient a_0		Coefficient a_1
			Horizontal (*10^6)	Vertical (*10^3)	
H	0	0.182	0.257	0.100	--
C	0	0.188	0.304	0.112	--
B	0	0.416	0.536	0.103	--
A	0	0.203	0.682	0.139	--

permeabilities. All experimental variograms exhibit transition structures with variogram values increasing with distance up to an upper limit. Subsequently, as distance increases, they exhibit no correlation tending towards or osciliating around a value (sill). Transition zones are much longer on the plane than vertically, indicating better continuity horizontally in all units. The variogram models of permeability are restricted by the theory used in the succeeding paragraphs on permeability estimation to exponential ones of the form

$$\gamma(h) = \sigma^2_f(1 - \exp\,[-(h/\lambda)]) \qquad (5.1)$$

where σ^2_f is the sill or variance of the log-permeability field and λ the correlation scale equal to a third of the apparent length of the transition zone of the experimental variogram. The parameters of the exponential models inferred for each unit of the Crystal reservoir are presented in Table 5.6.

5.7 Estimated Block Models of Reservoir-Rock Properties

The estimation of pertinent reservoir-rock properties is based upon the estimation of the boundaries of units H, EM, C, B and A. Accordingly these boundaries are first estimated using equations (2.9)

TABLE 5.6 - Exponential variogram models of core sample permeabilities per unit of the Crystal reservoir.

Unit	Correlation distance λ-horizontal (m)	Correlation distance λ-vertical (m)	Sill σ_f^2
H	150.0	4.0	4.04
C	490.0	1.8	2.43
B	700.0	2.0	3.27
A	600.0	4.0	3.96

and (2.10) and the generalized covariances inferred from the data. Tops and bottoms of reservoir units are estimated on a regular grid of 38 x 52 points at 300 x 300 meters grid spacing. The grid spacing is slightly larger than the average well spacing within the limits of the Crystal 'A' and 'H' pools. The estimated tops and bottoms of all Crystal units, as well as the associated estimation variance, are presented in the figures included in Appendix C. Isopachs of Crystal facies are also included in Appendix C.

Estimated models of porosity, permeability, water saturation and residual oil saturation at the megascopic scale are created by first superimposing over the entire reservoir a regular three-dimensional grid with a north-south orientation. The grid set-up is followed by the identification of the reservoir unit to which each grid block belongs, using the positions in space of the estimated tops and bottoms of the units. The grid spacing is 300 x 300 x 1 meters resolution, and is selected by considering several factors including the average well spacing, the average variation structures of the pertinent variables as well as both abilities of reservoir flow simulations and simulation strategies. It should be noted that although several factors must be taken into account, a very important criterion, as far as reservoir-rock properties are concerned, is their correlation structures. For example, in the present study, permeability variograms exhibit transition zones on the plane with distances ranging from about 450 to 2100 meters. Then, in order to express the horizontal variability and continuity of

permeability in all units, the horizontal grid resolution should be the smallest possible with respect to the minimum apparent correlation distance, i.e. the 450 meters in this case.

Based on the grid set-up described above, porosity, water and residual oil saturations for every block within the limits of the reservoir and per sandstone unit are estimated using the inferred generalized covariances. Estimation proceeds separately for every unit. Cross-sections from the constructed models showing the variation of each variable within the boundaries of each unit are presented for porosity, water saturation and residual oil saturation in Figures 5.22, 5.23 and 5.24 respectively. The corresponding estimation variances are shown in Figures 5.25, 5.26 and 5.27.

The estimation of permeabilities using specialized methodology is described in a separate section.

5.8 Conditionally Simulated Models of Reservoir-Rock Properties

Conditional simulations of pertinent properties are performed on the same grid set-up as in estimation, using the generalized covariance of each variable. As is demonstrated by the definition of conditional simulation in equation (3.21), the technique consists of an estimate of the variable plus a simulated correlation variate. Estimation under minimum variance constraints, although statistically best, is a

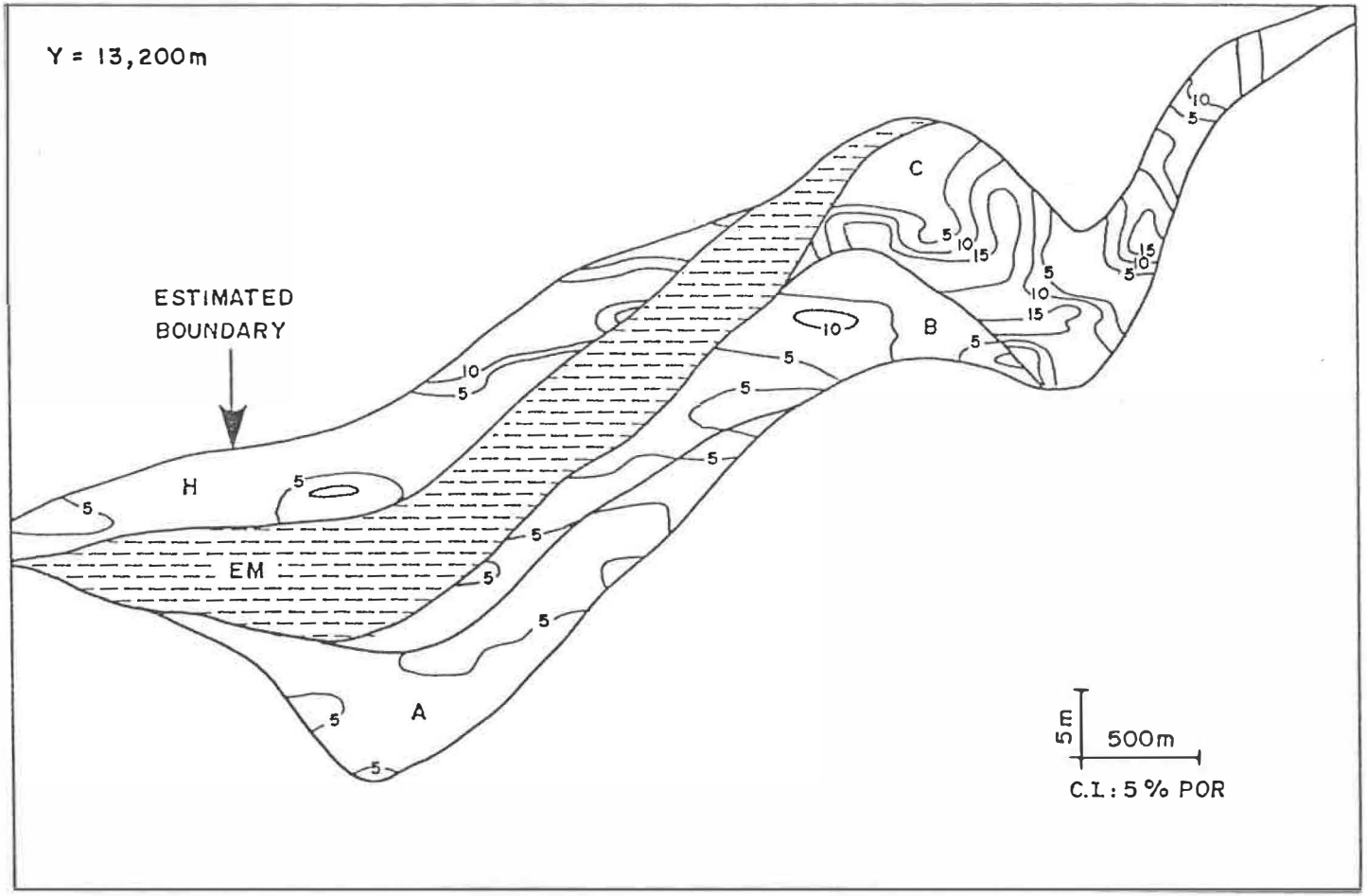

FIGURE 5.22: Cross-section from the estimated model of porosity of the Crystal reservoir .

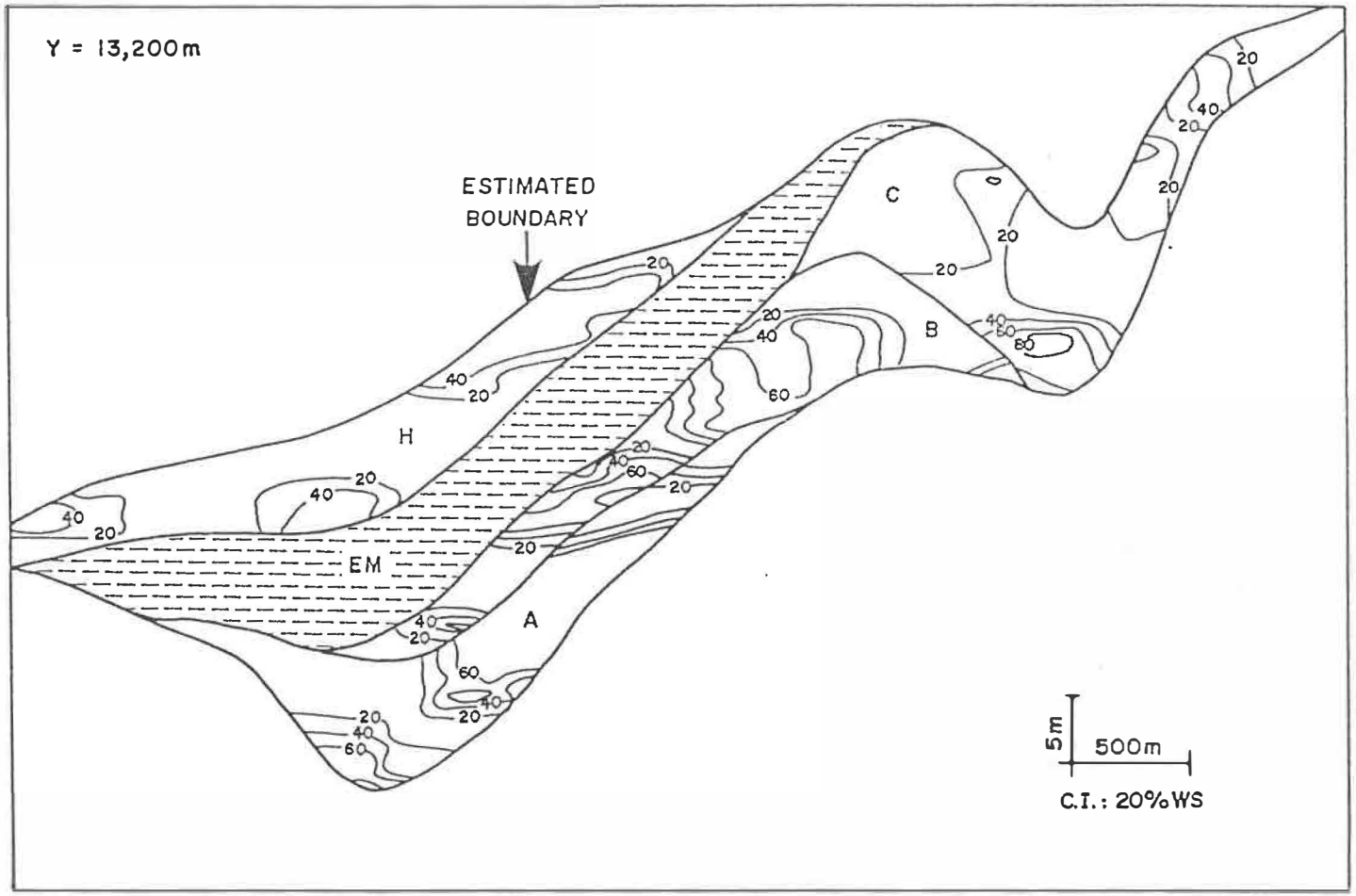

FIGURE 5.23: Cross-section from the estimated model of water saturation of the Crystal reservoir .

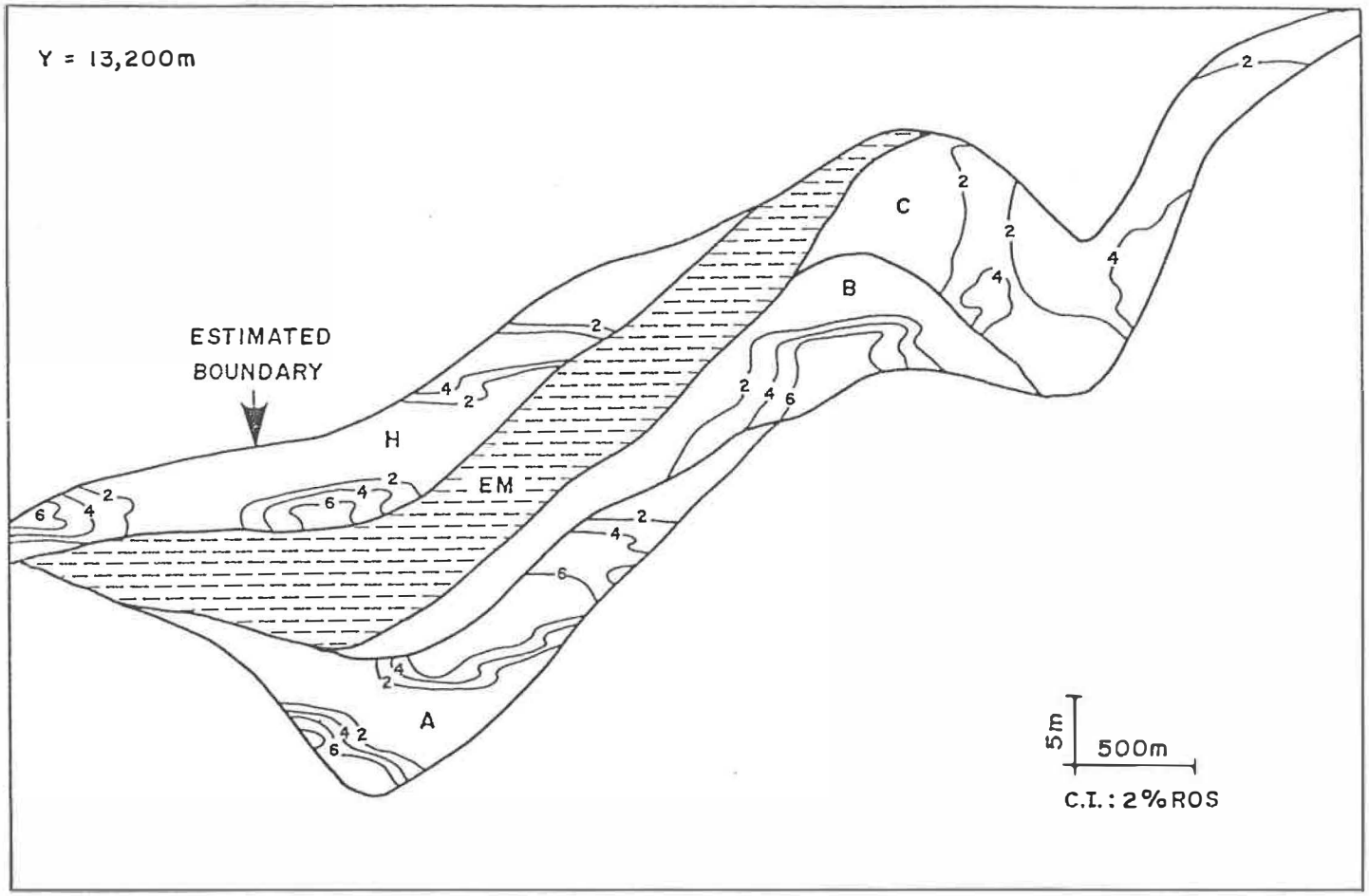

FIGURE 5.24: Cross-section from the estimated model of residual oil saturation of the Crystal reservoir .

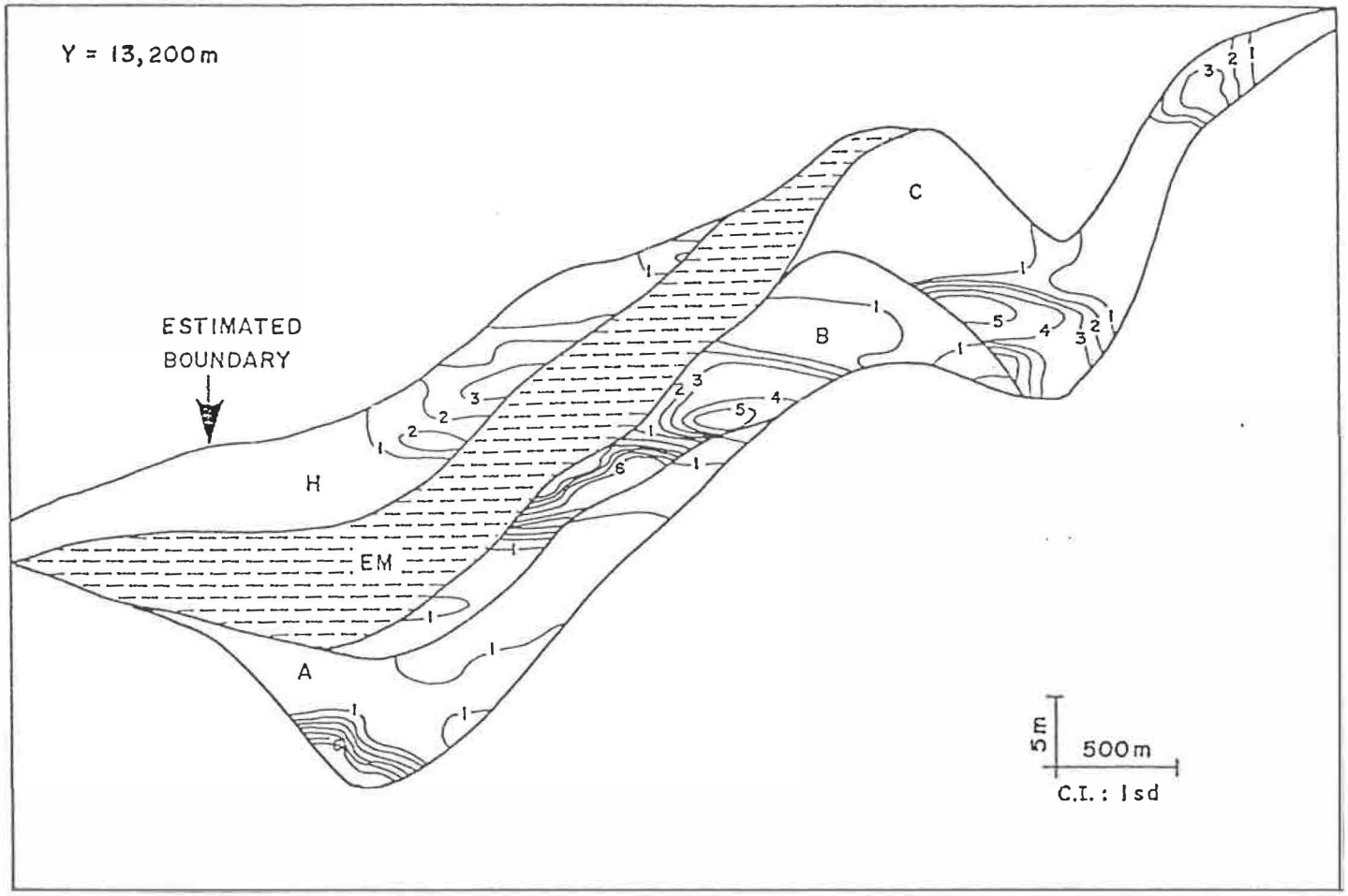

FIGURE 5.25: Estimation standard deviations corresponding to the cross-section of porosity in Figure 5.22 .

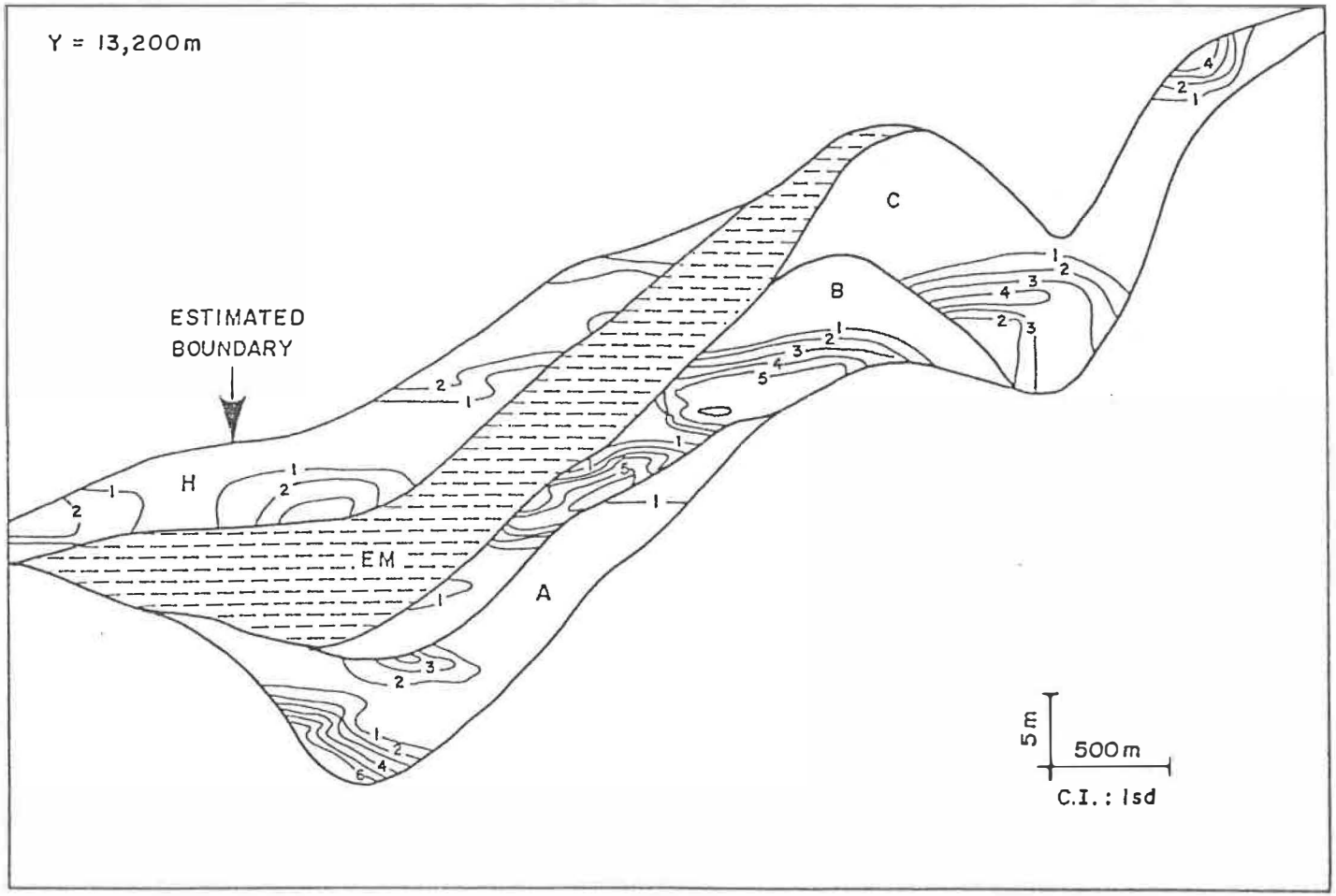

FIGURE 5.26: Estimation standard deviations corresponding to the cross-section of water saturation in Figure 5.23 .

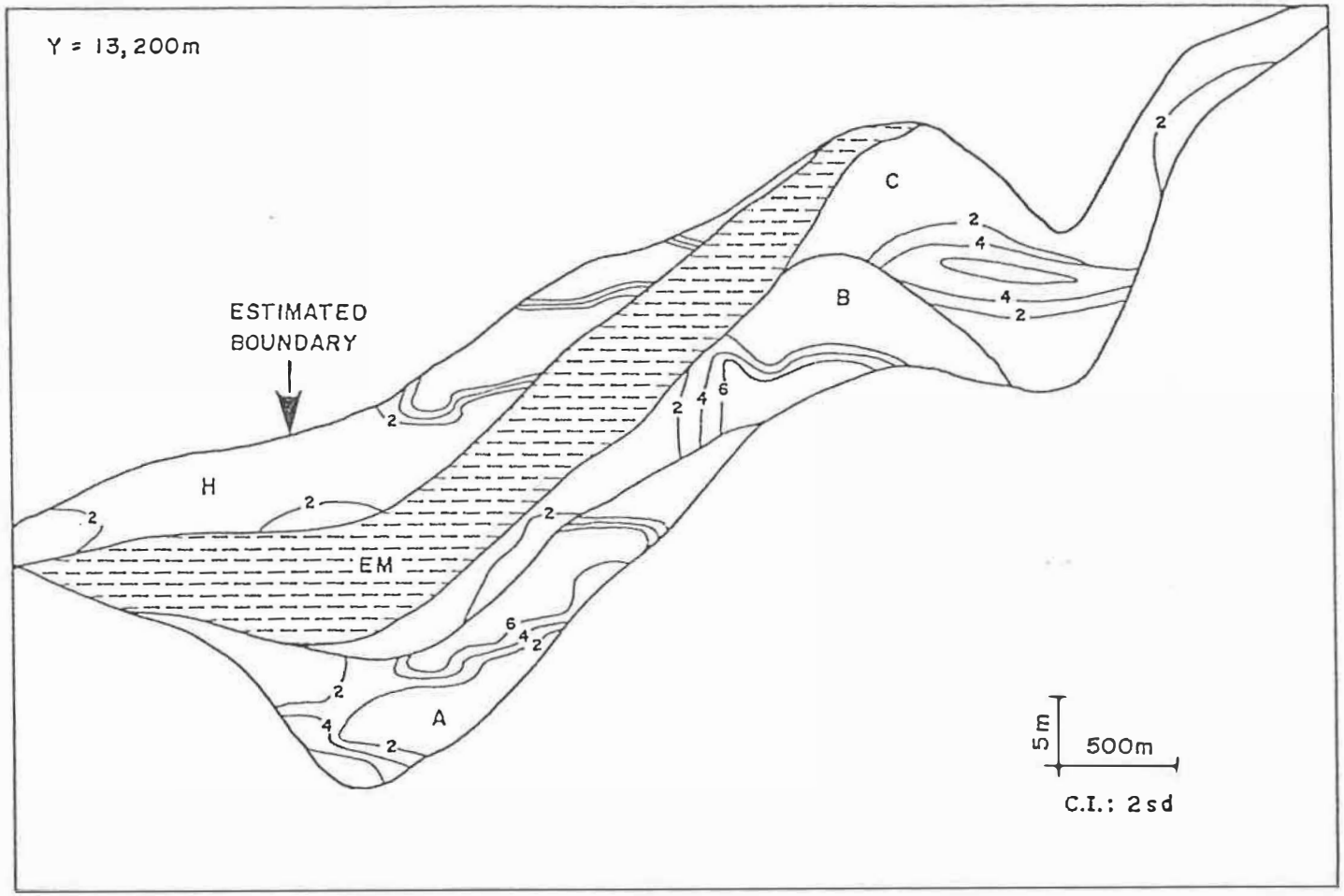

FIGURE 5.27: Estimation standard deviations corresponding to the cross-section of residual oil saturation in Figure 5.24 .

smoothing operation. To the contrary, conditional simulation is an attempt to reconstruct-represent actual fluctuation. Furthermore, the variate added to the estimate in equation (3.21) is not unique; thus, it is possible to generate different conditionally simulated models of the same variable.

The boundaries of the units H, EM, C, B and A are first conditionally simulated and two realizations of each are generated. Conditionally simulated tops and bottoms of all units are subsequently used to identify the unit to which every grid block of the reservoir at the megascopic scale belongs to.

Based on the generated realizations of unit boundaries, two realizations of each of the variables, porosity, water and residual oil saturation for every unit, are generated, representing their conditionally simulated models at the megascopic scale. Cross-sections from the first realization are depicted in Figures 5.28, 5.29, 5.30 and from the second one in Figures 5.31, 5.32, 5.33. Comparison of these cross-sections with the estimated ones graphically expresses the difference between estimation and conditional simulation.

Validation of all conditionally simulated variables is performed by comparing the generalized covariances of the generated realizations to the corresponding ones inferred from the data and used as input for the simulations. The comparisons for each of the conditional

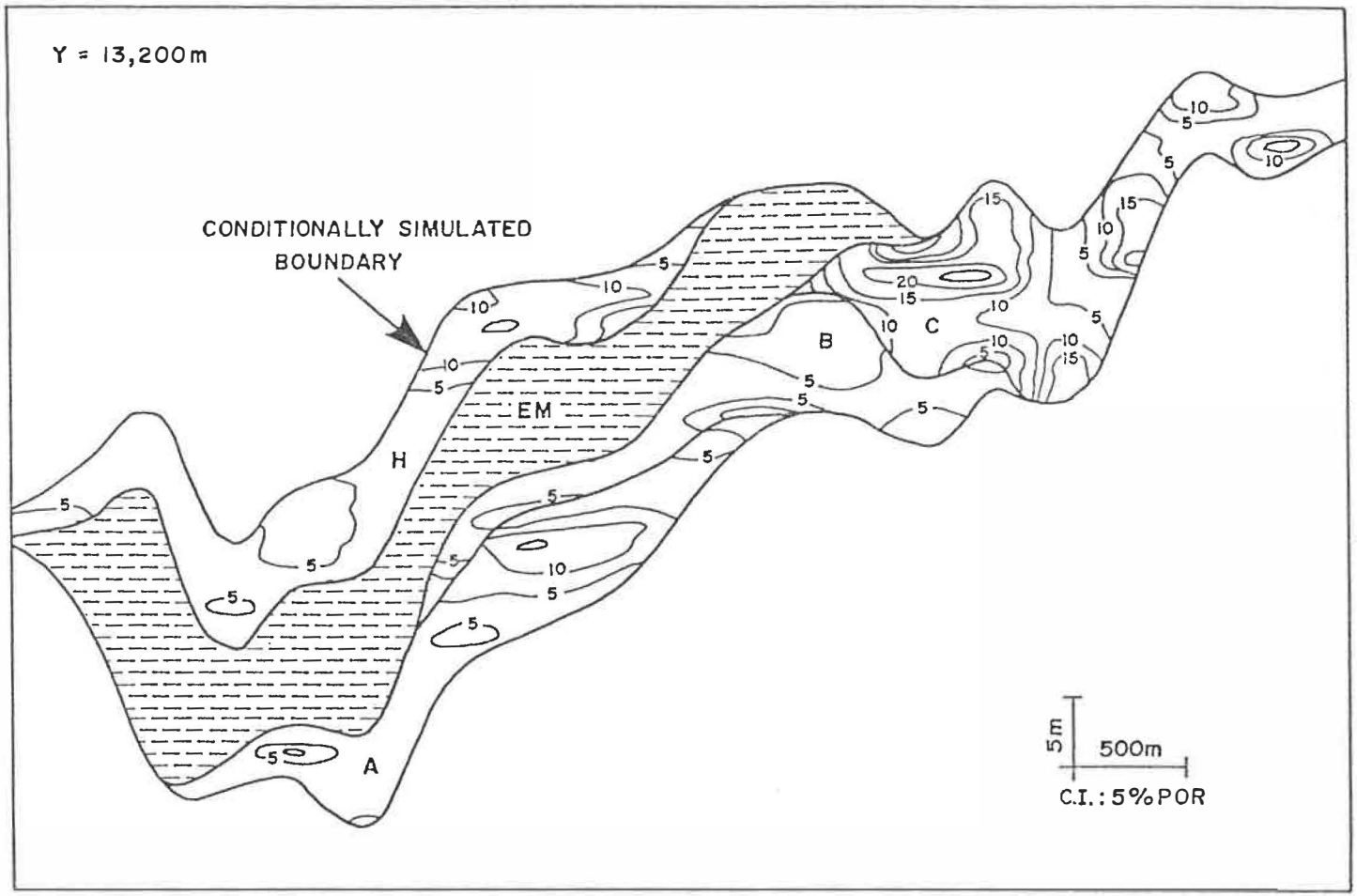

FIGURE 5.28: Cross-section from the first conditionally simulated realization of porosity of the Crystal reservoir .

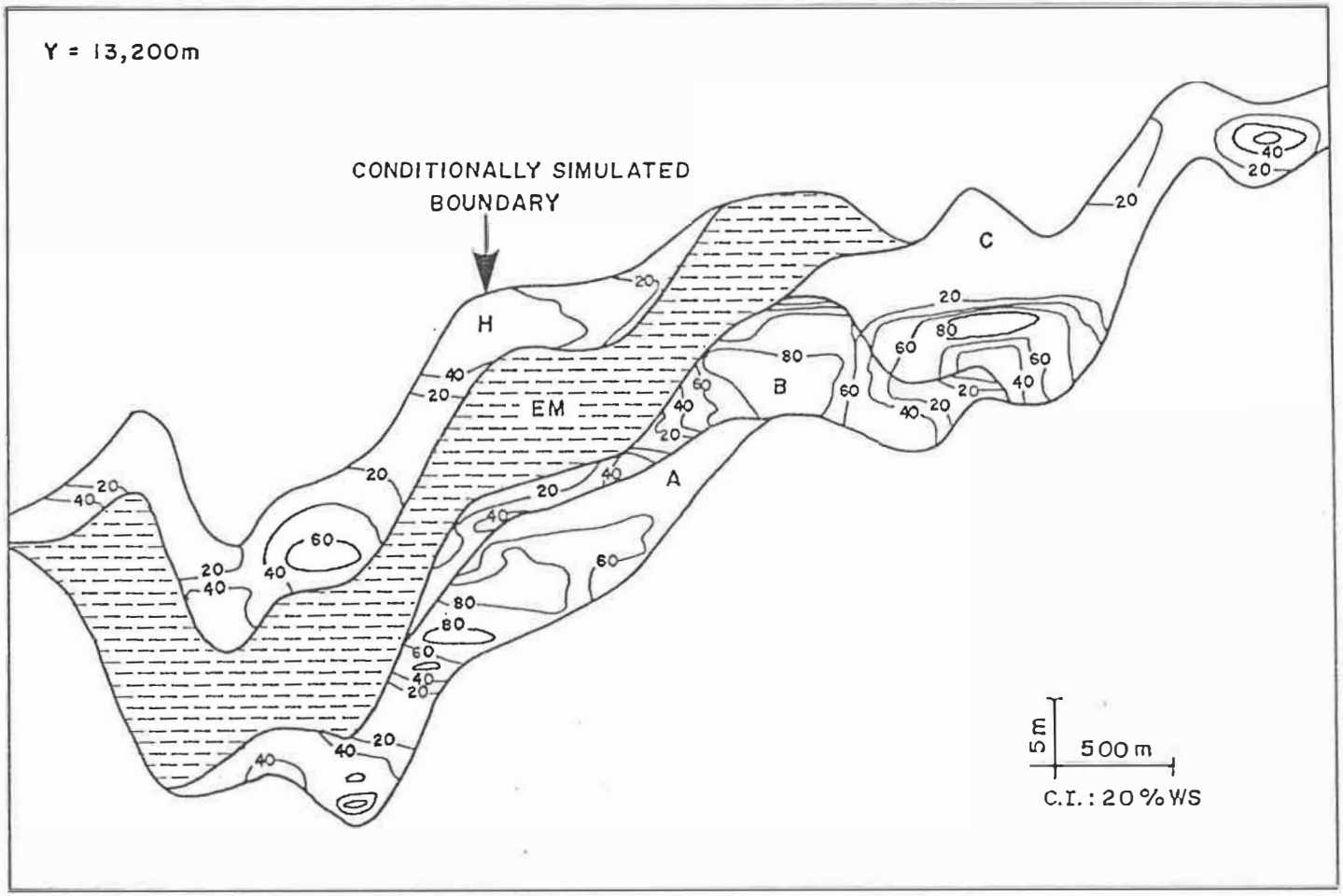

FIGURE 5.29: Cross-section from the first conditionally simulated realization of water saturation of the Crystal reservoir .

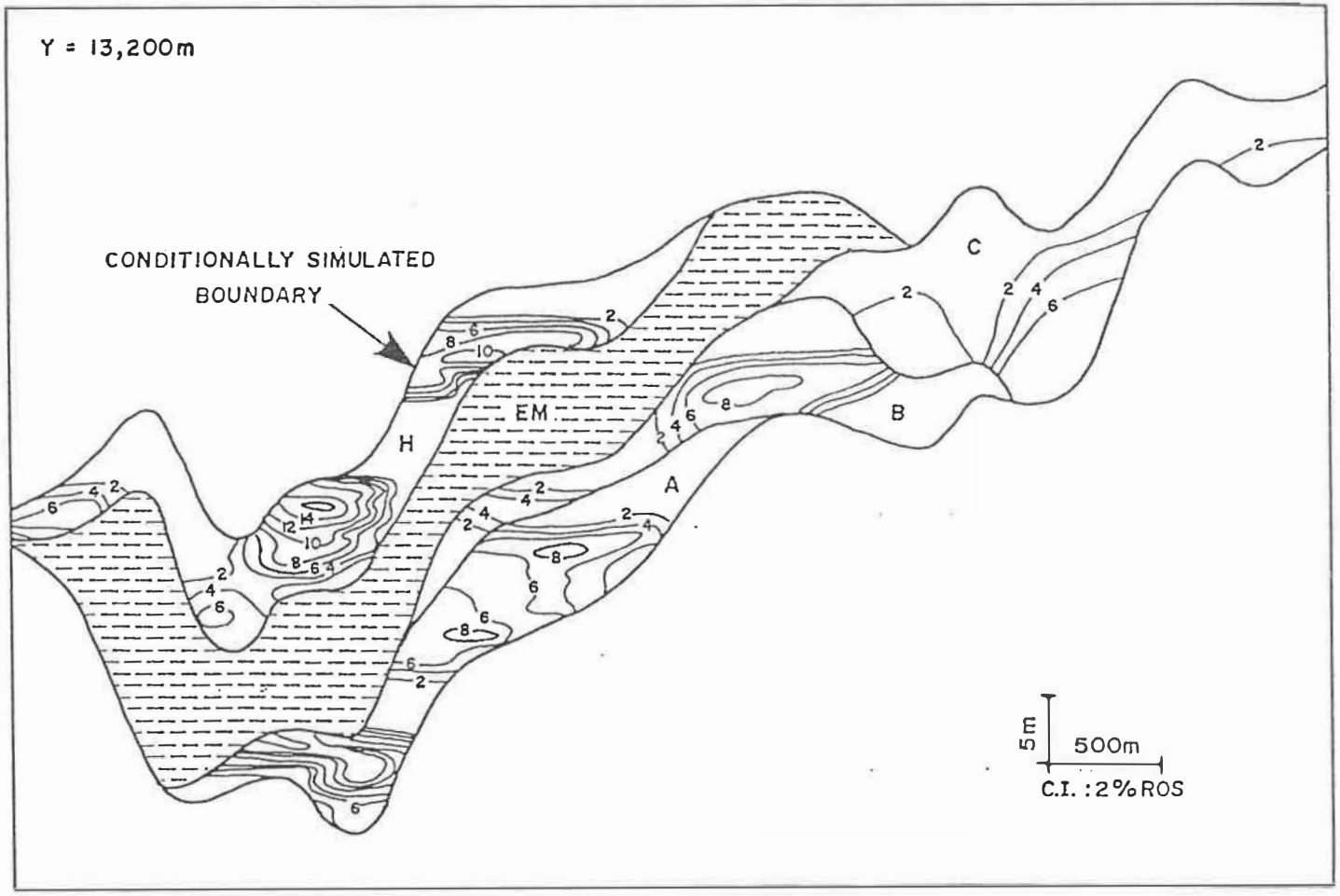

FIGURE 5.30: Cross-section from the first conditionally simulated realization of residual oil saturation of the Crystal reservoir .

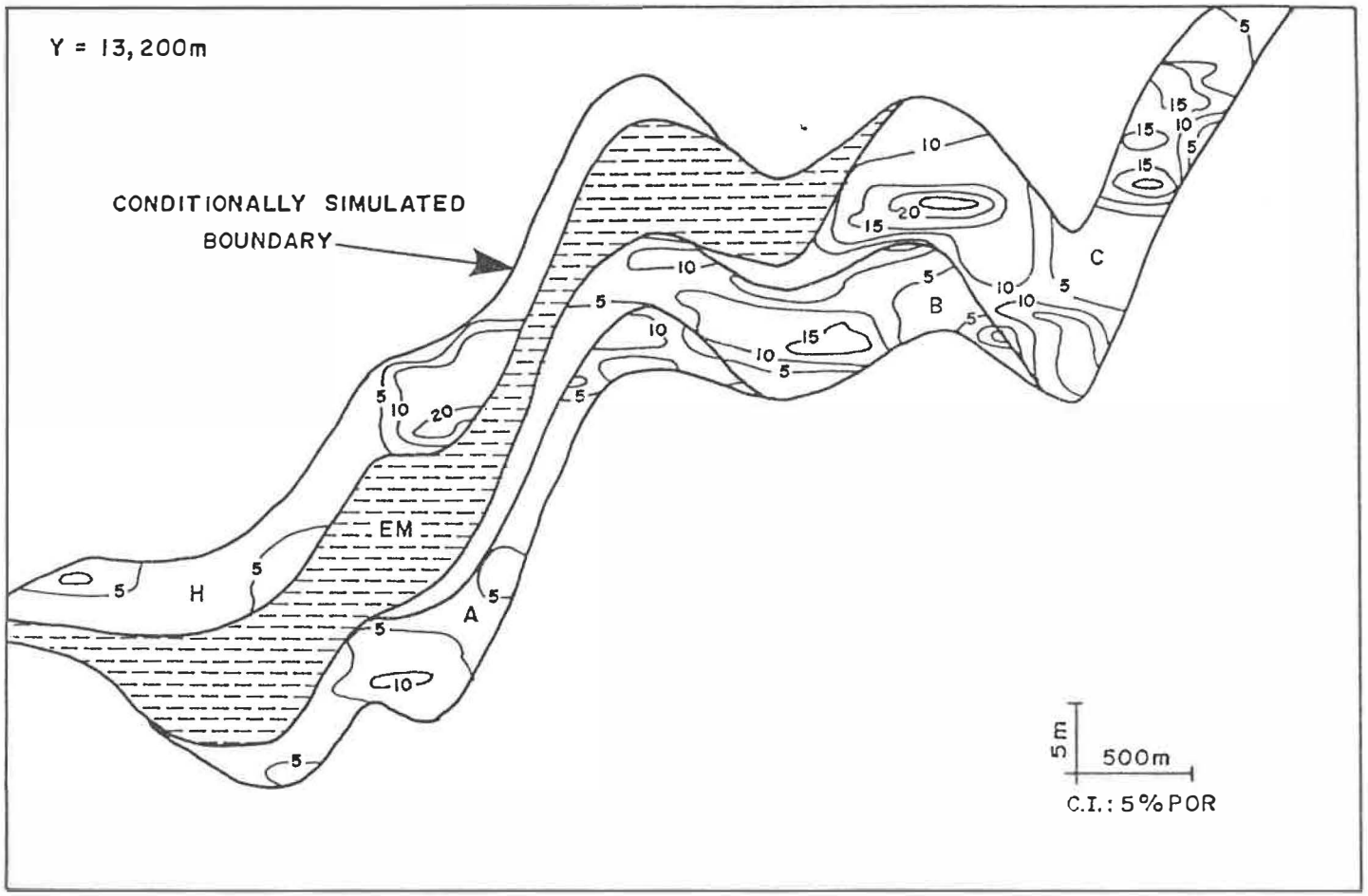

FIGURE 5.31: Cross-section from the second conditionally simulated realization of porosity of the Crystal reservoir

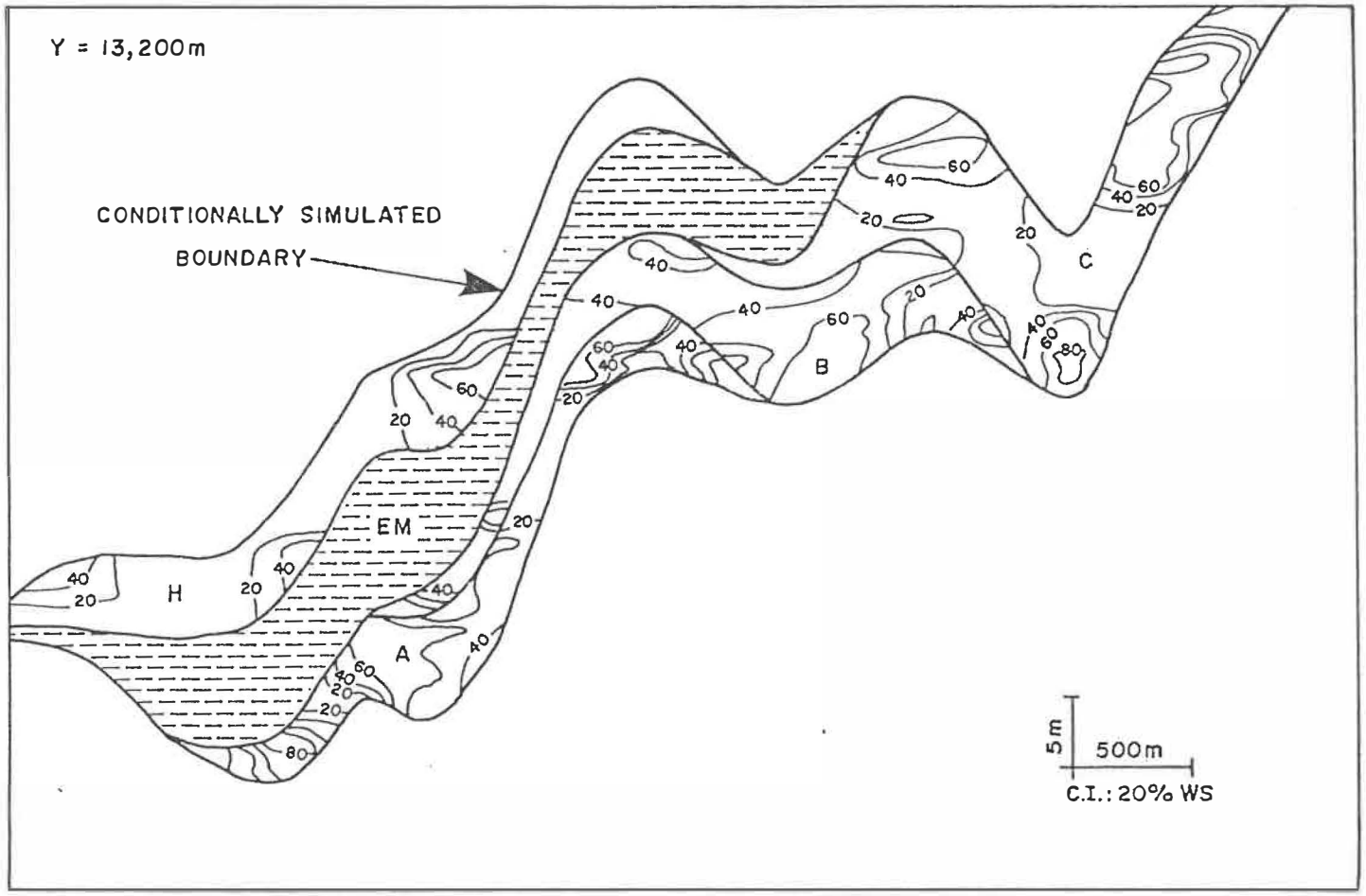

FIGURE 5.32: Cross-section from the second conditionally simulated realization of water saturation of the Crystal reservoir

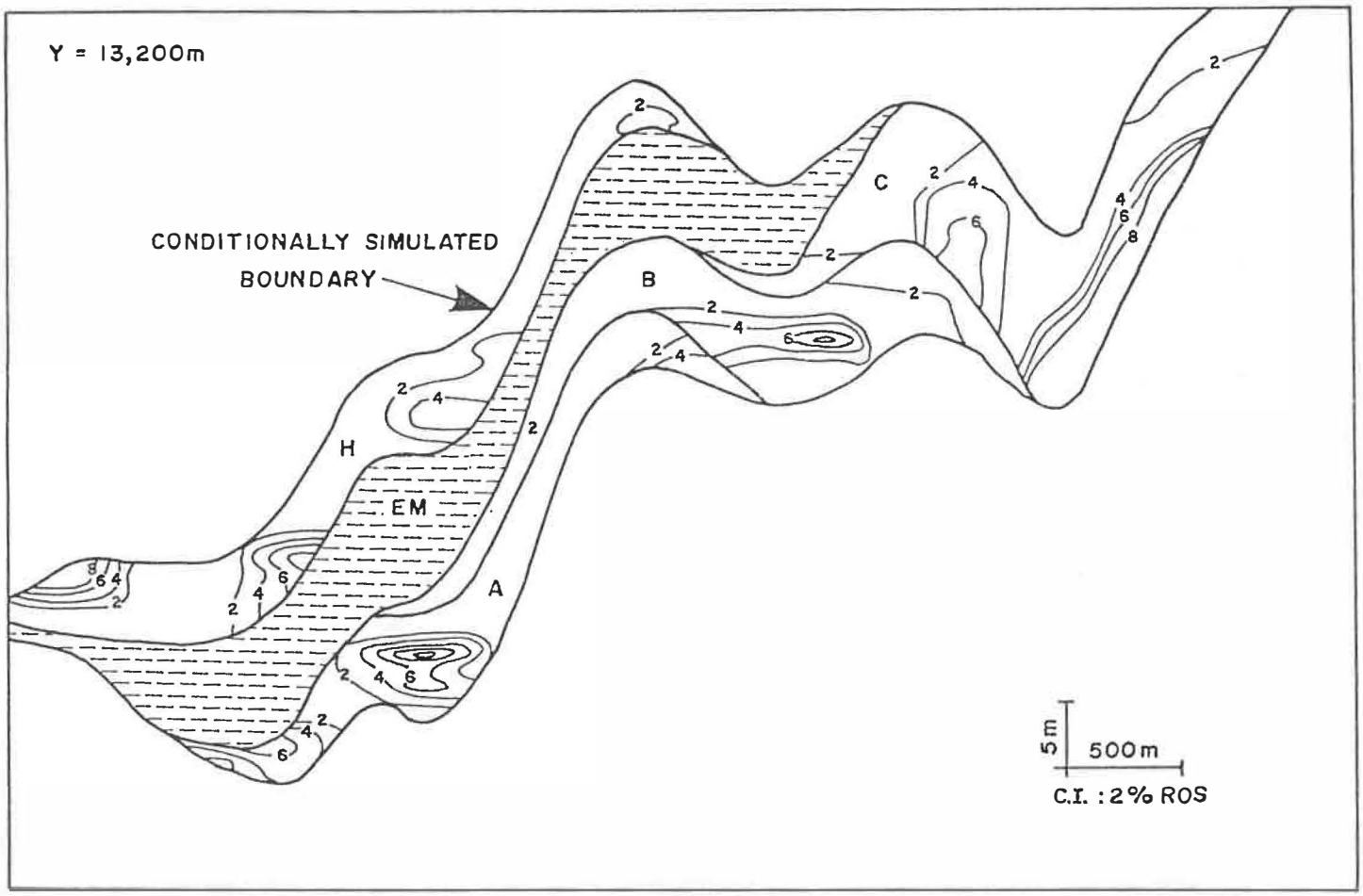

FIGURE 5.33: Cross-section from the second conditionally simulated realization of residual oil saturation of the Crystal reservoir

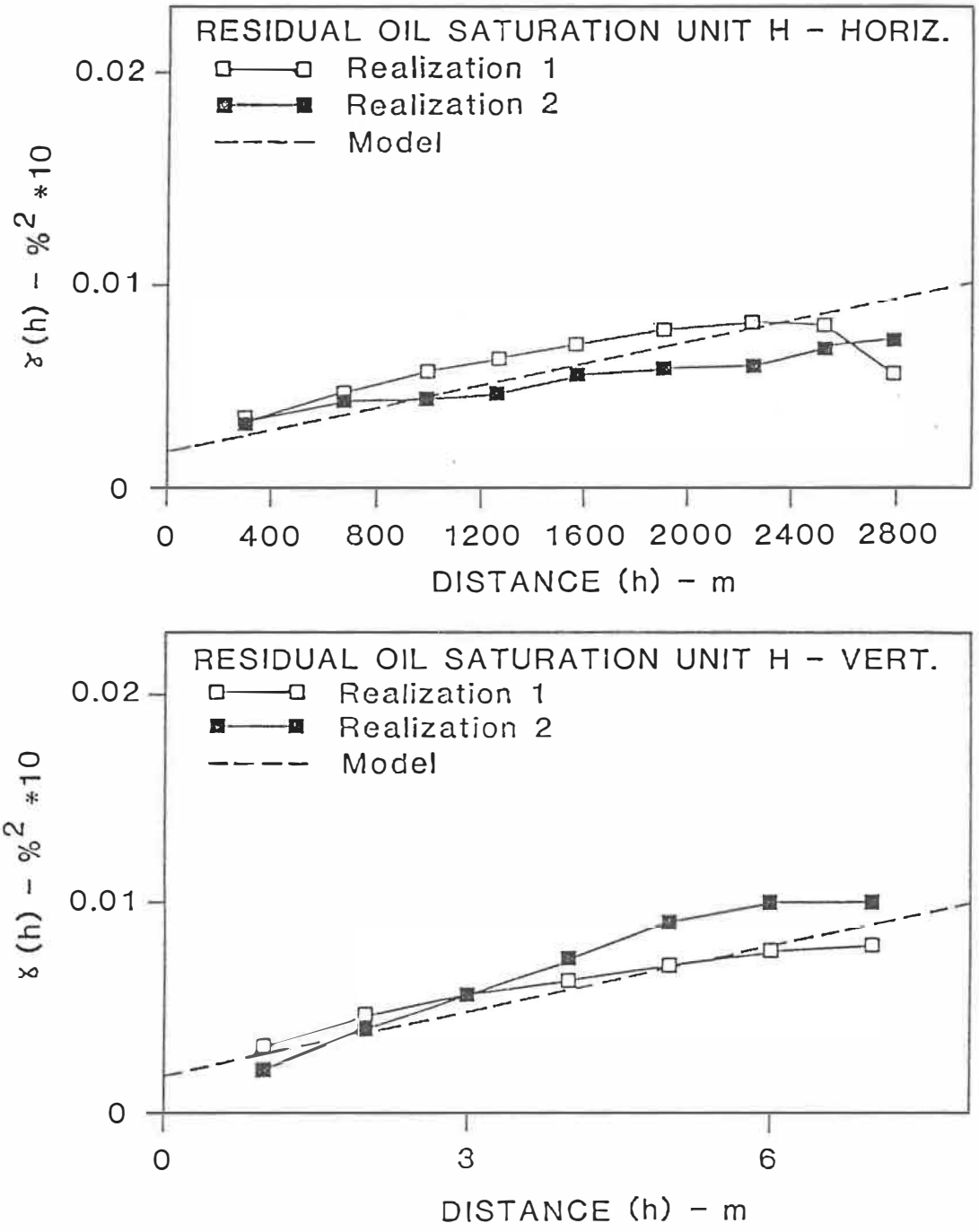

FIGURE 5.34: Comparison of the experimental variograms of two realizations of residual oil saturations in unit H to the theorical model; average horizontal (top) and vertical (bottom) .

simulations performed show a good reproduction of the generalized covariances. An example is shown in Figure 5.34. Additional figures comparing experimental and theoretical generalized covariances of the conditionally simulated variables are included in Appendix D.

Conditional simulations of reservoir-rock properties are of particular importance to reservoir flow simulations. It is standard practice to check the sensitivity of flow simulation results to variation of reservoir-rock input by arbitrarily altering parameter values. Conditionally simulated models can provide sound realistic representations of the actual parameter variability, thus providing viable alternatives as well as space for experimentation with other more uncertain flow simulation parameters.

5.9 Determination of the Effective Permeability Tensor

Permeability is not an intrinsic rock property like the other reservoir parameters whose modelling was presented in the previous sections. It is rather an entity arising when an attempt is made to describe flow through α porous medium using Darcy's equation and is expressed (Bear, 1968) as a second-rank symmetric tensor whose off-diagonal components reduce to zero when the principal components of the tensor coincide with the coordinate system, as is usually the case. Due to its character, the effective horizontal and vertical permeabilities of reservoir blocks cannot be estimated directly from core samples.

To this problem, different solutions have been used in different cases (Desbarats, 1987; Begg **et al.**, 1985; Begg and King, 1985; Haldorsen and Lake, 1982). An additional approach, consistant with the methodology followed in this study, is used for the modelling of the effective horizontal and vertical permeabilities in the Crystal reservoir. (See Chapter 4).

The approach that is followed in the present study is essentially a two step process. First, the grid set-up representing the reservoir at the megascopic scale, as used previously for the modelling of other pertinent variables, is discretized to a much denser grid with a resolution of 30 x 30 meters horizontally and 0.5 m vertically, so that a reservoir block is represented by 200 points at the macroscopic scale. Subsequently, the logarithmic transforms of core sample permeabilities are conditionally simulated at the macroscopic scale using equation (2.18) and the exponential variogram models derived from the data. The conditionally simulated models of units H, C, B and A are validated by comparing the variograms of each unit to the corresponding model. The validation shows that variograms have been well reproduced. In addition, the mean and variance and, in fact, histograms of the data are reproduced. The figures comparing variograms of the conditionally simulated point log-permeabilities and the corresponding histograms are included in Appendix E.

The effective horizontal and vertical components of the permeability tensor at the megascopic scale can be simultaneously reconstructed for any reservoir block from the simulated points within the block using an ad-hoc extension of analytical expressions derived by Gelhar and Axness (1983). According to the results in Chapter 4 it is:

$$\begin{cases} K_{E_{11}} = K_{E_{22}} = K_V \exp\left[s^2 \left(\tfrac{1}{2} - g_{11}\right)\right] \\ K_{E_{33}} = K_V \exp\left[s^2 \left(\tfrac{1}{2} - g_{33}\right)\right] \end{cases} \qquad (5.2)$$

where K_E is the effective permeability, K_V the spatial geometric average of point permeabilities, and s^2 the variance of simulated points within a block. g_{11} and g_{33} are functions of the anisotropy ratio calculated from charts.

Using formulae (5.2), the effective horizontal and vertical components of reservoir block permeabilities are estimated, using the anisotropy ratio of each unit. The anisotropy ratios of units H, C, B and A, derived from the correlation distances of the corresponding exponential variograms models, are 37.5, 272, 350 and 150 respectively. Cross-sections representing the variation of reconstructed horizontal and vertical permeabilities of the Crystal reservoir and within the estimated boundaries of each unit are depicted in Figures 5.35 and 5.36 respectively.

The derivation of the formulas in equations (5.2) and (5.3) imposes certain assumptions. Log transforms of core sample permeabilities are considered to follow a normal distribution and exhibit an anisotropic exponential correlation structure. The distributions of log-permeabilities in all units of the Crystal reservoir, as already pointed out, approximate normal ones. Furthermore, the exponential variogram models fit well to the experimental ones. Ergodicity is an implicit assumption of the method used. The operational consequence of ergodicity is that experimental variograms exhibit a sill at larger distances. Apparently, both horizontal and vertical variograms of permeability in all units clearly show an upper bound at larger distances.

Two additional factors of the methodology followed are the anisotropy ratios and the discretization of the reservoir blocks. It is evident from equations (5.2) and (5.3) that as the anisotropy ratio increases, horizontal and vertical permeabilities tend towards the arithmetic and harmonic means respectively. It is therefore expected that permeabilities in cases of very large anisotropy ratios such as in units C, B and A (ρ = 150 to 350) tend towards the above means of the conditionally simulated points in each block. The effect of discretization on the results is not clear. It should be noted, however, that density of the discretization grid reaches the limits of the available hardware. Furthermore, the 200 points corresponding to every reservoir block present a statisticaly sufficiently large number to estimate the spatial geometric mean of macroscopic permeabilities of the block.

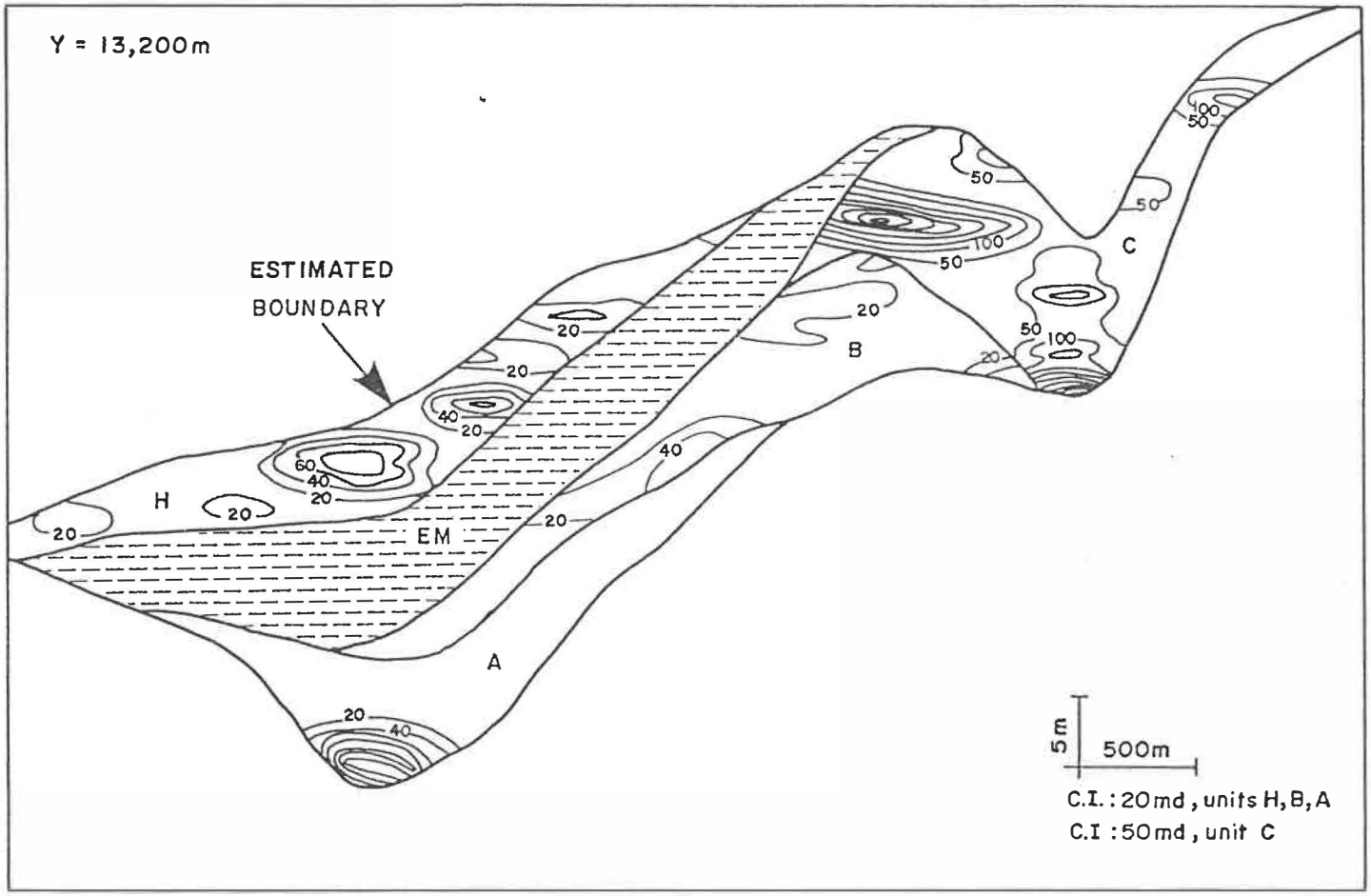

FIGURE 5.35: Cross-section of the horizontal permeability model of the Crystal reservoir .

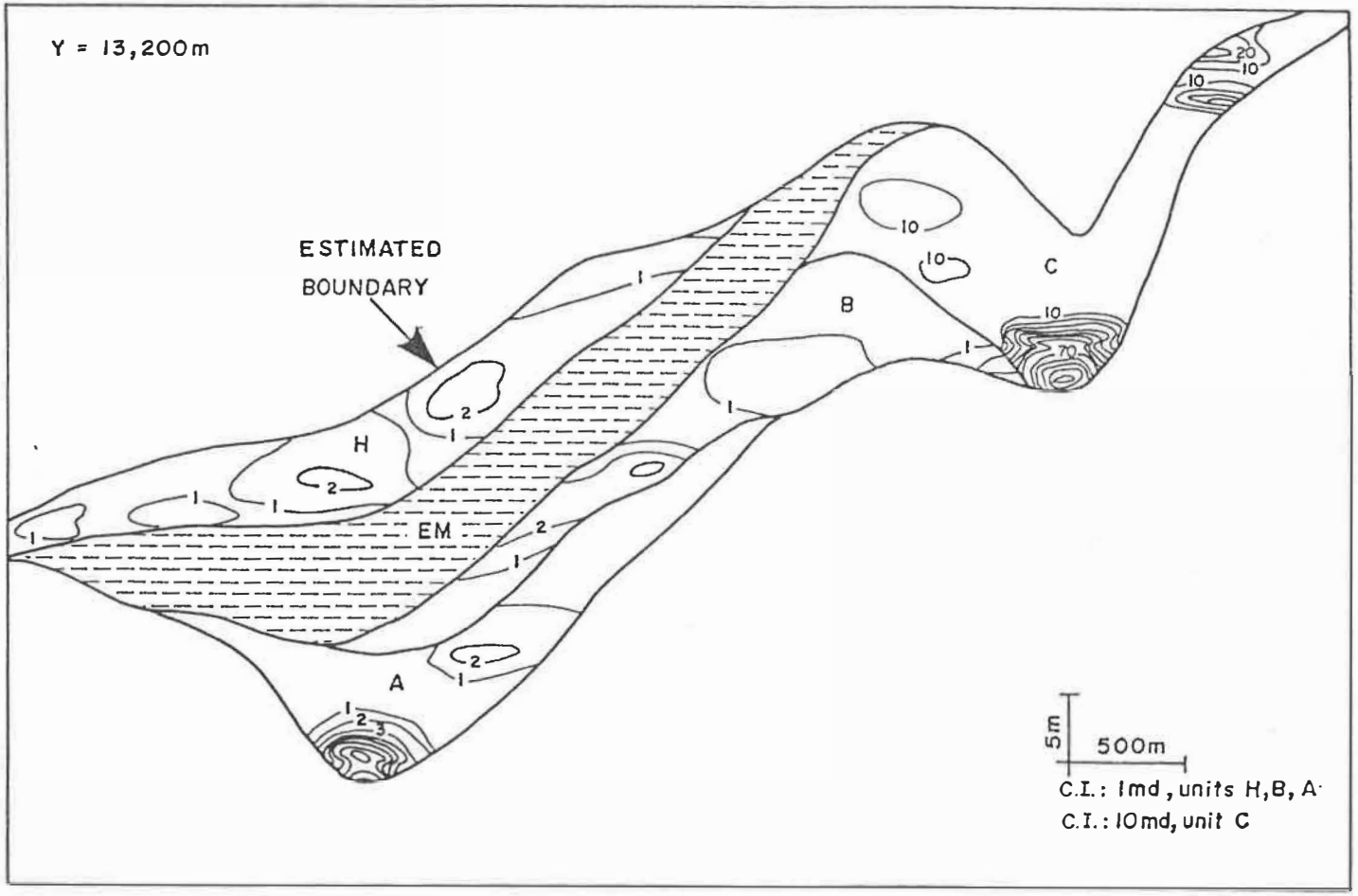

FIGURE 5.36: Cross-section of the vertical permeability model of the Crystal reservoir .

The approach used in modelling effective permeabilities of the Crystal reservoir is a simple, workable engineering approximation which seems to have provided reasonable results and which could be used in other reservoirs with similar characteristics.

5.10 Summary

In the present study, the complete quantitative-numerical characterization of the Crystal Viking reservoir, south-central Alberta, is presented and is based on a comprehensive qualitative-geological description. Geological variables including unit boundaries, porosities, water and residual oil saturations as well as permeabilities are considered.

An integrated approach is consistantly followed in the context of effectively combining quantitative information and quantitative models. Integration is founded on two major aspects. First, the natural heterogeneities of the Crystal reservoir are recognized, leading to the separation of the reservoir into distinct geologically homogeneous units (zonation). Second, geostatistical (stochastic) techniques are utilized. The latter quantify natural inherent characteristics of the anisotropies which are directly used in modelling the megascopic spatial variability of pertinent variables utilizing the techniques of best, minimum variance estimation and conditional simulation.

Estimated models capture average variation and provide detailed, reliable numerical descriptions of pertinent variables of the Crystal reservoir. Thus they will be used as geological input to reservoir flow simulation, while the associated estimation variances provide a confidence measure to be taken into account. The two conditionally simulated realizations generated reproduce the **in-situ** inherent fluctuation and will provide realistic alternatives in checking the sensitivity of flow simulation results to geological reservoir-rock describing input.

Effective horizontal and vertical permeabilities at the megascopic level of representation at Crystal are simultaneously reconstructed using core sample conditional simulation in combination with averaging formulae derived from the direct solution of the flow equation. The approach used at Crystal is simple, workable, and seems to present a reasonable engineering approximation far more elaborate than common practices in the Industry.

The present study on the Crystal Viking field demonstrates a methodology based on geostatistical techniques which provide sophisticated models in a synergetic effort to improve reservoir description and increase the certainty of reservoir representations. It is hoped that the methodology presented will be found useful in characterizing other reservoirs as well. To enhance the usibility of the presented methodology, and in general geostatistical techniques for numerical reservoir description, the problem of geostatistical knowledge transfer using expert systems will be examined in the following chapter.

6. THE EXPERT SYSTEM PERSPECTIVE: A THEORY OF ARTIFICIALLY INTELLIGENT GEOSTATISTICS

6.1 Introduction

Geostatistical techniques, in terms of the IRF-k theory, were reviewed, developed and applied in the previous chapters. The properties, abilities and advantages of these techniques were demonstrated. Furthermore, it was suggested that, since they improve the reliability of models describing reservoir-rock properties, they should be used for reservoir characterization by the Petroleum Industry. However, when one considers the Industry, that is a real life situation, as an inseparable guide of theoretical developments, one inevitably is forced to consider one additional reality. Simply, whether the knowledge and expertise required to put geostatistical techniques at work are available and if not, to provide a perspective in terms of knowledge transfer.

To understand the magnitude of the problem of knowledge transfer, as far as geostatistics is concerned, one may recall the example of the Mining Industry where the experts in the field declare: "After twenty years of geostatistics, it can be stated that from the technological transfer view, it is a quasi-total failure"; (David **et al.**, 1987). Considering that the Petroleum Industry has only discovered geostatistics in the last few years, one should realize that it is imperative to provide, at least, a perspective for the transfer of the knowledge and expertise involved. The latter may be examined in the light of technological developments in the field of Artificial Intelligence and particularly the area of Expert Systems. Expert systems are computer programs which contain knowledge in a domain and can therefore be used by non-experts to perform elaborate tasks. They have been used for knowledge transfer in other areas related to the Petroleum Industry, including well-log correlations (Olea and Davis, 1986; Kuo and Stratzman, 1987), dipmeter interpretations (Smith and Baker, 1983), sedimentary basin classification and resource assessment (Miller, 1986) and recognition of sedimentary environments (Shults **et al.**, 1988).

Expert system technology is suggested here as a perspective for geostatistical reservoir characterization. The suggestion, however, is not as simple as it may appear. The related knowledge is not a mere collection of rules of thumb, as it is, for example when one has to correlate the resistivity response of a sequence of rocks as expressed by its increase or decrease on well-log curves. Rather, one has to deal with an elaborate mathematical model and the intricacies arising

not only from the phenomenon to be studied but also from the model itself. It is therefore necessary that in order to provide a viable operational perspective such as an expert system, one must view geostatistics as a model and provide a new expanded view of the model itself, upon which new perspectives may be founded. This is attempted in the next paragraphs where the model is not geostastistics but the geostatistician as both a theoretician who develops geostatistical formulations and a practitioner dealing with everyday applications, exhibiting knowledge and intelligence.

6.2 Elements of Intelligence in Geostatistics: The Geostatistician

In scientific developments, theories, formulations, models or applications, there is an underlying characteristic expressed. This characteristic is intelligence. Intelligence is neither an inherent property of a theory, model or solution nor an entity in itself, but rather an ability exhibited by the Person who puts things together based on knowledge - understanding of an area of work or problem. It should therefore be evident that to examine the source of intelligence in geostatistics, one is bound to consider the geostatistician as the Person both developping and using a mathematical model, as well as his knowledge in the domain of application.

The Geostatistician involved in problem solving may be seen as engaged in a series of cognitive processes in order to perform his task. These processes are concerned with the effective and competent (i) selection of the parts of his knowledge relevant to the problem and (ii) the combination of them in the process of inventing a solution. If the existing knowledge is inadequate, then knowledge acquired from experience in problem solving guides the search for knowledge relevant to the problem in hand. At higher levels of difficulty, it may be required to interact and combine developments from other fields with geostatistical knowledge to discover new techniques capable of tackling the given problem. Next, if a solution has been invented or discovered then the results of application are assessed, in a similar manner as before, by effectively selecting, combining and comparing different pieces of knowledge. If the results are not satisfactory, the above processes are repeated taking into account what has been learned from the whole experience.

From the processes outlined above, it may be concluded that intelligence in geostatistics is the ability of the Geostatistician to invent and/or discover as well as assess, by effectively selecting and combining pieces of relevant knowledge using the relational know-how in the domain. Apparently, the source of intelligence in geostatistics lies in the dynamic interaction of the different parts of geostatistical knowledge as manipulated and processed by the cognitive tasks that the Geostatistician performs. It is therefore necessary to consider geostatistical knowledge and further identify its content.

Geostatistical knowledge may be seen as including (i) the strict stochastic model as it has been developed (Matheron, 1965) and the numerous associated techniques; (ii) operational intricacies of the model and techniques; (iii) applicational facts related to the field of application, variable under investigation and particular case study. To these, one may add (iv) the relational know-how, that is how all pieces of knowledge in (i) to (iii) are related, interact and could be efficiently and effectively combined as well as general methodological knowledge on how to search for a solution, and interact with other fields and developments. To suggest how the above knowledge is being used, one must suggest a medium and a form of expression. However, to do so one must first adopt a view of the Geostatistician itself. The latter, as it will be further discussed, directs the approach of how geostatistical knowledge should be conceptualized.

To provide scientifically sound formulations, it is necessary not only to state the objects of study such as the Geostatistician with his intelligence and knowledge, but also to provide the approach that is taken for the study. To put it in more proper terms, a paradigm (Kuhn, 1970) is needed. The paradigm chosen here is directly adopted from the field of Artificial Intelligence, from which the present paper heavily borrows. In Artificial Intelligence, the Person is viewed as a processor of symbols representing knowledge, a processor which exhibits intelligence by performing various cognitive tasks (Newell and Simon, 1972, 1976). Accordingly, it is simply rephrased that the Geostatistician, as

being a Person, is viewed as symbolic processor, but specialized rather than generic.

6.3 A Theory of Artificially Intelligent Geostatistics

Motivation drawn from the pragmatic need to transfer geostatistical knowledge and expertise led, in the previous paragraphs, to the examination of the intelligence and knowledge of the Geostatistician. The latter is conceived as an abstraction of "collective" knowledge in the domain to simultaneously represent a theoretician and a practitioner. The focus was implicitly shifted from the traditional geostatistical model expressed in the probabilistic formalism of random functions, to an attempt to conceive a different expanded model where the traditional one, although definitive, is clearly not the sole attribute.

Considering the view previously discussed it is possible to construct a theory establishing the abstraction of Geostatistician as a wide model of geostatistics, which may be termed "theory of Artificially Intelligent Geostatistics". "Artificially" should be seen as expressing the intent to consider the operational objective of building computer systems for geostatistics, while "Intelligent" signifies the intent to tackle deeper analytical objectives of demystifying, clarifying and explicating geostatistical knowledge, leading to a better understanding of intelligence as is required if operational objectives are to be

realized. The theory of Artificially Intelligent Geostatistics simply states that:

(i) The Geostatistician is a processor of symbols.
(ii) The Geostatistician performs cognitive processes which can be expressed as the effective combination of relevant pieces of knowledge.
(iii) The effective combination of knowledge is guided by relational knowledge.
(iv) Advice generated from geostatistical knowledge is always followed.
(v) Results of geostatistical problem solving may be assessed.

The above theory is founded, as explicitly stated, upon the view of the Geostatistician as a processor of symbols performing cognitive tasks in geostatistical problem solving. This view is in itself neither right nor wrong. It is adopted for the same reasons that it is adopted in Artificial Intelligence, that is, models with operational consequences and uses can be built upon it. It is adopted for the same reasons that the Person is viewed as an economic agent in Economics and not a biological organism as is viewed in Medicine. The theory of Artificially Intelligent Geostatistics, however, needs like any scientific theory to (a) unify a number of observations and (b) predict new effects that can be experimentally tested.

The Geostatistician is an instant of the general abstraction Person representing the "collective" human intelligence. As such it

unifies all observations about the Person as shown in the twenty years or more of research in Artificial Intelligence. The theory proposed here must also unify observations within the domain of specialization, mainly geostatistics. Some examples should therefore be considered.

Suppose that structural analysis is to be performed on porosity data from a horizontal sandstone unit representing a fluvial channel with northeast-southwest orientation. Several parameters will be considered including the directions at which variograms will be calculated. One way is to calculate variograms for many directions. However, the geometry and orientation of the sand body may be considered. The related knowledge will suggest that anisotropy is probably present and most likely the major axis of it will follow the major axis of the sand body i.e. the northeast. Thus, knowledge on variography and knowledge on the given study case are combined by the empirical knowledge that relates them. Consider now that experimental variograms do not exhibit clear transition zones. Then histograms of porosity are examined and found tailed to the right, indicating that outliers may exist. Exclusion and recalculations are undertaken to find if, as is very common, the new variograms do exhibit structures, which are then related to permissible variogram models. Thus, the variogram of porosity of the given sandstone unit has been revealed by consistantly using not only pieces of geostatistical knowledge but also knowledge on how they are related. Apparently, the advice from geostatistical knowledge has always been followed. Furthermore, the revealed variogram model can be assessed either by a jacknife technique or new field data, if available.

As a second example a real situation taken from the modelling of permeability in the previous chapters is considered. Permeability is not additive. Therefore estimation of block permeabilities from point ones cannot be direct. It is, however, known that point permeabilities can be conditionally simulated. Similarly, discretization of volumes is also a known procedure. Relating the two, a block can be seen as a collection of conditionally simulated point permeabilities. Next, a formulation is needed to relate the point permeabilities to the permeability of the block. It is known that permeability is an entity arising when flow is considered; therefore, it is evident that developments in subsurface stochastic hydrology should be considered. Indeed, developments in the latter field provide the formulation to derive the permeability of a block. Thus, by combining different pieces of knowledge as guided by the knowledge of their relations, a new method in estimating block permeabilities is discovered. The new method may be assessed by using the knowledge of the formulation or new field data.

The above examples show that the theory of Artificially Intelligent Geostatistics unifies observations on how geostatistical knowledge is being used in order for the Geostatistician to discover or invent. The same can be concluded by considering any of the numerous published papers on geostatistics. The theory must also be able to predict effects which can be tested experimentally. The latter can be demonstrated by the operational dynamic consequences of the theory in the form of computer programs which validate the theory. However, before the

dynamic aspects of the theory proposed here are examined and examples presented, there are two important aspects to be considered. First, how knowledge that is being used is expressed, represented and how it could be manipulated, that is processed.

6.4 Symbolic Realization and Epistemological Aspects of Geostatistical Knowledge

Symbols, or more generally, the symbolic realization of knowledge is inherent to the very notion of a processor of symbols (Newell, 1980). In the theory of Artificially Intelligent Geostatistics, the Geostatistician is therefore bound to operate in a world of symbols representing all aspects of his knowledge. This world is a (geostatistical) universe of discourse where everything can be expressed in terms of symbols associated with physical relationships. Symbols and their relationships, as for example, one symbol next to another, are symbolic structures which can encode and express knowledge in the universe of discourse. Geostatistical symbolic structures consist of elementary (primitive) entities such as distance, location, grade, etc., and elementary processes such as addition, power, expectation, etc. which have a fixed meaning and are not further analysed within the conceptualization of the domain. Symbolic structures have referents; in fact, this is precisely what makes a combination of tokens (elements) symbolic. Referents signify the ability of symbols and symbolic structures to designate. For instance, in geostatistics, the combination of the symbolic structure (RANGE, VARIOGRAM-1) and the primitive symbol 10km designate that the RANGE of VARIOGRAM-1 is 10 km. In addition,

symbolic structures are interpretive, in the sense that symbols designating a process can be performed by the symbolic processor. For example, interpretation of the symbolic structure (CALCULATE EXPERIMENTAL-VARIOGRAM) designates the process CALCULATE which can be performed on the EXPERIMENTAL-VARIOGRAM.

The symbolic realization provides the medium necessary to express knowledge. However, if it is to enhance representation and processing of complicated geostatistical symbolic structures, one must consider, in an epistemological sense, broad classes of symbolic structures representing geostatistical conceptual units. Furthermore, one must examine the relations of these conceptual units to provide some basic semantics. The above will then provide the means to examine forms that can represent knowledge. Accordingly, four major distinct associative conceptual units will be considered, namely concept, description, attribute and value.

Concepts are general formal geostatistical symbolic structures such as the conception of variogram, estimation, conditional simulation etc. For example, a spherical variogram is a specific description of a variogram. Attributes are also symbolic structures or symbols. A spherical variogram, for example, has range, still, nugget effect, and distance as attributes, and conversely these attributes are parts of the description of the spherical variogram. Values correspond to every attribute and are specific parts of it, expressed as primitive symbols, such as the primitive symbol 10km, which may be the value of the

attribute RANGE. In addition, values may be attached formulae or precedures which can be carried out to yield specific values.

The consideration of different conceptual units represents an abstraction mechanism (Lehnert, 1981). Two kinds of abstraction mechanisms may be distinguished (Levesque and Mylopoulos, 1979). The first is the distinction of concepts, sub-concepts and descriptions generating a taxonomy known as IS-A hierarchy. An IS-A expresses universal quantification. The second abstraction mechanism is the distinction of descriptions, attributes, and values. These conceptual units generate a taxonomy known as PART-OF hierarchy expressing existential quantification. The significance of the IS-A and PART-OF hierarchies is that characteristics and properties of one conceptual unit can be inherited by another. For example, one may consider the concept variogram and its sub-concept experimental variogram. From the IS-A hierarchy one can derive that an experimental variogram IS-A variogram and it therefore describes the spatial structure of a variable. Furthermore, the experimental variogram will inherit a description, say spherical variogram. From the PART-OF hierarchy, the experimental variogram with spherical description will inherit the existing attributes range, still, nugget effect as well as values through some heuristic or algorithmic procedure. In addition, the value of an attribute may be a known constant (default value), which has been selected according to prior knowledge in the domain.

Finally, individual real conceptual units are considered as instances of abstract ones. For example, the variogram $\gamma(h) = 0.5$ is an

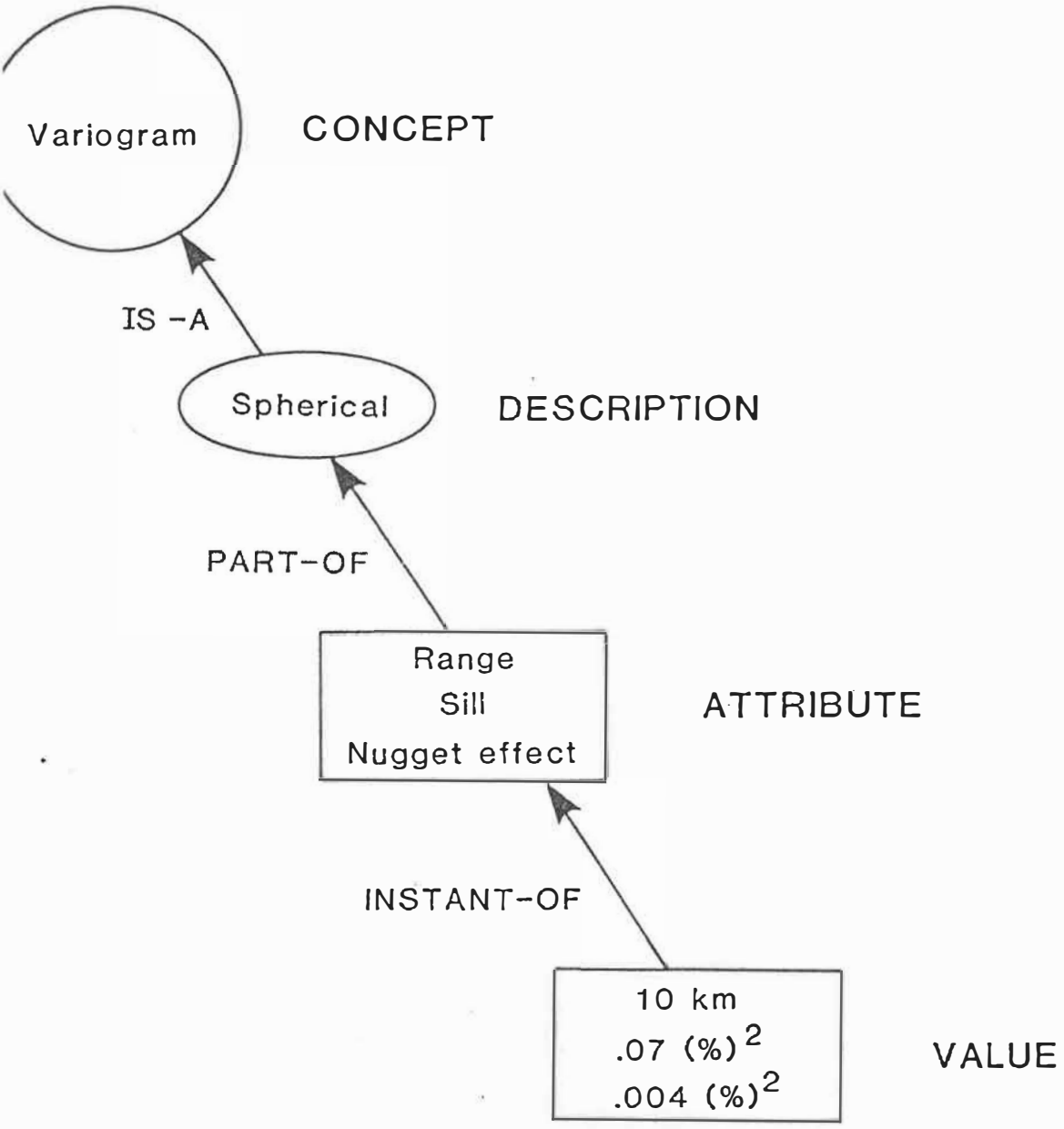

Figure 6.1: Formal geostatistical conceptual units and their semantics.

INSTANT-OF the concept variogram, the range 10 km is an INSTANT-OF the attribute range, etc. A graphical example of geostatistical conceptual units and their formal semantics are presented in Fig. 6.1.

6.5 Knowledge Representation and Inference

The paramount aspect of the realization of knowledge as a collection of symbolic structures is that it can be represented. Then inference of new knowledge can be attained. The most common representation of knowledge is in the form of predicate calculus as developed in logic (Kleene, 1967). Predicate calculus consists of formulas and every legitimate (syntacticly and semanticly valid) expression is called a well formulated formula (wff). Wff's are made of elementary (atomic) formulas consisting of predicates and arguments. For example, to express the relation between an individual range, say RANGE-1, and the conceptual units of range, spherical variogram and variogram, we may write the atomic formulas:

(INSTANCE-OF RANGE-1 RANGE)
(PART-OF RANGE SPHERICAL-VARIOGRAM)
(IS-A SPHERICAL-VARIOGRAM VARIOGRAM)

Atomic formulae can be connected with connectives and quantified with quantifiers. Connectives are the conjunction ($\wedge$), disjunction ($\vee$), negation ($\neg$), implication ($\rightarrow$), and equivalence($\leftrightarrow$). Quantifiers are the existential ($\exists$) and the universal ($\forall$). In addition, predicate calculus permits the use of variables. Consequently, complex

statements can be expressed. For example, we may express that every spherical variogram has sill, range, and possibly nugget effect in the form of a wff as follows:

$$
\begin{aligned}
&(\forall x)\ (\text{IS-A } x \text{ SPERICAL-VARIOGRAM}) \rightarrow \\
&\quad \exists\ y\ (\text{IS-A } y \text{ RANGE}) \wedge \\
&\quad \exists\ z\ (\text{IS-A } z \text{ SILL}) \wedge \\
&\quad \exists\ u\ (\text{IS-A } u \text{ NUGGET-EFFECT}) \vee \\
&\quad \neg\ u\ (\text{IS-A } u \text{ NUGGET-EFFECT}))
\end{aligned}
$$

Knowledge is also represented by semantic (associative) networks (Brachman, 1979; Shapiro, 1971; and others). Semantic networks consist of nodes representing conceptual units and arcs (links) between the nodes which correspond to relations. The knowledge represented previously in the form of predicate atomic formula can, for example, be represented in a semantic network as follows:

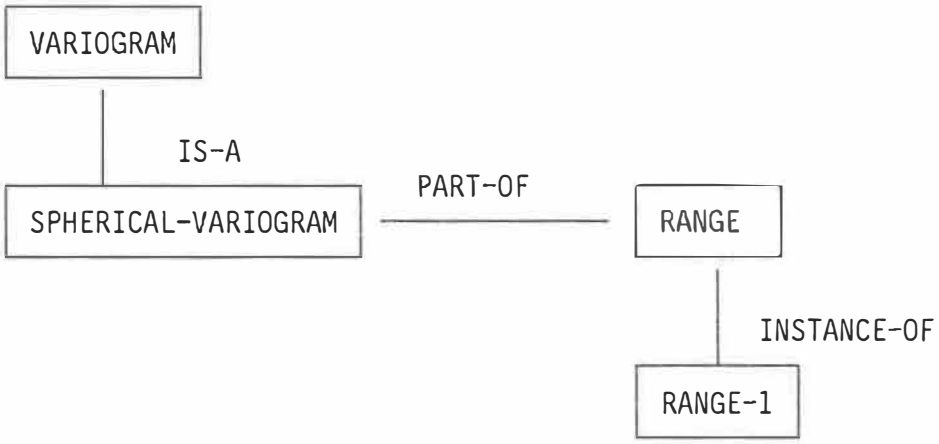

Networks may also be partitioned (Hendrix, 1979) into subnets (spaces) which can be considered separately, increasing the usability of network.

Frames (Minsky, 1975; Aikins, 1983) are special structures which tie together associated conceptual units and relations as well as instances. They are equivalent to a collection of semantic network nodes and arcs that describe a particular relation. For example, a frame describing a spherical variogram may be as follows:

```
(SPHERICAL-VARIOGRAM (HAS-A RANGE)
                     (HAS-A SILL)
                     (HAS-A NUGGET-EFFECT))
```

Knowledge is very commonly represented in the form of rules (Buchman and Shortliffe, 1984). Rules are conditional statements which consist of antecedent-consequent symbolic pairs in the general form:

$$A_1, A_2, \ldots, A_n \rightarrow C_1, \ldots, C_n$$

The condition for the validity rule is that it must be both syntactically and symbolically valid. Rules can capture empirical and judgmental knowledge in a universe of discourse. They express causal relations between antecedents and consequents; however, they do not in general include formal justifications. In general, rules do not represent in context explicitly stated knowledge in the domain (Clancey, 1983a). However, they can be grouped together on the basis of context

to represent knowledge explicitly. The latter may be obtained by combining rules and frames. In general, combinations of different knowledge representations (multiple representation) can be used to capture the knowledge in a universe of discourse. Furthermore, it is suggested that special attention should be paid in the representation schemes that are functionally more suitable to express geostatistical knowledge.

Knowledge represented in some form can be processed to infer new knowledge. The most common inference is deduction. Deduction is seen in formal logic (Kowalski, 1979), as being based on a set of axioms (truths) from which new axioms are derived using formal rules of inference. Deduction is a sound inference which means that every deduction is correct. The most simple rules of inference are:

1)**modus ponens;**

given $\left.\begin{matrix} x \\ x \rightarrow y \end{matrix}\right\}$ deduce y

2)**modus tolens;**

given $x \rightarrow$ deduce $\neg x \rightarrow \neg y$

3)**universal specification:**

given $\left.\begin{matrix} x\ W(x) \\ A \end{matrix}\right\}$ derive $\rightarrow W(A)$

More general rules of inference also exist, which subsume the simpler ones. The most general rule of inference is resolution (Robinson, 1965), presented extensively by Nilsson (1980) and Loveland (1978). Resolution is a complete rule of inference, which means that if an axiom can be deduced from a set of axioms, then resolution will prove it. Rules of inference and particularly resolution are subject to operational problems such as combinatorial explosion and halting (Winston, 1983).

Although formal logic provides significant rules of inference, it is not always the best or unique inference medium. Inference can be, in addition, formulated in the form of search (Nilsson, 1989; Gardner, 1981). Accordingly, a desired solution is seen as a goal and possible steps to achieve the goal as states. The search based on heuristics is performed to find the steps leading to the goal. For example, if it has geen decided that an experimental variogram has a specific sill, range

and nugget effect, the solution of the problem of fitting one of the appropriate models can be formulated as search in which the goal is to fit a model and the steps are to try the different available models. Search can then be performed by using a heuristic function measuring the goodness of fit of every possible variogram model. Search is also based on deduction as well as other kinds of inference such as abduction (Pople, 1973) and induction (Brown, 1973). Abduction is, in simple terms, expressed by the relation:

$$\left.\begin{array}{l} \text{given} \quad A \rightarrow B \\ \qquad\quad B \end{array}\right\} \text{ abduct } A$$

Induction represents the derivation of generalizations from specific facts applying to individual instances. Both abduction and induction are not sound kinds of inference and are guided by heuristics.

6.6 Dynamic Aspects of the Theory: The Explicit Knowledge Formalism

The theory of Artifically Intelligent Geostatistics is a rationalization of the performing Geostatistician. As such, it incorporates dynamic aspects, that is, operational models in the form of computer systems that can be built to exhibit what the theory calls for. In fact, operational models constitute the predictive aspect of the theory and are the new effects which can be experimentally tested.

The operational formalism expressing the dynamic aspects of the

theory and at the same time an inseparable part of it, is termed the explicit knowledge formalism. The formalism calls for computer systems which contain, explicitly, geostatistical knowledge in all its types and aspects as previously discussed.

To further elaborate on the explicit knowledge formalism one may first consider conventional geostatistical programs which, like any other conventional program, are based on the scheme:

$$\text{INPUT} \rightarrow \text{METHOD} \rightarrow \text{OUTPUT} \qquad (6.1)$$

where method is a numerical algorithm and INPUT, OUTPUT sets of numerical values. This scheme may be seen as posessing some knowledge on how to follow-perform a geostatistical procedure which can be carried out or not. However, the program does not have any 'consciousness' of what the input is, what the output represents or what the meaning of the operation it is designed to perform is about. Traditional programs as in (6.1) are, however, consistent with the traditional conception of geostatistics as a strict probabilistic model. They are designed to carry out the calculations geostatistical theory requires for its application, and in this sense fulfill their objectives. The explicit knowledge formalism as the operational side of an expanded geostatistical theory provides a different objective. This objective is to build geostatistical expert systems having all types of geostatistical knowledge is part of them and accordingly the ability to create, modify, reproduce or copy and destroy geostatistical knowledge.

The explicit knowledge formalism integrates the following: (i) all types and aspects of geostatistical knowledge; (ii) symbolic, non-algorithmic methods for knowledge representation, inference and reasoning; and (iii) numerical data processing. It can therefore provide a new formulation of geostatistical programs in the scheme:

INFORMATION → SYSTEM → JUSTIFIED RESULTS (6.2)

where INFORMATION is simple general information on a specific application; JUSTIFIED RESULTS is the output including numerical results, interpretations, evaluations as well as a detailed account of the steps followed, knowledge involved together with full explanations and reasoning; SYSTEM is a collection of a storage of different kinds of geostatistical knowledge and an engine for the processing of knowledge. Traditional programs as in scheme (6.1) one part of SYSTEM as simple attached procedures used to returned numerical values needed for geostatistical attributes (recall previous presentation of conceptual units also depicted in Fig. 6.1).

Implementation of systems according to scheme (2) one critically controlled by:

a) Theoretical foundations.

b) The acquisition of geostatistical knowledge and particularly the expertise for problem-solving in the domain.

c) The functional representation of geostatistical knowledge.

d) The inference mechanism (engine) for geostatistical knowledge processing.

e) The interface to the user of the collection of the required information and transformation of it to a processable form (representation).

f) The interface to conventional subroutines for calculation of specific values, results evaluation and interpretation.

6.7 BOU-1: A Prototypical Experimental System

BOU-1 is an experimental system entirely based on the theory presented in the previous paragraphs. It represents an exploratory attempt to investigate the feasibility of larger geostatistical systems, study aspects related to geostatistical knowledge representation, and finally evaluate the theory upon which it is based. In this sense, the calculation of experimental variograms which the system is able to perform or some further evaluation on variogram models is not its main contribution because it was never meant to be. What are indeed important are the properties the system has, that is essentially the knowledge it can contain, use and how it proceeds.

BOU-1 is implemented in Golden Common LISP (Gold Hill Computers,

1986) available on PCs. The choice of LISP (Charniack **et et.**, 1980) as the programming language is based on the facts that LISP provides a very flexible and relatively fast environment for symbolic manipulations, it is interpretive and is featured by functional modularity. Pros and cons of different programming languages for symbolic manipulations from an implementational point of view are discussed by Forsyth (1984a).

As a knowledge-based system, BOU-1 schematically consists of (Figure 6.2) (a) the knowledge-base which is the system's storage of symbolically represented knowledge about geostatistical domain subjects, namely calculation and evaluation of experimental variograms; (b) the inference mechanism which structurally controls the processing of the knowledge base; (c) interface with subroutine VARIO3 (Geostat Systems International Inc., 1983) for variogram calculation; (d) the user interface for the collection of information; and (e) a "blackboard" where numerical values of global variables are stored and accessed during consultations.

Multiple representation is used in BOU-1. Accordingly, knowledge is represented by rules, frames and networks. Rules consist of an IF (antecedent) and a THEN (consequent) part (Figure 6.3) and are used to capture empirical relationships among entities in the geostatistical domain. On the basis of content, rules can be disinguished as inferential and control. The former are directly related to the inference process, while the latter are directly related to the flow of the sys-

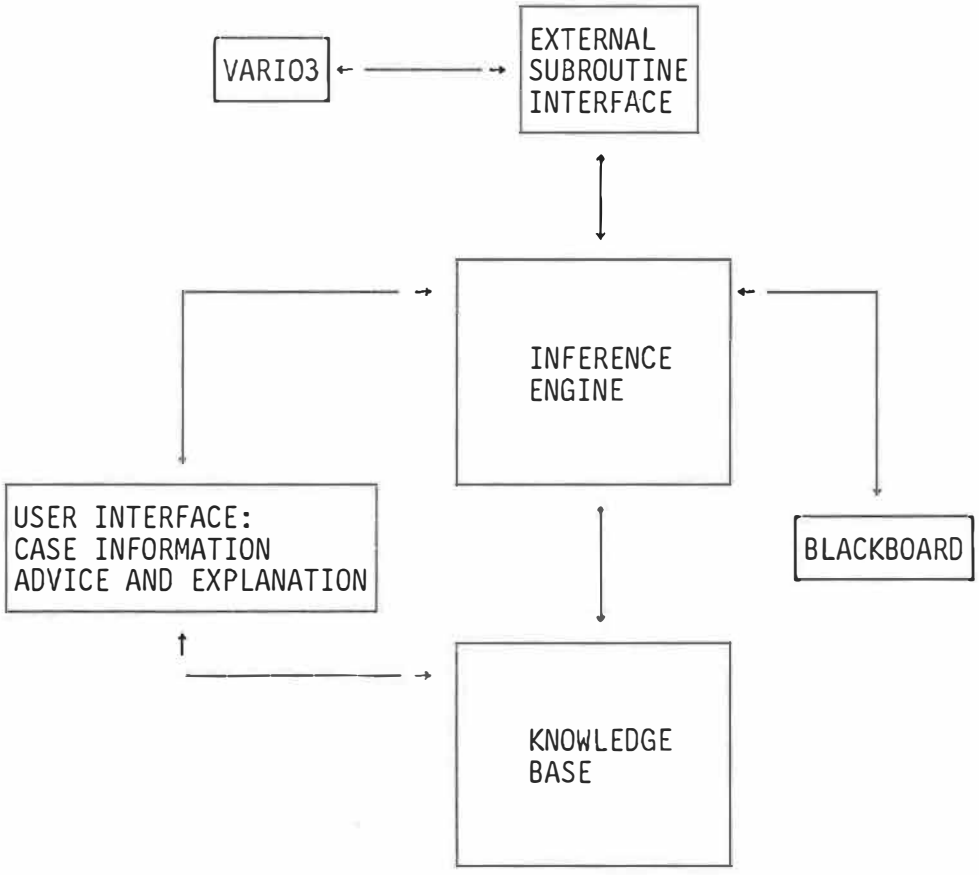

Figure 6.2: Main parts of BOU-1. Arrows indicate information flow.

```
(RULE 2-no-of-directions     (IF   (No-OF-SAMPLES is less than 150)
                                   (No-OF-SAMPLES is greater than 75)
                                   (PREFERENCE-IN-DIRECTION is NO)

                             (THEN (No-OF-DIRECTIONS-NDIR is 4)))

(RULE 2-Check-no-of-pairs    (IF   (No-OF-DIRECTIONS-NDIR is 1)
                                   (No-OF-PAIRS is greater than 49)
                                   (No-OF PAIRS is less than 100))

                             (THEN (TIME TO STOP)
                                   (FINISH PART-2)))
```

Figure 6.3: Sample rules from the knowledge-base of BOU-1.

tem. Both contextually and operationally, rules are classified into three groups. The first includes rules related to the initialization of the numerical values for the parameters needed to execute subroutine VARIO3; the second, rules related to the evaluation of the results that VARIO3 returns and; the last, rules related to the quantification of characteristics of the experimental variogram. Frames, implemented as nested association lists (Winston and Horn, 1985), are used to store and retrieve the current values of parameters for the execution of subroutine VARIO3, as well as describe taxonomic relations between concepts, descriptions, attributes, and values in the domain. Frames consist of their name, slots, facets, and values as shown in Figure 6.4. Simple networks (Figure 6.5) are used to transform or deduce facts from the information the user provides.

The inference process in BOU-1 proceeds in a forward-chaining fashion. Antecedents are matched against facts, rules trigger, consequents are new facts added to the initial ones, matching is repeated and so on until no rule triggers. The process is implemented using rules and facts in the form of lists which flow through algorithmically interconnected and invoked functions. Conflicting facts commonly deduced during consultation of the system are treated by always retaining the latest deduction and discarding the earlier for truth maintenance.

The control structure of the system is simple. The system executes the top task on an agenda as defined within the program, and then proceeds with the execution of the second one. A task corresponds

```
(INPUT-FOR-VARIO3   (No-OF-DIRECTIONS-NDIR     (MUST-BE-SET-TO 4)
                    (MAX-STEP-STEP             (MUST-BE-SET-TO 10)
                          •
                          •
                          •
                          •                                        )


(FPUT '2D-GEOMETRICALLY-ANISOTROPIC-3DV 'NUGGET-EFFECT 'IS (* 0.5
                                        (+ NUGGET-1 NUGGET-V)))

(FPUT '2D-GEOMETRICALLY-ANISOTROPIC-3DV 'SILL 'IS (* 0.5 (+ SILL-1
                                        SILL-V)))

(FPUT '2D-GEOMETRICALLY-ANISOTROPIC-3DV 'RANGE 'IS (MAX RANGE-1
                                        RANGE-V))

(FPUT '2D-GEOMETRICALLY-ANISOTROPIC-3DV 'ANISOTROPY-RATIO 'IS
                                        (/ (MAX RANGE-1 RANGE-V)
                                        (MIN RANGE-1 RANGE-V))

(FPUT '2D-GEOMETRICALLY-ANISOTROPIC-3DV 'DISTANCE 'IS 'FUNCTION-OF
                                        ANISOTROPY-RATIO)
```

Figure 6.4: Simple frame structures as used in BOU-1.

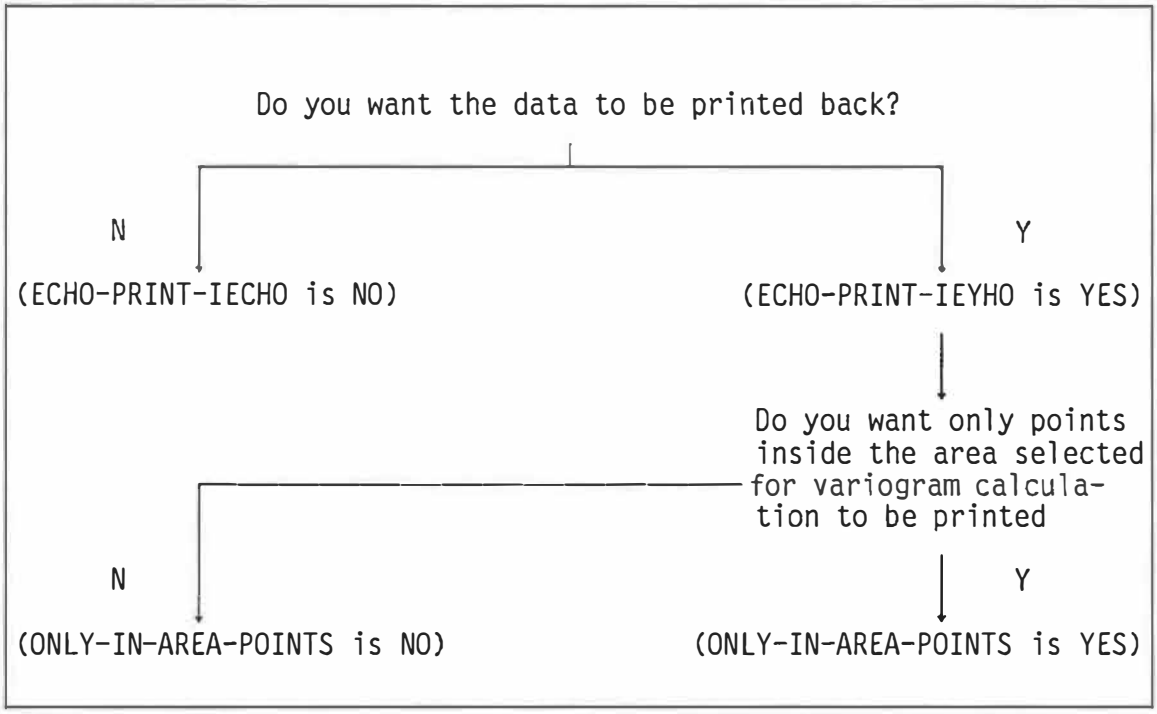

Figure 6.5: Sample network used to transform information to processable by system facts.

to an operational part of the system. Three such parts are distinguished. The first deals with the initialization of the parameters critical for the run of subroutine VARIO3, the second with the evaluation of the results of the run and the third with the suggestion of the characteristics of a possible variogram model. The system is so designed that tasks can be repeated if required. This is done through control rules and it is required in the second part if the results from VARIO3 are not considered by the system as satisfactory. The control flow of the system is given in Figure 6.6.

A consultation session with BOU-1 proceeds with the system asking simple questions as in Figure 6.7. Then the parameters for running VARIO3 are chosen and reported to the user as in Figure 6.8. Explanations in the choice of the parameters are also provided (Figure 6.9). Next VARIO3 is executed, the results are evaluated and if satisfactory, the system asks the user to give some simple judgments on the experimental variograms (Figures 6.10 and 6.11). Then BOU-1 evaluates the experimental variograms. Results (Figure 6.12 and 6.13) and explanations (Figure 6.14) complete the session with BOU-1.

BOU-1 is a prototypical experiment in the perspective of automating geostatistical operations. As an experiment, it has shown that geostatistical knowledge can be well represented in the form of rules, frames, and networks. It would be interesting, in future developments of the system, to examine the possibility of using more generalized forms for the representation of empirical relations such as "covering sets"

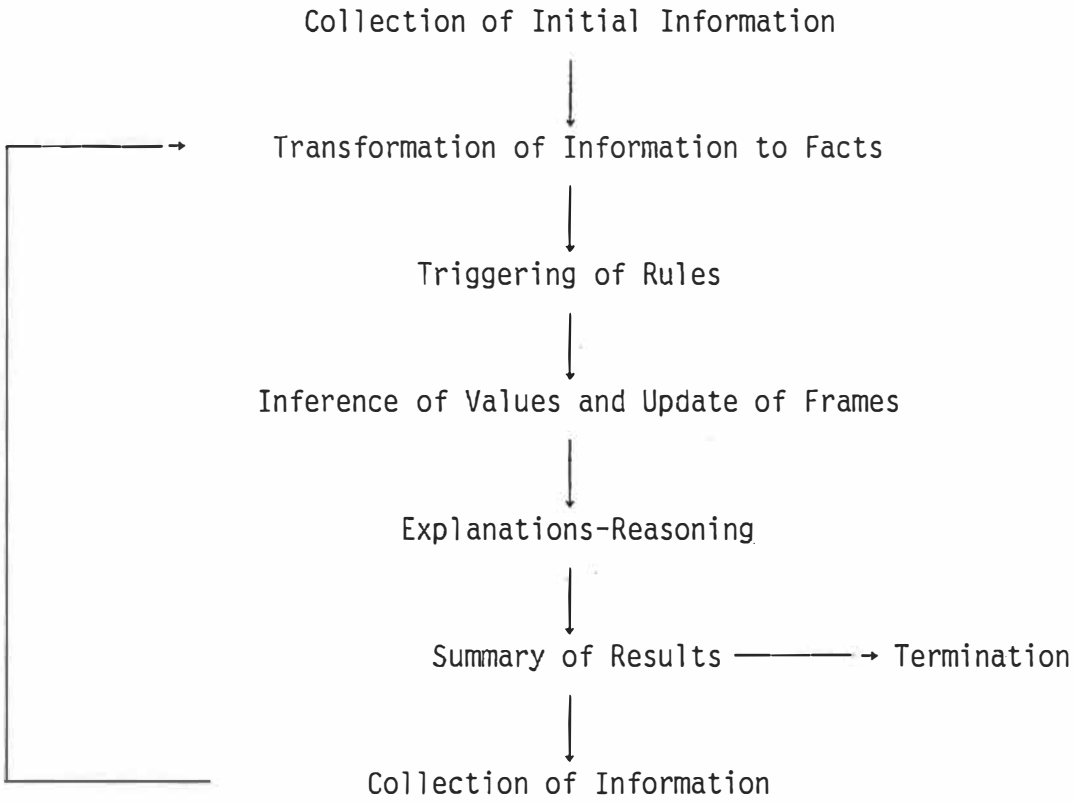

Figure 6.6: Overview of control flow in BOU-1.

```
Are we dealing with more than one variable?          (Y or N)     No
Are we dealing with two dimensional data?            (Y or N)     Yes
Give me the minimum X coordinate:  770.0
Give me the maximum X coordinate:  882.5
Give me the minimum Y coordinate:  730.0
Give me the maximum Y coordinate:  817.6
How many samples are involved:     112
```

Figure 6.7: Sample questions asked by BOU-1 for the collection of initial information.

Dear Roussos, I have reached the following conclusions for PART-1 according to what you have just told me. If you need more explanation, you can just ask me.

(IECHO IS 1)

(IACM IS 0)

(IVERT IS 0)

(ZDMAX IS 0)

(ZMIN IS 0)

(ZMAX IS 0)

(NO-OF-DIRECTION-NDIR IS 4)

Figure 6.8: Some conclusions reached by BOU-1.

```
Do you want to know why:          (Y or N)    Yes
Rule 2:  2-NO-OF-DIRECTIONS
         - concludes:  (NO-OF-FIRECTIONS-NDIR IS 4)

         - because:    (PREFERENCE-IN-DIRECTION IS NO)
                       (NO-OF-SAMPLES IS GREATER THAN 75)
                       (NO-OF-SAMPLES IS LESS THAN 150)
```

Figure 6.9: Sample of explanations provided by BOU-1.

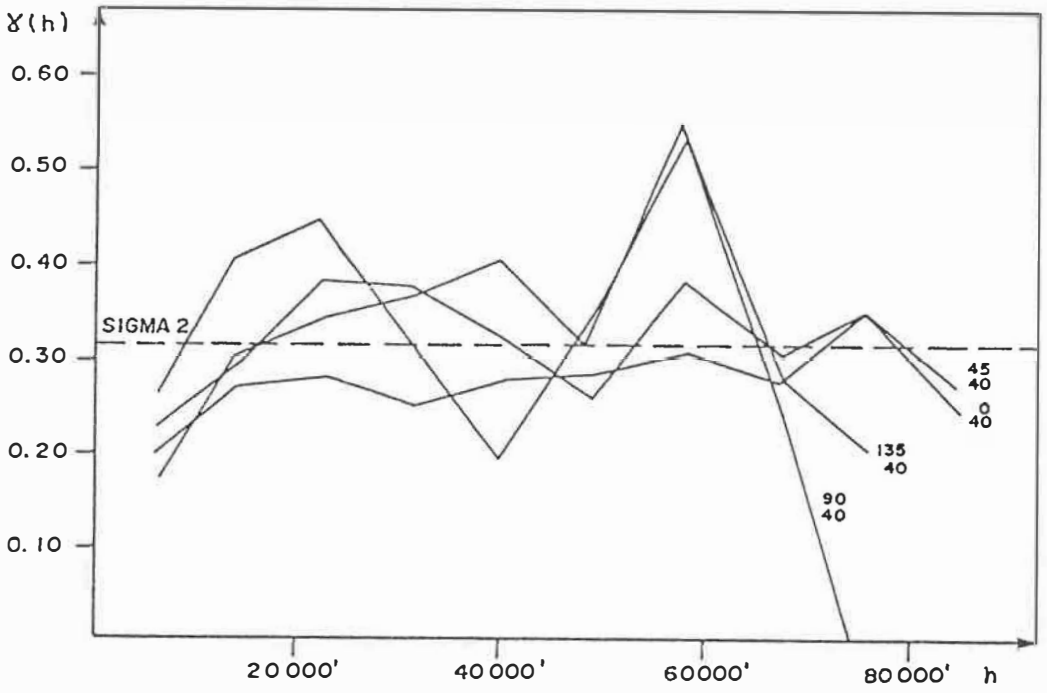

Figure 6.10: Experimental variograms, calculated by BOU-1.

```
Are you ready to continue with PART-2?          (Y or N)      Yes

Experimental variograms have been calculated in the directions:
                            (0 45 90 135)

Give me your estimates of the nugget effects in all directions in a
list form - in the same order as above:
                       (0,11  0,11  0,10  0,12)

Give me your estimates of the sills in all directions in a list
form - same order as above:
                       (0,32  0,30  0,33  0,33)

Give me your estimates of the ranges in all directions in a list
form - same as above:
                       (17,2  18,0  17,5  17,0)
```

Figure 6.11: Questions BOU-1 is asking the user in PART-2.

```
     Dear ROUSSOS, I have reached the following conclusions for
PART-2 according to what you have just told me.  If you need more
explanations you can just talk to me:

                (VARIOGRAM-MODEL IS 3D-ISOTROPIC-2DV)

                (SET VARIOGRAM-MODEL-FRAME NSR-FRAME)

                          (FINISH 'PART-2)
```

Figure 6.12: Report of deductions in PART-2.

I have concluded PART-2 and now I will give you a summary of my conclusions.

The variogram model: 4D-ISOTROPIC-2DV

WHERE

- the value of the NUGGET-EFFECT is: 0.11
- the value of the SILL is: 0.32
- the value of the RANGE is: 17.425

Figure 6.13: Conclusions of a consultation with BOU-1.

```
Do you want to know why?              (Y or N)      Yes
Rule:  8-4D-ISOTROPY-2D-VARIOGRAM
- concludes:  (VARIOGRAM-MODEL IS 4D-ISOTROPIC-2DV)
              (SET VARIOGRAM-MODEL-FRAME NSR-FRAME)
              (FINISH 'PART-2)
- because :   (RANGES ARE EQUIVALENT IN ALL DIRECTIONS)
              (SILLS ARRE EQUIVALENT IN ALL DIRECTIONS)
              (NUGGETS-EFFECTS ARE EQUIVALENT IN ALL DIRECTIONS)
              (2D-IVERT IS YES)
              (NO-OF-DIRECTIONS-NDIR IS 4)
```

Figure 6.14: Explanations on deductions made in PART-2.

(Reggia **et al.**, 1983) as a substitute for rules. Frames are shown to be more appropriate to represent conceptual units and their formal relations from the geostatistical theory as well as situational-prototypical knowledge in the domain. Frames could also be used to control the agenda of tasks that a larger geostatistical system will execute and possibly to group and classify rules in a contextual manner. Networks were found particularly flexible in transforming user provided information to facts processable by the system. It has been realized that networks could be used to guide the collection of information and reason about why a specific question is asked at different stages of the operation of a large system. Furthermore, networks could direct the classification of different cases of deposit and regionalized variables that may need special treatment by the system.

The current inference engine of BOU-1 can easily be expanded to process more advanced knowledge structures. A backward-chaining inference function could be added, although its need has not been obvious so far. In addition, the inference engine could be expanded to augment multiple representation with separate reasoning processes for every representational scheme in the direction of a hybrid representation and reasoning engine (Brachman **et al.**, 1985; Vilain, 1985). Probabilistic reasoning for uncertain information could also be implemented in a Bayesian type formalism (Duta **et al.**, 1978), fuzzy logic (Zadeh, 1965) or other formalisms of non-classic logic (Mandani and Efstathiou, 1984). However, questions about the operational meaning of probabilistic reasoning have been raised (Forsyth, 1974b).

6.8 Verification of Theory

The system BOU-1 presented in the previous section has some significant properties and abilities with respect to the theory of artificially intelligent geostatistics. First, it undoubtedly represents a processor of symbols, possessing and manipulating geostatistical domain knowledge in different forms. Second, the tasks it performs are based upon the combination of relevant pieces of knowledge. For example, different parts of the knowledge base are used for the task of initializing the input of subroutine VARIO3 than for the task of evaluating the results. Third, pieces of knowledge are related by relational knowledge. For example (Figure 6.3), different pieces of knowledge from experience, i.e. the number of samples and the number of directions to calculate variograms are related in the form of a rule, and in another rule the number of directions is related to the pairs of samples used to calculate points of the experimental variogram. Finally, the system has the ability to assess results; for example, the experimental variograms are assessed in terms of the number of pairs used in the calculation of the first variogram point. In short, BOU-1 has all the properties that the theory calls for.

A comparison may also be considered. Given a set of data on porosity from a petroleum reservoir, experimental variograms are calculated independantly by BOU-1 and a geostatistician. As it is depicted in Figure 6.15, the experimental variograms are very similar, due to the fact that similar parameters have been used for their calculations. The

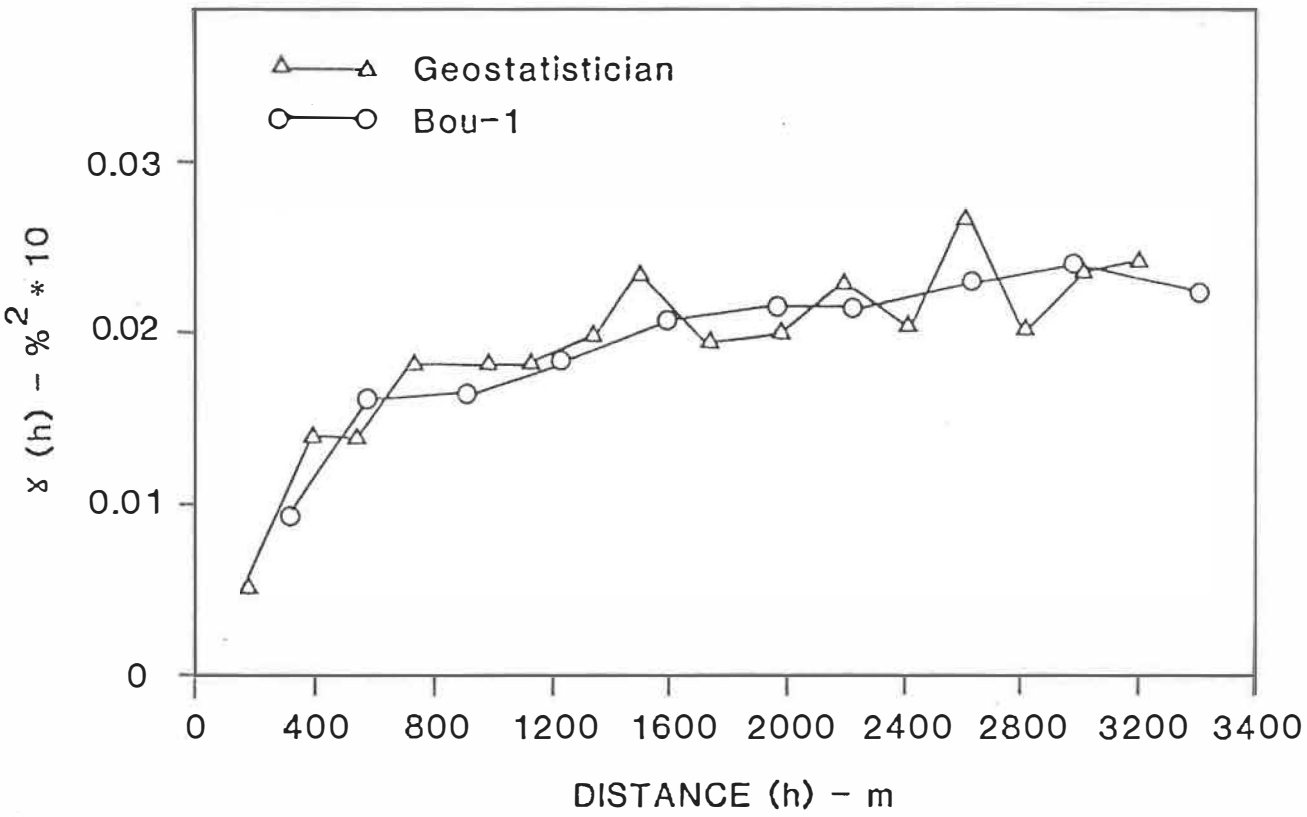

FIGURE 6.15: Comparison of experimental variograms of the same data set calculated independantly by BOU-1 and a geostatistician .

main difference is that the geostatistician used a step of 350 meters while BOU-1 used 500 meters. Although the task is simple, the comparison demonstrates the viability of building systems compatible to geostatisticians. In addition, BOU-1 verifies the proposed theory.

BOU-1 is at present the only system based on the theory proposed here. It is evident that more such systems will provide a more extensive verification. It should, in addition, be pointed out that BOU-1 represents a prediction that new systems can be built from the proposed theory.

6.9 Summary

Recognizing the need for transfer of geostatistical knowledge and expertise, a theory of Artificially Intelligent geostatistics has been proposed following the paradigm in the field of Artificial Intelligence. Accordingly, the Geostatistician is perceived as a processor of symbols, effectively combining all aspects of geostatistical knowledge represented by these symbols, in order to invent or discover. The operational side of the theory is termed explicit knowledge formalism and it is an integration of geostatistical knowledge, symbolic non-algorithmic techniques, and numerical data processing. An example has been presented in the form of an experimental system for calculation and evaluation of experimental variograms. The properties and abilities in representing and processing knowledge of the presented system support

the proposed theory; however, more systems are needed to sufficiently validate the theory.

The theory presented represents a perspective for the future development of geostatistical expert systems which can indeed provide the required transfer of knowledge and expertise in the Petroleum Industry as well as other areas of application of geostatistics. It should be, however, pointed out that the building of expert systems is not the goal of the presented theory. Expert systems are only the embodyment of the current (at each time) state of knowledge, technology, understanding and theoretical developments. The real goal is to further understand, explicate, demystify and comprehend geostatistical knowledge and skills, which in turn will be reflected upon the building of expert systems.

7. CONCLUSIONS AND RECOMMENDATIONS

The aim of this study was to present the conditional simulation of IRF-k, viewed as the generalization of geostatistical theory, in the quantitative-numerical characterization of petroleum reservoirs, and furthermore to provide a perspective for the transfer of the knowledge and expertise involved.

Following the specific objectives set in Chapter 1, the nature of reservoir properties was investigated and the basic elements of the IRF-k theory were presented indicating the suitability of geostatistical methods for modelling reservoir-rock variables. The technique for the conditional simulation of IRF-k was fully developed showing that non-stationary phenomena such as reservoir variables can be conditionally simulated to reproduce both available data and data structures as expressed by their generalized covariances. The modelling of permeability was also examined and a new approximate approach was proposed. Although the approach has limitations, it represents an improvement over practices in the Industry and could be found useful in reservoirs with good geological control and characteristics satisfying theoretical requirements imposed by the method.

Geostatistical techniques were used for the quantitative-numerical characterization of the Crystal Viking reservoir in south-central Alberta. Every unit of the reservoir was modelled separately. The quantification of variation patterns in terms of generalized covariances or variograms was used to subsequently estimate and conditionally simulate all pertinent variables. The produced models are intended to be used as input to reservoir flow simulations by the company operating the reservoir.

Finally, a perspective for building geostatistical expert systems was provided as the dynamic aspect of the theory of artificially intelligent geostatistics. The theory and an example suggest that indeed the perspective provided is realistic and feasible.

The major conclusions that can be drawn from this study are that geostatistical techniques have properties of particular interest and importance to reservoir characterization. They (i) quantify inherent geological reservoir properties such as zonation, continuity, trends and anisotropies; (ii) provide, directly from the scale of core and log data to the scale of the reservoir block model, unbiased estimates of reservoir-rock properties to be used as geological input to reservoir flow simulation studies; (iii) generate conditionally simulated representations of pertinent variables reproducing in-situ fluctuation of properties, to be used to check the sensitivity of flow simulation results to geological input; and (iv) can be transfered in the form of computer systems to be used by non-geostatisticians.

7.1 Future Developments

Several research subjects remain open to future developments, the major ones are emphasized next.

The problem of permeability estimation remains largely unsolved. Future research could be directed to study the quantity of flow, to somehow 'by pass' the estimation of permeability. Another direction could be to consider fractal pore geometry and related flow equations.

Reservoir-rock properties change as reservoir exploitation proceeds. It would be interesting to consider the development of techniques which could account for such changes given that laboratory data on physico-chemical alterations within the reservoir are available.

Qualitative information is often available in oil reservoirs. Techniques to account for this information such as Bayesian or Fuzzy geostatistics could be considered and assessed.

The expert system perspective opens a new area of research and developments. One area is research on the level of the Geostatistician, which could lead to better understanding and demystifying geostatistical knowledge, as well as explicate geostatistical skills. A second area of research includes the development of geostatistical expert systems for reservoir characterization. Such systems could be seen to contain,

along with geostatistical expertise, information on groups or oil plays, that is families of genetically related reservoirs in a sedimentary basin. This information could be used to guide reservoir characterization of a given oil pool even in the case that the available well data are not sufficient.

BIBLIOGRAPHY

AIKINS, J.S., 1983, Prototypical knowledge for expert systems. Artificial Intelligence, vol. 20, pp. 163-210.

AITCHISON, J. and BROWN, J.A.C., 1957, The Log normal distribution, Cambridge Univ. Press, Cambridge, MA.

ANTELMAN, G. and SAVAGE, I.R., 1965, Surveillance Problems: Wiener Processes. Naval Research Logistics Quarter, vol. 12, no. 1, pp. 35-55.

AZIZ, K., and SETTARI, A., 1979, Petroleum reservoir simulation. Applied Science Publications, London.

BAKR, A.A., GELHAR, L.W., GUTJAHR, A.L., and MacMILLAN, J.R., 1979, Stochastic analysis of spatial variability in subsurface flows. 1. Comparison of one and three-dimensional flows. Water Resour. Res., vol. 14, pp. 263-271.

BAVEYE, P. and SPOSITO, G. 1984, The operational significance of the continuum hypothesis in the theory of water movement through soils and aquifers. Water Resources Research, vol. 20, no. 5, pp. 521-530.

BEAR, J., 1968, Dynamics of fluids in porous media. Elsevier, New York.

BEAR, J., and BRAESTER, C., 1972, On the flow of two immiscible fluids in fractured porous media. Proc., First Symposium on Fundamentals of Transport Phenomena in Porous Media, Elsevier, New York, pp. 177-198.

BEAUMONT, E.A., 1984, Retrogradational self sedimentation. Lower Cretaceous Viking Formation, Central Alberta. In R.W. Tillman and C.T. Seimers, eds., Siliciclastic Shelf Sediments. Society of Economic Paleontologists and Mineralogists, Special Publication no. 34, pp. 163-178.

BEGG, S.H., CHANG, D.M., and HALDORSEN, H.H., 1985, A simple statistical method for calculating the effective vertical permeability of a reservoir containing discontinuous shales. SPE 14271, presented at the 60th Ann. Conf. and Exh., Las Vegas, Sept. 22-25.

BEGG, S.H., and KING, P.R., 1985, Modelling of the effects of shales on reservoir performance: calculation of effective vertical permeability. SPE 13529, presented at the 8th Symposium on Reservoir Simulation, Dallas, Feb. 10-13.

BRACHMAN, R.J., 1979, On the epistemological status of semantic networks. **In** N.V. Findler, ed., Associative Networks, Academic Press, New York, pp. 3-50.

BRACHMAN, R.J. GILBERT, V.P., and LEVESQUE, H.J., 1985, An essential hybrid reasoning systems: knowledge and symbol level accounts of KRYPTON. Proc. IJCAI-85, pp. 532-539.

BROWN, J.S., 1973, Steps towards automatic theory formation. Proc. IJCAI-73, pp. 121-129.

BUCHANAN, B.G., and SHORTLIFFE, E.H., 1984, Rule-based expert systems: The MYCIN experiments of the Stanford Heuristic Programming Project. Addition-Wesley Publishing Co., Reading, Massachusetts.

CHARNIAK, E., RIESBERG, C.K., and McDERMONTT, D.V., 1980, Artificial intelligence programming. Lawrence Erlbaum Associate Publishers, Hillsdale, New Jersey.

CHAUVET, P., and GALLI, A., 1982, Universal kriging. Internal report C-96, Centre de Morphologie Mathématique, Fontainebleau.

CHILES, J.P., 1976, How to adapt kriging to non-classical problems - three-case studies. **In** M. Guarascio **et al.**, eds., Advanced Geostatistics in the Mining Industry, D. Reidel Publishing Co., Dordrecht, pp. 69-90.

CHILES, J.-P., 1977, Géostatistique des phénomènes non stationnaires (dans le plan). Thèse de docteur-ingénieur, Université de Nancy-I.

CHILES, J.P., 1979, Le variogramme généralisé. Int. Rep. N-612, Centre de Géost., Fontainebleau.

CHRISTAKOS, G., 1984, On the Problem of permissible covariance and variogram models. Water Resour. Res., vol. 20, no. 2, pp. 251-265.

CHRISTAKOS, G., 1987, Stochastic Simulation of spatially correlated geo-Processes. Math. Geol., vol. 19, no. 2, pp. 807-831.

CLANCEY, W.J., 1983, The epistemology of a rule-based expert system - a framework for explanation. Artificial Intelligence, vol. 20, pp. 215-251.

CLANCEY, W.J., 1983b, The advances of abstract control knowledge in expert system design. Proc. AAAAI-83, pp. 74-78.

COATS, D.H., 1982, Reservoir simulation: state of the art. J. Pet. Tech., pp. 1633-1642, Aug. 1982.

DA COSTA E SILVA, A.J., 1985, A new approach to the characterization of reservoir heterogeneity based on the geomathematical model and kriging technique. SPE 14275, presented at the 60th, Ann. Tech. Conf. and Exh., Las Vegas, September 22-25.

DAGAN, G., 1979, Models of groundwater flow in statistically homogeneous porous formations. Water Resour. Res., vol. 15, pp. 47-63.

DAVID, M., 1977, Geostatistical ore reserve estimation. Elsevier, Amsterdam.

DAVID, M. DIMITRAKOPOULOS, R. and MARCOTTE, D., 1987, Geostat-1: A prototype expert system for the explicit knowledge approach to geostatistics. APCOM'87, vol. 3, pp. 121-126.

DAVID, M., CROZEL, D., and ROBB, J.M., 1986, Automated mapping of the ocean floor using the theory of intrinsic random functions of order k. Marine Geophysical Research, vol. 8, pp. 49-74.

DAVIS, M.W., 1987, Production of conditional simulations via the LU decomposition of the covariance matrix. Math. Geol., vol. 19, no. 2, pp. 91-98.

DAVIS, M., and DAVID, M., 1978, Automatic kriging and contouring in the presence of trends (Universal kriging made simple). J. Can. Pet. Tech., pp. 1-10.

DEFFEYES, K.S., RIPLEY, B.D., and WATSON, G.S., 1982, Stochastic geometry in petroleum geology. Math. Geol., Vol. 4, pp. 419-431.

DELFINER, P., 1976, Linear Estimation of non stationary spatial phenomena. **In** M. Guarascio **et al.** (eds), Advanced Geostatistics in the Mining Industry. D. Reidel Publishing Co., Dordrecht, pp. 49-68.

DELFINER, P., and CHILES J.P., 1977, Conditional simulations: A new Monte-Carlo approach to probabilistic evaluation of hydrocarbons in place. Internal report N-526, Centre de Morphologie Mathématique, Fontainebleau.

DELFINER, P., DELHOME, J.P., and PELISSIER-COMBESCURE, J., 1983, Application of geostatistical analysis to the evaluation of the petroleum reservoirs with well logs. Paper presented at the 24th Annual Logging Symposium of the SPWLA, Calgary, June 27-30, 1983.

DELHOMME, J.P., 1979, Spatial variability and uncertainty in ground water flow parameters: a geostatistical approach. Water Resour. Res., vol. 15, pp. 269-282.

DESBARATS, A., 1988, Estimation of effective permeabilities in the Lower Stevens Formation of the Paloma field, San Joaquin Valley, California. SPE Reservoir Engineering, November 1988, pp. 1301-1307.

DESBARATS, A., 1987a, Numerical estimation of effective permeability in sand-shale formations. Water Resour. Res., vol. 23, pp. 273-286.

DESBARATS, A., 1987b, Stochastic modeling of flow in sand-shale sequences. Ph.D. Thesis, Stanford University, Stanford, CA.

DEUTSCH, C., 1986, Estimating block effective permeability with geostatistics and power averaging. Soc. Petrol. Eng. paper No. 015991.

DIMITRAKOPOULOS, R., 1985, Conditional simulation and kriging as an aid to oil sands development: An application in part of the Athabasca deposit. M.Sc. Thesis, The University of Alberta.

DOWD, P.A., 1984, Conditional simulation of interrelated beds in an oil deposit. **In** G. Verly **et al**, eds, Geostatistics for Natural Resources Characterization, Part 2, D. Reidel Publishing Co., Dordrecht, pp. 1031-1093.

DOWD, P.A., and ROYLE, A.G., 1977, Geostatistical applications in the Athabasca tar sands. **In** Proc. 15th APCOM Symposium, Brisbane, Australia, pp. 235-242.

DUBRULE, D., and KOSTOV, C., 1986, An interpolation method taking into account inequality constraints: I. Methodology. Mathematical Geology, vol. 8, pp. 33-51.

DUDA, R.O., HART, P.E., NILSSON, N.J., and SUTHERLAND, G., 1978, Semantic network representations in rule-based inference systems: **In** D.A. Waterman and F. Hayes-Roth, eds., Pattern-Directed Inference Systems, Academic Press, New York, pp. 203-221.

FORSYTH, R., 1974a, The architecture of expert systems. **In** R. Forsyth, ed., Expert Systems, Principles and Case Studies, Chapman and Hall Comptuting, London, pp. 9-17.

FORSYTH, R., 1974b, Fuzzy reasoning systems. **In** R. Forsyth, ed., Expert Systems, Principles and Case Studies, Chapman and Hall Computing, London, pp. 51-62.

GALLI, A., GERDIL-NEUILLET, F., and DADOU, C., 1984, Factorial kriging analysis: A substitute to spectral analysis of magnetic data. **In** G. Verly **et al**, eds., Geostatistics for Natural Resources Characterization, Part 2, D. Reidel Publishing Co., Dordrecht pp. 543-557.

GARDNER, A., 1981, Search. **In** A. Barr and E.A. Feigenbaun, eds., Handbook of Artificial Intelligence, vol. 1, William Kaufman, Los Altos, CA., pp. 19-139.

GEL'FAND, I.M. and VILENKIN, N.Y., 1964, Generalized functions 4. Academic Press, New York.

GELHAR, L.W., and AXNESS, C.L., 1981, Stochastic analysis of macrodispersion in three-dimensionally heterogeneous acquifers. Report H-8, Hydrology Resources Program, New Mexico Institute of Mining and Technology, Socoro.

GELHAR, L.W., and AXNESS, C.L., 1983, Three dimensional stochastic analysis of microdispersion in Aquifers; Water Resour. Res., Vol. 19, p. 161.

GELHAR, L.W., 1984, Stochastic analysis of flow in heterogeneous porous media. In fundamentals of Transport Phenomena in Porous Media, J. Bear and M.Y. Carapcioglou, eds., Martinus Njhoff Publishers, Dordrecht, Netherlands, pp. 673-720.

GUTJAHR, A.L., GELHAR, L.W., BAKR, A.A. and MacMILLAN, J.R., 1978, Stochastic analysis of spatial variability in subsurface flows. 2. Evaluation and application. Water Resour. Res., 14, pp. 953-959.

HAAS, A., and VIALLIX, j.R., 1976, Krigeage applied to Geophysics - The answer to the problem of estimates and contouring. Geophysical Prospecting, Vol. 24, pp. 49-69.

HAAS, A., and JOSSELIN, C., 1975, Geostatistics in the petroleum industry. **In** M. Guarascio **et al.** eds, Advanced Geostatistics in the Mining Industry, D. Reidel Publishing Co., Dordrecht, pp. 334-347.

HASS, A., and MOLLIER, M., 1974, Un aspect du calcul d'erreur sur les réserves en place d'un gisement. Revue de l'Institut Français du Pétrole, vol. 29, pp. 507-527.

HALDORSEN, H.H., 1983, Reservoir characterization procedures for numerical simulation. Ph.D. Thesis, The University of Texas at Austin.

HALDORSEN, H.H., 1986, Simulator parameter assignment and the problem of scale in reservoir engineering. **In** Reservoir Characterization, eds. Lake, L. W. and Carroll, Jr., H.B., Academic Press Inc., pp. 293-323.

HALDORSEN, H.H., and LAKE, L.W., 1984, A new approach to shale management in field-scale models. Soc. Pet. Eng. J., pp. 447-457, Aug. 1984.

HART, P., 1982, Directions for AI in the eighties. SIGART Newsletter, vol. 79, pp. 11-16.

HAUGELAND, J., 1985, Artificial Intelligence: The very idea. MIT Press, Cambridge, Massachusetts.

HELWICK, SS., Jr., and LUSTER, G.R., 1984, Fluid-flow modeling using a conditional simulation of porosity and permeability. **In** M. Guarascio **et al.**, D. Reidel Publishing Co., Dordrecht, pp. 635-650.

HENDRIX, G.G., 1979, Encoding knowledge in partitioned networks. **In** N.V. Findler, ed., Associative Networks: representation and use of knowledge by computers. Academic Press, New York, pp. 51-92.

HEWETT, T.A., 1986, Fractal Distributions of reservoir heterogeneity and their influence on fluid transport. SPE 15386, presented at the 61st Ann. Tech. Conf. and Exh., New Orleans, October 5-8.

JONES, T.A., 1984, Problems in using geostatistics for petroleum applications. **In** G. Verly **et al.**, eds. Geostatistics for Natural Resources Characterization, Part 2, D. Reidel Publishing Co., Dordrecht, pp. 651-667.

JOURNEL, A.G., 1974, Geostatistics for conditional simulation of ore bodies. Econ. Geol., vol. 69, pp. 673-687.

JOURNEL, A., and HUIJBREGTS, C.J., 1978, Mining geostatistics. Academic Press, London.

KITANIDIS, P.K., 1983, Statistical estimation of polynomial generalized covariance functions and hydrologic applications. Water Resour. Res., vol. 19, pp. 909-917.

KLEENE, S.C., 1967, Mathematical logic. John Wiley and Sons, New York.

KORVIN, G., 1981, Axiomatic characterization of the general mixture rule. Geoexploration, vol. 19, pp. 267-276.

KOSTOV, C., and DUBRULE, O., 1986, An interpolation method taking into account inequality constraints: II. Practical approach. Mathematical Geology, vol. 8, pp. 53-73.

KOSTOV, C., and JOURNEL, A.G., 1985, Coding and extrapolating expert information for reservoir description. Proc. of the Reservoir Characterization Technical Conference, Dallas, April 1985.

KOWALSKI, R., 1979, Logic for problem solving. North-Holland, Amsterdam.

KRAUSE, F.F., COLLINS, H.N., NELSON, D.A., MACHEMER, S.D., and FRENCH, P.R., 1987, Multiscale anatomy of a reservoir, geological characterization of Pembina-Cardium pool, west-central Alberta, Canada. Am. Ass. Petrol. Geol. Bull., vol. 71, pp. 1233-1248.

KUHN, T.S., 1970, The structure of scientific revolutions. 2nd ed., University of Chicago Press, Chicago.

KUO, T.B. and STRATZMAN, R.A., 1987, Field-scale stratigraphic correlation using artificial intelligence. Geobyte, vol. 2, pp. 30-35.

LAKE, L.W., and CARROL, Jr., H.B., 1986, Reservoir characterization. Academic Press Inc., Orlando.

LE LOC'H, G., 1987, Étude de la composition des perméabilités par des méthodes variationnelles, Thèse de Docteur-Ingénieur, École Nationale Supérieure des Mines de Paris, Fontainebleau, France.

LEHNERT, W.G., 1981, Pilot units and narrative summarization. Cognitive Science, vol. 4, pp. 293-331.

LEVESQUE, H.J., and MYLOPOULOS, J., 1979, A procedural semantics for semantic networks. **In** N.V. Findler, ed., Associative Networks, Academic Press, New York, pp. 93-120.

LIAKOPOULOS, A.C., 1965, Darcy's coefficient of permeability as symmetric tensor of second rank. AIHS X^{e} année, no. 3, pp. 41-48.

LOVELAND, D., 1978, Automated theorem proving: A logical basis. Elsevier North-Holland, New York.

LUSTER, G.R., 1985, Raw Materials for Portland Cement: Applications of Conditional Simulation of Coregionalization. Ph.D. thesis, Stanford University, Stanford, CA.

MANDANI, E.H., and EFSTATHIOU, J., 1984, An analysis of formal logics as inference mechanisms in expert systems. International Journal on Man-Machine Studies, vol. 21, pp. 213-227.

MANTOGLOU, A., 1987, Digital simulation of multivariate two-and three-dimensional stochastic processes with a spectral turning bands method. Math. Geol., vol. 19, pp. 129-149.

MARECHAL, A., 1984, Kriging seismic data in presence of faults. **In** G. Verly **et al.**, eds, Geostatistics for Natural Resources Characterization, Part 2, D. Reidel Publishing Co., Dordrecht, pp. 271-294.

MATHERON, G., 1965, Les variables régionalisées et leur estimation. Masson, Paris.

MATHERON, G., 1967, Éléments pour une théorie des milieux poreux. Masson et Cie., Paris.

MATHERON, G., 1969, Le krigeage universel. Les Cahiers du Centre de Morphologie Mathématique, Fasc. 1, CG Fontainebleau.

MATHERON, G., 1973, The intrinsic random functions and their applications. Advan. Appl. Prob., vol. 5, pp. 439-468.

MILLER, B.M., 1986, Building an expert system helps classify sedimentary basins and assess petroleum reservoirs. Geobyte, vol. 1, pp. 44-50.

MINSKY, M., 1975, A framework for presenting knowledge. **In** P.H. Winston, ed., The Psychology of Computer Vision, McGraw-Hill Book Co., New York, pp. 211-277.

MYLOPOULOS, J., 1980, An overview of knowledge representation. **In** M. Brodie and S.N. Zillers, eds., Proc. of the Workshop of Data Abstraction, Databases and Conceptual Modeling, ACM SIGMOD, vol. 11, pp. 5-12.

NEUMAN, S.P., 1982, Statistical characterization of aquifer heterogeneities: an overview Recent Trends in Hydrogeology. Geological Society of America, Spec. pap. 189, pp. 81-102.

NEWELL, A., 1980, Physical symbol systems. Cognitive Science, vol. 4, pp. 135-183.

NEWELL, A. and SIMON, H.A., 1976, Computer science as empirical inquiry: symbols and search. 1975 ACM Turing Award Lecture, CACM, vol. 19, pp. 113-126.

NEWELL, A., and SIMON, H.A., 1972, Human problem solving. Prentice-Hall, Englewood Cliffs, New Jersey.

NILSSON, N.J., 1980, Principles of artificial intelligence. Tioga Publishing Co., Paolo Alto, CA.

OMBRE, H., 1988, Halvorsen, K.B., and Berteig, V., 1988, A Bayesian approach to kriging. **In** preprints of Third International Geostatistics Congress. Avignon, Sept.5-9, vol. II, pp. 274-298.

OLEA, R.A., and DAVIS, J.C., 1986, An artificial intelligence approach to lithostratigraphic correlation using geophysical well logs. SPE paper no. 15603, vol. 61, pp. 558-572.

OLEA, R.A., and DAVIS, J.D., 1977, Regionalized variables theory or evaluation of petroleum accumulation in Magellan Basin, South America. American Association of Petroleum Geologists Bulletin, vol. 61, pp. 558-572.

ORFEUIL, J.P., 1972, Simulation du Wiener-Levy et de ses Intégrales. Int. Rep. N-290, Centre de Morphologie Mathématique, Fontainebleau.

PARZEN, E., 1962, Stochastic Processes. Holden-Day Inc., San Francisco.

PICKENS, J.F., CHERRY, J.A., GILLHAM, R.W., and MERRITT, W.F., 1977, Field studies of dispersion in a shallow sandy aquifer. Proc., DOE Invitational Well Testing Symposium, Berkley, pp. 55-69, Oct. 19-21.

POPLE, H.E., 1973, On the mechanization of abductive logic. Poc. IJCAI-73, pp. 147-152.

PRAGER, S., 1961, Viscous flow through porous media. Physics of Fluids, vol. 4, pp. 1477-1492.

REGGIA, J.A., NAU, D.S., and WANG, P.Y., 1983, Diagnostic expert systems based on a set covering model. International Journal on Man-Machine Studies, vol. 19, pp. 437-460.

REINSON, G.E., 1985, Facies analysis and reservoir geometry of the Crystal Viking field, Tp. 45 and 46, Rg. 3 and 4W5, central Alberta. Open File Report No. 1193, Institute of Sedimentary and Petroleum Geology, Calgary.

REINSON, G.E., and FOSCOLOS, A.E., 1986, Trends in sandstone diagenesis with depth of Burial, Viking Formation, South Alberta. Bulletin of Canadian Petroleum Geology, vol. 34, pp. 185-202.

REISON, G.E., CLARK, J.E., and FOSCOLOS, A.E., 1988, Reservoir geology of the Crystal Viking field - A lower Cretaceous estuarine tidal channel-bay complex, south-central Alberta. Am. Ass. Petrol. Geol. Bull., vol. 10, pp. 1270-1294.

RENDU, J.-M., and DAVID, M., 1979, A new geostatistical model for the estimation of coal deposits and other sedimentary deposits. **In** T.S. O'Neil, ed., 16th APCOM, pp. 182-195.

SHAPIRO, S.C., 1971, A net structure for semantic information storage deduction and retrival. Proc. IJCAI-71, pp. 512-523.

SHULTZ, A.W., FANG, J.H., BURSTON, M.R., CHEN, H.C., and REYNOLDS, S., 1987, XEOD: An expert system for determining clastic depositional environments. Geobyte, vol. 3, no 2, pp. 22-23.

SMITH, L., and FREEZE, R.A., 1979, Stochastic analysis of steady state groundwater flow in a bounded domain, 2, two-dimensional simulations. Water Resour. Res., vol. 15, pp. 1543-1559.

SMITH, L., and SCHWARTZ, F.W., 1981, Mass transport, 3, role of hydraulic conductivity data in prediction. Water Resour. Res., vol. 17, pp. 1463-1479.

SMITH, R.G. and BAKER, J.D., 1983, The dipmeter advisor system: A case study in commercial expert system development. Proc. IJACI-83, pp. 122-129.

VILAIN, M., 1985, The restricted language architecture of a hybrid representation system. Proc. IJCAI-85, pp. 547-551.

WARREN, J.E., and PRICE, H.S., 1961, Flow in heterogeneous porous media. Soc. Petrol. Eng. S., vol. 1, pp. 153-169.

WIENER, N., 1949, Extrapolation, interpolation and smoothing of stationary time series with engineering applications. J. Wiley, New York.

WINSTON, P.H., and HORN, B.K.P., 1985, LISP, second edition. Addison-Wisley Publishing Co., Reading, Massachusetts.

ZADEH, L., 1965, Fuzzy sets. Information and Control, vol. 8, pp. 338-353.

ZWICKY, R.W., 1977, Preliminary geostatistical investigation of tar-bearing sands, lease-13. Athabasca tar sands, Canada. Journal of Canadian Petroleum Technology, vol. 16, pp. 25-30.

APPENDIX A: DERIVATION OF THE GENERALIZED COVARIANCE k_{pq}

Let $W_p(x)$ be the p^{th} integration of the Wiener-Levy process $W_o(x)$ n R^1, in the sense of Eq. (7). The latter equation gives

$$\frac{dW_p(x)}{dx} = \int_o^x \frac{\partial}{\partial x}\left[\frac{(x-u)^{p-1}}{(p-1)!} W_o(u)\right] du = \int_o^x \frac{(x-u)^{p-2}}{(p-2)!} W_o(u)\, du$$

$$= W_{p-1}(x), \text{ or}$$

$$W_p(x) = \int_o^x W_{p-1}(u)\, du. \qquad \text{(A1)}$$

$_p(x)$ is an IRF-k and the corresponding GI-k is

$$\Delta_k^W(x,h,p) = \sum_{i=0}^{k+1} (-1)^i C_{k+1}^i W_p(x+ih) \qquad \text{(A2)}$$

/ applying (A1), Eq. (A2) writes

$$\Delta_k^W(x,h,p) = \sum_{i=0}^{k+1} (-1)^i C_{k+1}^i \int_x^{x+ih} W_{p-1}(u)\, du$$

$$\sum_{i=0}^{k+1} (-1)^i C_{k+1}^i \int_o^x W_{p-1}(u)\, du + \sum_{i=1}^{k+1}\sum_{j=1}^{k+1} (-1)^j C_{k+1}^j \int_{x+(i-1)h}^{x+ih} W_{p-1}(u)\, du \qquad \text{(A3)}$$

$\text{It } \sum_{i=0}^{k+1} (-1)^i C_{k+1}^i = 0$, and

$$\sum_{j=i}^{k+1} (-1)^j C_{k+1}^j = \sum_{j=i}^{k} (-1)^j C_k^{j-1} + \sum_{j=i}^{k} (-1)^j C_k^j + (-1)^{k+1}$$

$$= (-1)^{k+1} - \sum_{\ell=i-1}^{k-1} (-1)^\ell C_k^\ell + \sum_{j=i}^{k} (-1)^j C_k^j$$

$$= (-1)^i \, C_k^{i-1}$$

nserting the last two equations into Eq. (A3) one gets

$$\Delta_k^W (x,h,p) = \sum_{i=1}^{k+1} (-1)^i \, C_k^{i-1} \int_{x+(i-1)h}^{x+ih} W_{p-1}(u) \, du$$

$$= - \sum_{i=0}^{k} (-1)^i \, C_k^i \int_x^{x+h} W_{p-1} (u+ih) \, du$$

$$= - \int_x^{x+h} \Delta_{k-1}^W (u,h,p-1) \, du. \qquad \text{(A4)}$$

Let

$$P_{pp} = E[\Delta_k^W (x,h,p)]^2; \qquad \text{(A5)}$$

then

$$P_{pp} = \sum_{i=0}^{k+1} \sum_{j=0}^{k+1} (-1)^{i+j} \, C_{k+1}^i \, C_{k+1}^j \, k_p((i-j)h). \qquad \text{(A6)}$$

applying Eq. (A4) onto Eq. (A5) one obtains

$$P_{pp} = \int_x^{x+h} du \int_x^{x+h} dv \; E[\Delta_{k-1}^W (u,h,p-1) \, \Delta_{k-1}^W (v,h,p-1)]$$

$$= \int_x^{x+h} du \int_x^{x+h} dv \sum_{i=0}^{k} \sum_{j=0}^{k} (-1)^{i+j} \, C_k^i \, C_k^j \, k_{p-1} (v-u+(j-i)h)$$

this point Appendix B is used to get

$$P_{pp} = (-1)^k \int_x^{x+h} du \int_x^{x+h} dv \sum_{i=0}^{2k} (-1)^i C_{2k}^i \; k_{p-1} (v-u-kh+ih) \quad (A7)$$

Let $I_\mu k_{p-1}(h) = \int_o^h du_\mu \ldots \int_o^{u_2} du_1 \; k_{p-1} (u_1)$.

By applying Eq. (A4) twice, first in terms of $k_{p-1}(.)$ and then in erms of $I_1 \; k_{p-1} (.)$ one finds

$$P_{pp} = (-1)^k \sum_{i=0}^{2k+2} (-1)^i C_{2k+2}^i \; I_2 \; k_{p-1} ((i-k-1)h)$$

$$= -\sum_{i=0}^{k+1} \sum_{j=0}^{k+1} (-1)^{i+j} C_{k+1}^i \; C_{k+1}^j \; I_2 \; k_{p-1} ((i-j)h) \quad (A8)$$

ıere Appendix B has been used. Comparing equations (A6) and (A8) one gets

$$K_p(h) = -I_2 \; k_{p-1}(h) = - \int_o^h du \int_o^u dv \; k_{p-1} (v), \quad (A9)$$

· by applying (A9) several times

$$k_p(h) = (-1)^p \int_o^h du_{2p} \ldots \int_o^{u_2} du_1 \; k_o \; (u_1)$$

$$= (-1)^p \int_o^h \frac{(h-u)^{2p-1}}{(2p-1)!} \; k_o(u) \; du, \quad (A10)$$

ich is the GC-k corresponding to the $W_p(x)$. In order to find now the oss-GC of two IRF $W_p(x)$ and $W_q(x)$ let us take $p \geq q$, so that $W_q(x)$ can be nsidered an IRF-p also. Then

$$P_{pp} = E[\Delta_k^W (x,h,p) \; \Delta_k^W (x,h,q)] \quad (A11)$$

$$= \sum_{i=0}^{k+1} \sum_{j=0}^{k+1} (-1)^{i+j} C_{k+1}^{i} C_{k+1}^{j} k_{pq} ((i-j)h). \qquad (A12)$$

By applying Eq. (A4) $\ell = p-q$ times on $\Delta_k^W (x,h,p)$ of Eq. (A11) one ets

$$P_{pq} = \theta_\ell E[\Delta_{k-\ell}^W (x,h,p-\ell) \Delta_k^W (x,h,q)]$$

$$= \theta_\ell \sum_{i=0}^{k+1-\ell} \sum_{j=0}^{k+1} (-1)^{i+j} C_{k+1-\ell}^{i} C_{k+1}^{j} k_q (u_1-x+(i-j)h), \qquad (A13)$$

here $\theta_\ell = (-1)^\ell \int_x^{x+h} du_\ell \ldots \int_{u_2}^{u_2+h} du_1$. By using Appendix B once more

$$P_{pq} = (-1)^{k+1} \theta_\ell \sum_{m=0}^{2k+2-\ell} (-1)^m C_{2k+2-\ell}^{m} k_q (u_1-x+(m-k-1)h)$$

nd by applying Eq. (A4) $\ell = p-q$ times in terms of k_q (.) one obtains

$$P_{pq} = (-1)^{k+1} \sum_{m=0}^{2k+2} (-1)^m C_{2k+2}^{m} I_\ell k_q (u_1-x+(m-k-1)h)$$

, taking Appendix B into account

$$P_{pq} = \sum_{i=0}^{k+1} \sum_{j=0}^{k+1} (-1)^{i+j} C_{k+1}^{i} C_{k+1}^{j} I_\ell k_q (u_1-x+(i-j)h) \qquad (A14)$$

mparing equations (A12) and (A14) one finds

$$k_{pq} (h) = I_{p-q} k_q (h). \qquad (A15)$$

f $K_o(h) = -\omega|h|$, Eq. (A10) and (A15) yield respectively

$$k_q(h) = (-1)^{q+1} \frac{w|h|^{2q+1}}{(2q+1)!} \qquad \text{(A16)}$$

$$k_{pq}(h) = (-1)^{q+1} \frac{w|h|^{p+q+1}}{(p+q+1)!} \qquad \text{(A17)}$$

APPENDIX B: CALCULATIONS ON GENERALIZED INCREMENTS

It will be demonstrated that for a function f(x) and j and k tegers, the following relation holds

$$\sum_{0}^{k}\sum_{q=0}^{} (-1)^{p+q} C_{j}^{p} C_{k}^{q} f(x+(p-q)h) = (-1)^{k} \sum_{r=0}^{j+k} (-1)^{r} C_{j+k}^{r} f(x+(r-k)h) \quad (B1)$$

Indeed if P is the left hand side of Eq. (B1) and n=p-q

$$P = \sum_{n=-k}^{j} (-1)^{n} \left[\sum_{q=0}^{j-n} C_{k}^{q} C_{j}^{n+q} \right] f(x+nh)$$

wever,

$$\sum_{q=0}^{j-n} C_{k}^{q} C_{j}^{n+q} = C_{j+k}^{n+k}$$

d hence

$$P = \sum_{n=-k}^{j} (-1)^{n} C_{j+k}^{n+k} f(x+nh)$$

ich by setting r=n+k concludes

$$P = \sum_{r=0}^{j-k} (-1)^{r-k} C_{j+k}^{r} f(x+(r-k)h)$$

$$= (-1)^{k} \sum_{r=0}^{j+k} (-1)^{r} C_{j+k}^{r} f(x+(r-k)h)$$

APPENDIX C: MAPS OF THE ESTIMATED TOPS AND BOTTOMS OF ALL CRYSTAL UNITS, CORRESPONDING ESTIMATION VARIANCE AND ISOPACHS

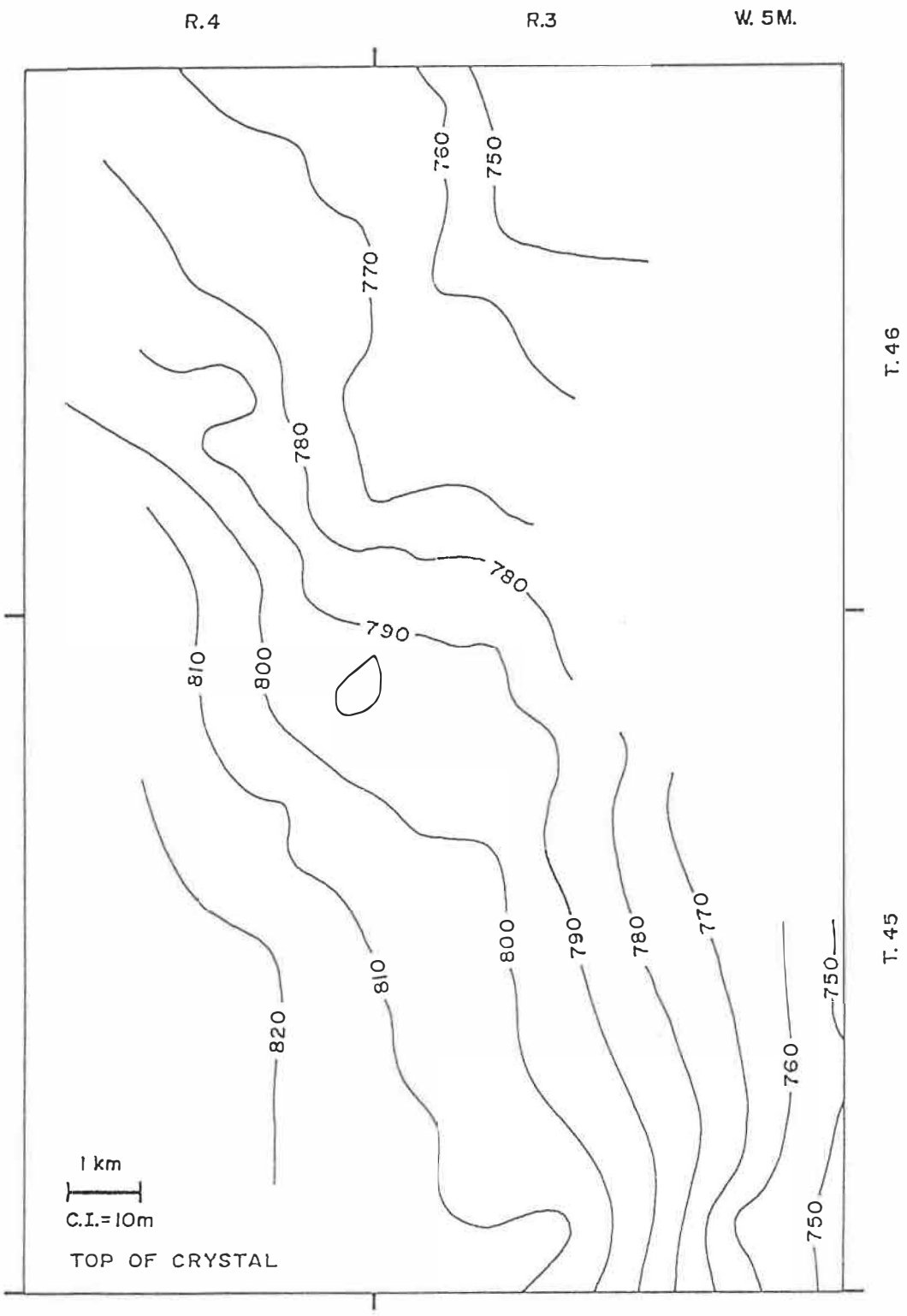
R.4
R.3
W. 5M.
T. 46
T. 45
760
750
770
780
780
790
810
800
820
810
800
790
780
770
760
750
750
1 km
C.I.= 10m
TOP OF CRYSTAL

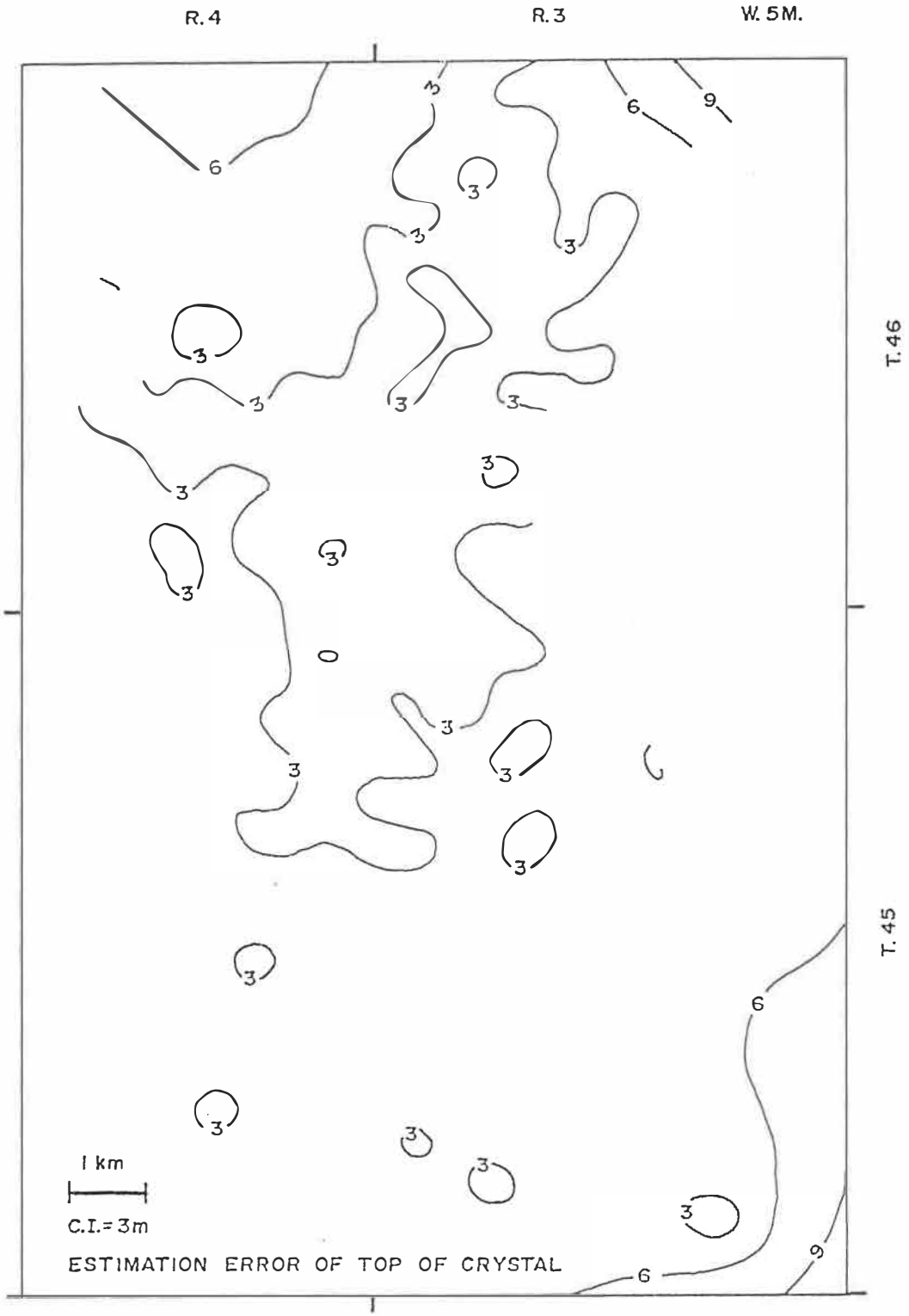
R. 4
R. 3
W. 5M.
T. 46
T. 45
1 km
C.I. = 3m
ESTIMATION ERROR OF TOP OF CRYSTAL

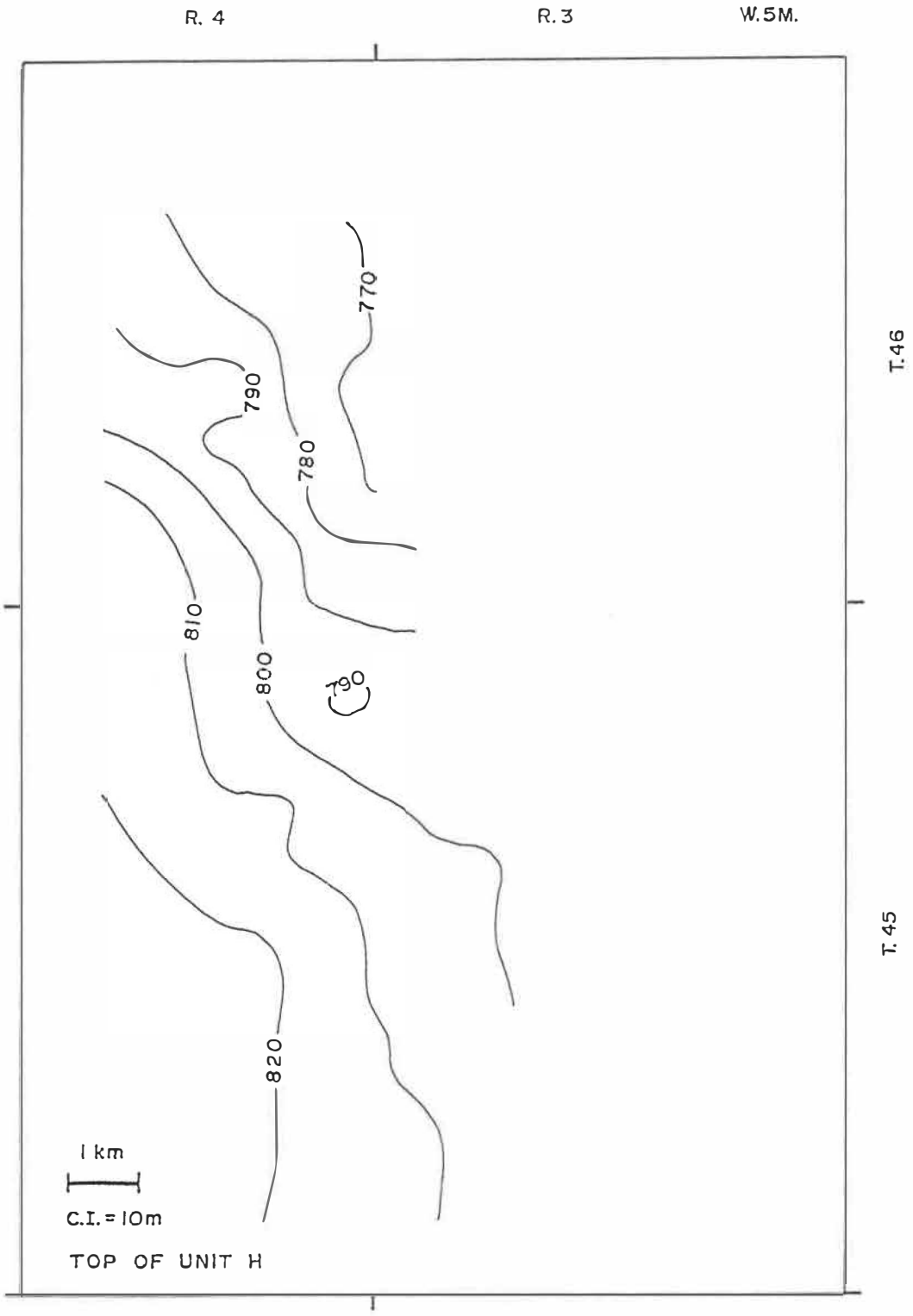
R. 4
R. 3
W. 5M.
T. 46
T. 45
770
780
790
800
810
820
790
1 km
C.I. = 10m
TOP OF UNIT H

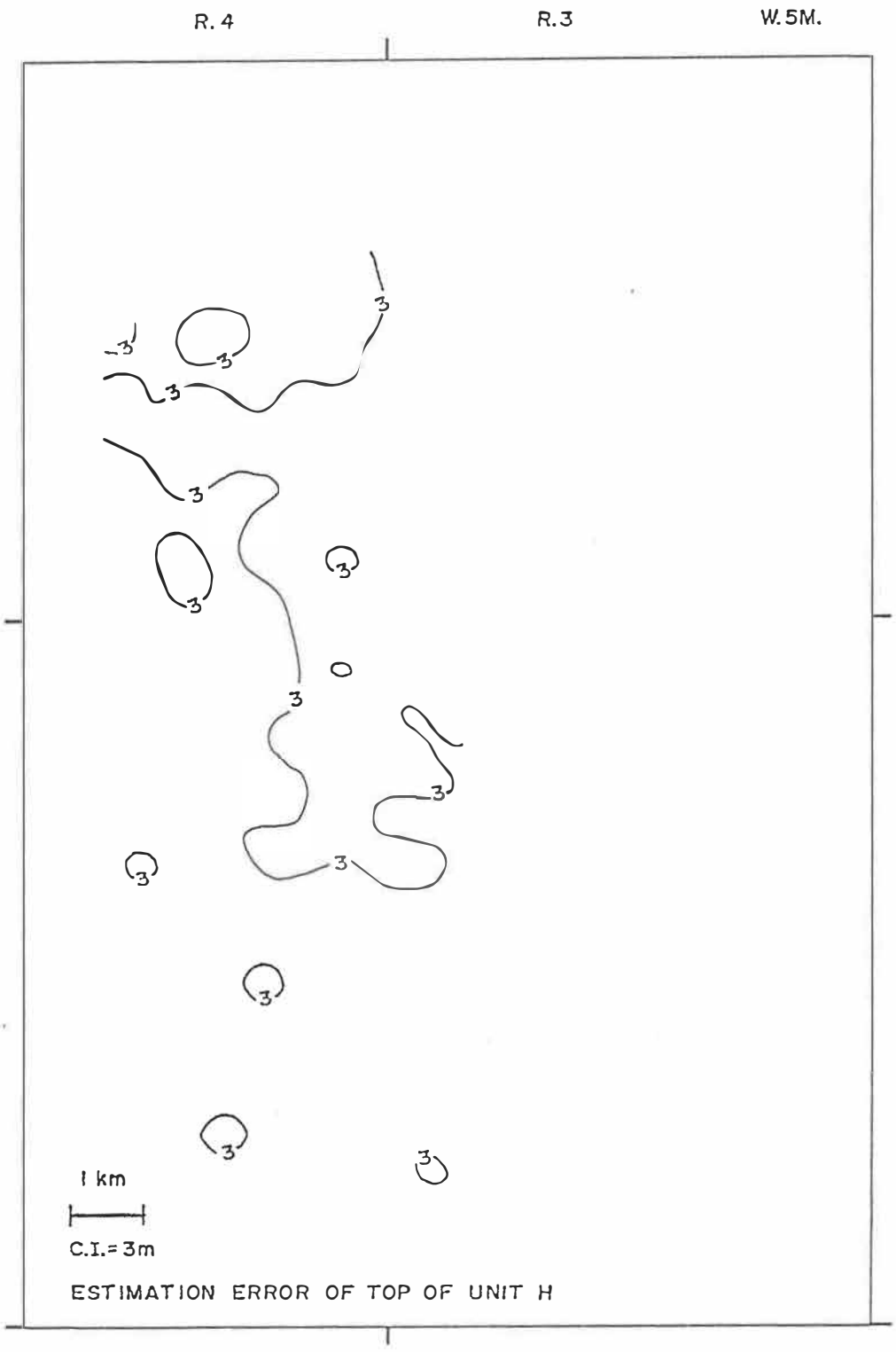

ESTIMATION ERROR OF TOP OF UNIT H

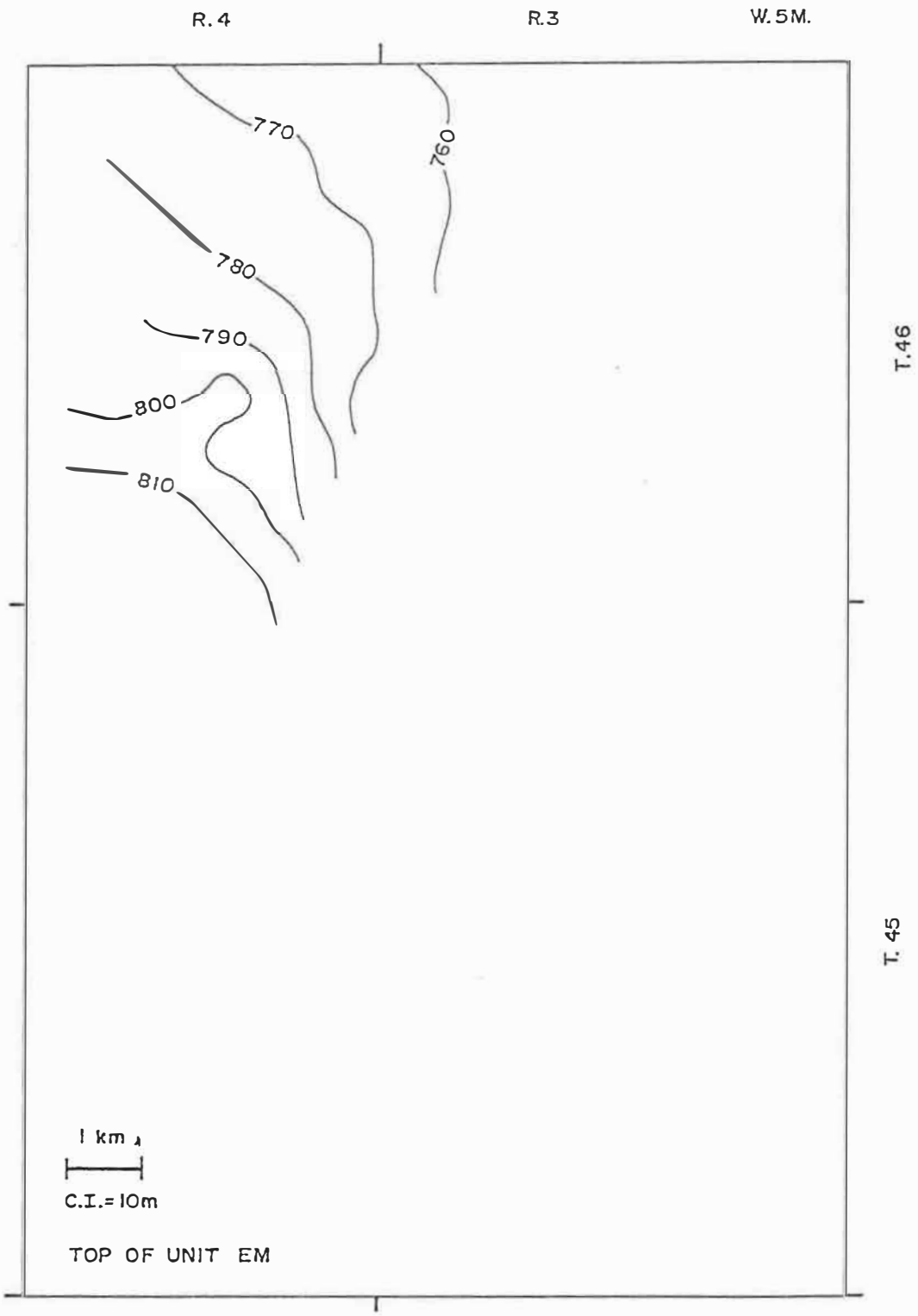
R. 4
R. 3
W. 5M.
T. 46
T. 45
770
760
780
790
800
810
1 km
C.I. = 10m
TOP OF UNIT EM

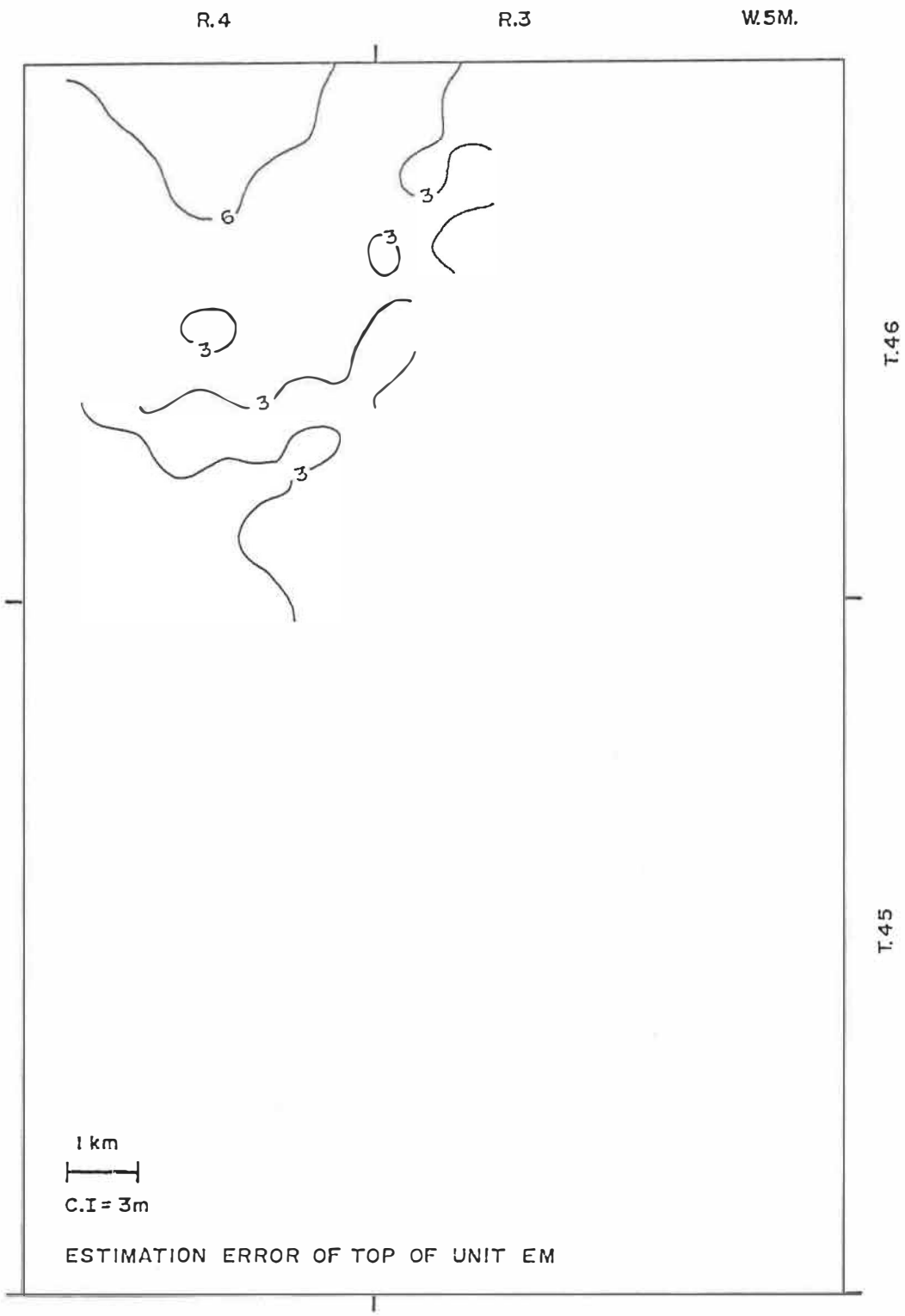
R.4
R.3
W.5M.
T.46
T.45
6
3
3
3
3
3
1 km
C.I = 3m
ESTIMATION ERROR OF TOP OF UNIT EM

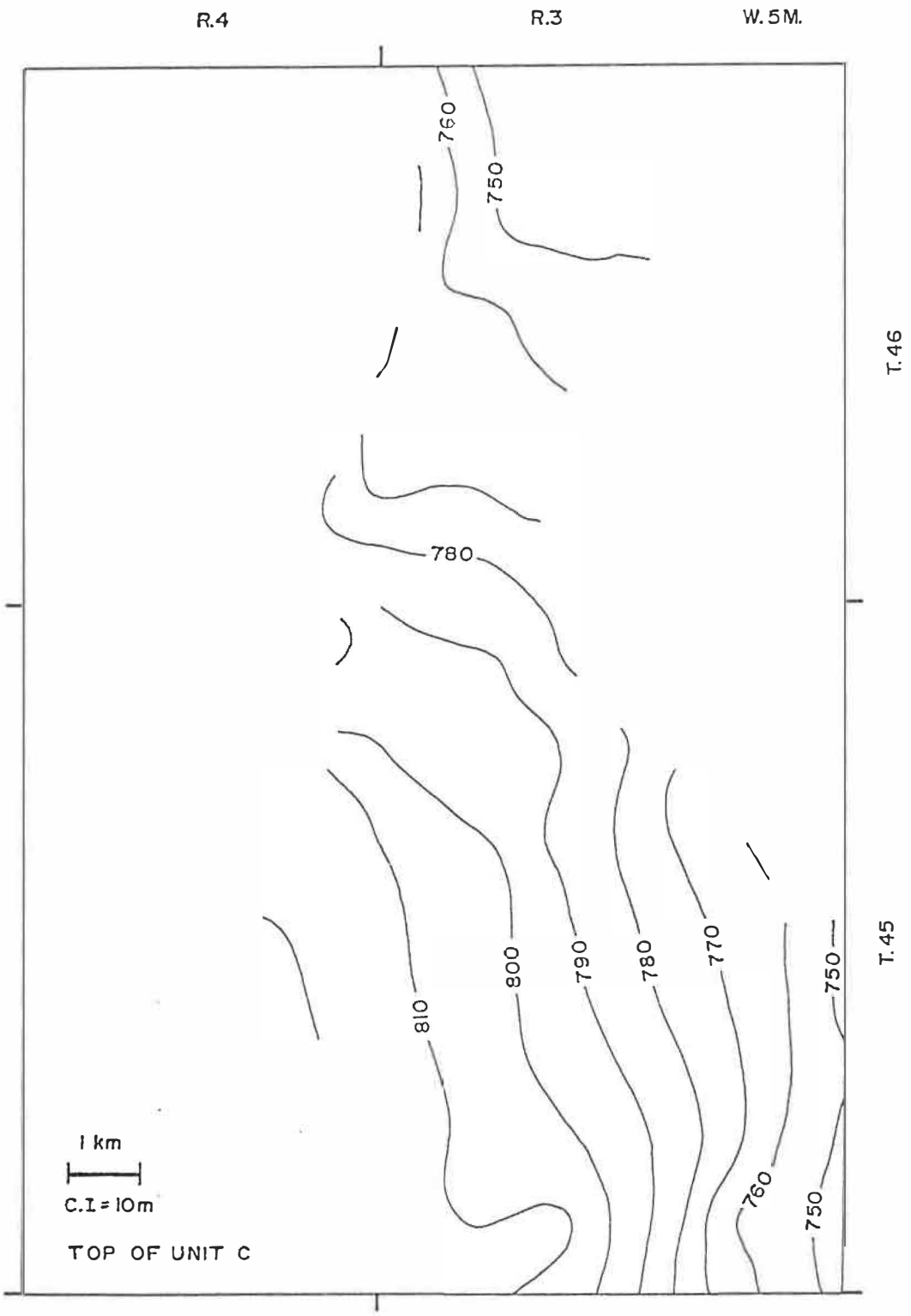
R.4
R.3
W. 5M.
T. 46
T. 45
760
750
780
810
800
790
780
770
760
750
750
1 km
C.I = 10m
TOP OF UNIT C

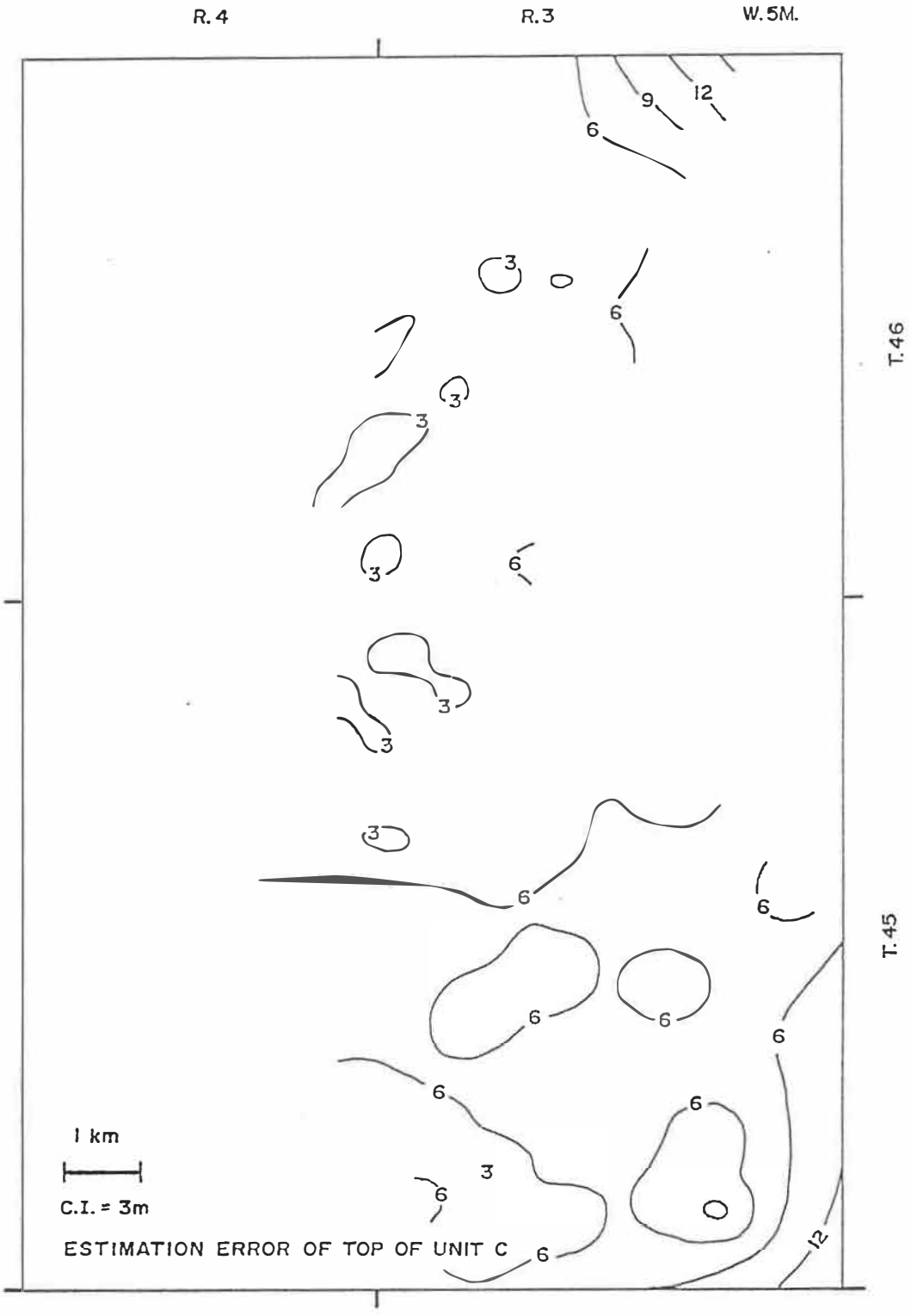
R. 4
R. 3
W. 5M.
T. 46
T. 45
1 km
C.I. = 3m
ESTIMATION ERROR OF TOP OF UNIT C

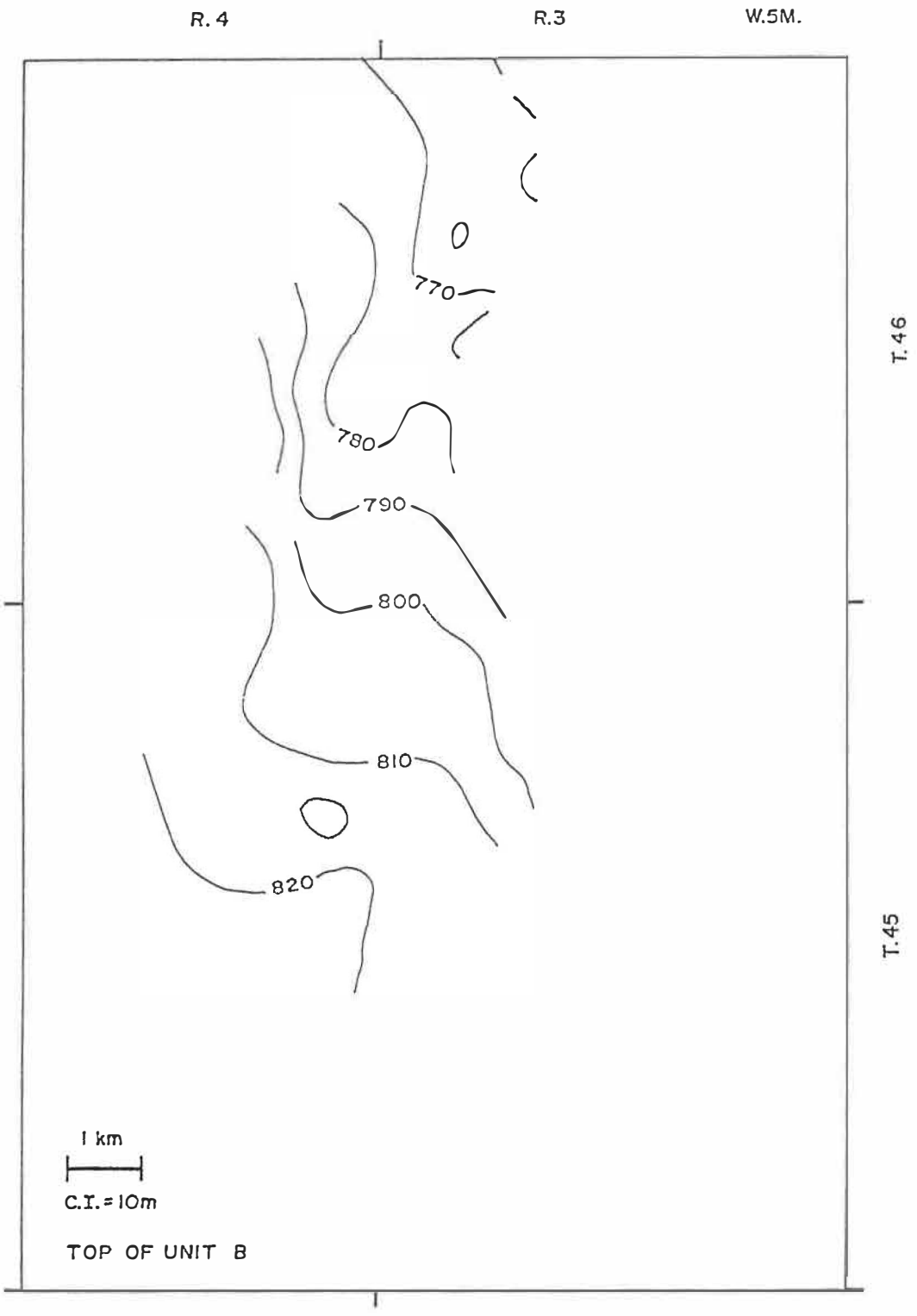
R. 4
R.3
W.5M.
T. 46
T. 45
0
770
780
790
800
810
820
1 km
C.I. = 10m
TOP OF UNIT B

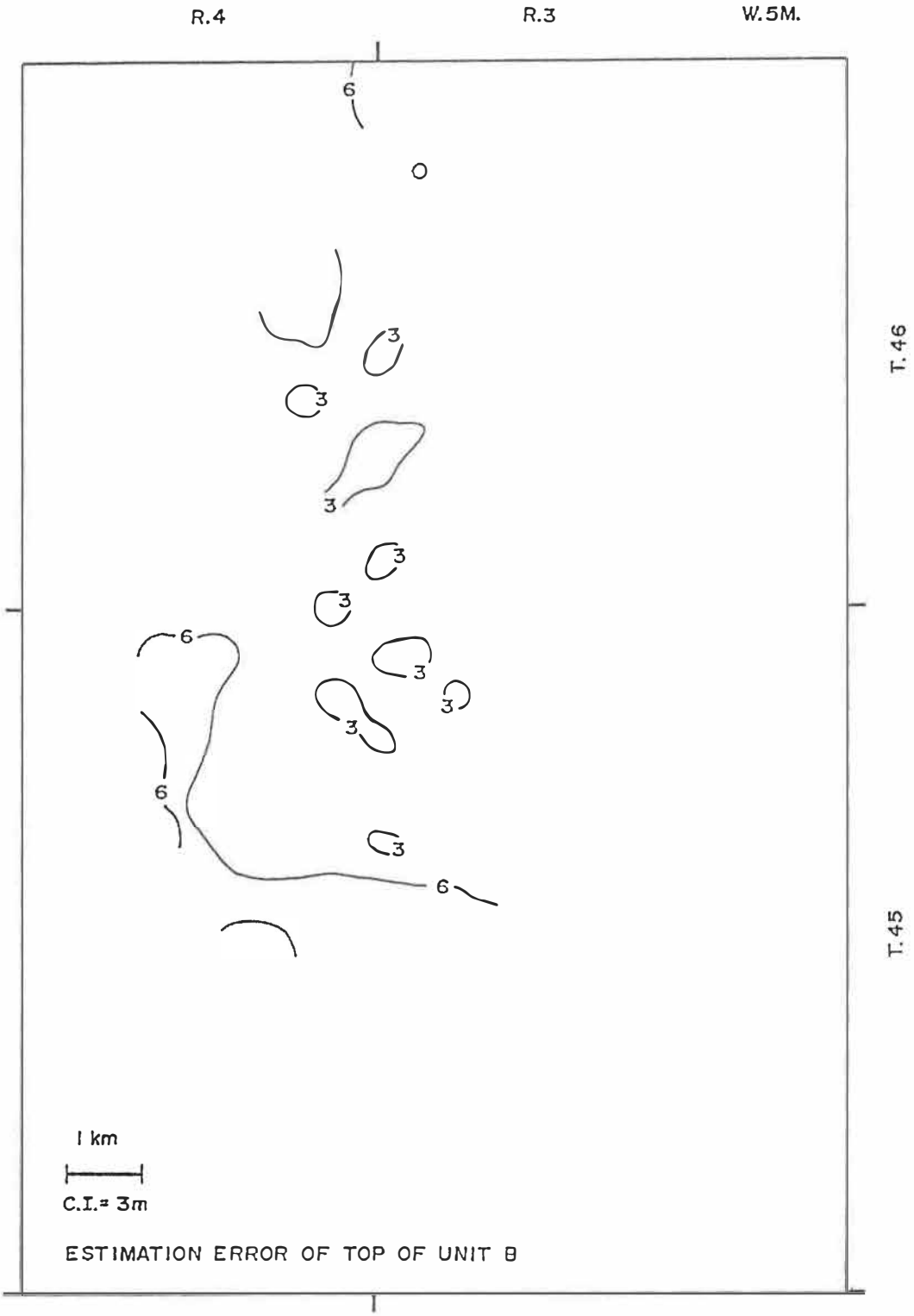

ESTIMATION ERROR OF TOP OF UNIT B

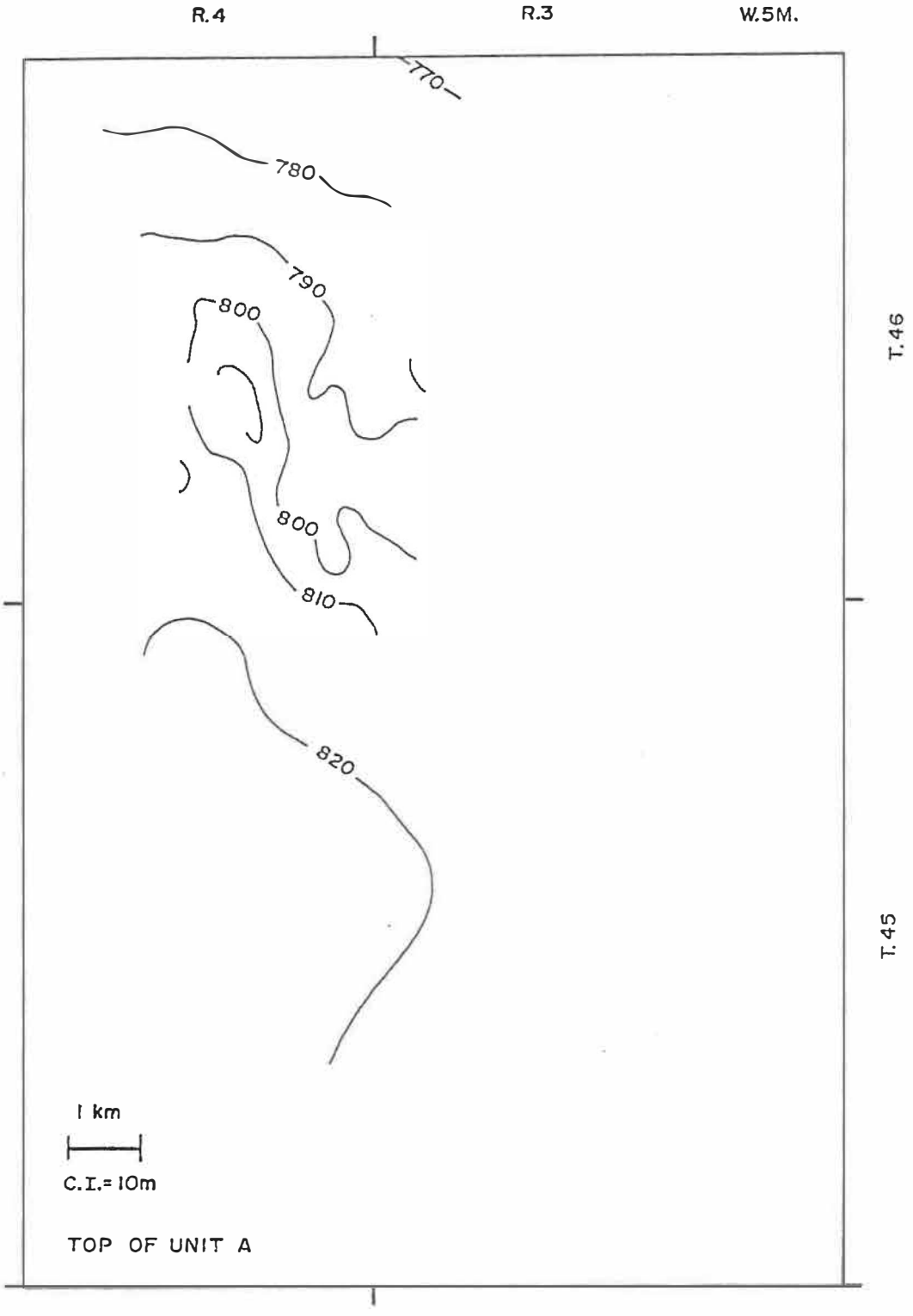
R.4
R.3
W.5M.
770
780
790
800
800
810
820
T.46
T.45
1 km
C.I.= 10m
TOP OF UNIT A

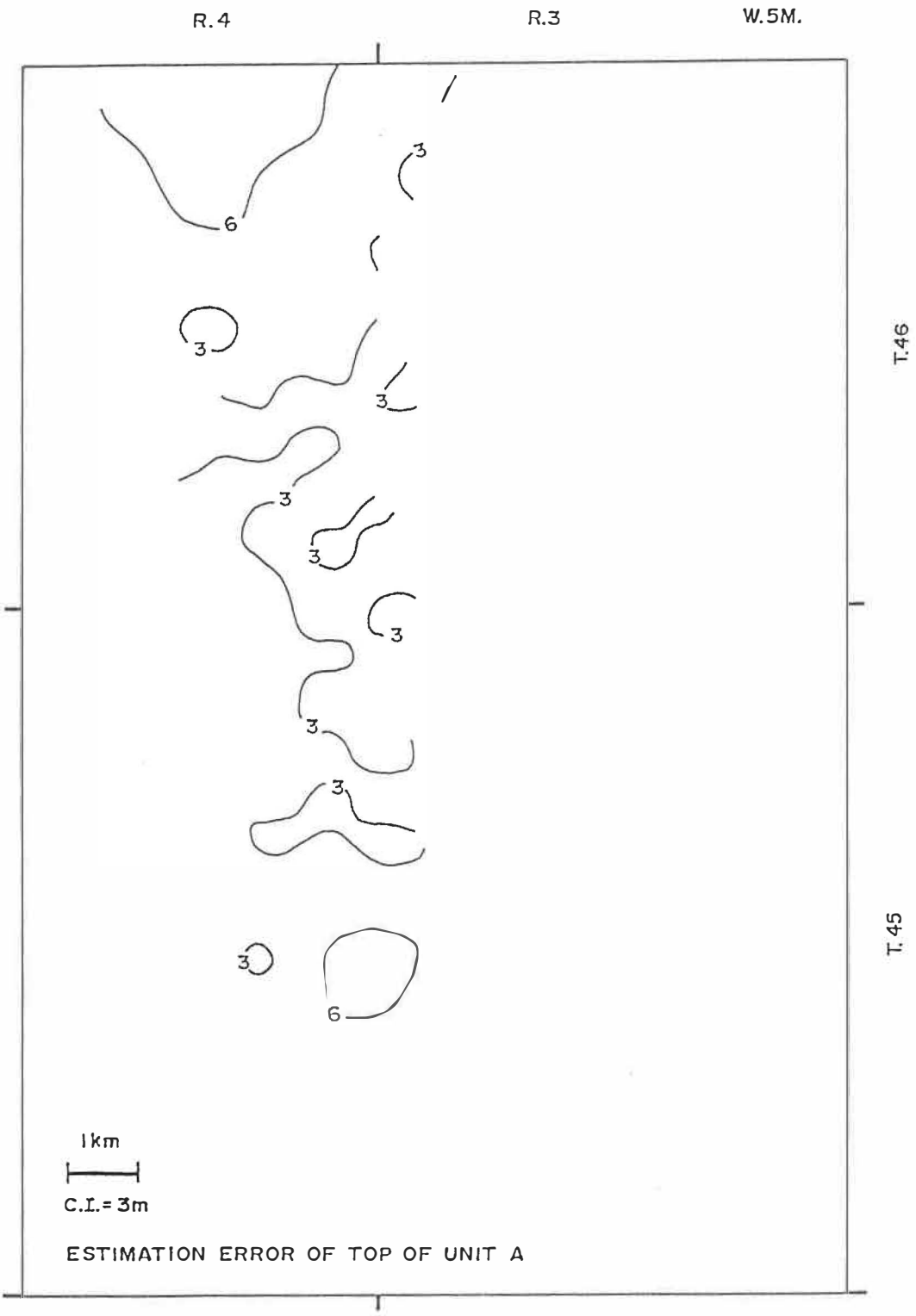

ESTIMATION ERROR OF TOP OF UNIT A

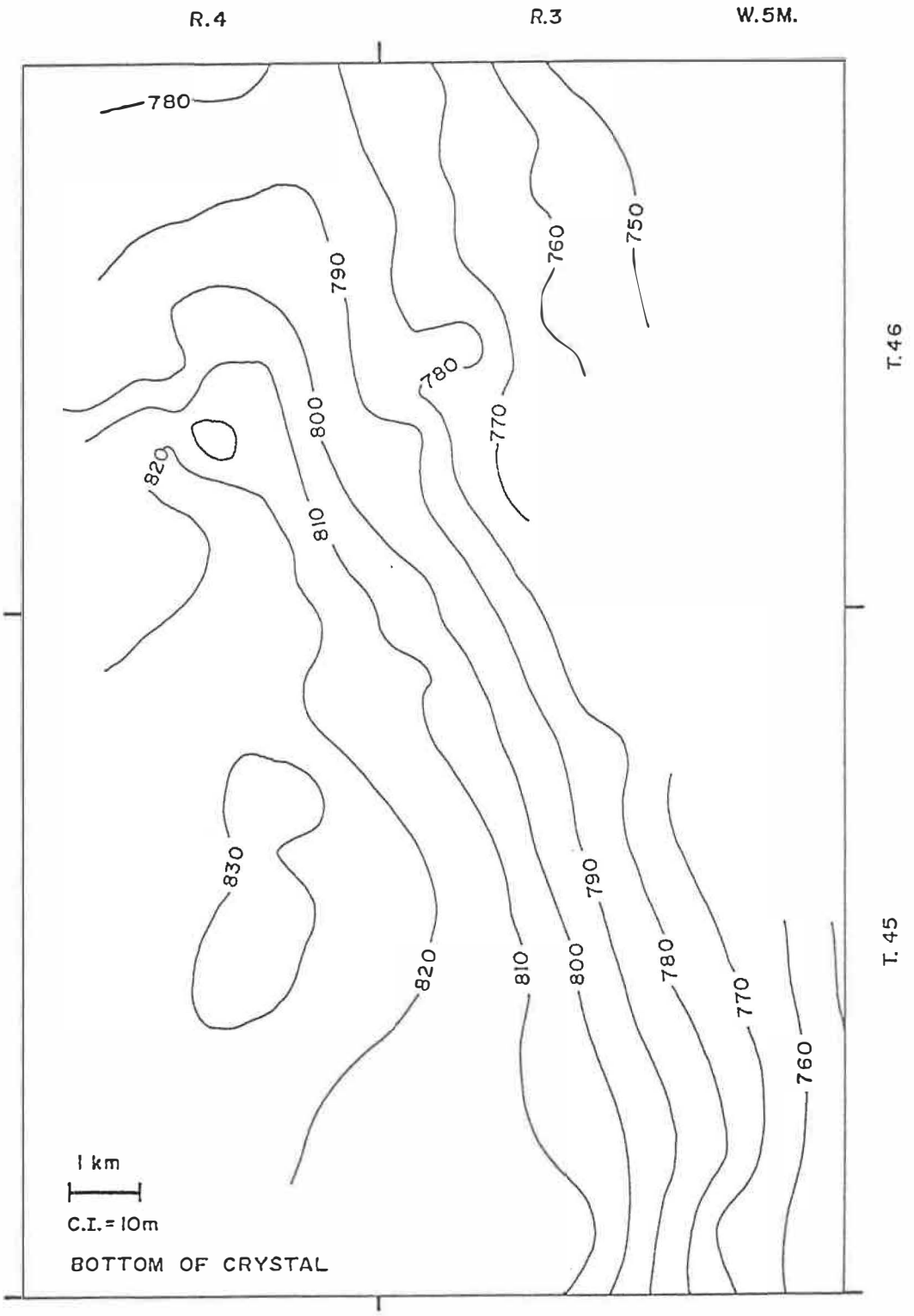
R.4
R.3
W.5M.
T.46
T.45
780
790
800
810
820
830
770
760
750
1 km
C.I. = 10m
BOTTOM OF CRYSTAL

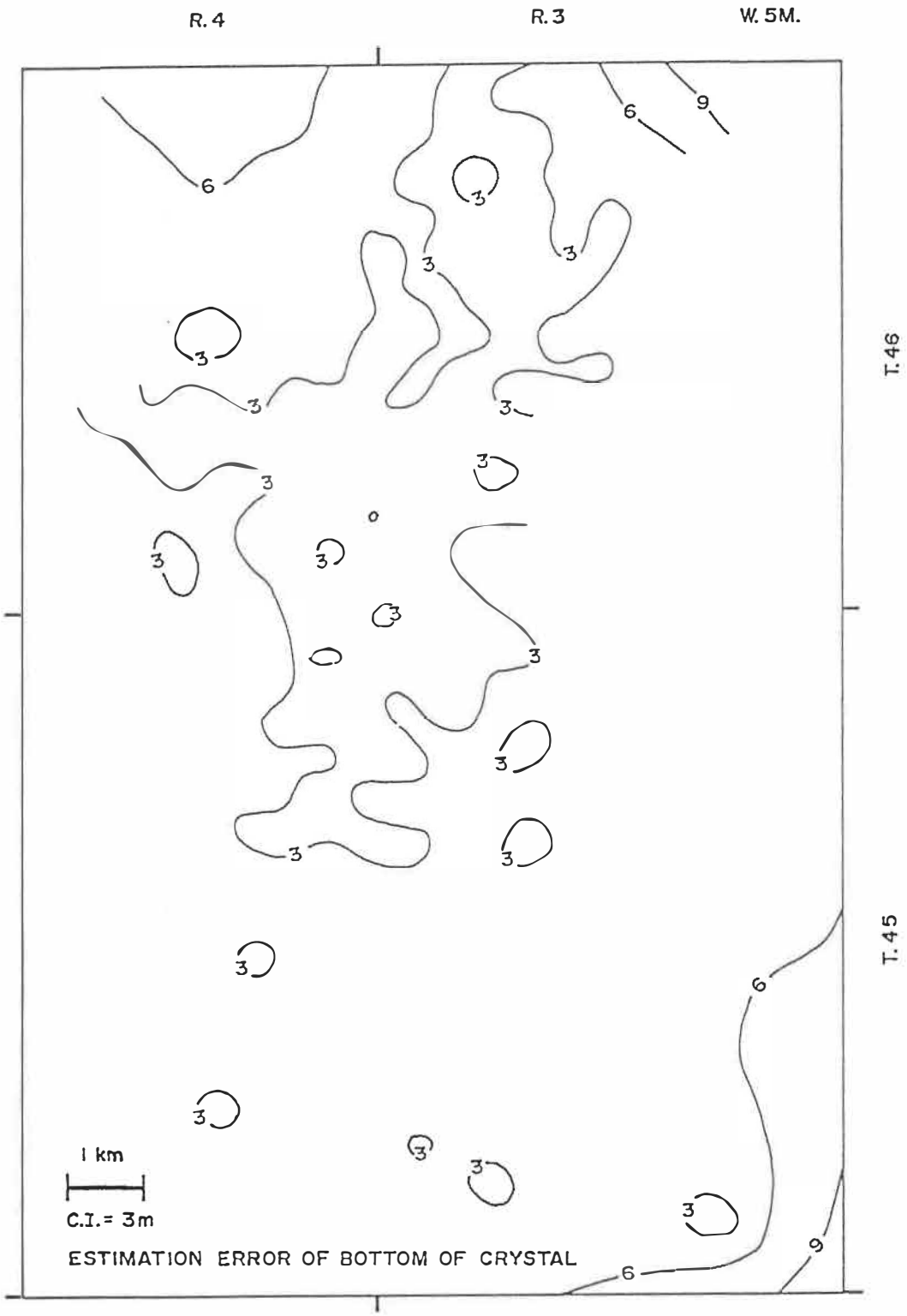
R. 4
R. 3
W. 5M.
T. 46
T. 45
6
9
3
1 km
C.I. = 3m
ESTIMATION ERROR OF BOTTOM OF CRYSTAL

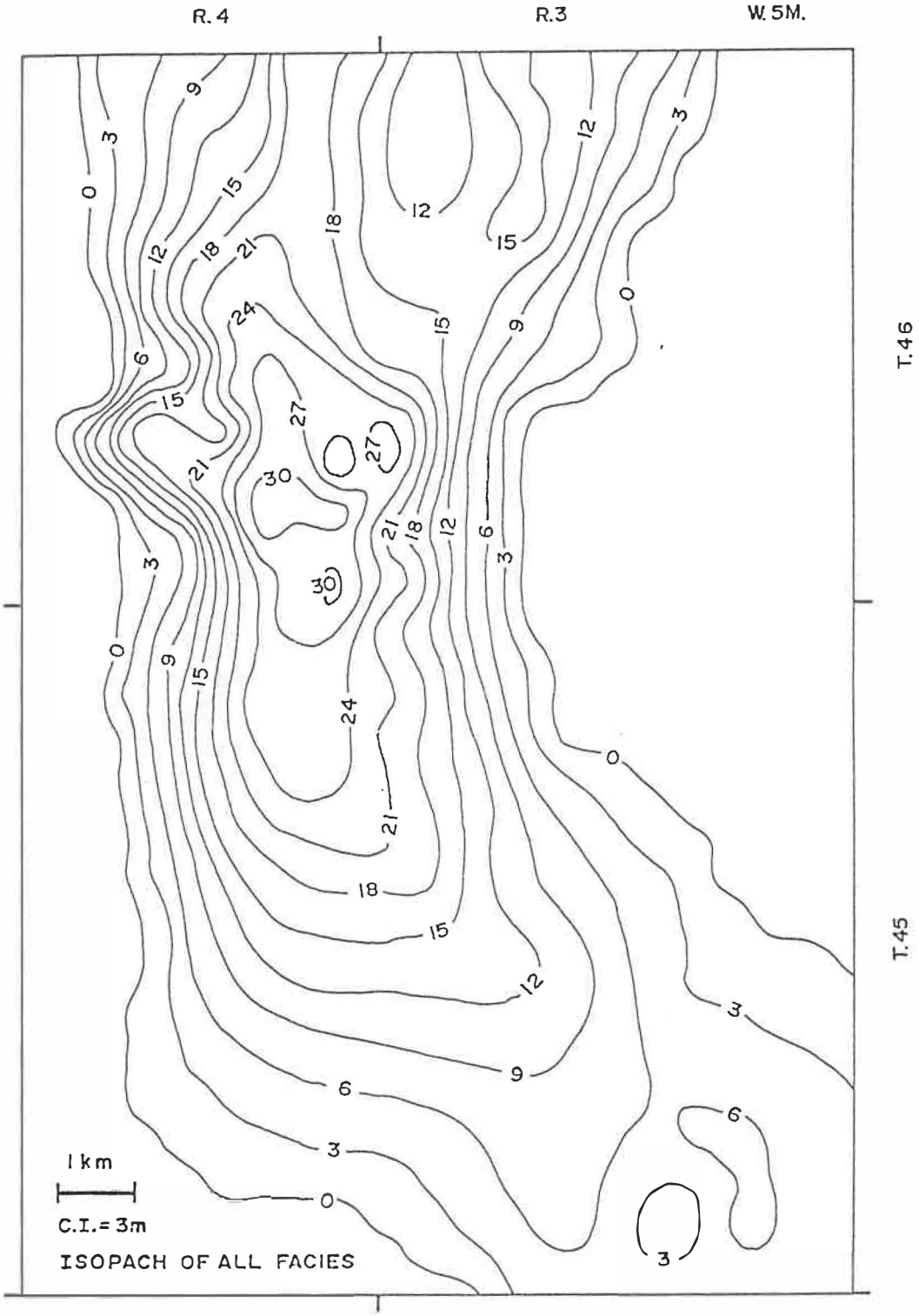
R. 4
R.3
W. 5M.
T.46
T.45
1 km
C.I. = 3m
ISOPACH OF ALL FACIES

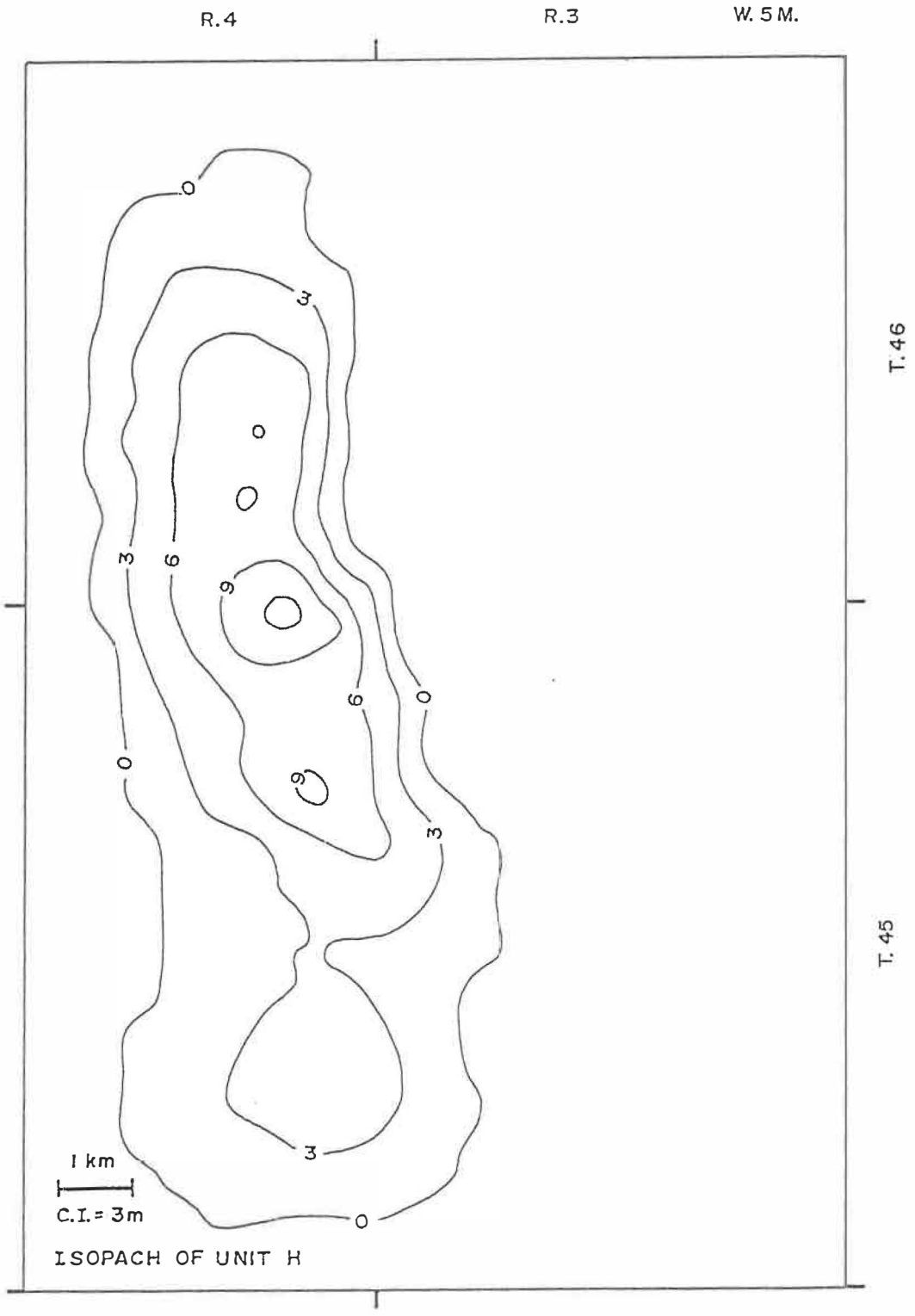

ISOPACH OF UNIT H

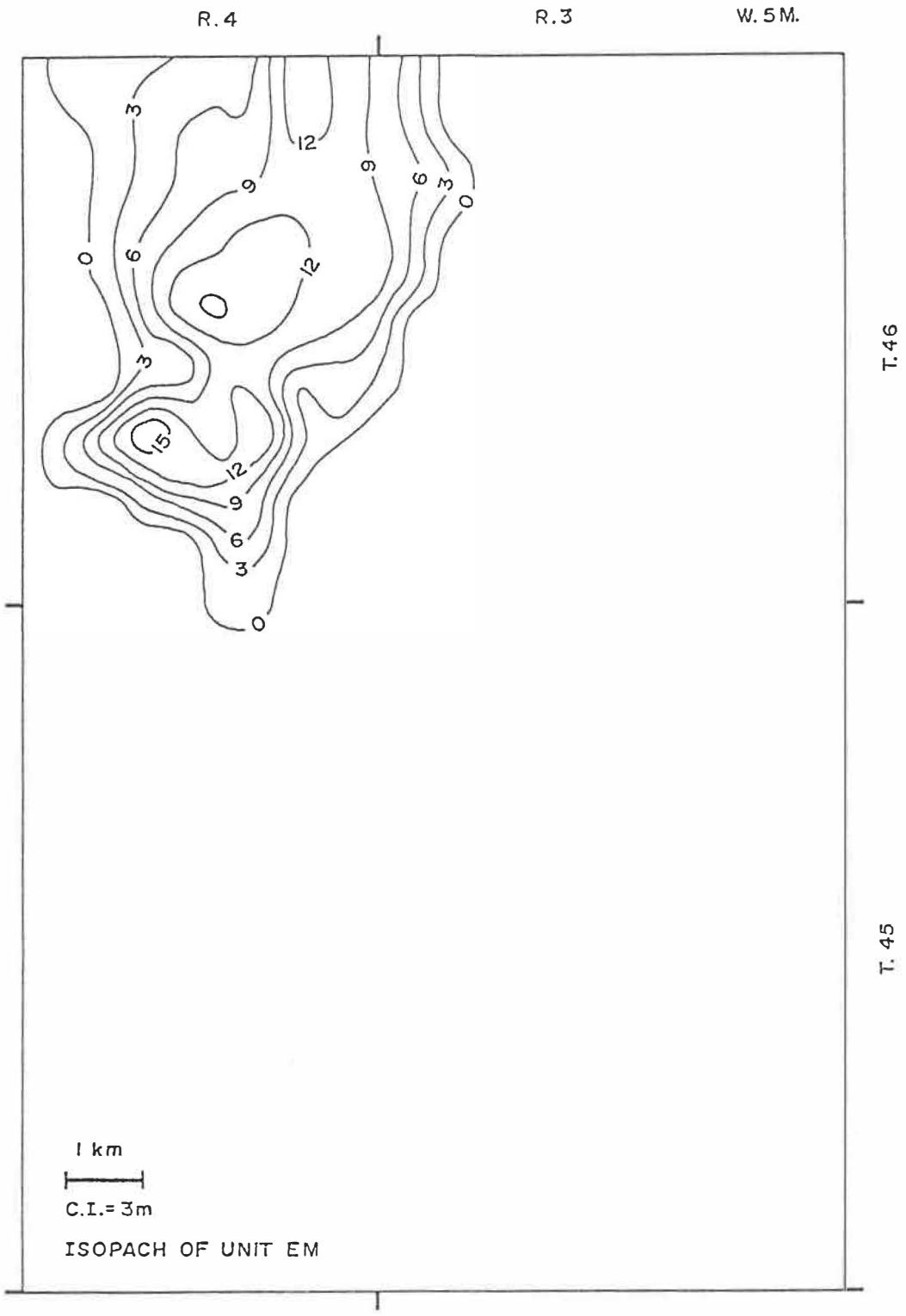
R. 4
R. 3
W. 5 M.
T. 46
T. 45
0
3
6
9
12
15
1 km
C.I. = 3m
ISOPACH OF UNIT EM

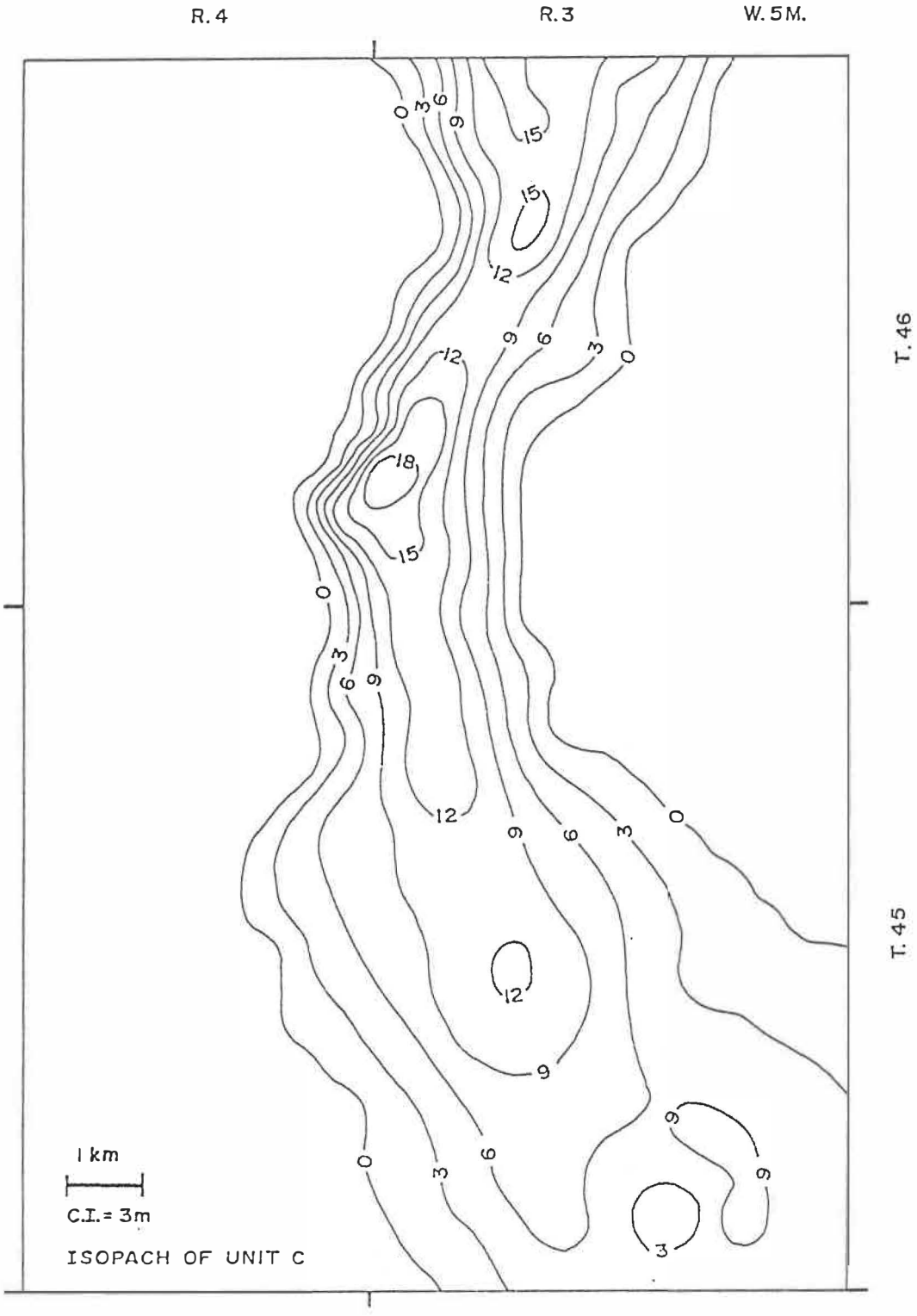
R. 4
R. 3
W. 5M.
T. 46
T. 45
0
3
6
9
12
15
18
1 km
C.I. = 3m
ISOPACH OF UNIT C

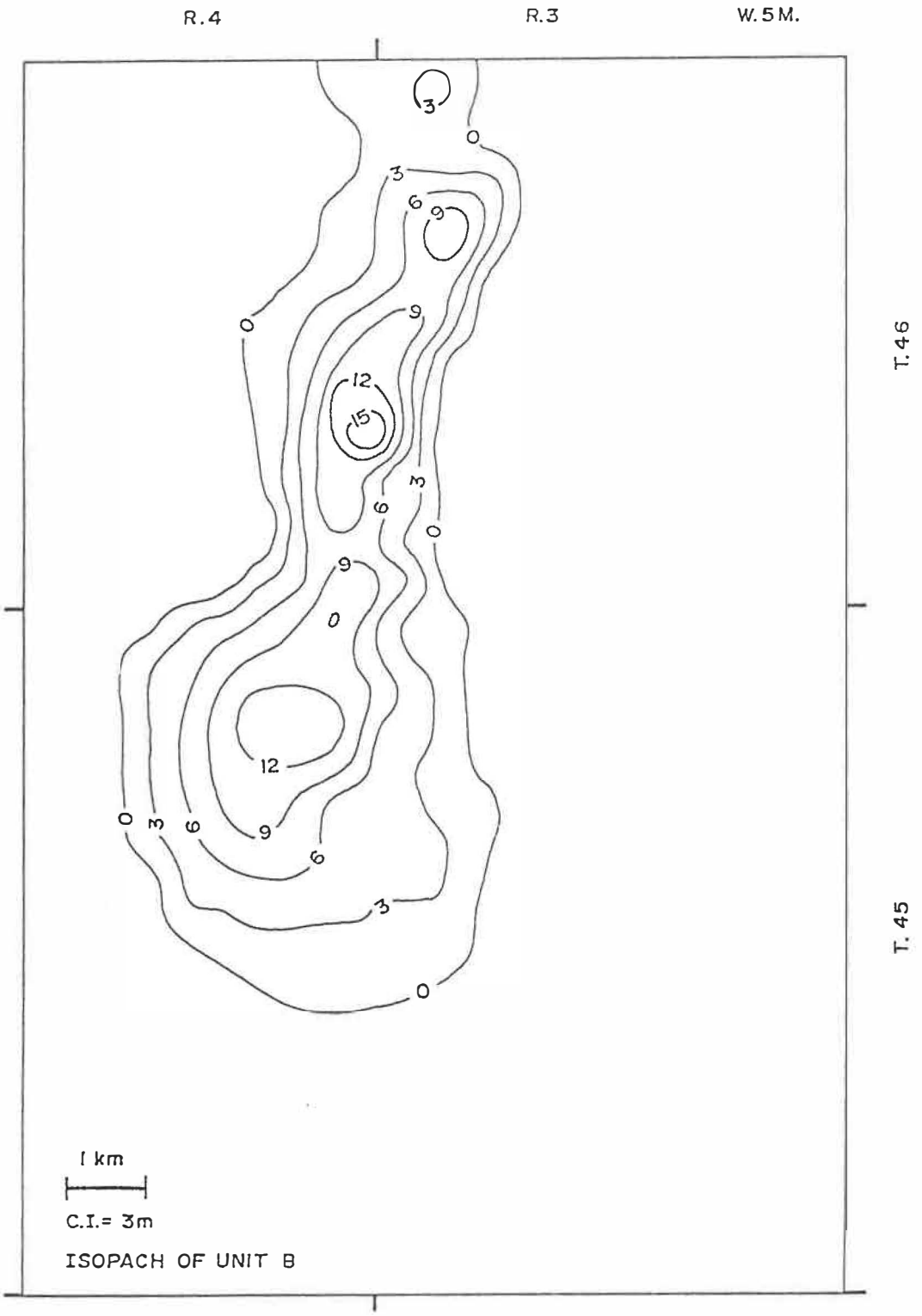

ISOPACH OF UNIT B

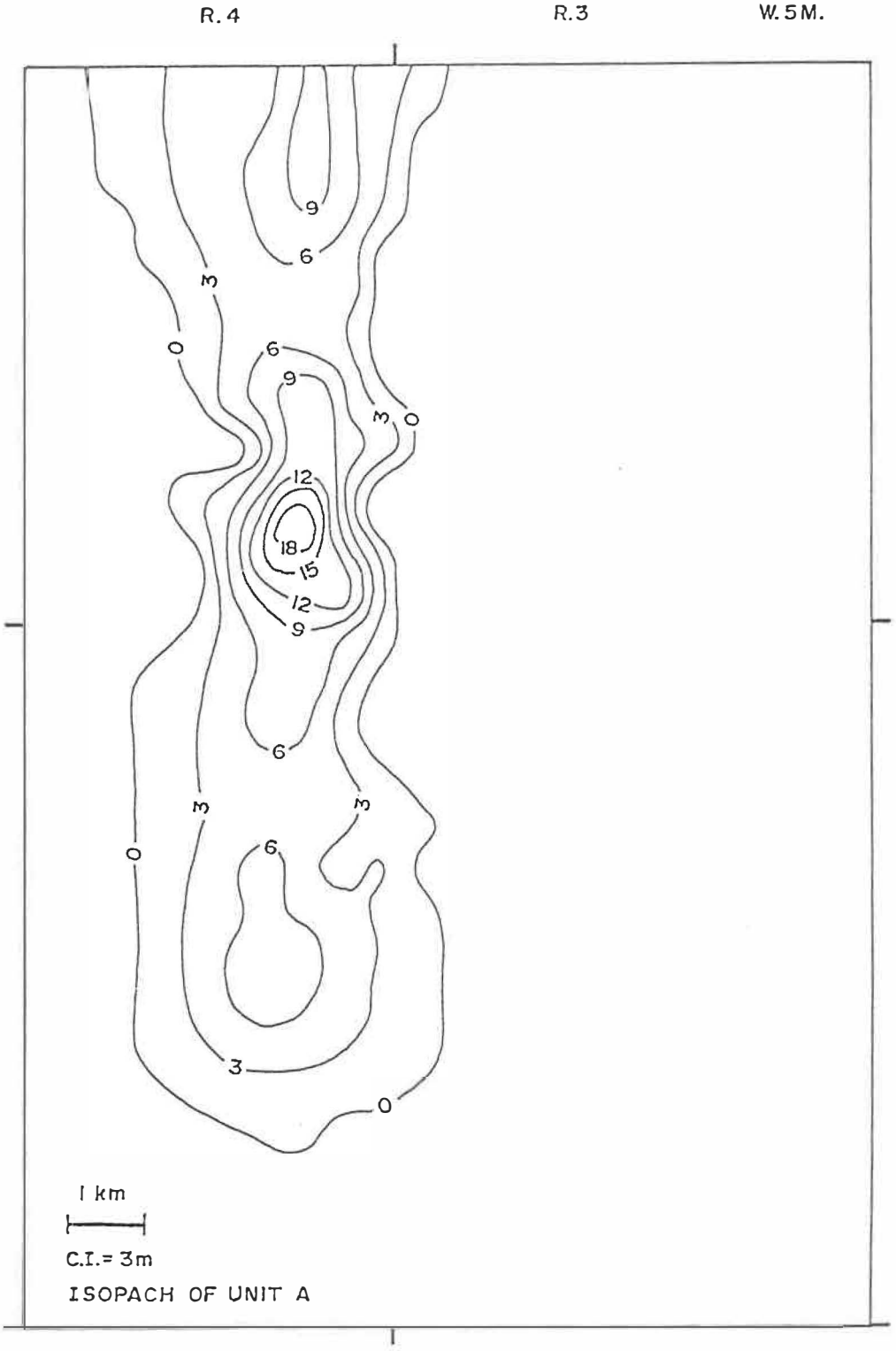
R. 4
R. 3
W. 5 M.
T. 46
T. 45
0
3
6
9
12
15
18
1 km
C.I. = 3m
ISOPACH OF UNIT A

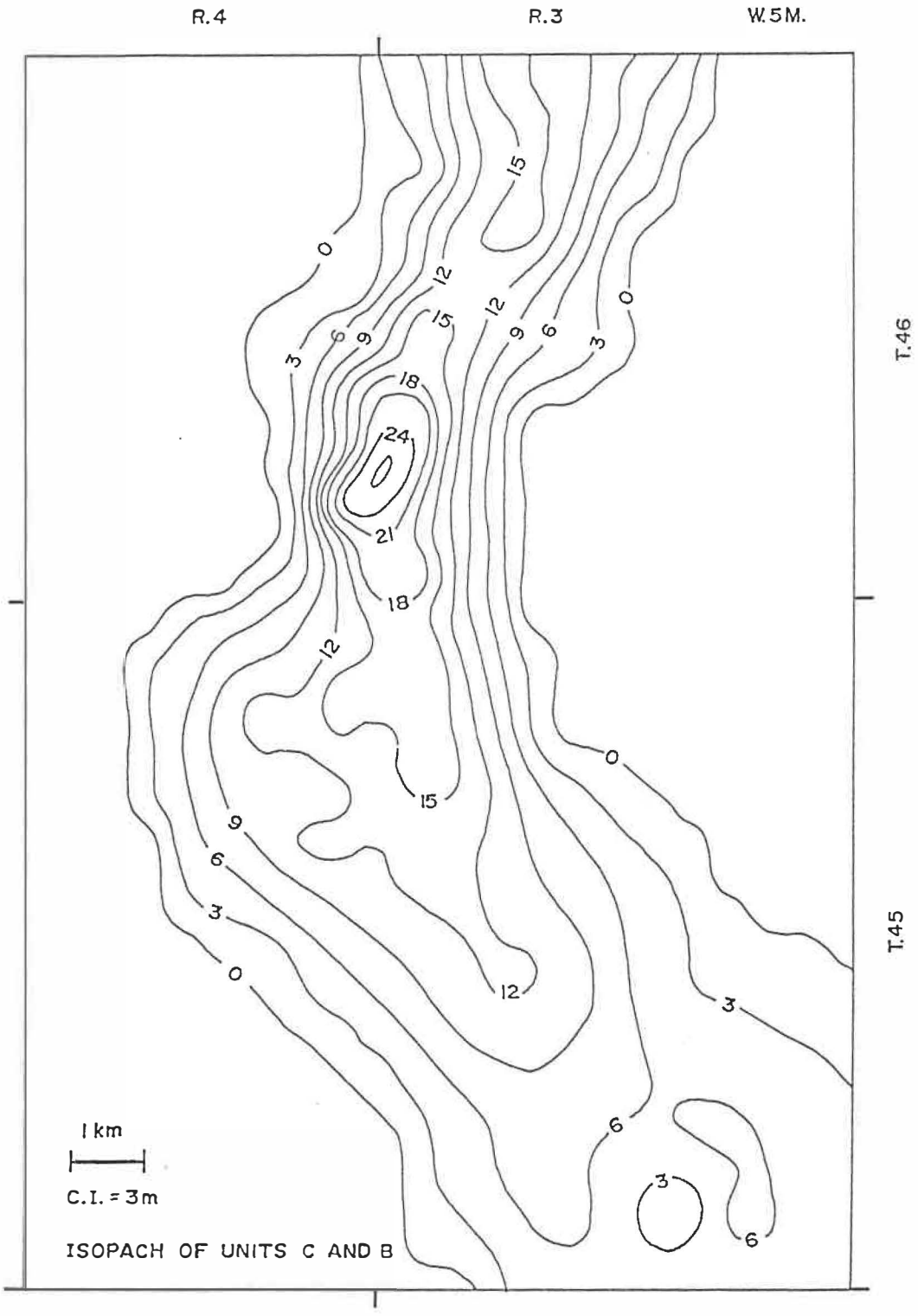
R.4
R.3
W.5M.
T.46
T.45
0
3
6
9
12
15
18
21
24
1 km
C.I. = 3m
ISOPACH OF UNITS C AND B

APPENDIX D: COMPARISONS OF THE VARIOGRAMS OF CONDITIONALLY SIMULATED FIELDS OF ROCK PROPERTIES OF THE CRYSTAL UNITS TO THE CORRESPONDING THEORETICAL MODEL

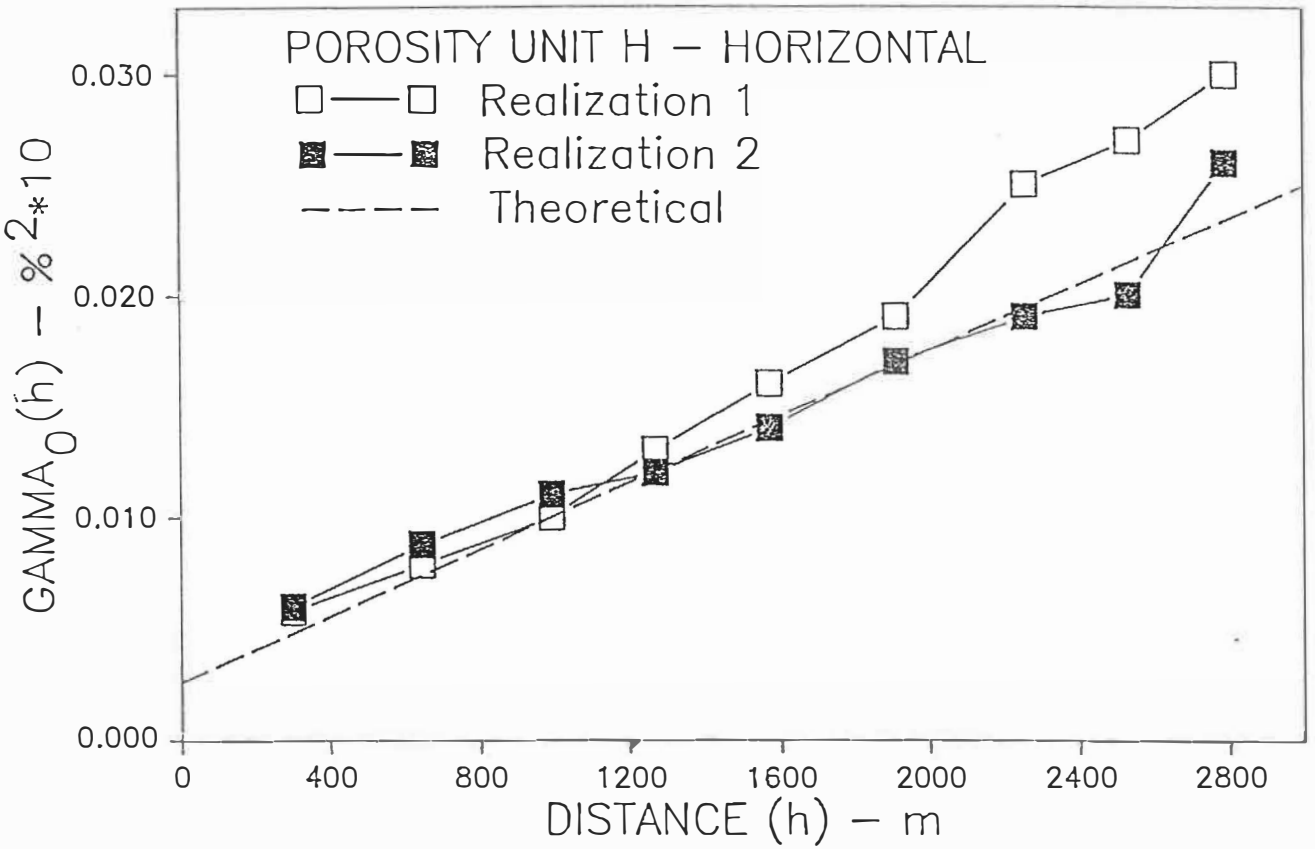
POROSITY UNIT H – HORIZONTAL
Realization 1
Realization 2
Theoretical
GAMMA$_0$(h) – %^{2}*10
0.030
0.020
0.010
0.000
0
400
800
1200
1600
2000
2400
2800
DISTANCE (h) – m

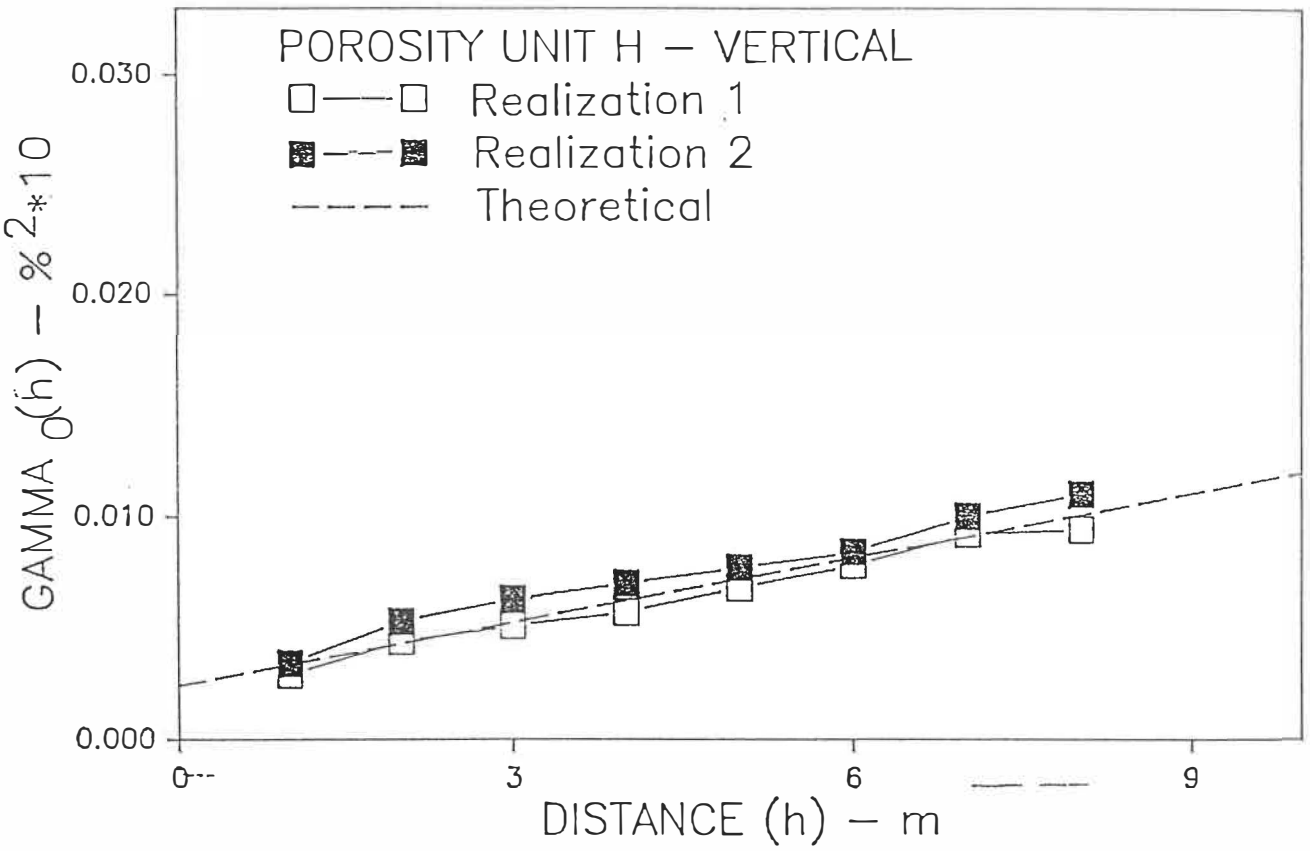
POROSITY UNIT H – VERTICAL
Realization 1
Realization 2
Theoretical
GAMMA σ(h) – %2*10
0.030
0.020
0.010
0.000
0
3
6
9
DISTANCE (h) – m

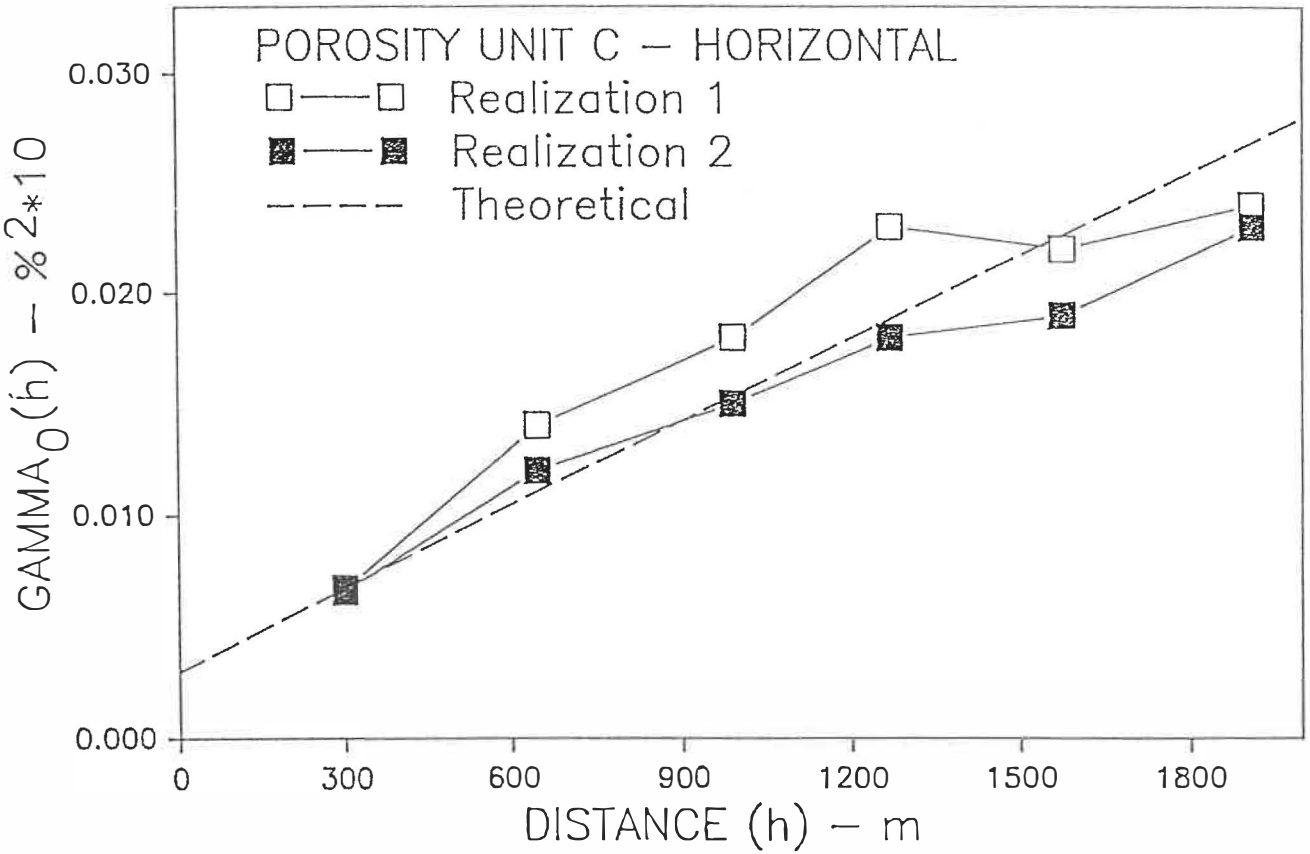
POROSITY UNIT C – HORIZONTAL
Realization 1
Realization 2
Theoretical
0.030
0.020
0.010
0.000
GAMMA$_0$(h) – %2*10
0
300
600
900
1200
1500
1800
DISTANCE (h) – m

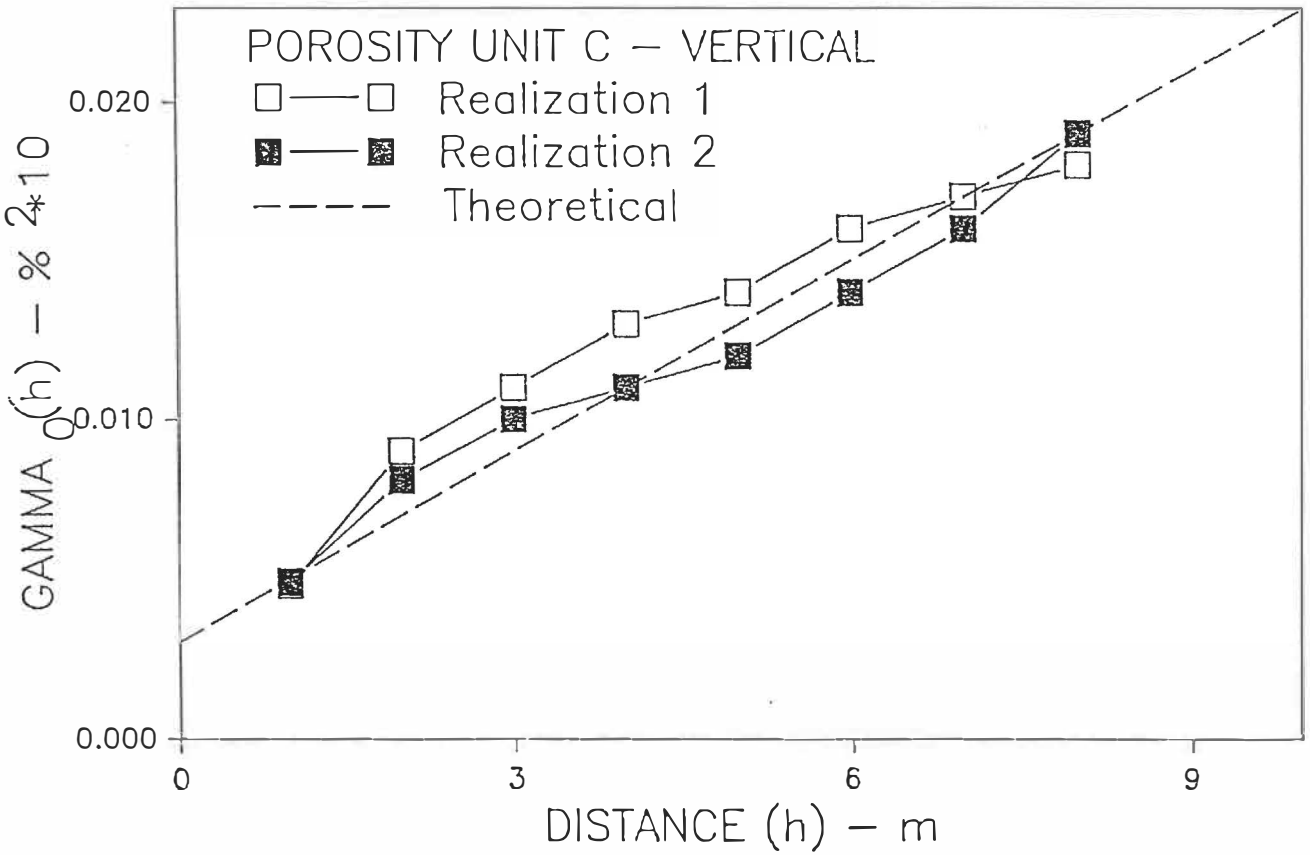
POROSITY UNIT C – VERTICAL
Realization 1
Realization 2
Theoretical
0.020
0.010
0.000
GAMMA (h) – % 2*10
0
3
6
9
DISTANCE (h) – m

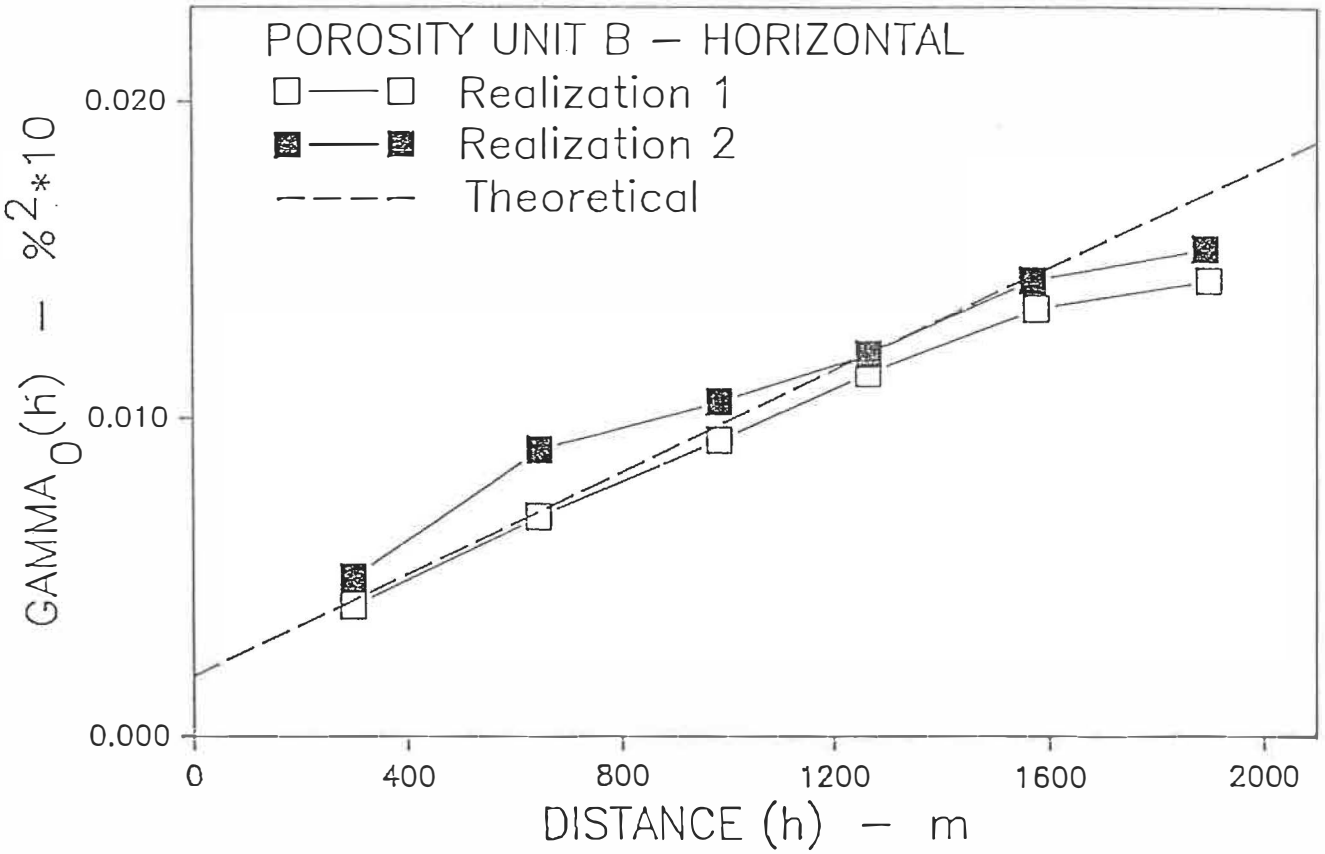
POROSITY UNIT B – HORIZONTAL
Realization 1
Realization 2
Theoretical
0.020
0.010
0.000
GAMMA0(h) – %2*10
0
400
800
1200
1600
2000
DISTANCE (h) – m

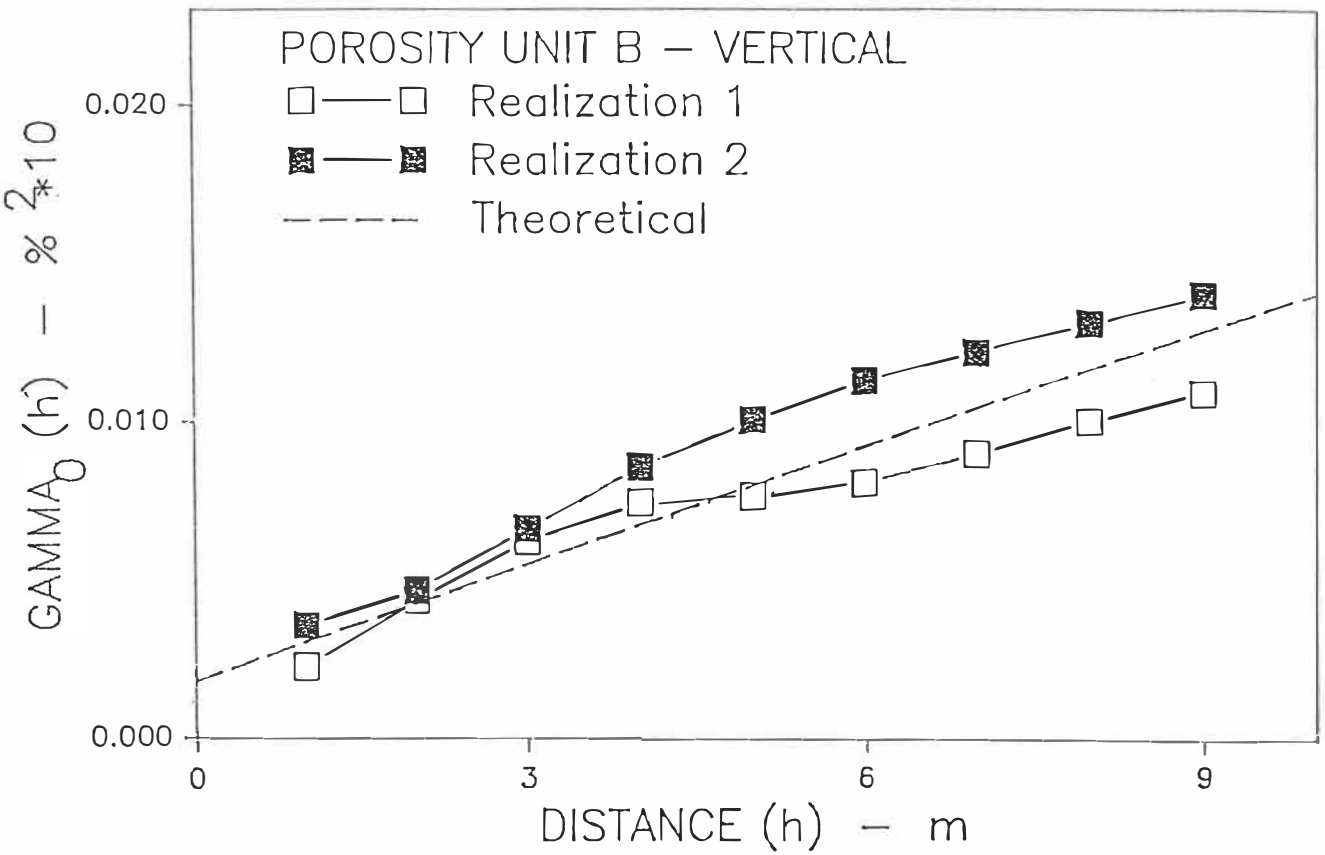
POROSITY UNIT B – VERTICAL
Realization 1
Realization 2
Theoretical
0.020
0.010
0.000
GAMMA0 (h) – % 2*10
0
3
6
9
DISTANCE (h) – m

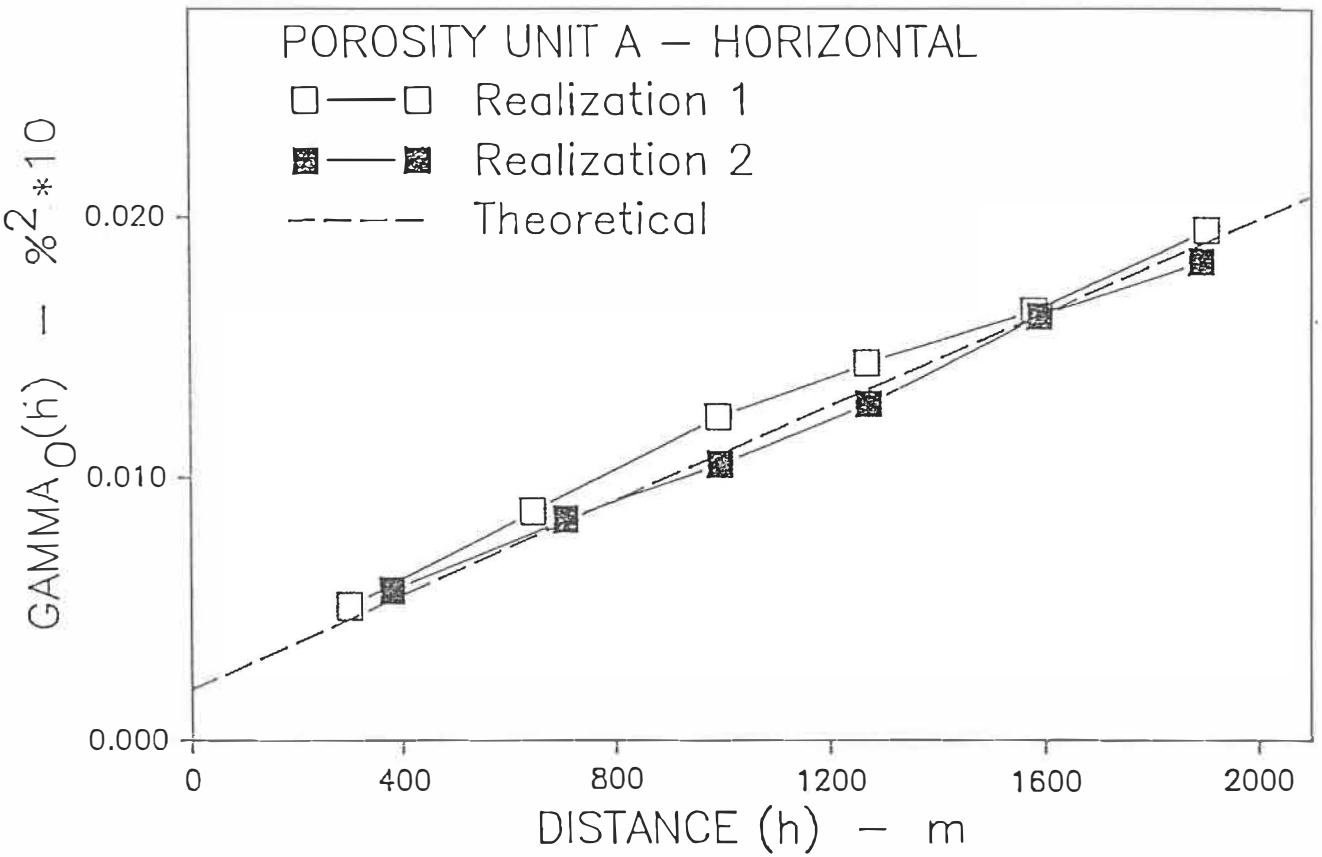
POROSITY UNIT A – HORIZONTAL
Realization 1
Realization 2
Theoretical
GAMMA O(h) – %2*10
0.020
0.010
0.000
0
400
800
1200
1600
2000
DISTANCE (h) – m

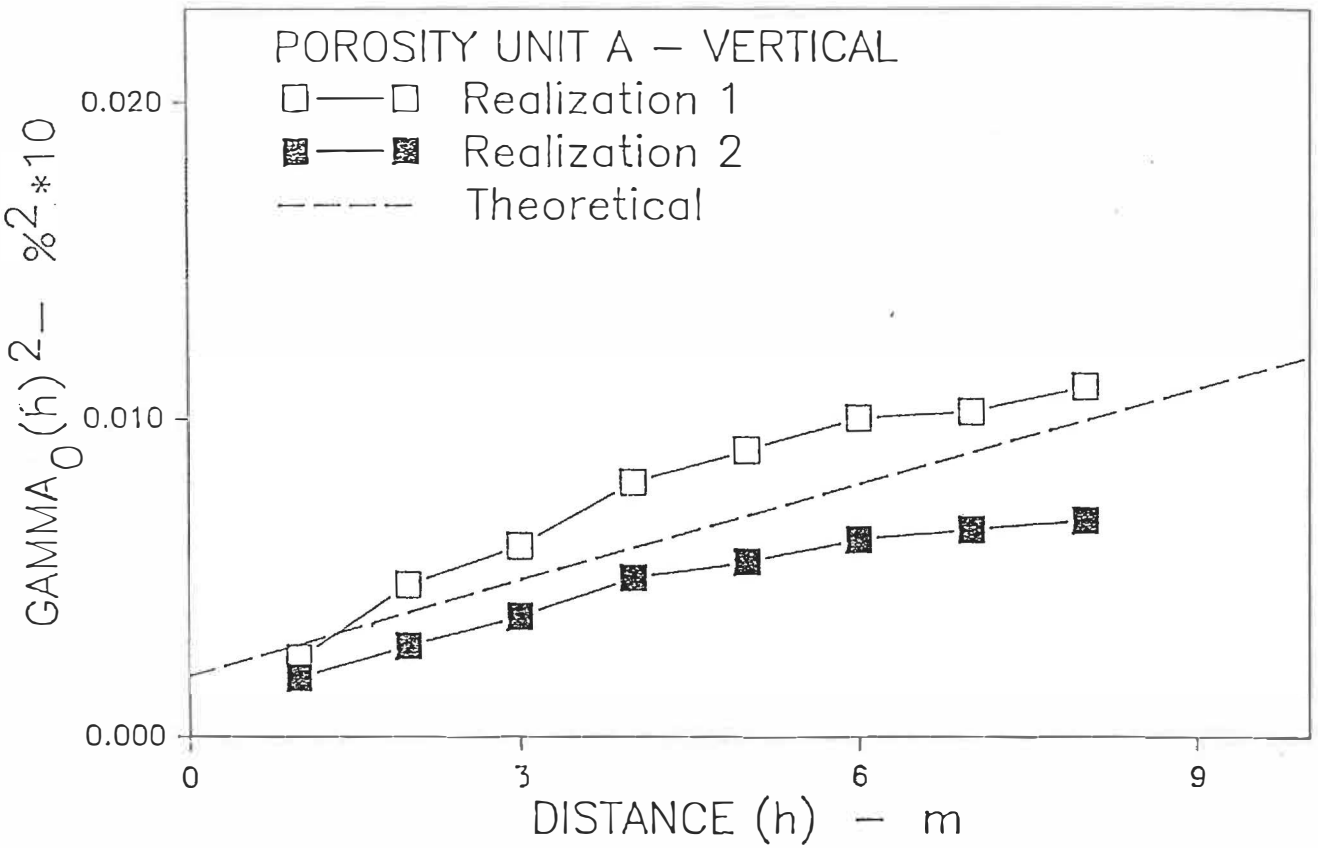
POROSITY UNIT A – VERTICAL
Realization 1
Realization 2
Theoretical
0.020
0.010
0.000
GAMMA0(h) 2– %2*10
0
3
6
9
DISTANCE (h) – m

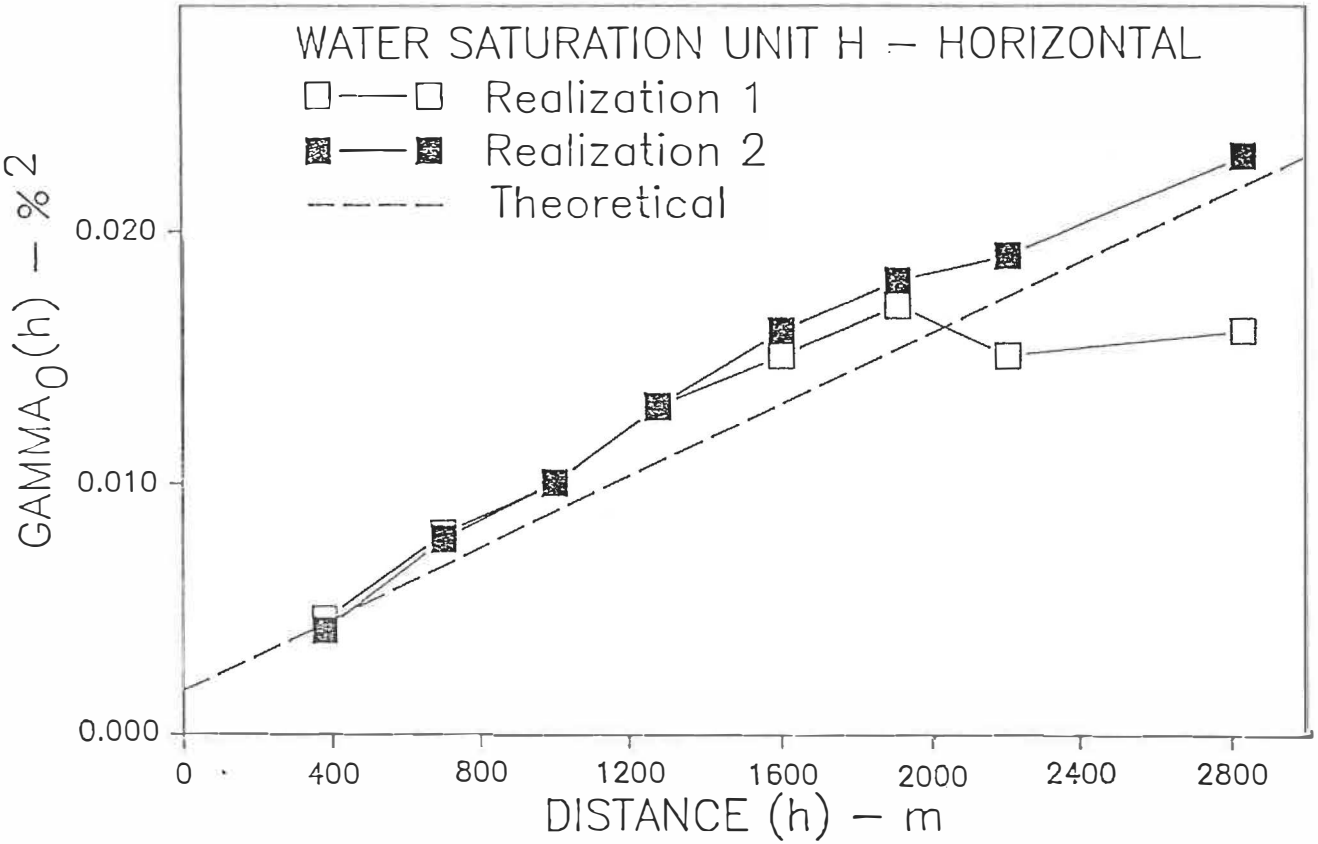
WATER SATURATION UNIT H – HORIZONTAL
Realization 1
Realization 2
Theoretical
GAMMA$_O$(h) – %2
0.020
0.010
0.000
0
400
800
1200
1600
2000
2400
2800
DISTANCE (h) – m

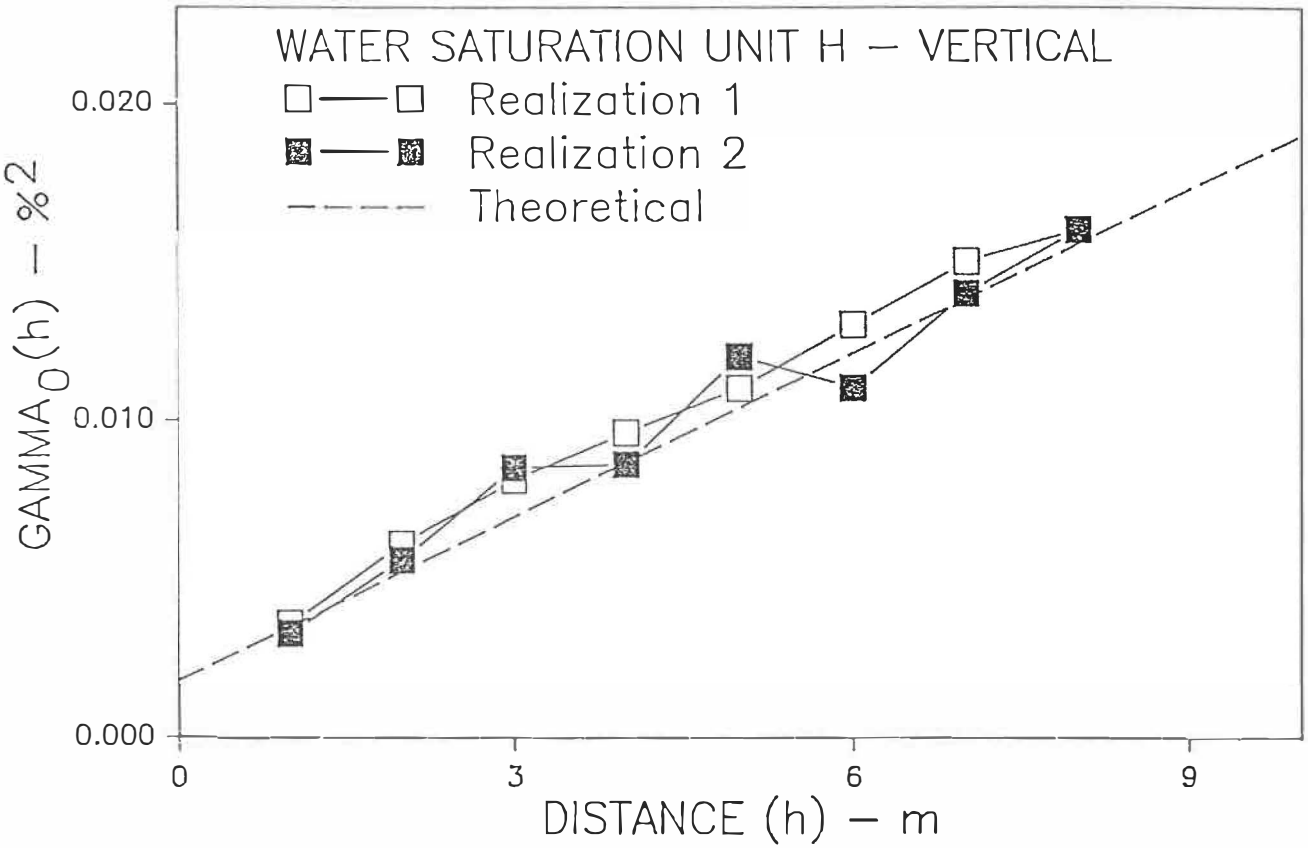
WATER SATURATION UNIT H – VERTICAL
Realization 1
Realization 2
Theoretical
0.020
0.010
0.000
GAMMA0(h) – %2
0
3
6
9
DISTANCE (h) – m

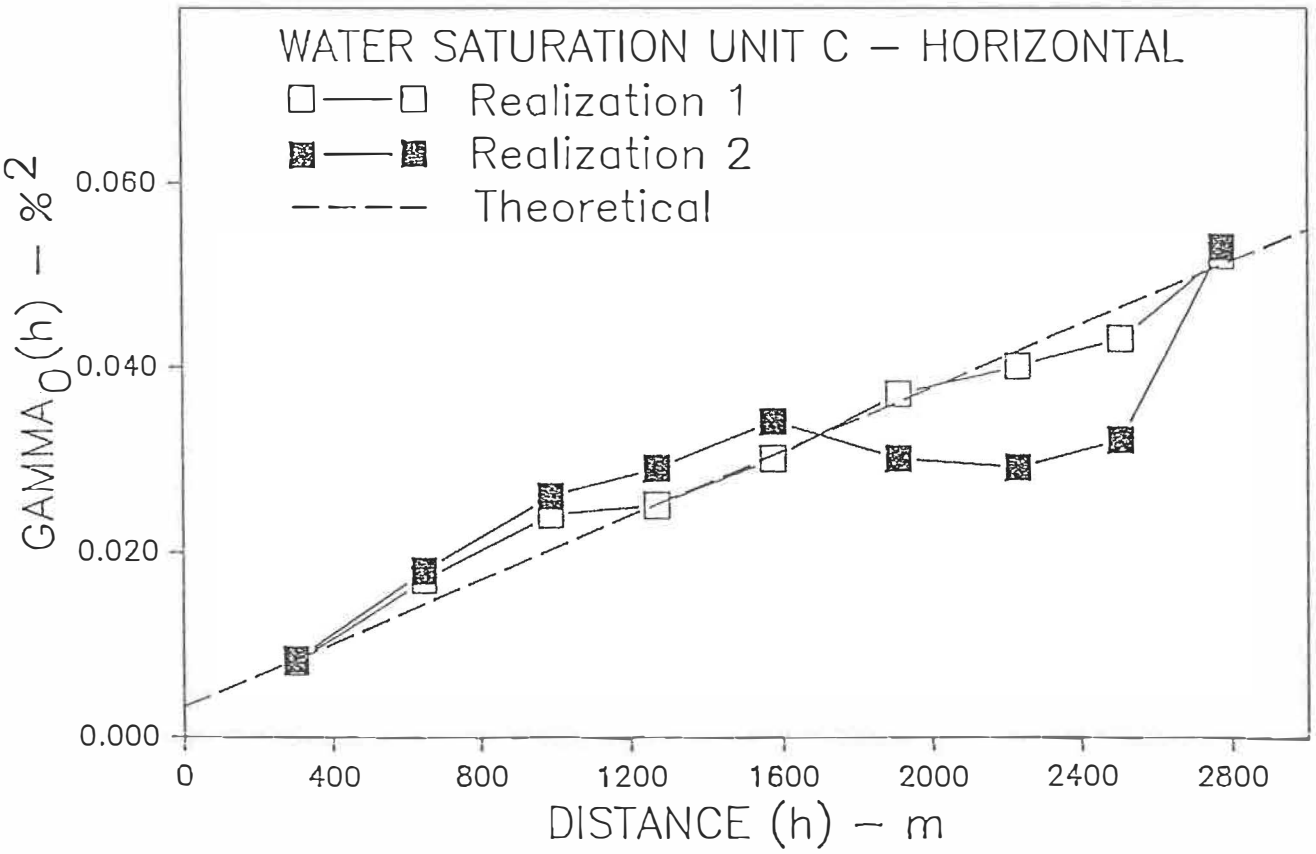
WATER SATURATION UNIT C – HORIZONTAL
Realization 1
Realization 2
Theoretical
GAMMA$_O$(h) – %2
0.060
0.040
0.020
0.000
0
400
800
1200
1600
2000
2400
2800
DISTANCE (h) – m

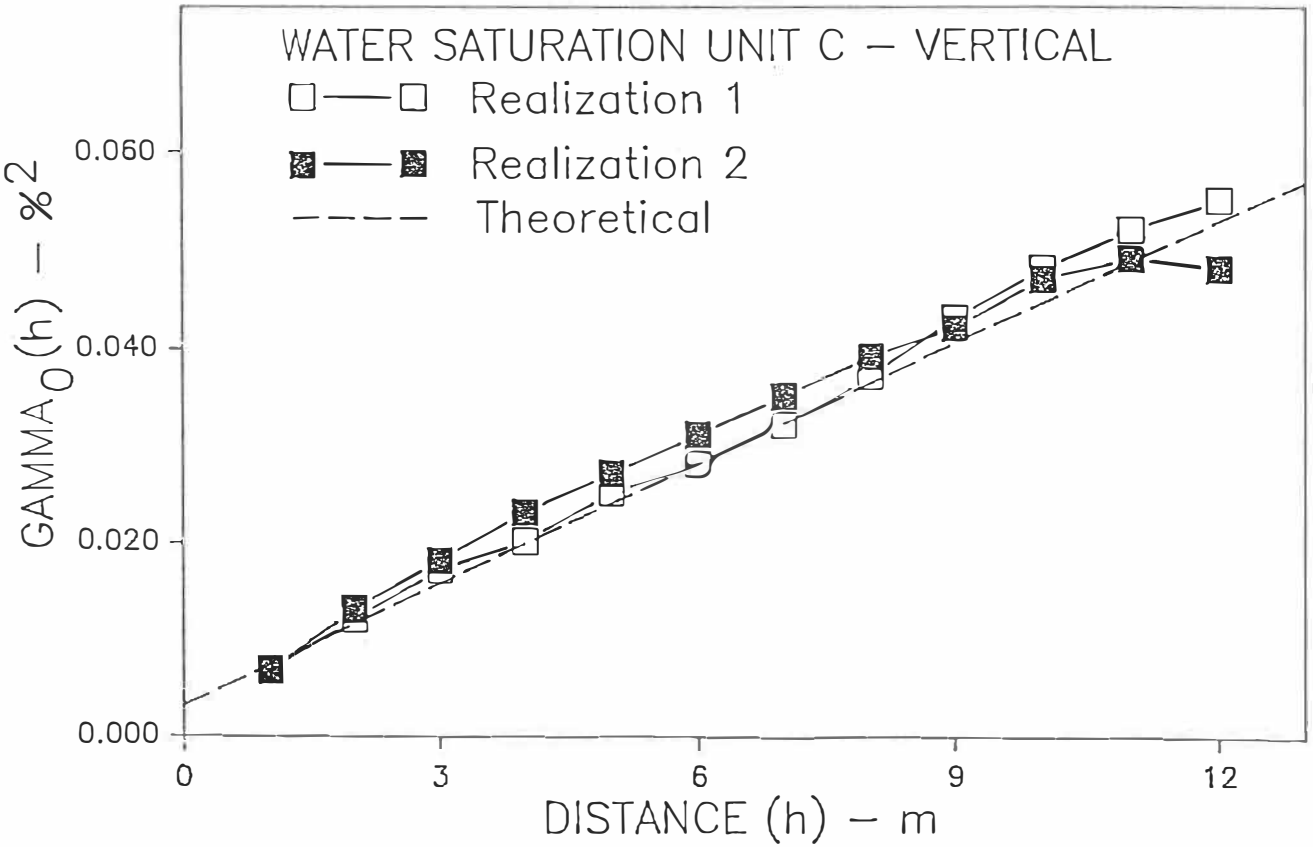
WATER SATURATION UNIT C – VERTICAL
Realization 1
Realization 2
Theoretical
GAMMA$_0$(h) – %^{2}
0.060
0.040
0.020
0.000
0
3
6
9
12
DISTANCE (h) – m

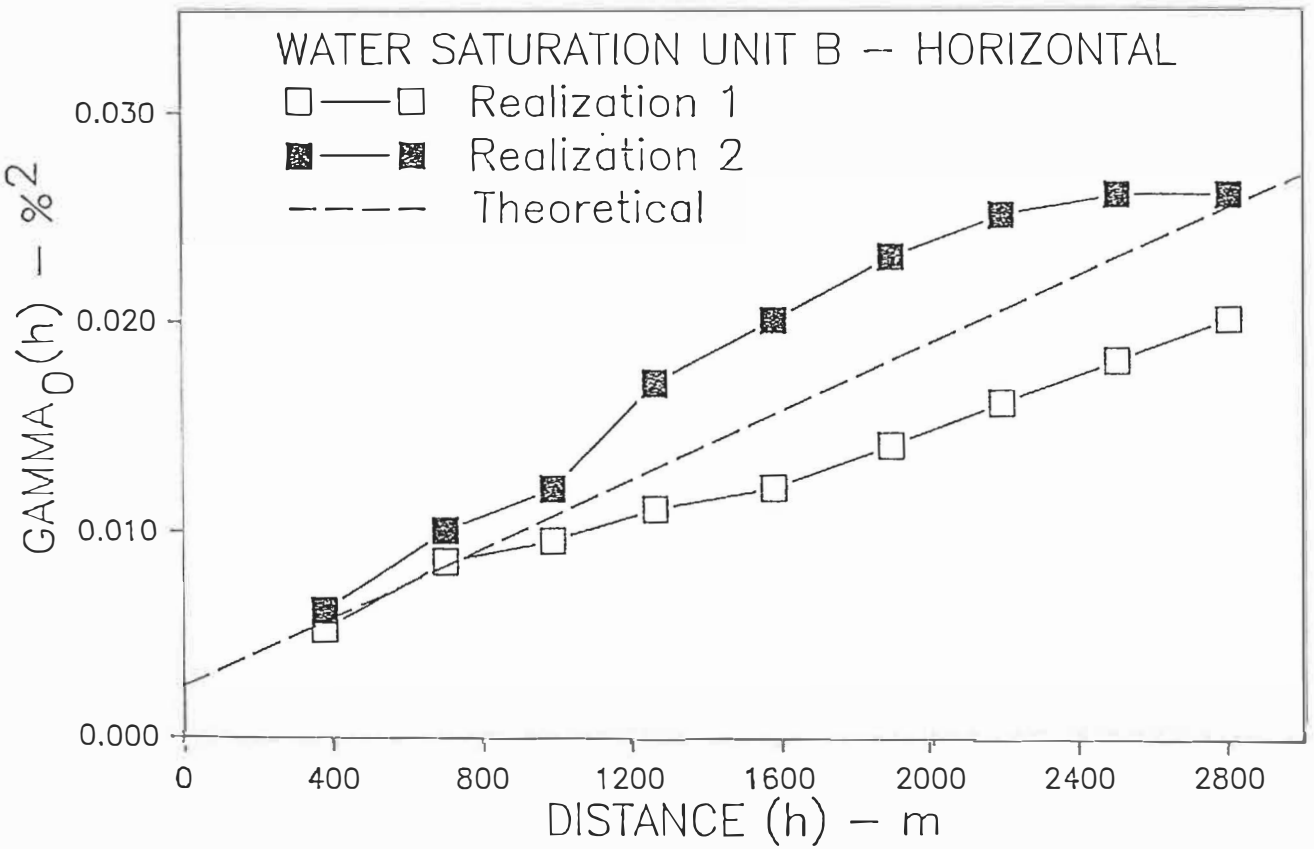
WATER SATURATION UNIT B -- HORIZONTAL
Realization 1
Realization 2
Theoretical
GAMMA$_0$(h) - %2
0.030
0.020
0.010
0.000
0
400
800
1200
1600
2000
2400
2800
DISTANCE (h) - m

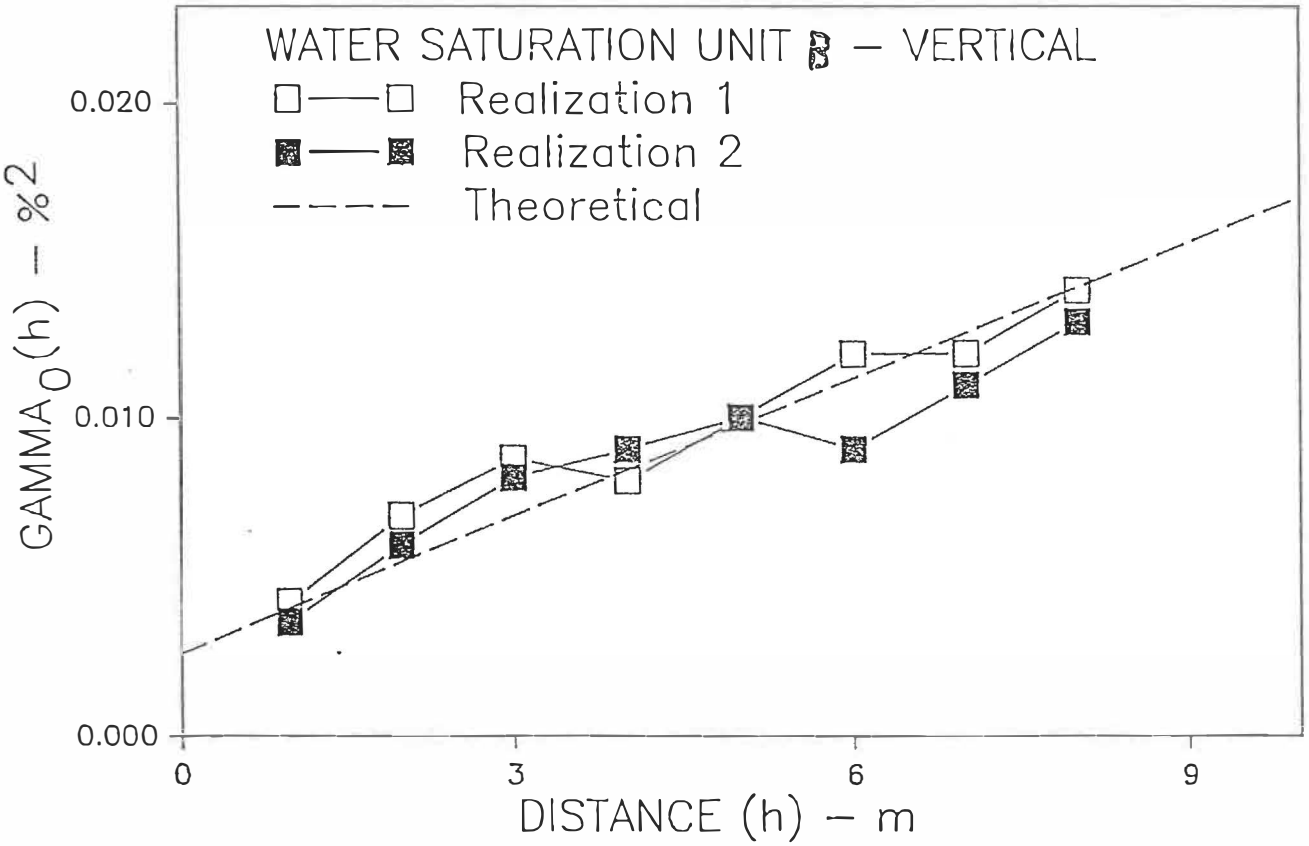
WATER SATURATION UNIT 2 – VERTICAL
Realization 1
Realization 2
Theoretical
0.020
0.010
0.000
GAMMA0(h) – %2
0
3
6
9
DISTANCE (h) – m

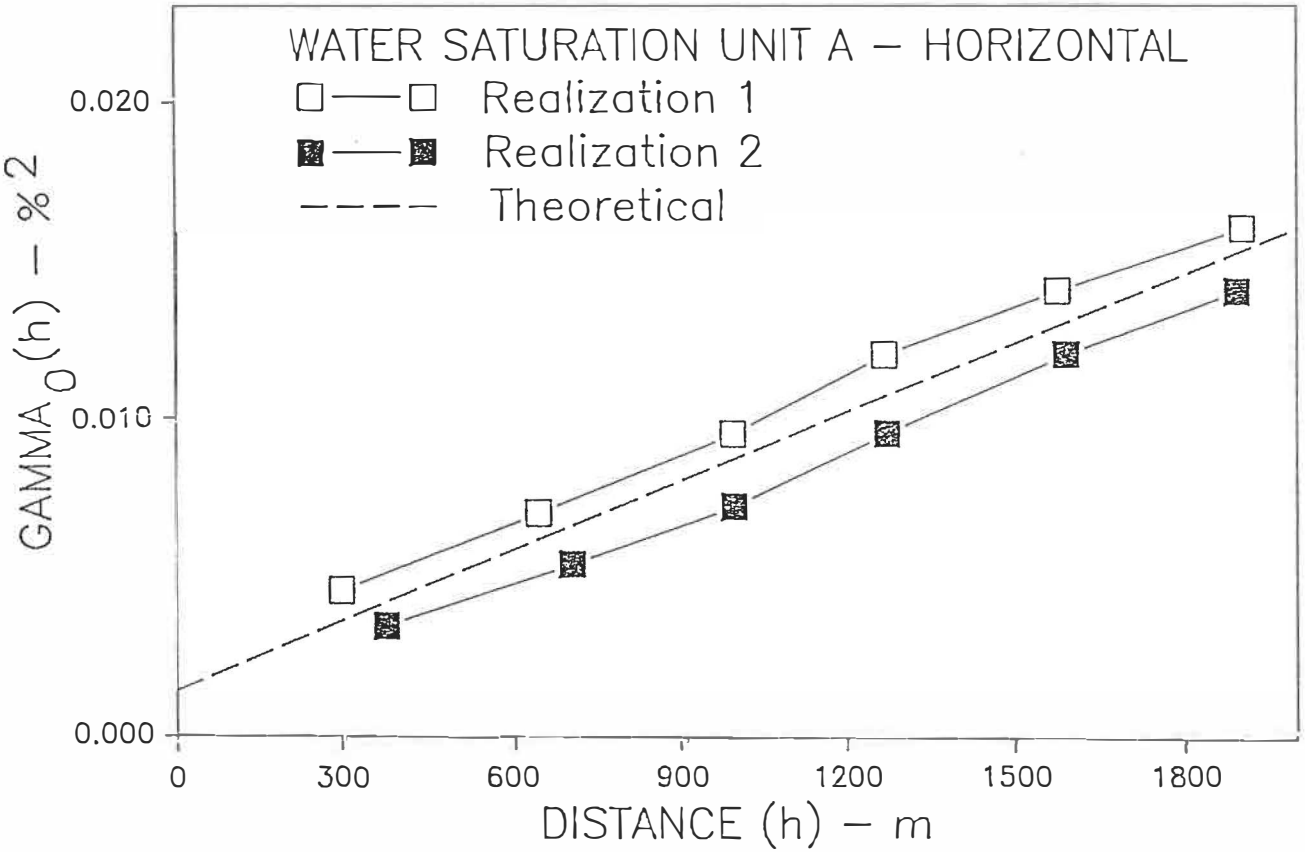
WATER SATURATION UNIT A – HORIZONTAL
Realization 1
Realization 2
Theoretical
GAMMA O(h) – %2
0.020
0.010
0.000
0
300
600
900
1200
1500
1800
DISTANCE (h) – m

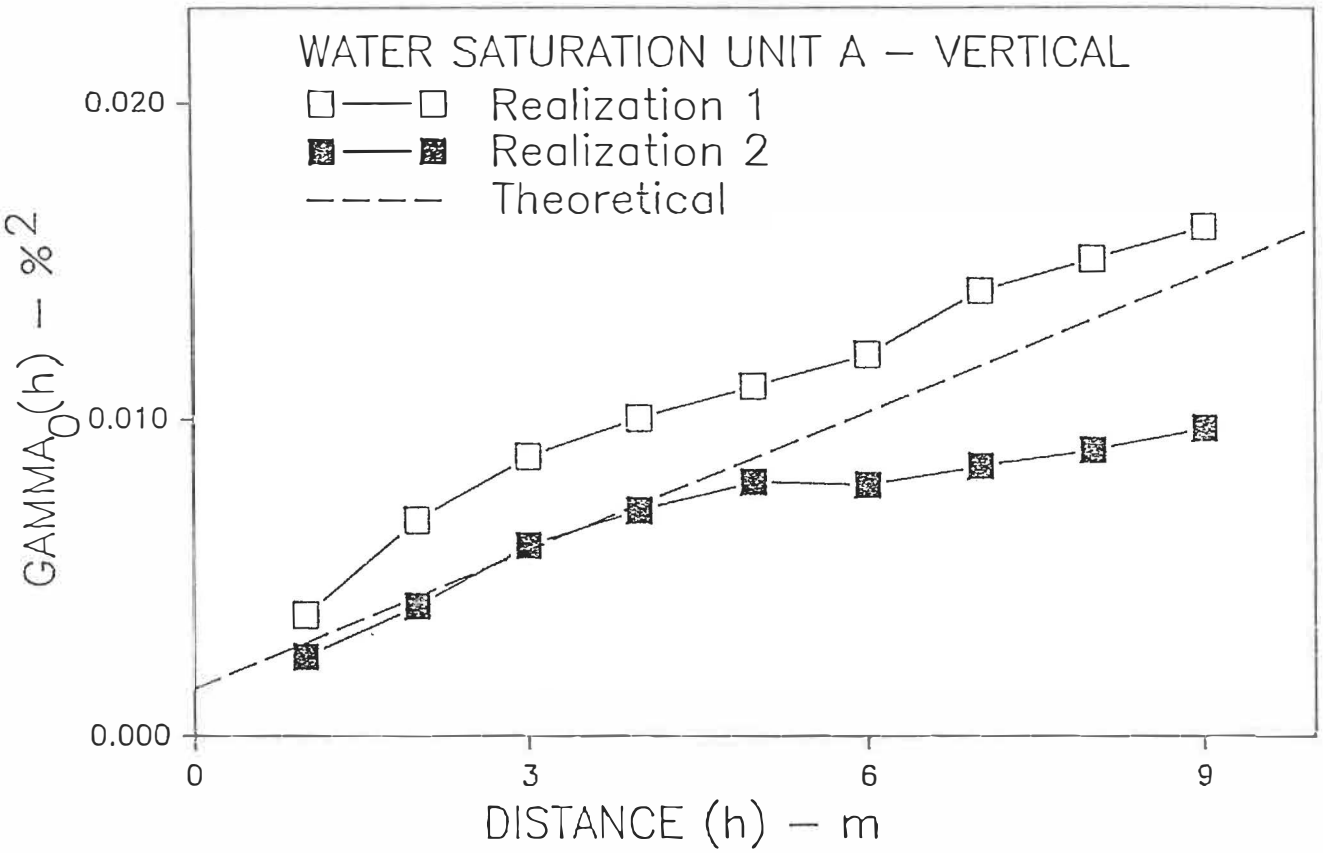
WATER SATURATION UNIT A – VERTICAL
Realization 1
Realization 2
Theoretical
0.020
0.010
0.000
GAMMA$_0$(h) – %2
0
3
6
9
DISTANCE (h) – m

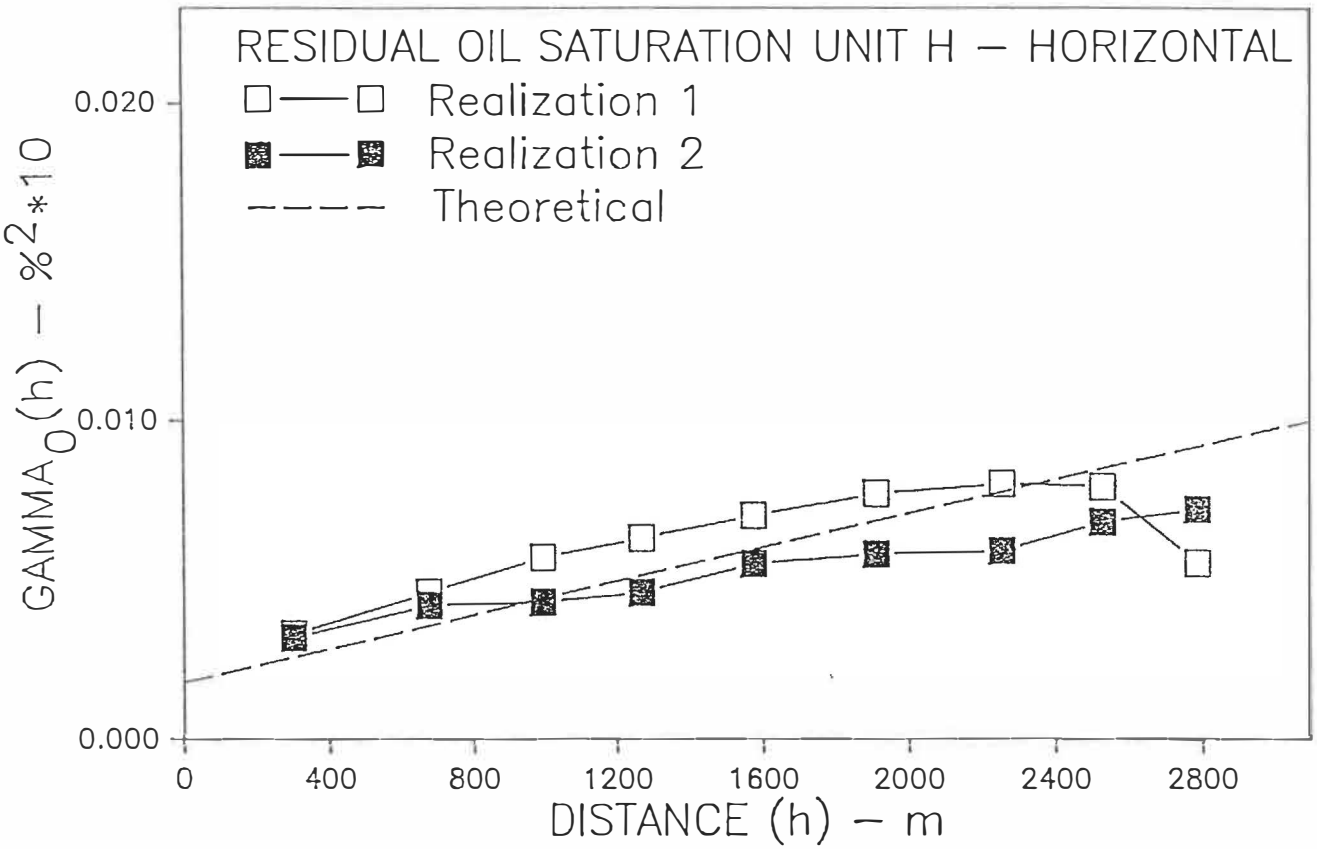
RESIDUAL OIL SATURATION UNIT H – HORIZONTAL
Realization 1
Realization 2
Theoretical
0.020
0.010
0.000
GAMMA$_0$(h) – %^{2}*10
0
400
800
1200
1600
2000
2400
2800
DISTANCE (h) – m

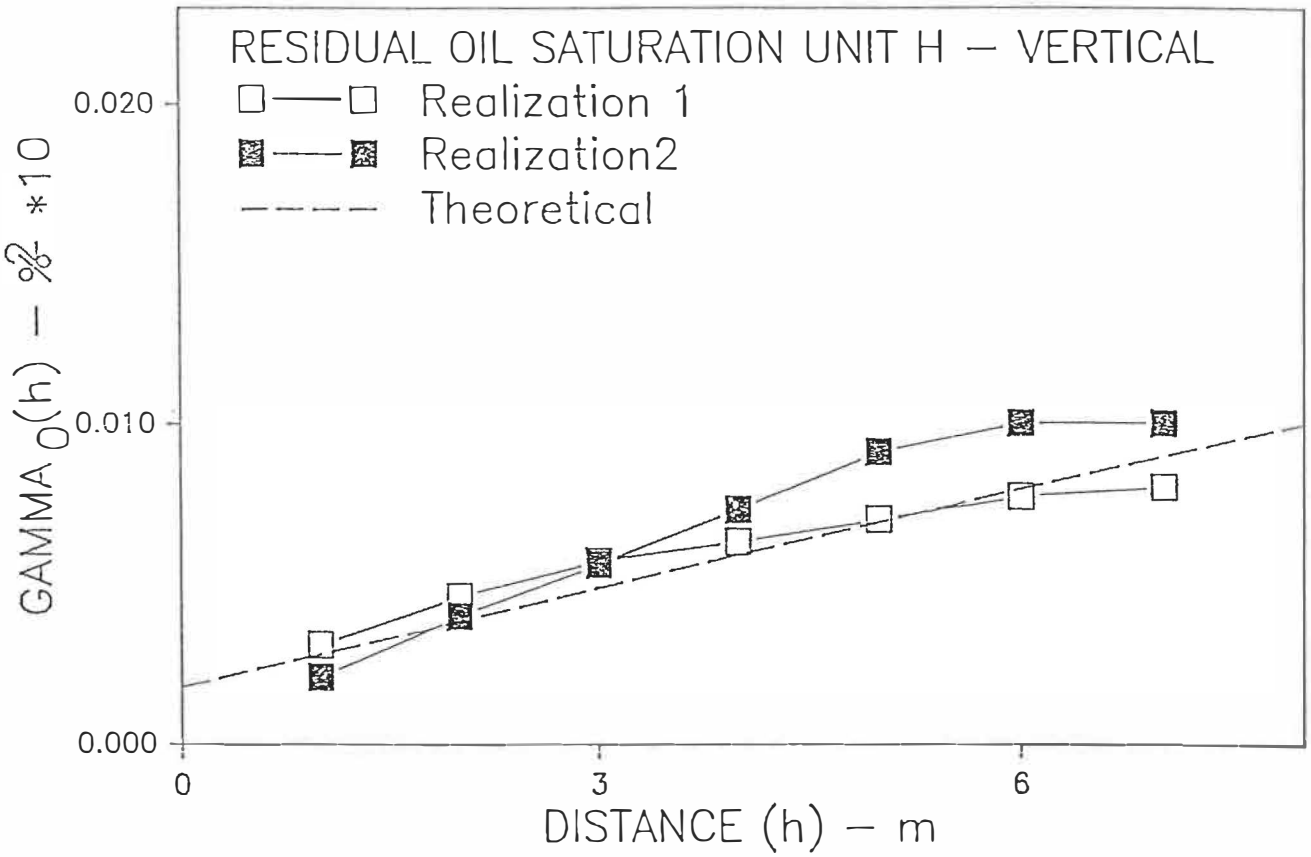
RESIDUAL OIL SATURATION UNIT H – VERTICAL
Realization 1
Realization2
Theoretical
0.020
0.010
0.000
GAMMA O(h) – %2 *10
0
3
6
DISTANCE (h) – m

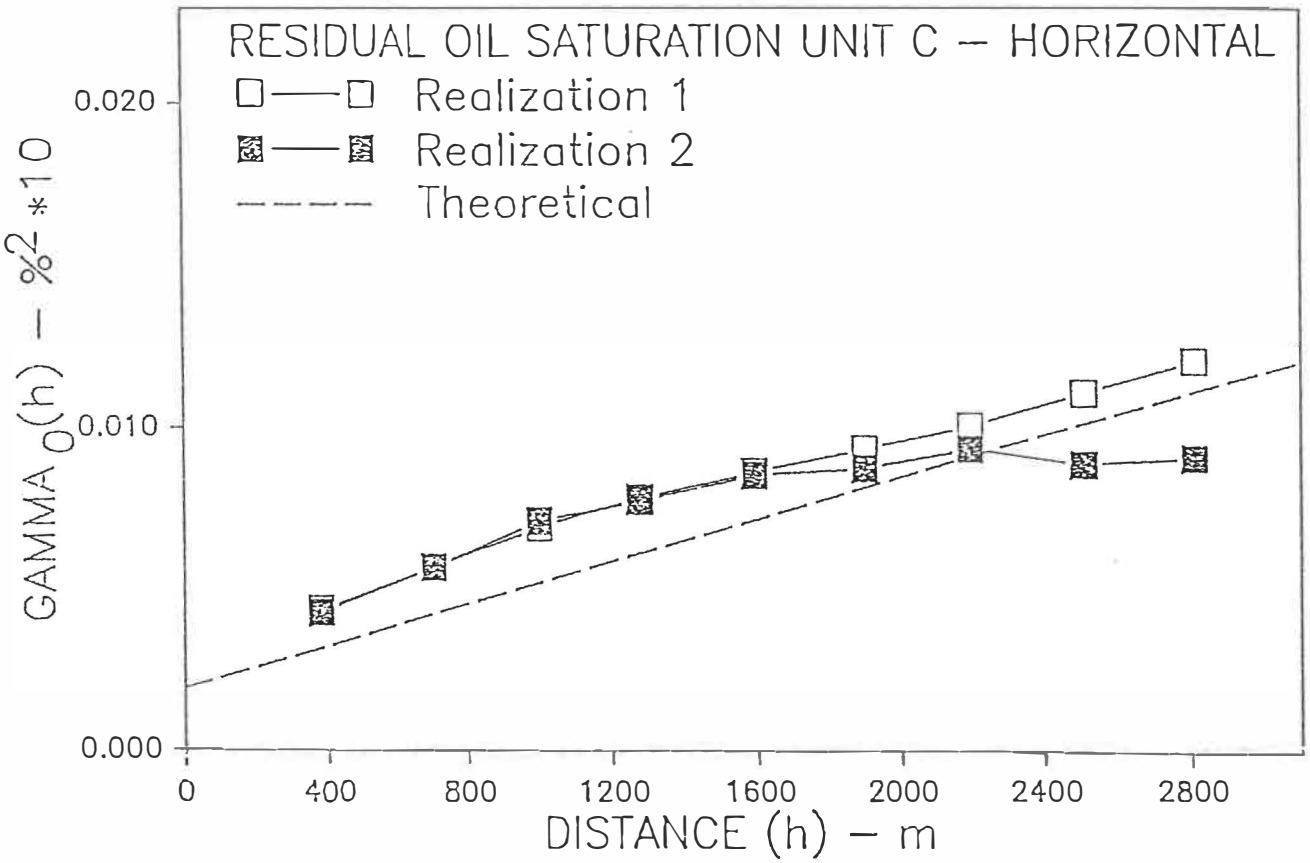
RESIDUAL OIL SATURATION UNIT C – HORIZONTAL
Realization 1
Realization 2
Theoretical
GAMMA O(h) – %2 *10
0.020
0.010
0.000
0
400
800
1200
1600
2000
2400
2800
DISTANCE (h) – m

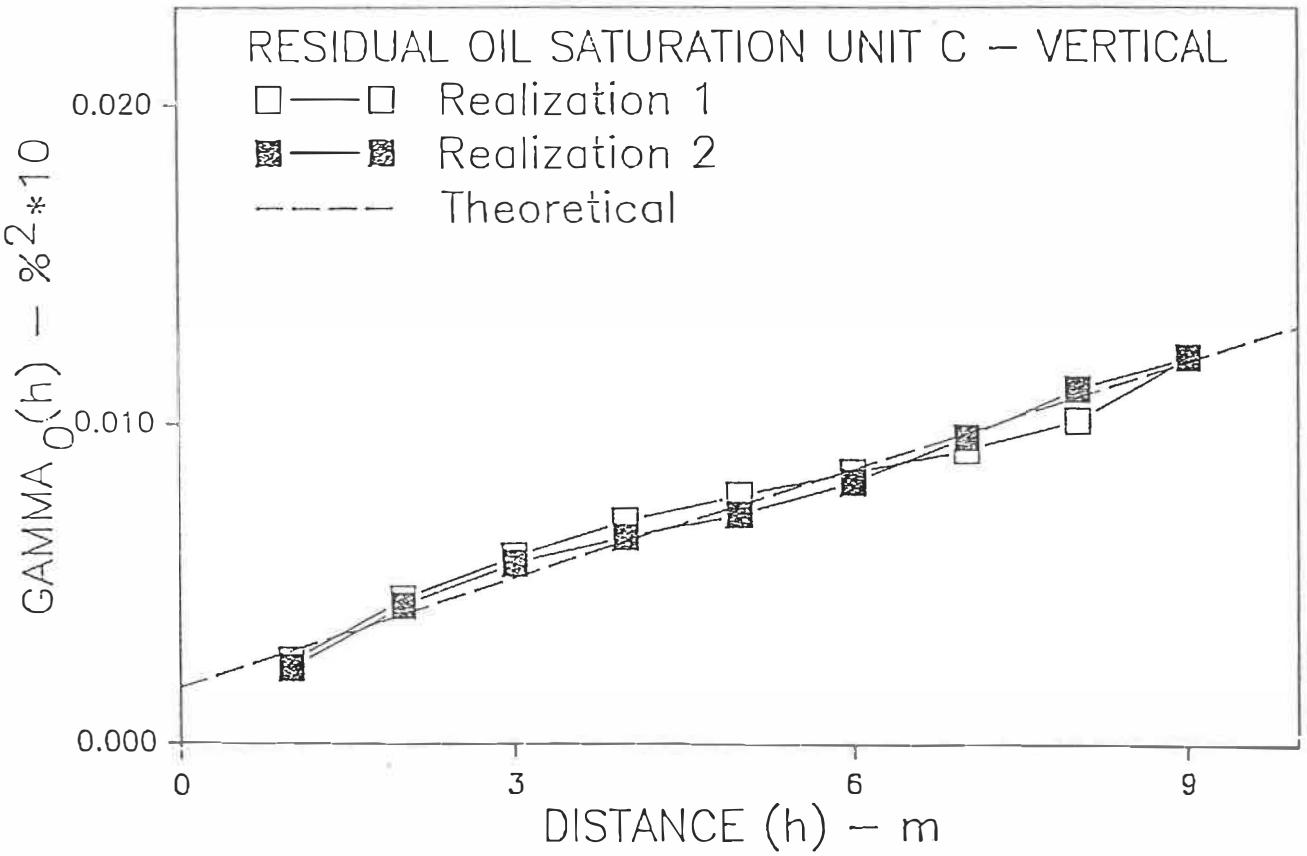
RESIDUAL OIL SATURATION UNIT C – VERTICAL
Realization 1
Realization 2
Theoretical
0.020
0.010
0.000
GAMMA O(h) – %2*10
0
3
6
9
DISTANCE (h) – m

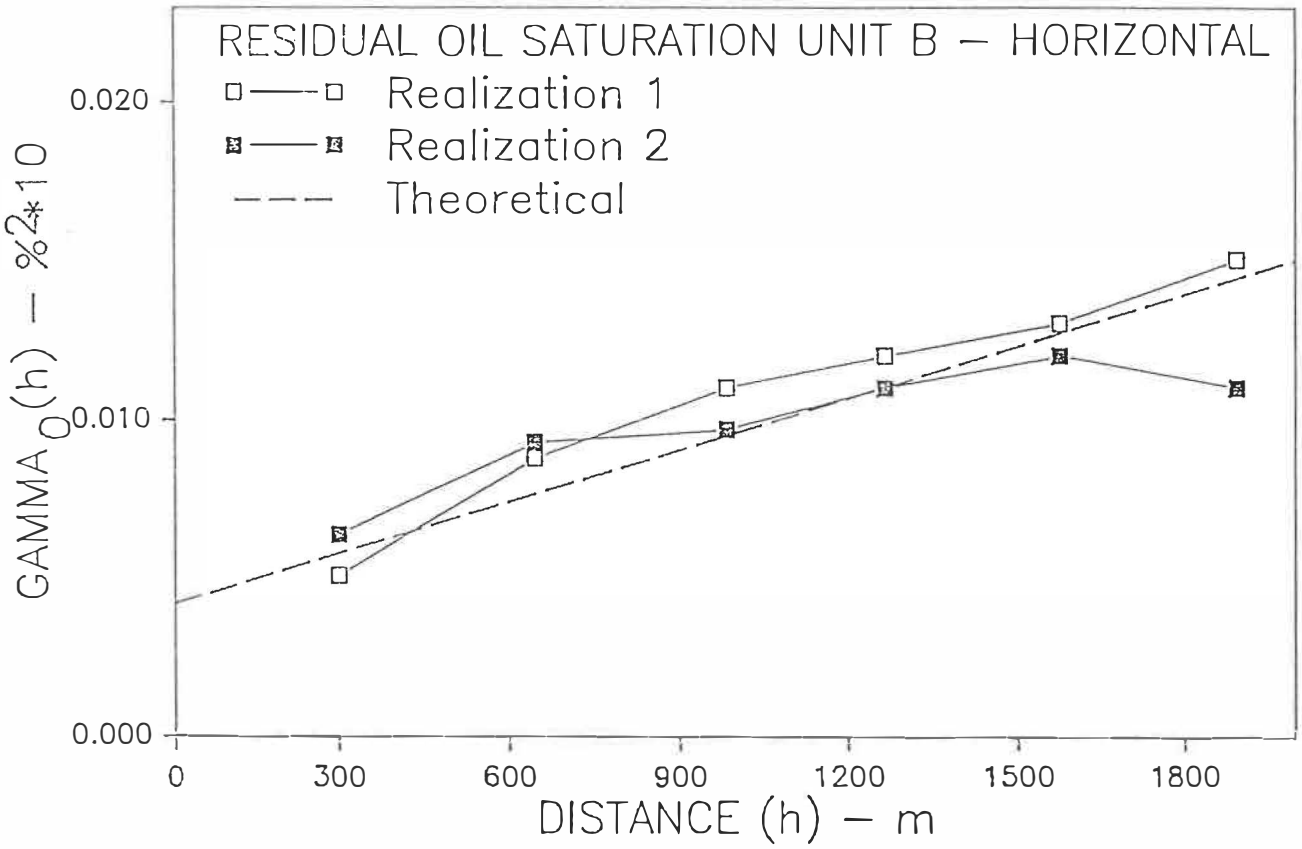
RESIDUAL OIL SATURATION UNIT B – HORIZONTAL
Realization 1
Realization 2
Theoretical
GAMMA_O(h) – %2*10
0.020
0.010
0.000
0
300
600
900
1200
1500
1800
DISTANCE (h) – m

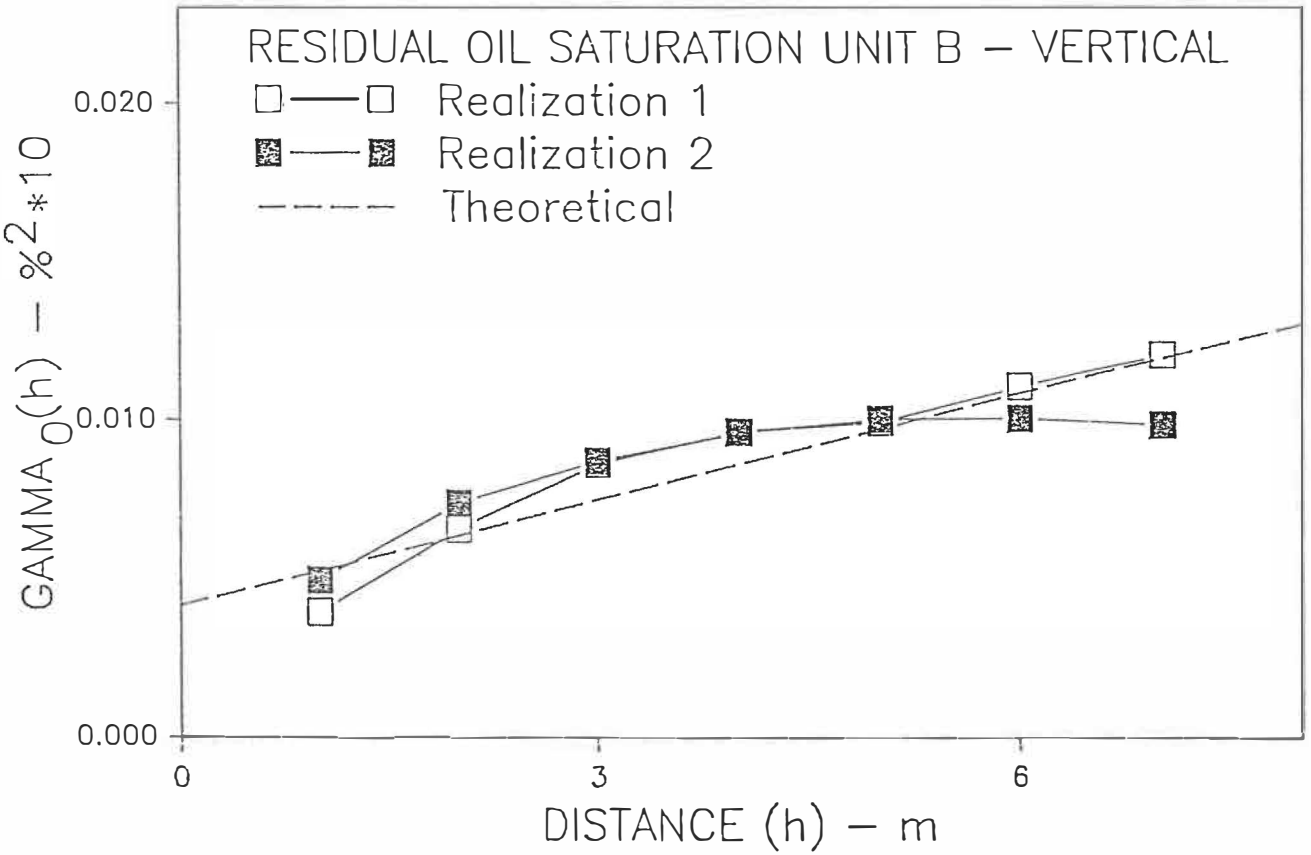
RESIDUAL OIL SATURATION UNIT B – VERTICAL
Realization 1
Realization 2
Theoretical
0.020
0.010
0.000
GAMMA O(h) – %2*10
0
3
6
DISTANCE (h) – m

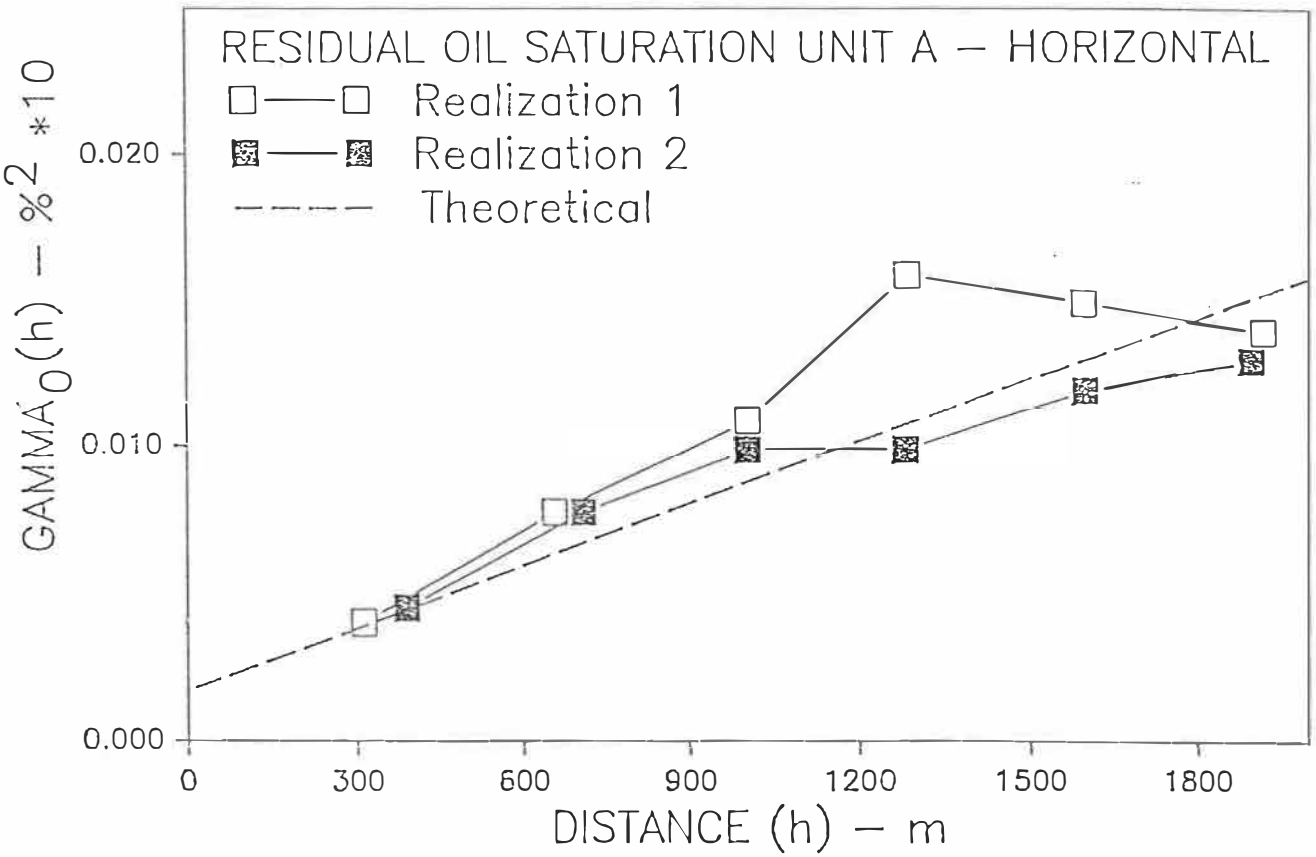
RESIDUAL OIL SATURATION UNIT A – HORIZONTAL
Realization 1
Realization 2
Theoretical
GAMMA$_O$(h) – %2 *10
0.020
0.010
0.000
0
300
600
900
1200
1500
1800
DISTANCE (h) – m

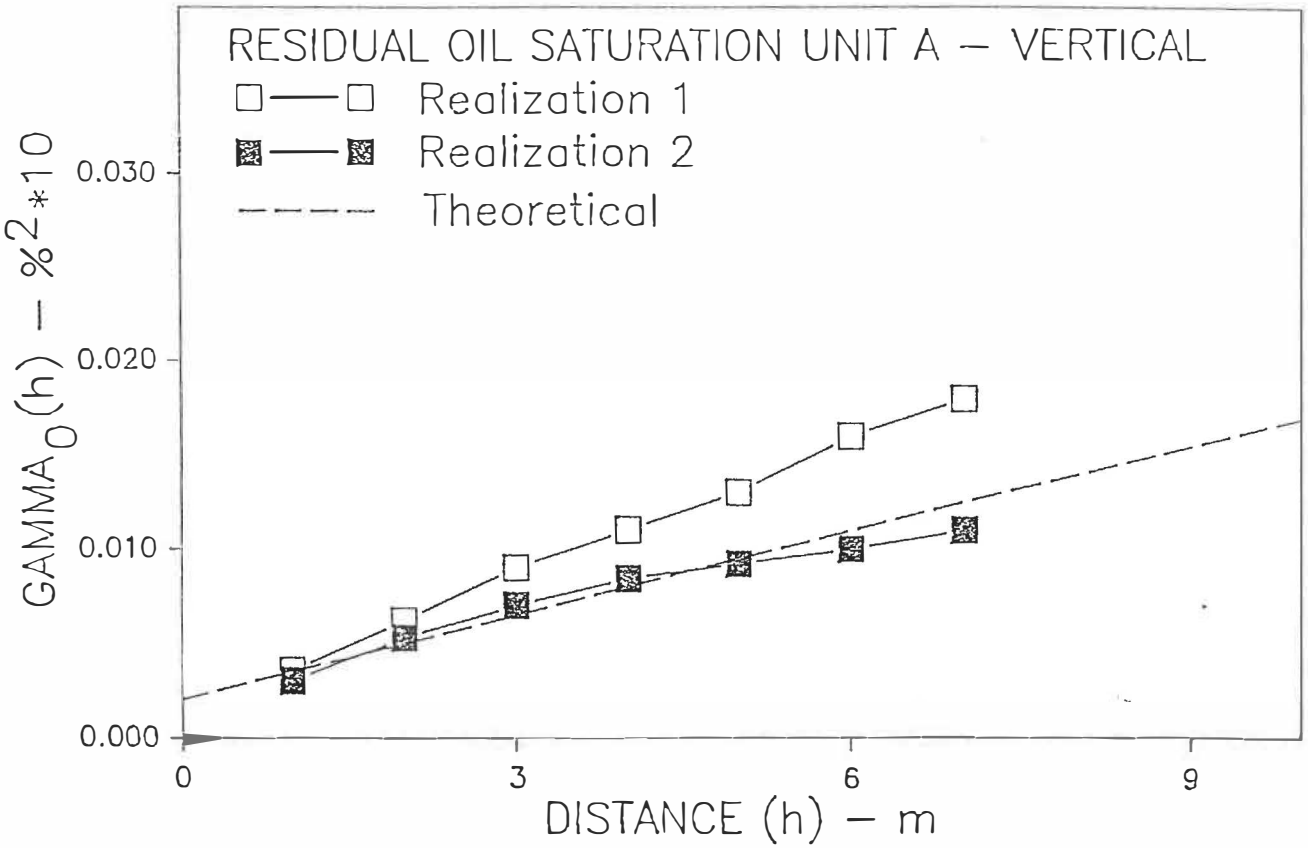
RESIDUAL OIL SATURATION UNIT A – VERTICAL
Realization 1
Realization 2
Theoretical
GAMMA$_0$(h) – %^{2}*10
0.030
0.020
0.010
0.000
0
3
6
9
DISTANCE (h) – m

APPENDIX E: COMPARISON OF LOG-PERMEABILITY VARIOGRAMS OF CONDITIONALLY SIMULATED REALIZATION OF THE CRYSTAL UNITS AND HISTOGRAMS OF REALIZATIONS

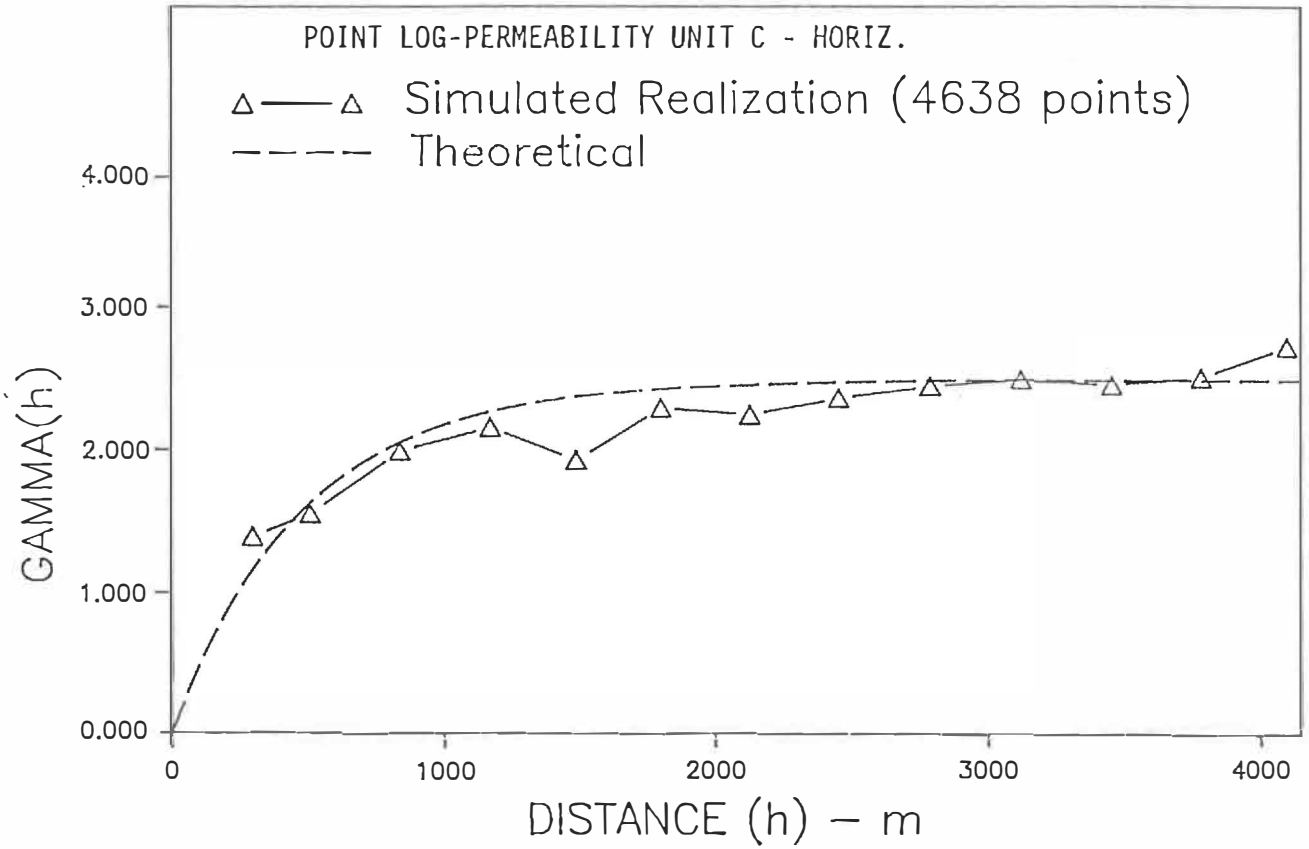
POINT LOG-PERMEABILITY UNIT C - HORIZ.
Simulated Realization (4638 points)
Theoretical
GAMMA(h)
4.000
3.000
2.000
1.000
0.000
0
1000
2000
3000
4000
DISTANCE (h) – m

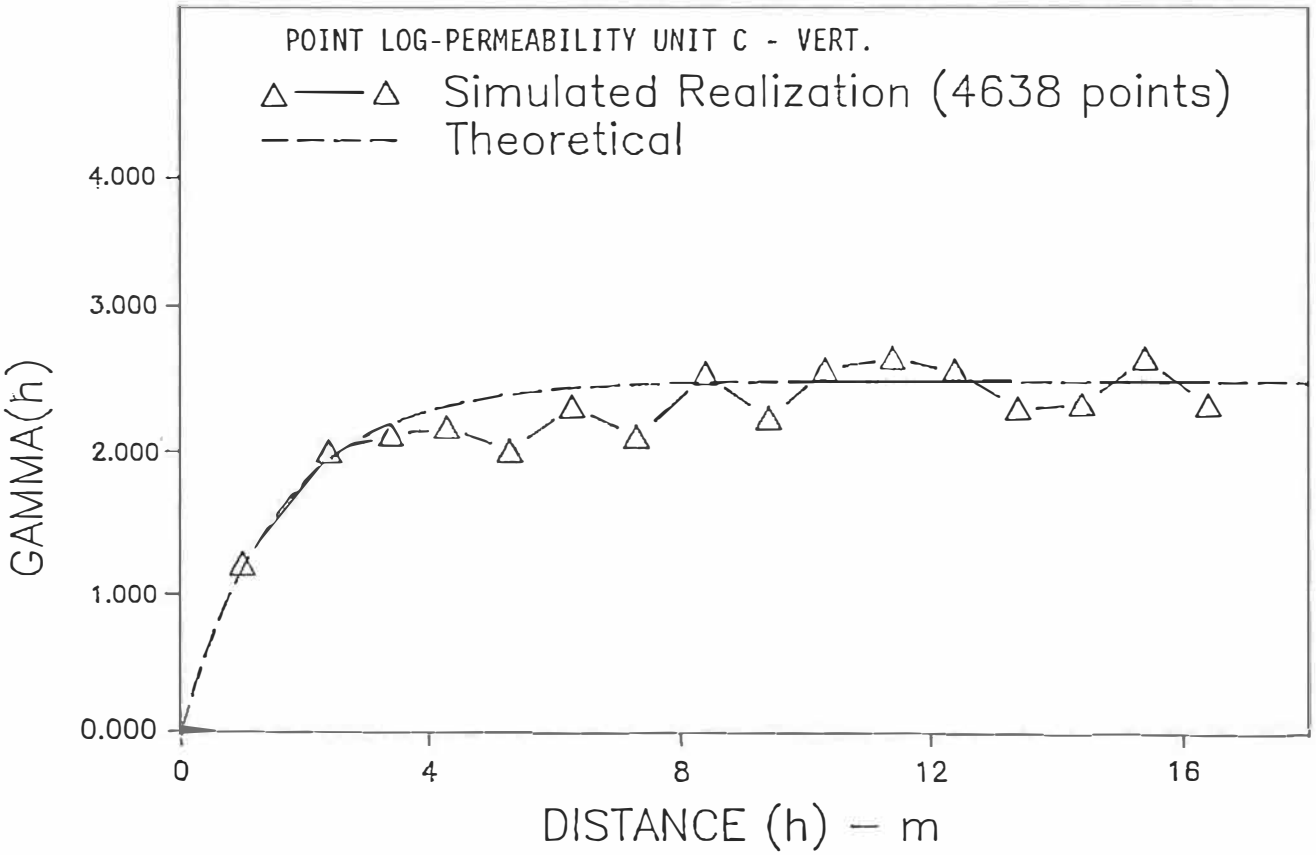
POINT LOG-PERMEABILITY UNIT C - VERT.
Simulated Realization (4638 points)
Theoretical
GAMMA(h)
4.000
3.000
2.000
1.000
0.000
0
4
8
12
16
DISTANCE (h) — m

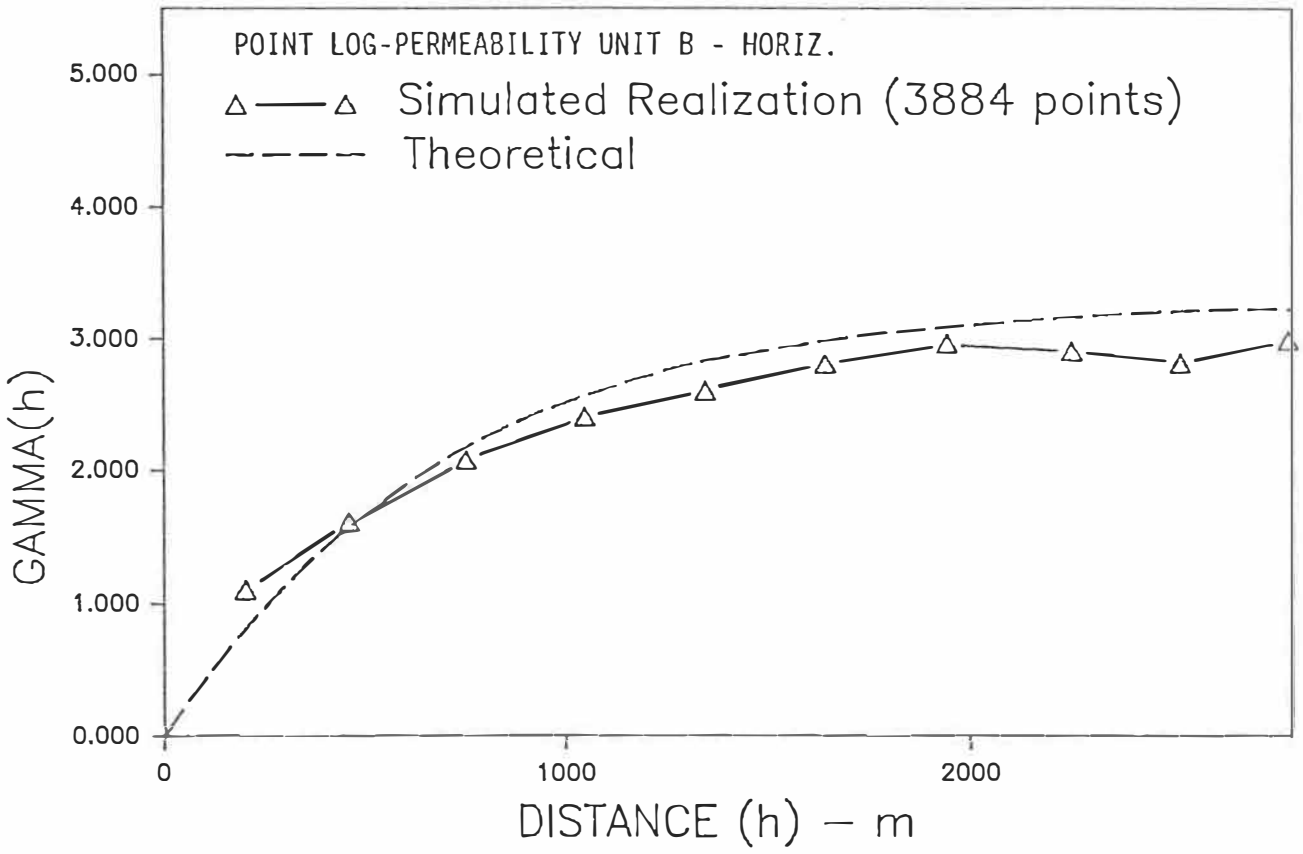
POINT LOG-PERMEABILITY UNIT B - HORIZ.
Simulated Realization (3884 points)
Theoretical
5.000
4.000
3.000
2.000
1.000
0.000
GAMMA(h)
0
1000
2000
DISTANCE (h) – m

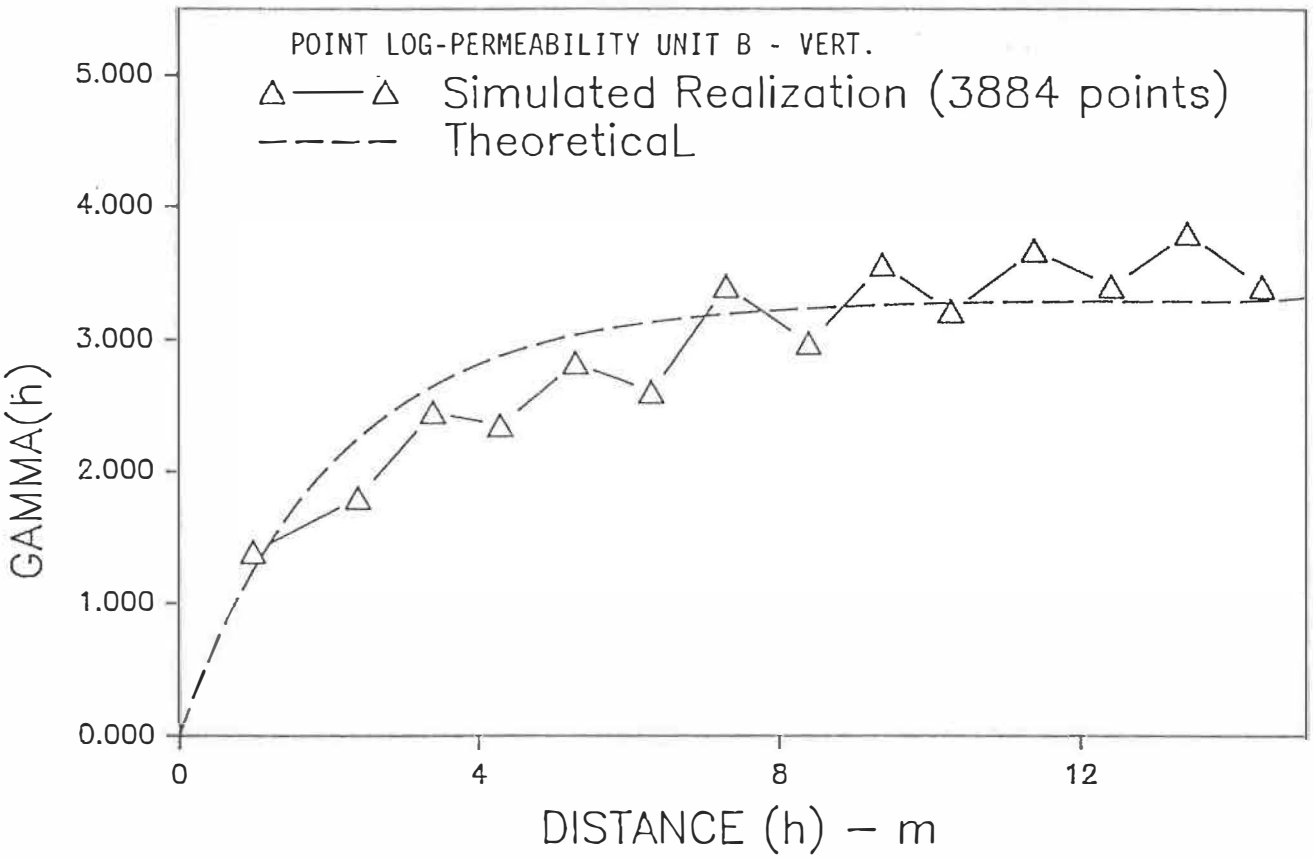
POINT LOG-PERMEABILITY UNIT B - VERT.
Simulated Realization (3884 points)
TheoreticaL
5.000
4.000
3.000
2.000
1.000
0.000
GAMMA(h)
0
4
8
12
DISTANCE (h) – m

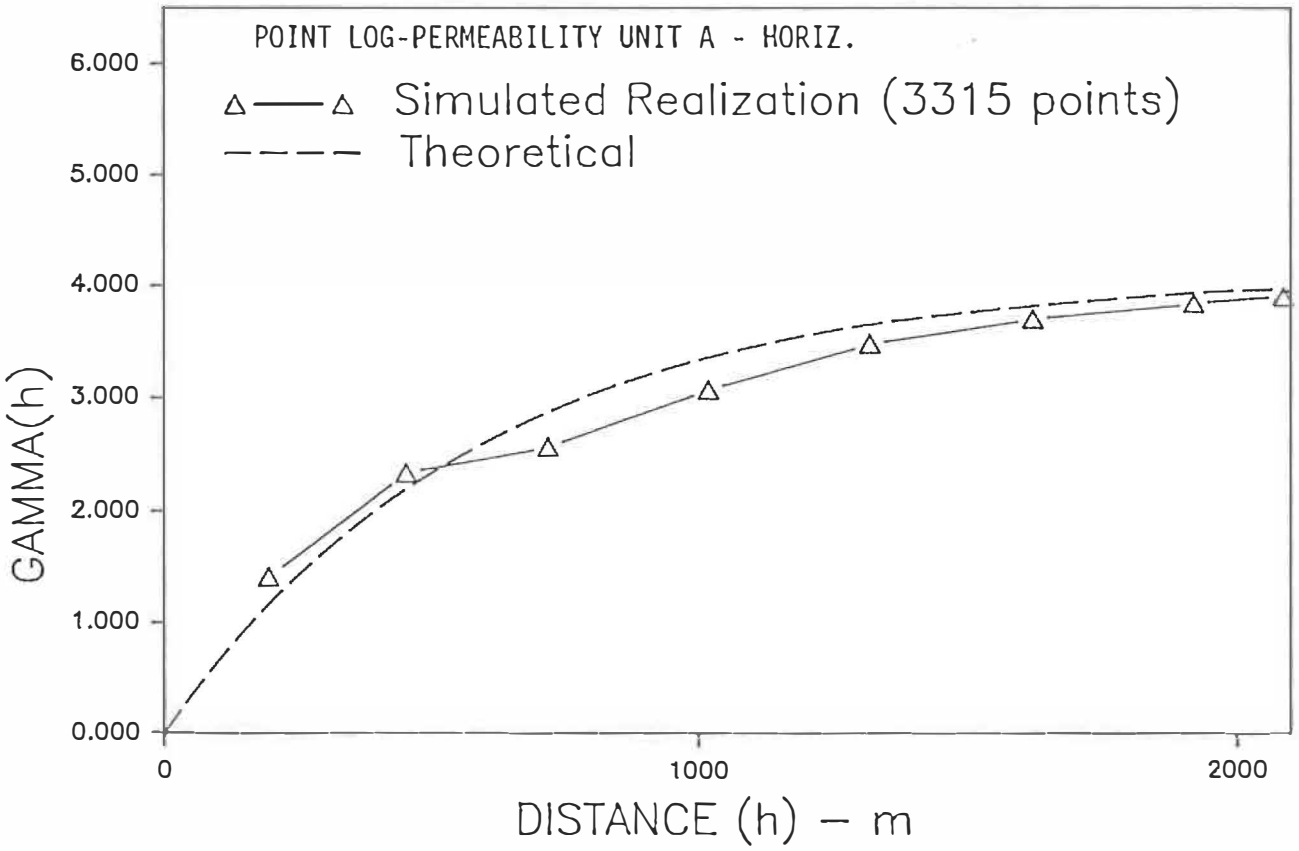
POINT LOG-PERMEABILITY UNIT A - HORIZ.
Simulated Realization (3315 points)
Theoretical
6.000
5.000
4.000
3.000
2.000
1.000
0.000
GAMMA(h)
0
1000
2000
DISTANCE (h) – m

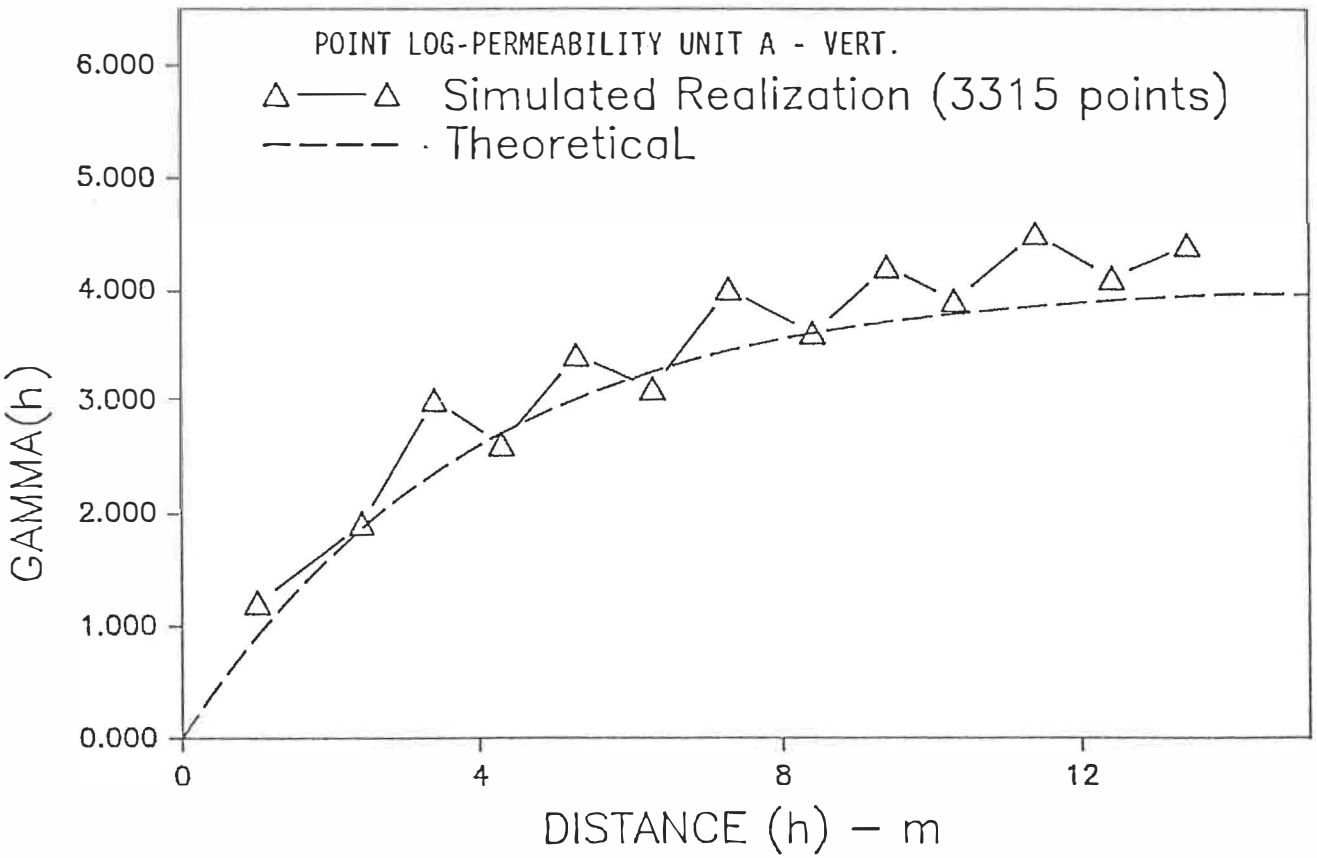
POINT LOG-PERMEABILITY UNIT A - VERT.
Simulated Realization (3315 points)
Theoretical
6.000
5.000
4.000
3.000
2.000
1.000
0.000
GAMMA(h)
0
4
8
12
DISTANCE (h) – m

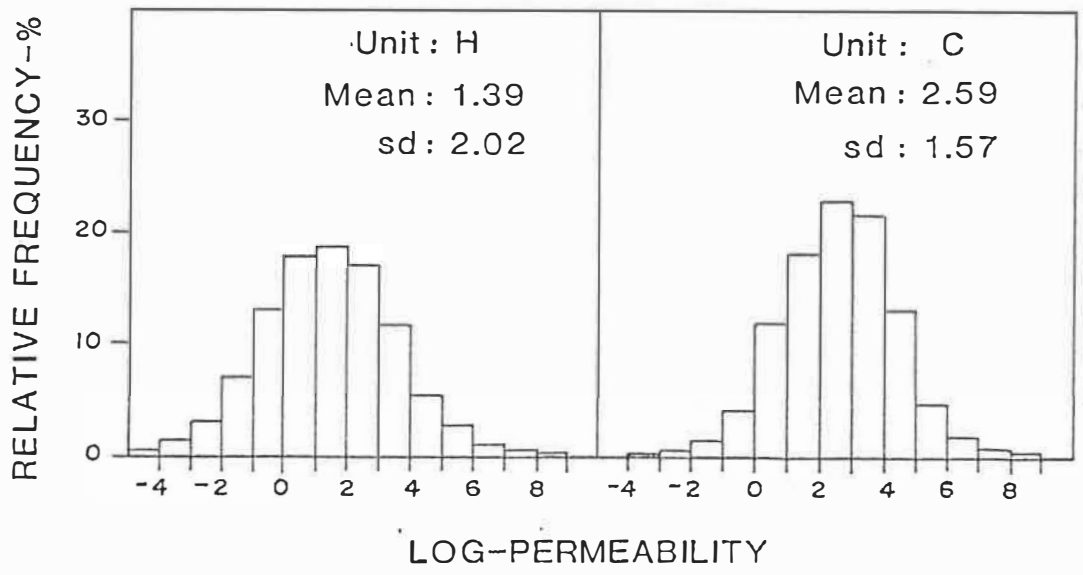
Unit : H
Mean : 1.39
sd : 2.02
Unit : C
Mean : 2.59
sd : 1.57
RELATIVE FREQUENCY-%
30
20
10
0
-4 -2 0 2 4 6 8
-4 -2 0 2 4 6 8
LOG-PERMEABILITY

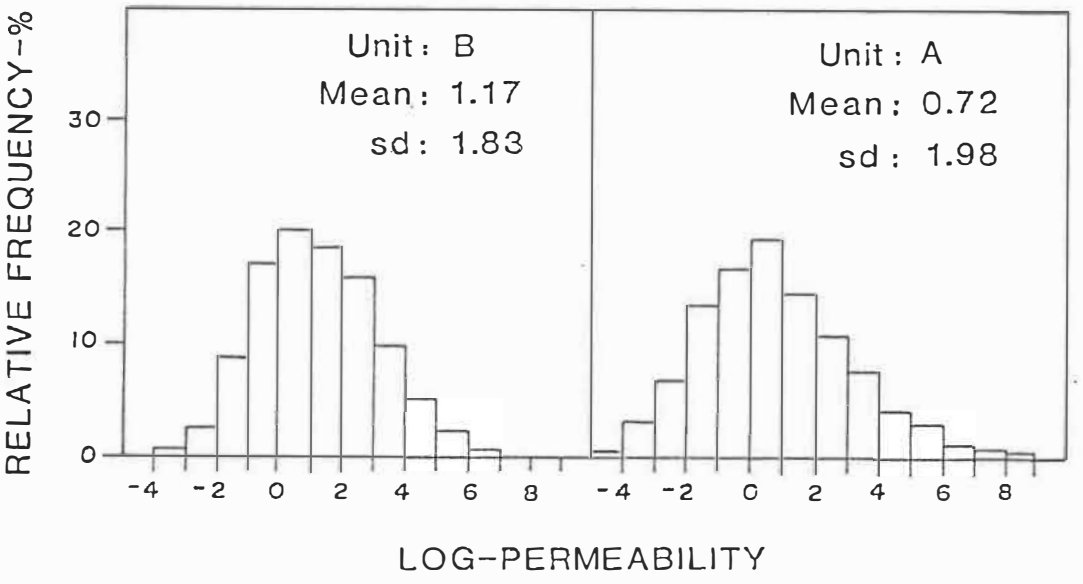
Unit : B
Mean : 1.17
sd : 1.83
Unit : A
Mean : 0.72
sd : 1.98
RELATIVE FREQUENCY-%
30
20
10
0
-4 -2 0 2 4 6 8
-4 -2 0 2 4 6 8
LOG-PERMEABILITY